STUDIES ON ANTIPROLIFERATIVE AND ANTIBACTERIAL PROPERTIES OF SOME QUINAZOLINE-4(3H)-ONES AND THEIR DIMERS

A Thesis Submitted to the University of North Bengal

For the Award of

Doctor of Philosophy
in
Biotechnology

By

BIPRANSH KUMAR TIWARY

Guide

Prof. Ranadhir Chakraborty

Co-Guide

Dr. Ashis Kumar Nanda

DEPARTMENT OF BIOTECHNOLOGY

UNIVERSITY OF NORTH BENGAL

April, 2016

Dedicated to
"My beloved Parents"

Without their blessings I would have never made it through

DECLARATION

I hereby declare that the research work embodied in this thesis has been carried out by me in the Department of Biotechnology, University of North Bengal, Darjeeling-734 013, West Bengal, India, under the supervision of Dr. Ranadhir Chakraborty, Department of Biotechnology, University of North Bengal, Darjeeling-734 013, West Bengal, India and Co-supervision of Dr. Ashis Kumar Nanda, Department of Chemistry, University of North Bengal, Darjeeling-734 013, West Bengal, India. I also affirm that this work is original and has not been submitted before in part or full for any degree/diploma or any other academic award to this or any other University or Institution.

Bipransh kumar Tiwary
04/04/2016

(Bipransh Kumar Tiwary)
Research Scholar
Department of Biotechnology
University of North Bengal -734 013

UNIVERSITY OF NORTH BENGAL

DARJEELING-734 013, WEST BENGAL, INDIA

CERTIFICATE

The research work of **Mr. Bipransh Kumar Tiwary**, presented in this thesis entitled "**Studies on Antiproliferative and Antibacterial properties of some Quinazoline-4(3H)-Ones and their Dimers**", carried out under our direct supervision, is original and has not been submitted for any degree or diploma to this or any other University or Institution.

4.4.2016

(Ranadhir Chakraborty)
Department of Biotechnology
[Guide]

Dr. R. Chakraborty
Deptt. of Biotechnology
NBU

Ashis Kr. Nanda · 4.4.2016.

(Ashis Kumar Nanda)
Department of Chemistry
[Co-Guide]

Associate Professor
Department of Chemistry
University of North Bengal
Darjeeling - 734013

Abstract

The Quinazoline-4(3H)-one and its derivatives constitute an important class of fused heterocycles that has been extensively studied and used in certain specific biological activities. The stability of the quinazolinone nucleus has encouraged researchers to introduce many bioactive moieties to this nucleus to create new potential therapeutic agents. With progress of time, newer and more complex variants of the quinazolinone structures are being discovered.

Quinazoline-4-(3H)-ones are emerging as new generation drugs, which motivated us to study some of their special features. In this study, self association property of some 2-substituted-benzo[d][1,3] oxazin-4-ones were explored. The existence of dimerization in 2-substituted-benzo[d] [1, 3] oxazin-4-was established. From the obtained results, attention was drawn towards an apparent paradoxical event where aryl C-H---O=C DA-AD pair stabilized the molecular assembly remarkably. Inresestingly, this stability was even found in the solution state. All were found to exist in solution as DA-AD pair with remarkable stability which was supported by infrared, ultraviolet, NMR and mass spectral studies. Since such DA-AD pair have large enough dimerization constant value, it could be regarded as a good model to study other properties of (hyper) polarizable dimers and study of polymorphism in solution state.

In course of our investigation during the synthesis of the 2-substituted-benzo[d][1,3] oxazin-4-ones (1d), the existence of two metamorphic forms in solid state of the compound were oberved. One polymorph has melting point (mp)81 ^{0}C (Form-I) and the other with mp 188 ^{0}C (Form-II); where Form-I was capable of complete transformation to Form-II on keeping for 15 days at room temperature. On the other hand, Form-II was re-converted to Form-I by vacuum sublimation at an elevated temperature. The existence of the compound 1d as two polymorphs was thus proved by DSC and PXRD. It was revealed in PXRD that both polymorphs are of same chemical constitution, same stacking pattern but only differ in their compactness of stacking. As two lone pairs in the carbonyl plane flank the carbonyl oxygen, we theorize some change in direction of H-bond may be responsible for the metamorphism.

Intriguingly, the dimerization of 2-substituted-benzo[d] [1, 3] oxazin-4-ones was found to hinder their antibacterial activity. It was found that the molar inhibition of bacterial growth gradually increased with dilution. The independent contribution by monomer and dimer was mathematically calculated. The monomer was found to be more active than the dimer. The findings bear considerable relevance in SAR studies of similar pharmacophores.

After uncovering the reasons behind the low antibacterial activity of 2-substituted-benzo[d][1,3] oxazin-4-ones, we have shifted our interest to explore the potential of 3-aryldeneamino-2-phenyl-quinazoline-4(3H)-ones in other biological activity. First of all, *In silico* studies were performed with an aim to evaluate the drug candidature of some quinazoline-4-(3H)–ones in future. The study consisted of compounds belonging to quinazoline-4-(3H)-ones. All the studied derivatives have qualified the Lipinski's Rule of Five, CMC like rule, WDI like rule and MDDR like rule. Every compound possessed pertinent pharmacological properties based on the results of Lipinski's Rule, hydrophobicity (based on log P value), drug likeliness and drug score. Moreover, the compounds have been predicted to have low toxicity value.

The high drug score and drug likeliness of these derivatives encouraged us to carry out molecular docking study with the human dihydrofolate reductase (hDHFR). hDHFR was chosen because literature supported that Quinazoline-4(3H)-ones have the capability to bind with it. Again, hDHFR, for its metabolic importance, was considered as better therapeutic target for cancer. Strikingly, the compounds used in this study occupied the same cavity in the protein molecule as seen to be occupied by the natural ligand like folic acid or the standard drug methotrexate.

High binding affinity of these compounds in molecular docking, instigated us to perform DHFR inhibition assay in the wet-lab. The synthesized compounds showed IC_{50} value less than that obtained with methotrexate. Two of our compounds, 3d and 3g, showed four times less IC_{50} value than methotrexate.

All the synthesized compounds (1a, 2a and 3a-3j) along with methotrexate and curcumin (as a reference drug) were screened for their anti-proliferative activities against three cancerous cell lines; HepG2 (human liver cancer cell line), MCF-7 (human breast cancer cell line) and HeLa (human cervical cancer cell line) using 3-(4,5-Dimethylthiazol-2-yl)-2,5-Diphenyltetrazolium Bromide (MTT) assay. Among

the three cell lines used, HepG2 was found to be the most sensitive against all the compounds used. All the cell lines were susceptible to compounds, 3a and 3i. Hence, features like drug likeliness, inhibition of hDHFR activity and antiproliferative activity of 3-(arylideneamino)-2-phenylquinazoline-4-(3H)-ones were evaluated.

In the journey of a compound to be established as a lead and finally to a drug, the problem of solubility is a major challenge for medicinal chemists and formulation scientists. The major predicament of Quinazoline-4-(3H)-one derived drugs is their low water solubility. In the present study, we have tried to solubilize molecule by making a host-guest complex with β-cyclodextrins. Kneaded method was found to be the best one to prepare the host guest complex. The compounds and its complexation with β- cyclodextrin were analyzed by spectral methods, DSC and PXRD. The encapsulated compound fitted better into the cavity of β-CD and thus improved their solubility. Taken together all the results, it was shown that our approach to enhance the solubility of quinazoline-4(3H)-one compounds by β-Cyclodextrin is an easy and economical method.

The present study has therefore generated certain genuine thrust to pursue medicinal chemistry research in combating overwhelming human sufferings like cancer.

PREFACE

The art to solve mysteries of natural phenomena, afflicts the progress of human civilization. Time and again several scientific searches have flip-flopped. During the past years Quinazoline-4(3H)-ones have once again come out as an important nucleus showing varied pharmaceutical and biological activities. A few of them are worth mentioning - antibacterial and anticancer activities. The tremendous therapeutic potential demonstrated by the nucleus prompted us to synthesize and evaluate biological activities of some Quinazoline-4(3H)-one. This idea has led to pursue the Ph.D. work entitled "Studies on Antiproliferative and Antibacterial properties of some Quinazoline-4(3H)-ones and their dimers". Our aim was to explore the intrinsic impediments of this pharmacophore to achieve better antibacterial activity and also to explore their potential as anti-proliferative agents.

The study was carried out in three sections. First section dealt with the characterization of dimerization in 2-substituted-benzo[d][1,3]-oxazine-4(3H)-one. The CH-O-C H-bond was found to be responsible for self association. This association was also established in solution state. The effect of this dimerization on hindrance of their antibacterial activity was also studied.

In second section, the drug likeliness behaviour and drug score was predicted by *In silico* studies. Again, *In silico* studies were validated by performing hDHFR activity inhibition assay. After validation by measuring inhibition of dihydrofolate reductase enzyme, cell-line studies demonstrating the antiproliferative potential of these compounds were done.

In concluding section of this study, we have tried to increase the solubility of Quinazoline-4(3H)-one by forming inclusion complexes with β-cyclodextrins. The formation of inclusion complexes were characterized by different spectroscopic and other methods. In this way, we have addressed the two major intrinsic problems of Quinzoline-4(3H)-ones as a therapeutic agents, first the self association properties of this pharmacophore and the second one - the problem of solubility.

ACKNOWLEDGEMENTS

My laborious days at the laboratory of the Department of Biotechnology, University of North Bengal during the course of this work would not have been a pleasing experience had it not been for the presence of many good-hearted individuals at the working place and caring family members at home. It would not have been possible to realize this work without the friendly help and advice of all of them, to whom I take this opportunity, to acknowledge and thank.

First and foremost I acknowledge my heartfelt and sincere gratitude to my supervisor Prof. Ranadhir Chakraborty, Department of Biotechnology, University of North Bengal, Darjeeling-734 013, West Bengal, India, and Co-supervisor Dr. Ashis Kumar Nand, Associate Professor, Department of Chemistry, University of North Bengal, Darjeeling-734 013. Under their guidance, I was given the freedom to take my research into the areas that interests me the most. Not only are they a valuable information source, but they are also an excellent mentor. It has been my pleasure to work with someone who truly loves what he does and refreshing to see somebody who enjoys science so much. I consider myself fortunate enough to be associated with them whose vast scientific knowledge, personal care and spirit has resulted in this present endeavor. Due to them my time at this department has been excellent.

I would like to take opportunity to thank all Faculty members as well as Non-teaching staff members of the Department of Biotechnology and Department of Chemistry for their help during this course of study.

I wish to express my deep sense of gratitude and respect to Dr. Anoop Kumar for taking out his time and personally helping me for the antiproliferative studies. I express my sincerest gratitude to Dr. Dipanwita Saha for always encouraging me and helping me with my work. I am also grateful to Dr. Shilpi Ghosh for her constant encouragement and blessings.

I record my special thanks to all my seniors' research scholars and friends of my laboratory: Dr. Shriparna Mukherjee, Dr. Suparna Saha Bhowal, Dr. Arvind Kumar, Dr. Krishna Kant Yadav, Mr. Amit Kumar Mandal, Vivek Kumar Ranjan and Mr. Subhanil Chakraborty for their kind help and co-operation.

I reserve my special thanks to Dr. Kiran Pradhan, my senior lab-mate, who was always there to help and encourage me.

It's a great pleasure to express my sincere thanks to Dr. Asim Kumar Bothra, Department of Chemistry (Raiganj University)and and Ravikant Pathak, Department of bioinformatics, Lovely professional University for their co-operation and helpful suggestions for Bioinformatics studies. I would also like to take this opportunity to thank Dr. Santa Sabuj Das, Department of Immunology, NICED, Kolkata, West Bengal, India, for helping me in antiproliferative studies.

I wish to thank the authorities of the University for providing me with the required facilities and financial assistant.

I am extremely thankful to CDRI Lucknow, Utter Pradesh and AIRF, Jawaharlal University, Delhi, India for carrying out Raman spectra and PXRD.

I can't express my profound regards to my parents in words for their support of all my life's choices and their unconditional love which is a constant source of strength for everything I do. My parent has been the beacon of light in my life and every successful endeavor of mine silently draws inspiration from them. I have constantly received significant support from my two my elder sisters, Madhu Upadhyay and Subhasha Mishra. I express my gratitude to my brother-in-laws Arun Kumar Upadhyay and Sanjay Mishra. Their blessings, affection and care have been the constant source of my insipiration throughout the entire period of my academic career. I also express my love to younger brother (Mr. Brahmansh Kumar Tiwary) and younger sister (Nitasha Pandey) for encouragement during the whole course of my work. Finally my wife, Anshu Pandey, has been my constant source of encouragement in the end of this journey. It is very difficult to mention every individual name and his/her contribution in my life. This thesis could not be completed without them. I am highly indebted to all of them.

Dated: 04/04/2016

Bipransh Kumar Tiwary

(Bipransh Kumar Tiwary)

TABLE OF CONTENTS

LIST OF TABLES

LIST OF FIGURES

LIST OF SCHEMES

APPENDIX A

ABBREVIATIONS

°C	Degree Celsius
µm	micrometer
1D	1-Dimensional
2D	2-Dimensional
AFM	Atomic fluorescence microscopy
C	Carbon
CD	Cyclodextrin
CFU	Colony-forming unit
CH_3OH	Methanol
$CHCl_3$	Chloroform
cm	Centimeter
d	diameter
Da	Dalton
DMSO	Dimethyl-sulfoxide
DOSY	Diffusion-Ordered NMR Spectroscopy
DSC	Diffrantial scanning calorimetry
EtOH	Ethanol
FTIR	Fourier transform infrared spectroscopy
g	gram
h	Hour(S)
HMBC	Heteronuclear multiple bond correlation
HSQC	Heteronuclear single quantum coherence
Hz	Heartz
H	Hydrogen
J	Coupling constants
Kg	Kilogram
KND	Inclusion complex by Kneaded method
M	Molar

mg	miligram
MHz	Mega hertz
min	minutes
ml	Mililiter
mm	Millimeter
mM	Millimolar
NaOH	Sodium hydroxide
$NaHCO_3$	Sodium carbonate
NMR	Nuclear magnetic resonance
NOESY	Nuclear overhauser enhancement spectroscopy
PBS	Phosphate buffered saline
ppm	Parts per million
PXRD	Powder X- Ray Diffraction
PM	Physical mixture
rpm	Rotation per minute
SEM	Scanning electron microscope
TGA	Thermo gravimetric analysis
TOCSY	Total correlation spectroscopy
UV	Ultraviolet
v/v	Volume by volume ratio
vis	Visible
µg	microgram
µl	microliter
µM	micromolar

Review of Literature

Review of Literature

I. Brief introduction of Benzoxazine

4H-3,1-benzoxazinones are known for more than a century. They, being found in nature, are frequently utilized as suitable skeletons for the design of biologically active compounds (El-Mekabaty, 2013). They are also used in organic synthesis for building natural and designed synthetic compounds. Hence, they are considered as chemical synthons of various physiological significances and pharmaceutical utilities. Benzoxazine skeleton is known for their versatility, relative simplicity and accessibility, which put them up amongst the most promising sources of bioactive compounds (Macias *et al*., 2006). The general name given to members of this family is acylanthranils. Apparently, they are early synthesized from 2,1- benzisoxazole (anthranil) and an acylating agent (Coppola, 1999). The phenyl derivative 1a was first synthesized (Friedländer & Wleugel, 1883) and after seventeen years the methyl analog 1b was synthesized (Figure 1). Compounds possessing this ring system are also found in nature. e.g. Phytoalexins, Avenalumin, Dianthalexins and some hydroxylated derivatives (Hofman & Hofmanova, 1969).

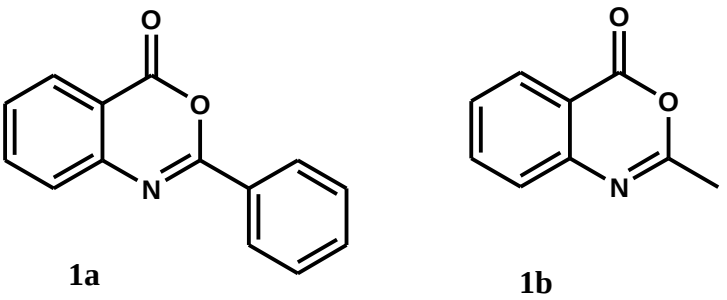

1a **1b**

Figure 1: Structure of (1a) 2-phenyl-benzo[d][1,3]oxazine-4-one; (1b) 2-methyl-benzo[d][1,3]oxazine-4-one.

Table 1: Timeline representing Development of Quinazoline scaffold

Year	Discovery	Number of Quinazoline compounds known till date
1869	Griess prepared the first quinazoline derivative, 2-cyano-3,4-dihydro-4-oxoquinazoline	>300000 Quinazoline as a substructure compounds available in SciFinder. Interestingly, nearly 40000 compounds were found to be biologically active
1887	The name quinazoline (German: Chinazolin) was first proposed for this compound by Weddige	
1889	Paal and Bush suggested the numbering of quinazoline ring system	
1903	More satisfactory synthesis of quinazoline was subsequently devised	
1951	The first renowned quinazoline marketed drug – Methaqualone is used for its sedative–hypnotic effects	
1957	Chemistry of quinazoline was reviewed by Williamson	
1959	Chemistry of quinazoline was further reviewed by Lindquist	
1963	Brought up to date by Armarego in 1963	
1960-2010	More than hundred drugs containing Quinazoline moieties have made their way to the market	

II. Properties of Benzoxazine

(a) Physical properties

Benzoxazine has the ability to provide effective bleaching at as low as 40°C. It is cost effective as well as environment-friendly. Moreover, polybenzoxazines showed admirable strong thermal stability and near-zero shrinkage without showing any release of volatiles during polymerization. They exhibited low viscosity, no need of harsh catalysts, and rich molecular design flexibility (Ambujakshan *et al.*, 2008). The flexibility occurred in their molecular design, enable to develop several high performance benzoxazines, naphthazozines, phthalonitrile and phenylnitrile functional polybenzoxazines (Kim *et al*., 1999; Brunovska *et al.*, 2000).

(b) Chemical properties

4H-3,l-benzoxazin-4-one derivatives can be believed as semi-acid anhydrides because formed by cyclodehydration of acylanthranilic acids. They undergo many reactions of true acid anhydrides, but at slower rate (El-Hashash *et al.,* 2012). However, rarely electrophilic reactions on the benzene ring of the benzoxazinone nucleus occurred and are probably unnecessary due to the plethora of diversely available substituted anthranilic acids. It is considered that the synthesis of electronically unsaturated character of unstable benzoxazinones (4*H*)-3,1-benzoxazinones) which are bearing saturated substituents such as CH_3, CH_2COCH_3, CH_2CN and $CH_2CH_2CO_2H$ at position 2 renders their synthesis difficult. They are not considered as satisfactorily stable rings. But, they are indeed useful intermediates in organic synthesis affording through reaction with nitrogen nucleophiles 4(3*H*)quinazolinones **(**Essawy *et al.,* 1982; Mohamed *et al.,* 1981).

Reactions with hydrazine hydrate (Hydrazinolysis)

Heating 4H-3,1-benzoxazin-4-ones in neat hydrazine hydrate or in pyridine or xylene solutions produces the 3-amino-4-quinazolones (Patil *et al.,* 2009; Shweta *et al.,* 2009; El-Hashash *et al.,* 2012).

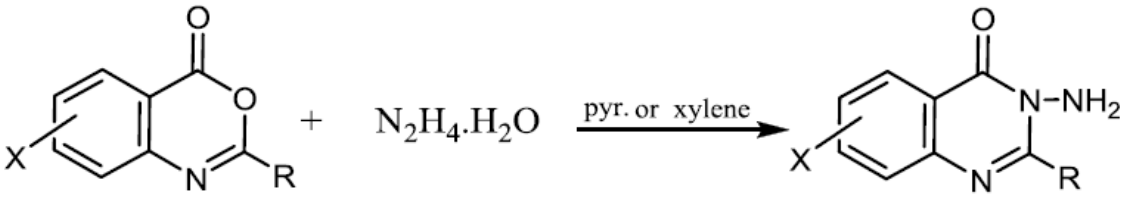

Figure 2: Heating of benzoxazinone derivatives with hydrazine hydrates

Similarly, heating benzoxazinone derivatives with hydrazine hydrate in n-butanol afford 3-aminoquinazolone derivatives (Madkour, 2014).

Reactions with Oxygen nucleophiles

The simplest and sometimes the most unwanted reaction of some 4H-3,1-benzoxazin-4-ones is hydrolysis. Where, the *4H*-3,1-benzoxazin-4-ones are

exceedingly labile to hydrolysis and the initial cleavage to N-acylanthranilic acids parallels that of benzoxazoles to acylarninophenol (Bolotin *et al.*, 1976).

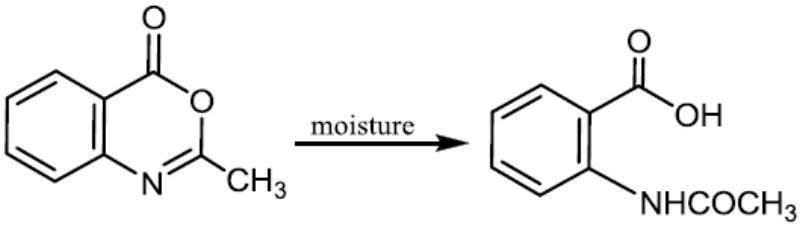

Figure 3: Hydrolysis of benzoxazine-4-one

III. Brief introduction of Quinazoline-4(3H)-one

Quinazoline-4(3H)-one and its derivatives constitute an important class of fused heterocycles that are found in more than 200 naturally occurring alkaloids. In 1950, medicinal chemists started to take interest after the elucidation of a quinazolinone alkaloid, 3-[β-keto-g-(3-hydroxy-2- piperidyl)- propyl]-4-quinazolone. This quinazolinone derivative was isolated from Traditional Chinese herbal *Dichroa febrifuga*, which is found to be effective against malaria (Koepfly *et al.,* 1947). Quinazolinones are the oxidized form of quinazoline. These structures are defined by the location of the oxygen and the oxygen and the hydrogen on the nitrogen (NH). Gabriela obtained quinazoline in good yield by oxidation of 3,4-dihydroquinazoline with alkaline pottsaium ferricyanide. This fused bicycle compound was earlier known as benzo-1,3-diazine. The name quinazoline (German: Chinazolin) was first proposed for this compound by Weddige, on observing that this was isomeric with the compounds cinnoline and quinoxaline (Asif, 2014). In 1889 the commonly accepted numbering for quinazolines and quinazolinone was first adopted by Paal and Buch, as suggested by Knorr and designated individual atoms of a ring with numbers. The most important class of compounds containing the quinazoline nucleus is composed of those compounds, which have hydroxyl group in the 2 or 4 positions in the quinazoline ring, adjacent to a heterocyclic nitrogen atom. Those quinazolines having a functional group, which is easily derived on conversion to hydroxyl group like alkoxy, aryloxy, chloro, amino, thioethers and seleno etc. are also included in important class**.** . Depending upon the position of the keto or oxo group, these compounds may be classified into two types: 2-(1H) quinazolinones and 4-(3H) quinazolines (Mhaske & Argade, 2006). Thus 4-hydroxyquinazoline, tautomeric with

4-keto-3,4-dihydroquinazoline, is commonly named 4(3H)-quinazolone, or simply 4-quinazoline (Mahato *et al*., 2011).

The major subclasses of quinazolinones based on the substituents present on different positions are as follows- .

- 2-Substituted-4(3H)-quinazolinones
- 3-Substituted-4(3H)-quinazolinones
- 4-Substituted-quinazolines
- 2,3-Disubstituted-4(3H)-quinazolinones

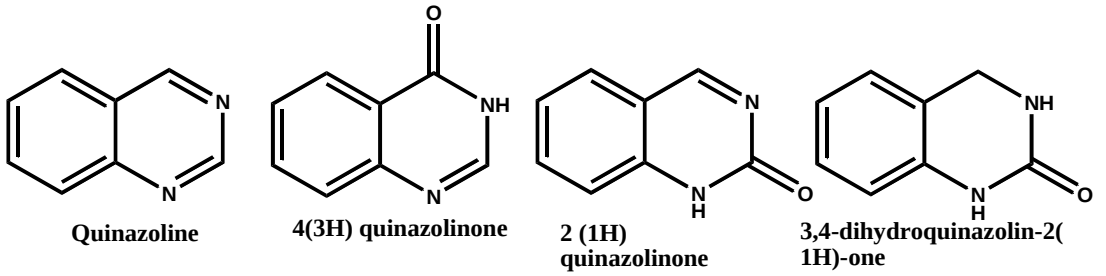

Figure 4: Different types of quinazoline

Among the four quinazolinone structures, 4(3H)-quinazolinones are most prevalent, either as intermediates or as natural products in many proposed biosynthetic pathways. This is partly due to the structure being derived from the anthranilates while the 2(1H)-quinazolinone is predominantly a product of anthrailonitrile, or benzamide with nitriles. Through the process of auto-oxidation quinazoline precursors can be converted to the corresponding 4(3H)-quinazolinone.

IV. Properties of Quinazolinone/Quinazoline-4(3H)-one

(a) Physical properties

Quinazolinones are known for high melting crystalline solids, extremely stable to light, heat, and air. It is insoluble in water and in most organic solvents but soluble in aqueous alkali, because of tautomerism. They are generally insoluble in dilute acids

but are sometimes soluble in concentrated acids. Although, simple 4-(3H)-quinazolinones are insoluble in dilute acids, but soluble in 6N hydrochloric acid. They form stable chloroplatinate, monohydrochlorides, chloroaurates and picrates . They also form stable metal salts of silver, mercury, zinc, copper, sodium and potassium. (Soderbaum & Widman, 1889; Korner, 1900).

(b) Chemical properties

Despite quinazolinone chemistry being considered to be an established area, day by day newer and more complex variants of the quinazolinone structures are still being discovered (Shobha & Raju, 2015). The first reported synthesis of a quinazolinone occurred in 1869, which was prepared from anthranilic acid and cyanide in ethanol, creating 2-ethoxy-4(3H)-quinazolinone. These findings were further confirmed by the synthesis of the derivatives 2-amino-4(3H)-quoinazolinone and 2,4(1H,3H)-quinazolinedione by reaction with ammonia and water respectively. A strong lactam-lactim tautomeric interaction is observed in quinazolinones as shown in Figure 5 (Weber *et al.,* 2003). This tautomeric interaction can also be observed when a 4(3H)-quinazolinone containing a methyl in the 3-position is subjected to chlorination with $POCl_3$, the methyl group is lost and chlorination proceeds (Bogert & Seil, 1907) and when the methyl group is present in the 2-position, the tautomeric effect is extended generating an exo methylene carbon. As result of these extended tautomeric effects, the reactivity of the substituted-4(3H)-quinazolinones is increased (Marr & Bogert, 1935). Hence, the quinazolinones are regarded to be a "privileged structure" for drug development and discovery (Cavalli *et al.,* 2009; Akbari *et al.,* 2013). Moreover, various literatures including Structure activity relationship studies of quinazolinone ring system revealed that position 2, 6 and 8 are very much important for structure activity studies. It is also suggested that chemotherapeutic activity could be increased by attachment of position 3 to different heterocyclic rings.

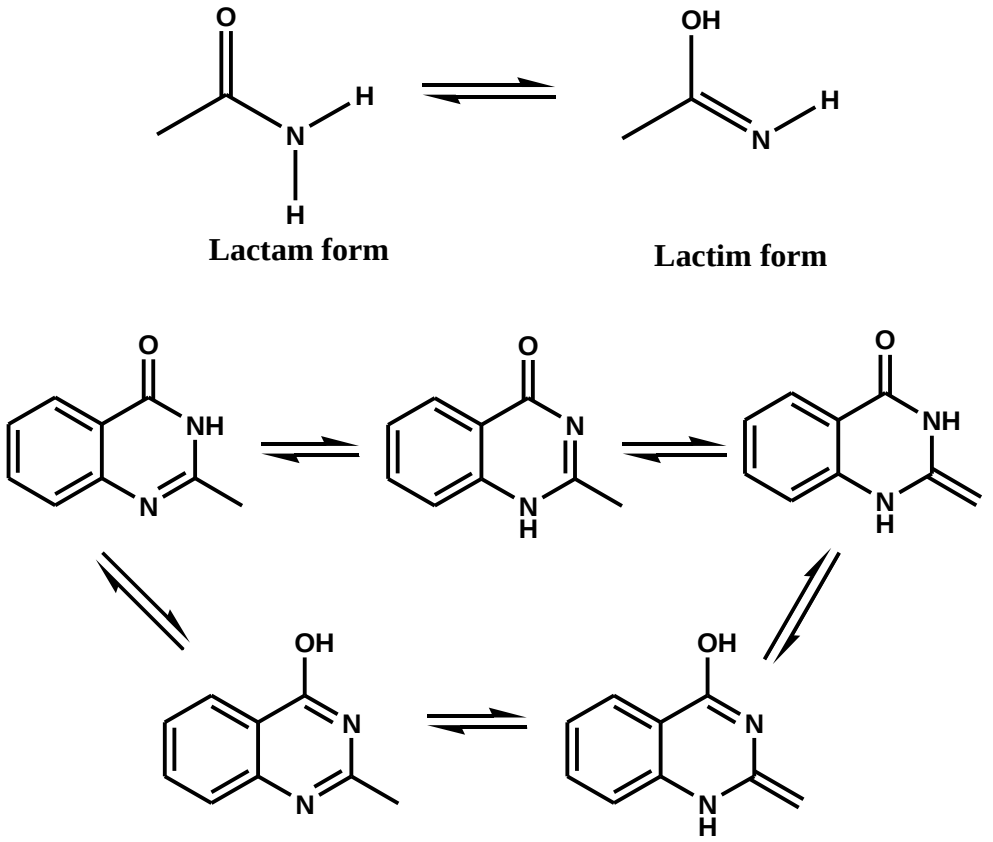

Figure 5: Representation of the different tautomeric forms of 2-methyl-4(3*H*)-quinazolinone

Aromatisation

When a simple and 2-substituted 4-(3H) quinazolinone is heated with an equivalent amount of phosphorous pentachloride in phosphorous oxychloride, the corresponding 4-chloroquinazoline is obtained. If a methyl group is present at 3-position, prohibiting the usual tautomerism, the methyl group is lost during the chlorination (Bogert & May, 1909).

Stability of the ring system

It was reported that the quinazolinone ring is quite stable towards oxidation, reduction and hydrolysis reactions. No reactions of ring degradation via simple chemical oxidation were cited till date (Armarego, 1963).

Chemical reactions

Oxidation

It is reported that after the absorption of one molecule of hydrogen catalytic hydrogenation of quinazoline ended and yields 3,4-dihydroquinazoline (Figure 6) (Armarego, 1963).

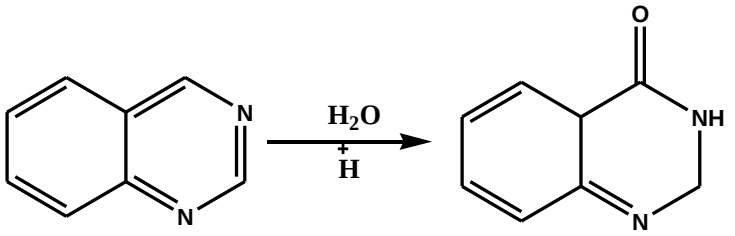

Figure 6: Oxidation of Quinazoline

Reduction

Reduction with sodium amalgam produce 1,2,3,4-tetrahydroquinazoline. However, Lithium aluminum hydride and sodium borohydride gave 3,4-dihydro and 1,2,3,4- tetrahydroquinazoline. The reduction of 3-methyl-4(3*H*)-quinazolinone with lithium aluminium hydride (LiAIH4) in benzene give 2-Hydro-3-methyl- 4(1*H*)-quinazolinone (Figure 7) (Akbari *et al.,* 2013).

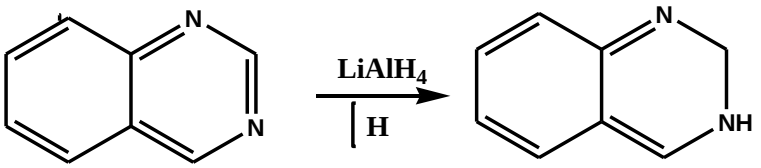

Figure 7: Reduction of Quinazoline

Nitration

It was observed that on boiling with nitric acid 4(3H)-Quinazolinone give 6-nitro-4 (3*H*)-quinazolinone (Figure 8) by substitution. It was also found that on further nitration, the second nitro group enters the 8-position to provide 6,8-dinitro derivatives. It is reported that under such conditions 2-substituted-4(3*H*)-quinazolinones were also behave similarly (Akbari *et al.,* 2013).

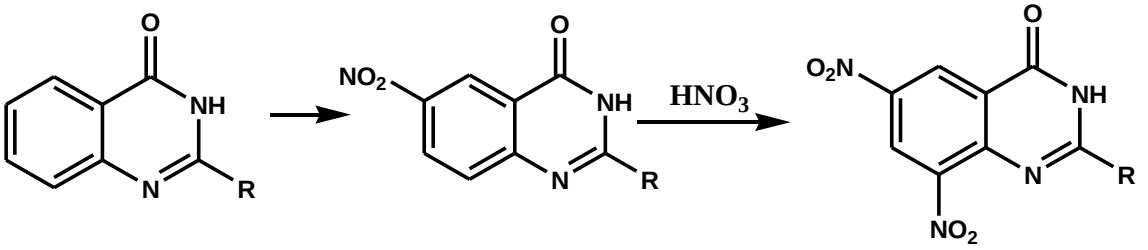

Figure 8: Nitration of Quinazolonone

IV. Methods of synthesis of 4-(3H) Quinazolinones

Most of the methods used for the synthesis of 4-(3H)-quinazolinones make use of anthranilic acid or one of their functional derivatives as the preparatory materials. Pharmacologically, quinazoline particularly quinazolin-4-one or quinazolinone are among the most important classes of heterocyclic compounds. Quinazolin-4-one is synthesized when the keto group is introduced in the pyrimidine ring of quinazoline. Based on this factor, the general methods of synthesis are listed as follows:

(a) Condensation of anthranilic acid with acid amides

A simple and easy conversion to 4-(3*H*) quinazolinones can be achieved when anthranilic acid is heated in an open container with excess of formamide at 120 °C. In this reaction, water is removed and proceeds via an o-amidobenzamide intermediate (Scheme 1) (Armarego, 1963). Commonly, this method is known as Niementowski synthesis. Howerever, Besson et al modified Niementowski synthesis to improve the yields and reaction time by using microwave irradiation techniques (He *et al.*, 2014).

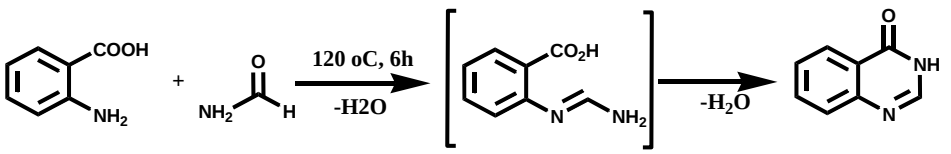

Scheme I: The Niementowski reaction

(b) Condensation of acetanilides with urethanes

Another effective conversion is to condense a urethane derivative with aniline to give 4-(3*H*) quinazolinone. 2-methyl-4-(3*H*) quinazolinone was synthesized by

heating of urethane and acetanilide for 3 hours with phosphorus pentoxide in toluene (Scheme 2). Quinazolinones may also be synthesized directly from the corresponding N-acylanthranilic acid by heating with ammonia or substituted amines. 2-methyl-3-alkyl-6- nitro- 4-(3H) quinazolinones prepared from N-acyl-5-nitroanthranilic acid and a variety of primary amines (Armarego, 1963).

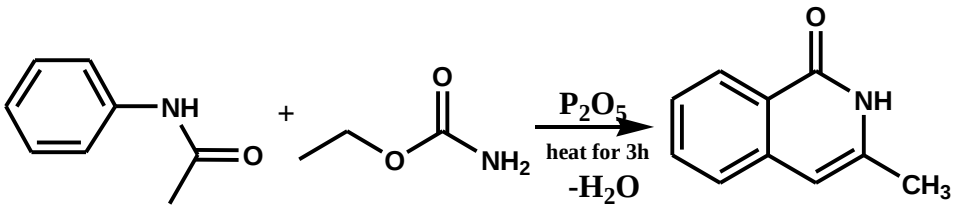

Scheme II: Synthesis of 2-methyl-4-(3H) quinazolinone

(c) Condensation of N-acylanthranilic acids with primary amines

A survey of the literature suggests that 4-(3*H*) Quinazolinones may also be synthesized directly from the corresponding N-acylanthranilic acid by heating with ammonia or substituted amines (Scheme 3). Therefore, a variety of primary amines and N-acyl-5-nitroanthranilic acid were condensed to synthesize 2-methyl-3-alkyl-6-nitro- 4-(3*H*) quinazolinones in good yields (Armarego, 1963).

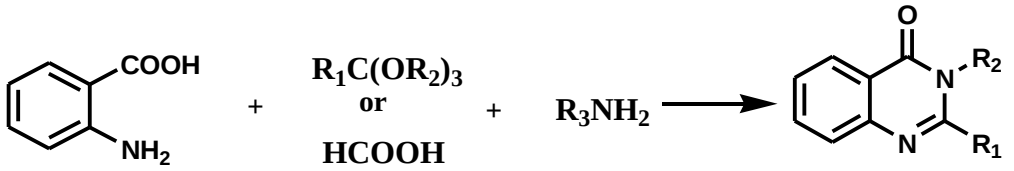

Scheme III: Condensation of anthranilic acids with primary amines

V. Biological activities of Benzoxazine and Quinazolinone

. **(a) Biological activities of benzoxazine-4-one**

The phytochemists and researchers started to take interest in benzoxazine with the first isolation of 2, 4-dihydroxy-2H-1, 4-benzoxazin-3(4H)-one (DIBOA) and 2, 4- dihydroxy-7-methoxy-(2H)-1,4-benzoxazin-3(4H)-one (DIMBOA) benzoxazine derivatives (Macias et al, 2006). This has led to the discovery of a wide variety of

compounds that are of high interest from the point of view of antimicrobial, antimycobacterial, antidiabetic and antidepressant effects among others. They possess a variety of biological effects including antitubercular (Petrlíkova, 2010) antifungal (Shirodkar *et al.,* 2000; Grover & Kini, 2006), antimalarial, anticancer, anti-HIV (Grover & Kini, 2006; Habib *et al.,* 2013; Kandale *et al.,* 2014), antiviral and antibacterial activities (Grover & Kini , 2006; Habib *et al.,* 2013; Ozden *et al.,* 2000). They also act as DNA binding agents (Sugiyama *et al.,* 1986) and HSV-1 protease inhibitors (Jarves *et al.,* 1996). A literature survey identified several benzoxazine derivatives in the development phase as potential new drugs (Siddiquia *et al.,* 2010).

The 4H-3,1-benzoxazin-4-one core is a key structural fragment in a range of biologically active compounds and led to a number of drugs (Siddiquia *et al.,* 2010). They have attracted considerable attention as inhibitors of Serine proteases. Hays et al. have screened a series of 2- substituted 4H-3,1-benzoxazin-4-ones as inhibitors of Clr serine protease of the complement system (Hays *et al.,* 1998). 4H-3,1-benzoxazin-4-ones core linked to heterocycle or heteroaryl were disclosed as Serine hydrolase inhibitors. They were also found to be potent elastase inhibitor (Colson *et al.,* 2005; Oshida *et al.,* 1992).

5-Methyl-4H-3,1-benzoxazin-4-one derivatives are accomplished as specific inhibitors of Human Leukocyte Elastase (HLE), where they showed strong and highly specific inhibition of Human Sputum Elastase (HSE), which is equivalent to HLE (Hsieh, 2005). 4H-3,1-benzoxazin-4-one derivatives are accomplished as specific inhibitors of Human Leukocyte Elastase (Stein *et al.,* 1987; Krantz *et al.,* 1990; Uejima *et al.,* 1993; Arcadi *et al.,* 1999; Hsieh, 2005). Moreover, 2-substituted-4H-3,1-benzoxazin-4-one derivatives showed good cytotoxic activity (Pavlidis & Perrya, 1994). A series of 4H-3,1-benzoxazin-4-ones with different aromatic substitution pattern were evaluated as HIV-1 Reverse transcriptase inhibitors (Patel *et al.,* 1999). 2-Aryl-substituted 4H-3,1-benzoxazin-4-ones act as novel active substances for the cardiovscular system (Rose, 1991). The benzoxazine derivatives also showed anti-convulsant activity (Hays *et al.,* 1998).

Moreover, some 2-substituted 4H-3,1-benzoxazin-4-ones are also found to lower the levels of cholesterol and triglycerides in plasma, and to raise the proportion of total cholsterol carried by high-density lipoproteins (Fenton *et al.,* 1989).

The importance of these 4H-3,1-benzoxazin-4-one also resides in that, these compounds are useful precursors for the preparation of other pharmaceutically active heterocyclic compounds, mainly quinazoline derivatives (Baumann *et al.,* 2013). Extensive structure activity relationship studies suggest that the entire quinazolinon structure was required, but activity was further enhanced by halides or small hydrophobic substituents at position-6 (Jiang *et al.,* 1990). Particularly, hetero substituents and chemically active functional groups on C-2 position affect their reactivity and reaction rate. Thus, one of the most important features in (4H)-3,1-benzoxazinones chemistry is their use as key starting materials for further transformations in design and synthesis of biologically active compound (Nikpour *et al.,* 2014).

(b) Biological importance of Quinazolin-4(3H)-ones

The stability of the quinazolinone nucleus has inspired medicinal chemists to introduce many bioactive moieties to this nucleus to synthesize new potential medicinal agents. The quinazolinone skeleton is a frequently encountered heterocycle in medicinal chemistry literature with applications including antibacterial, analgesic, anti-inflammatory, antifungal, antimalarial, antihypertensive , CNS depressant, anticonvulsant, antihistaminic, antiparkinsonism, antiviral and anticancer activities (Cao *et al.,* 2005; Giri *et al.,* 2009; Helby *et al.,* 2003; Kadi *et al.,* 2006; Jatav *et al.,* 2008; Xia *et al.,* 2001; Jessy *et al.,* 2007; Alagarsamy *et al.,* 2006; Asif , 2014). However, few quinazolinones were reported for treatment of tuberculosis e.g 3-aryl-6,8-dichloro-2H-1,3-benzoxazine-2,4(3*H*)-diones and 3-arylquinazoline-2,4(1H,3H)-diones are reported as anti-mycobacterial agents (Mahto *et al.,* 2011). In the last few decades quinazoline heterocycles got much importance due to their wide range of biological properties.

Antileishmanial agents

Chauhan and co-workers reported four novel series of quinazolinone hybrids bearing interesting bioactive scaffolds (pyrimidine, triazine, tetrazole, and peptide). Most of the synthesized analogues exhibited potent leishmanicidal activity against intracellular amastigotes (Chauhan *et al.,* 2013). The SAR analysis revealed that among the synthesized quinazolinone hybrids, quinazolinone pyrimidine, triazine, and ferrocene containing quinazolinone peptide displayed potent antileishmanial activity (Sharma & Ravani, 2013).

Anticonvulsant agents

Gupta and co-workers (Gupta *et al.,* 2013) reported a new series of 2-phenyl-3- (3-(substituted-benzylideneamino))-quinazolin-4(3*H*)-one derivatives and screened for their anticonvulsant activity against standard models MES (maximal electroshock seizure test) for their ability to reduce seizure spread. Zheng and co-workers (Zheng *et al.,* 2013) described the syntheses and anticonvulsant activity of 5-phenyl[1,2,4]triazolo[4,3-c] quinazolin-3-amine derivatives. El-Azab and co-workers (El-Azab *et al.,* 2013) designed and synthesized a new series of quinazoline analogues and evaluated for their anticonvulsant activity. Khan and Malik (Malik & Khan, 2014) reported a new synthesis of quinazolin-4(3H)-one substituted 1H and 2H-tetrazole derivatives and evaluated for anticonvulsant screening based on the NIH anticonvulsant drug development (ADD) program protocol. Zayed and co-workers (Zayed & Hassan, 2014) synthesized some novel derivatives of 6,8-diiodo-2-methyl-3-substituted-quinazolin-4(3H)-ones and evaluated for their anticonvulsant activity by the maximal electroshock-induced seizure and subcutaneous pentylenetetrazole tests. The neurotoxicity was assessed using rotarod test. All the tested compounds showed considerable anticonvulsant activity in at least one of the anticonvulsant tests.

Antiinflammatory agents

Hussain (Hussain, 2013) reported the synthesis of 2,3-dihydro-2-(3,4-dihydroxyphenyl) pyrazolo [5,1-b] quinazolin-9(1*H*)-one and tested for their anti-inflammatory activity. Eweas and co-workers (Eweas *et al.,* 2013) designed and synthesized some novel 2-pyridyl (3H)-quinazolin-4-one derivatives and evaluated for

their anti-inflammatory activity. All the tested compounds showed good anti-inflammatory activity. Saravanan and co-workers (Alagarsamy & Saravanan, 2013) synthesized a new series of novel quinazolin-4(3H)-one derivatives and tested for their anti-inflammatory activity. A series of novel 2-(2,4-disubstituted-thiazole-5-yl)-3- aryl-3H-quinazoline-4-one derivatives which became good inhibitors of NFκB and AP-1 mediated transcription activation (Giri *et al.,* 2009). Zayed and Hassan synthesized some novel 6,8-diiodo-2-methyl-3-substituted-quinazolin-4(3H)-ones bearing sulfonamide derivatives and evaluated for their anti-inflammatory activity by carrageenan-induced hind paw edema test using ibuprofen as a standard drug. Among the screened compounds, aliphatic side chain bearing compounds were found to be more active than those with aromatic ones (Zayed *et al.,* 2014).

Antitumor Activity

Quinazoline scaffold resembles both the purine nucleus as well as the pteridine one. As a consequence, some compounds which are able to inhibit the purinic (Dempcy & Skibo, 1991) or the folic acid (Martin *et al.,* 1947; Davoll & Johnson, 1970; Oatis and Hynes, 1977; Scanlon *et al.,* 1979) metabolic pathways were discovered. Structure modification of folic acid has also led to the discovery of a number of antifolates as efficient anticancer agents (Nzila, 2006). In an effort to look for the possible non-classical antifolates acting as antitumor agents, Cao *et al*. (2005) incorporated the dithiocarbamate moiety with 4(3H)-quinazolinone. Thus, a series of 4(3H)-quinazolinone derivatives with dithiocarbamate side chains were synthesized and tested for their *in vitro* antitumor activity against human myelogenous leukemia K562 cells by MTT (3-(4,5-dimethylthiazol-2-yl) -2,5- diphenyl-tetrazolium bromide) assay. Among them, few exhibited significant inhibitory activity against K562cells with IC_{50} value of 0.5 μM (Cao *et al.,* 2005).

Antimicrobial Activity

It is well documented that 4-(3H)-Quinazolinones with 3-substitution are associated with antimicrobial properties (Nagarajan *et al.,* 2010). The 3-substitution which was reported, bridged phenyl rings, heterocyclic rings and aliphatic systems. It was also reported that hydrazine derived Schiff's bases have potential antibacterial activity. In our previous study, we have synthesized 3-(Arylideneamino)-2-

phenylquinazoline-4(3*H*)-ones by placinng two potential bio-active sites, a quinazolone moiety as well as a Schiff base in the system to increase biological activity. The compounds were found to inhibit the growth of both Gram-positive (*Staphylococcus aureus* 6571 and *Bacillus subtilis*) and Gram-negative bacteria (*Escherichia coli* K12 and *Shigella dysenteriae*). We have proposed the promising effect of such compounds against Multiple Antibiotic Resistant Gram-negative enteric bacteria could lead to the development of new drugs (Nanda *et al.,* 2007). Recently, Bouley *et al.,* (2015), have discovered E)-3-(3-carboxyphenyl)-2- (4-cyanostyryl)quinazolin-4(3*H*)-one as an antibiotic effective in vivo against methicillin-resistant *Staphylococcus aureus* (MRSA). They also found that this antibiotic damage cell-wall biosynthesis by binding penicillin-binding protein (PBP). They proposed this as a promise antibiotic in fighting MRSA infections.

A new series of novel 2-methyl-3-(1’3’4-thiadiazol-2-yl)-4-(3*H*) quinazoline was synthesised by reacting 2-amino-5-aryl/alkyl-1’3’4’-thiadiazoyl with 2-substituted benzoxazin-2-one (Jatav *et al.,* 2008). These compounds possessed antibacterial activity on *Staphylococcus aureus, Bacillus subtilis* and *Escherichia coli*. Antifungal activity was screened against *Candida albicans, Aspergillus niger* and *Curvularia lunata*. Moreover, synthesized compounds showed both antibacterial and antifungal activity.

VI. Quinazoline-4(3H)-ones drugs available in market

The limitation of the drug agents is not only the rapidly emergence of drug resistance but also the drug side effects. This fact creates a crisis in the usage of antimicrobial drugs. The unsatisfactory status of the present drugs has forced scientists to develop new antibacterial agents having broad antimicrobial spectrum. Moreover, in the present scenario, it has become imperative to resolve the setback of emergence of microbial resistance towards conventional antimicrobial agents and also to minimize the side effects of existing drugs.

It is well known that quinazolinone skeleton containing drugs have been considered as very important class of therapeutic agents; hence large number of quinazoline compounds were synthesized and evaluated for their different biological activities. This rapid development indicates that there will be more quinazoline

derivatives in clinical trials in the near future. These compounds are likely to surpass the available organic based pharmaceuticals in the very near future. The first renowned quinazoline marketed drug – Methaqualone is used for its sedative–hypnotic effects since 1951 (Mhaske & Argade ,2006). Presently, a large number of quinazoline derivates are patented and available in market as potential drug for various diseases. The following table lists out a few marketed quinazolinone drugs used for treatment of various diseases (Table 2).

Table 2- Some marketed available drugs contain quinazolinone moiety

S.no	Drug	IUPAC Name	Activity	References
1	Afloqualone	6-amino- 2(fluoomethyl)- 3-(2-methylphenyl) quinazolin- 4-one	Sedative, Hypnotic, Anticancer, Anti-Anxiety Agents	Ochiai and Ishida , 1982; Chen et al, 2006
2	Albaconazole	7-chloro-3-[(2R,3R)- 3-(2,4-difluorophenyl)-3-hydroxy-4-(1,2,4-triazol- 1-yl)butan-2-yl]quinazolin-4-one	Antifungal	Sorbera et al, 2003
3	Balaglitazone	5-[[4- [(3,4-dihydro-3-methyl-4-oxo-2-quinazolinyl) methoxy]phenyl]methyl]-2,4-thiazolidinedione	Peroxisome proliferator-activated receptor (PPAR) gamma agonist , Antidiabetic	Henriksen et al, 2009; Henriksen et al, 2011
4	Cloroqualone	3-(2,6-Dichlorophenyl)-2-ethyl-4-quinazolinone	Sedative	Ochiai and Ishida , 1982; Chen et al, 2006
5	Diproqualone	3-(2,3-dihydroxypropyl)-2-methyl-quinazolin-4-one	Analgesic, Antihistamine, Rheumatoid Arthritis	Audeval et al, 1988; Chen et al, 2006
6	Etaqualone	3-(2-ethylphenyl)-2-methyl-quinazolin-4-one	Sedative, Hypnotic	Parmar et al, 1969
7	Fluproquazone	4-(4-fluorophenyl)-7-methyl-1-propan-2-ylquinazolin- 2-one	Antipyretic activity, NSAID	Mohing et al, 1981; Wheatley, 1982

8	Halofuginone	7-Bromo-6 chloro-3-[3-[(2S,3R)-3-hydroxy-2-piperidinyl]-2-oxopropyl]-4-quinazolinone	Antitumor, Autoimmune disorders	Sundrud et al, 2009
9	Isaindigotone	3-[(3,5-dimethoxy-4-oxocyclohexa-2,5-dien-1-ylidene)methyl]-2,4-dihydro-1H-pyrrolo[2,1-b]quinazolin-9-one	Acetylcholinesterase and butyrylcholinesterase	Tan et al, 2009
10	Ispinesib	N-(3-aminopropyl)-N-[(1R)-1-[7-chloro-3,4-dihydro-4-oxo-3-(phenylmethyl)-2-quinazolinyl]-2-methylpropyl]-4-methyl-benzamide	Anticancer	Blagden et al, 2008
11	Methaqualone	2-methyl-3-o-tolyl-4(3H)-quinazolinone	Hypnotic	Smith et al, 1973
12	Nolatrexed	2-Amino-6-methyl-5- (4-pyridylthio)-1H-quinazolin-4-one	Thymidylate synthase inhibitor, Anticancer	Andy et al, 2012
13	Piriqualone	3-(2-methylphenyl)-2-[(E)-2-pyridin-2-ylethenyl]quinazolin-4-one	Anticonvulsant	Koe et al, 1986
14	Quinethazone	7-chloro-2-ethyl-4-oxo-1,2,3,4-tetrahydroquinazoline-6-sulfonamide	Antihypertensive	Cohen et al, 1960
15	Raltitrexed	*N*-[(5-{methyl[(2-methyl-4-oxo-1,4-dihydroquinazolin-6-yl)methyl]amino}-2-thienyl)carbonyl]-L-glutamic acid	Anticancer	Wideman et al, 1999
16	Tempostatin	7-bromo-6-chloro-3-[3-[(2R,3S)-3-hydroxy-2-piperidyl]-2-oxo-propyl]quinazolin-4-one	inhibiting the deposition of collagen	Asif, 2014
17	Tiacrilast	(E)-3-[6-(Methylthio)-4-oxoquinazolin-3(4H)-yl]propenoic acid	Antiallergic	Welton et al, 1986
18	Rutaecarpine	8,13-Dihydroindolo[2',3':3,4]pyrido[2,1-b]quinazolin-5(7H)-one	Alzheimer's disease	Decker, 2005
19	Proquazone	1-Isopropyl-7-methyl-4-phenyl-2(1H)-quinazolinone	non-steroidal anti-inflammatory potential	Mohri, 2001

20	Fluproquazone	4-(4-Fluorophenyl)-1-isopropyl-7-methyl-2(1H)-quinazolinone	non-steroidal anti-inflammatory potential	Mohri, 2001
21	Diproqualone	3-(2,3-dihydroxypropyl)-2-methyl-quinazolin-4-one	analgesic effects	Mohri, 2001

In addition to all these, the other quinazoline marketed drugs are Gefitinib, Erlotinib, Trimetrexate, Vandetanib, Evodiamine, Dacomitinib, Barasertib, Cediranib, Elinogrel, Letermovir, Milciclib, Sotrastaurin, Tandutinib, Varlitinib etc (Selvan & Kumar, 2011).

Chapter 1

Synthesis of 2-substituted-benzo[d][1,3]oxazin-4-ones and Quinazoline-4(3H)-ones

Chapter 1

Synthesis of 2-substituted-benzo[d][1,3]oxazin-4-ones and Quinazoline-4(3H)-ones

1.1 General Remarks:

The commercially available aldehydes, ketones, acyl chlorides and amines needed for ligand synthesis were used without further purification and were procured from Merck. Other reagents were purchased from the companies Across, Sigma-Aldrich, Merck and Thomas Baker. ^{1}H and spectra were recorded on a *Bruker Avance* 300 spectrophotometer (300MHz). C NMR spectra were recorded on a *Bruker Avance* 300 spectrometer (75 MHz) Chemical shifts were quoted in parts per million (ppm) referenced to the appropriate solvent peak or 0.0 ppm for tetramethylsilane. Coupling patterns are described by the following abbreviations: s (singlet), d (doublet), t (triplet), q (quarter), m (multiplet). Solvents are specified in each case. The NMR peak assignments have been done by using TOCSY, COSY, HSQC and HMBC. The electrospray mass spectra were recorded on a MICROMASS QUATTRO II triple quadruple mass spectrometer. The ESI capillary was set at 3.5 kV and cone voltage was 40 V. The DART-MS was recorded on a JEOL-AccuTOF JMS-T100LC Mass spectrometer. Dry Helium was used with 4 LPM flow rate for ionization at 350 ^{o}C. Infrared spectra were recorded on a FTIR-8300 SHIMADZU spectrophotometer in the 4000-400 cm^{-1} region as KBr pellets. Only characteristics absorption bands are reported. Absorptions are given in wave number (cm^{-1}); abbreviations: s= strong, m= medium, w= weak, b= broad. UV/VIS spectra were taken on a JASCO V-530 UV/VIS spectrophotometer. A thermostatic controlled water bath was attached to the spectrophotometer to carry out temperature dependent spectra. DSC studies were carried out in the 30-230^{o}C temperature range at a heating range of 5^{o}C per min on a Perkin Elmer Pyris D6 Differential Scanning Calorimeter. The phase contrast microscopic images were carried out in OLYMPUS CK – 40. The curve fitting for the studies were done using ORIGIN 6.1, owned by

Department of Physics, North Bengal University. Quantum mechanical calculations have been carried out on a Desk Top PC with an intel Pentium IV Core 2 Duo processor. The semi empirical program package MOPAC 2000 (Fujitsu) program, in Chem 3D Ultra 8.0 Graphic interface under CambridgeSoft software Chem Office 3D Ultra 8.0 Graphic interface under CsmbridgeSoft software Chem Office Ultra 2004 was used for visualization. For each compound, computations were carried out with the PM3 method. The semi-empirical (MOPAC) method for the quantum mechanical calculations was. The molecular structures obtained in this were used in a configurational interaction calculation to compute dipole moments, bond orders, and electronic transition energy.

1.2. General Synthetic Procedures and Analytical Data:

1.2.1 General procedure for the synthesis of 2-substituted-benzo[d] [1, 3] oxazin-4-ones (1a-1d)

The synthesis of 2-substituted-benzo[d] [1, 3] oxazin-4-ones was carried out by following the previous reported methods. (Niementowski, 1895; Bain & Smalley, 1968).

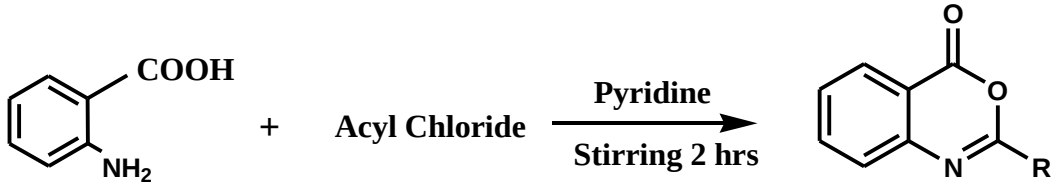

Scheme 1.1: 2-Substituted benzo[d] [1, 3] oxazin-4-ones.[R=phenyl(1a); p-Me-phenyl(1b); p-Cl-phenyl(1c); methyl(1d)]

1.2.1.1 Synthesis of 2-phenyl benzo[d] [1, 3] oxazin-4-one (1a).

A mixture of anthranilic acid (2-aminobenzoic acid) MW- 113.14 (0.03 mole i.e 4.01g) and benzoyl chloride (0.06 mole, 8.4 g) was dissolved in pyridine (60 ml). The mixture was stirred for 2 hours with occasional cooling. The mixture was diluted with water (300ml) when light brown solid separates out. It was filtered and washed. The product was dried and recrystallized from ethanol.

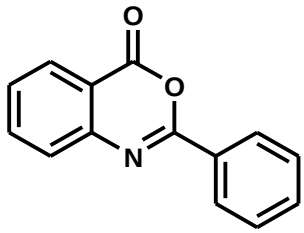

(1)

Yield 78%; Light Yellow solid; m.p. 120^{o}C

Anal. Calcd for ($C_{14}H_9NO_2$): C, 75.33; H, 4.06; N, 6.27. Found: C, 75.86; H, 4.23; N, 6.02

^{1}HNMR (300 MHz, $CDCl_3$): δ 8.33 (5-H); δ 8.31 (7-H); δ 7.84 (8-H); δ 7.72 (6-H); δ 7.56 (2'-H); δ 7.51 (3'-H); δ 7.26 (4'-H).

^{13}CNMR (300 MHz, $CDCl_3$): 158.78 (C-4); 156.35 (C-2); 146.20 (C-8b); 136.79 (C-7); 132.65 (C-5); 129.98 (C-4'); 128.93 (C-1'); 128.52 (C-2'); 127.99 (C-3'); 127.74 (C-6); 126.85 (C-8); and 116.86 (C-5a).

m/z found for ($C_{14}H_9NO_2$): 224(M+1), 246 (M+Na), 469 (2M+Na).

1.2.1.2 Synthesis of 2-p-tolyl-benzo[d] [1, 3] oxazin-4-one (1b).

The toulic acid MW- 136.15 (0.11 mole) was taken in a round bottom flask and thionyl chloride was added in a less amount to dissolve the toulic acid. During the addition of thionyl chloride, HCl fumes released. When the fumes became less, the solution was heated until it dissolved. Following dissolution, the solution was refluxed for 30 minutes at low temperatures because at high temperature solution churns to brown colour. After reflux, the excess solvent was distilled out and the remaining liquid tolyl chloride in round flask was collected.

The stirred solution of anthranilic acid (0.11mole) in pyridine (60ml), tolyl chloride was added dropwise, maintaining the temperature near 0-5 ^{o}C for 1 hour. The reaction mixture was stirred for another 2h at room temperature until a solid product was

formed. The reaction mixture was neutralized with $NaHCO_3$ solution and the pale yellow solid, which separated, was filtered. Finally the product was recrystallized from ethanol after washing with water

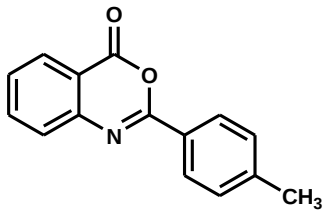

(2)

Yield 82%; Light Yellow solid; m.p. 152.7^{o}C

Anal. Calcd for ($C_{15}H_{11}NO_2$): C, 75.94; H, 4.67; N, 5.90. Found: C, 75.36; H, 4.84; N, 5.54

^{1}HNMR (300 MHz, $CDCl_3$): δ 8.25 (5-H); δ 8.19 (7-H); δ 7.85 (8-H); δ 7.79 (6-H); δ 7.69 & δ 7.52 (2'-Hs); δ 7.33 & δ 7.26 (3'-Hs); δ 2.45 (CH_3);

^{13}CNMR (300 MHz, $CDCl_3$): 159.71 (C-4); 157.37 (C-2); 147.16 (C-8b); 143.44 (C-4'); 136.53 (C-7); 129.53 (C-5); 128.59 (C-3'); 128.35 (C-2'); 128.02 (C-6); 127.46 (C-1'); 127.10 (C-8); 116.96 (C-5a) and 21.70 (CH_3).

m/z found for $C_{15}H_{11}NO_2$: 238(M+1), 260 (M+Na), 497 (2M+Na).

1.2.1.3 Synthesis of 2-p-chlorophenyl-benzo[d] [1, 3] oxazin-4-one (1c).

The thionyl chloride was added in a less amount to p-chlorobenzoic acid MW-156.56 (0.11 mole). The p-chlorobenzoic acid was dissolved in thionyl chloride after heating. The solution was then refluxed for 30 minutes at low temperatures. The excess solvent was distilled out after reflux and the remaining liquid p-chloro benzoyl chloride was collected. The stirred solution of anthranilic acid (0.11mole) in pyridine (60ml), p-chloro benzoyl chloride was added dropwise, maintaining the temperature near 0-5 ^{o}C for 1 h. The reaction mixture was stirred for another 2 hours at room temperature until a solid

product was formed. The reaction mixture was neutralized with $NaHCO_3$ solution and the pale yellow solid, which separated was filtered. Finally it was recrystallized from ethanol after washing with water.

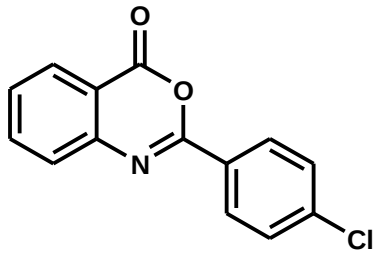

(3)

Yield 79%; Light Yellow solid; m.p.- 188.8^{o}C

Anal. Calcd for ($C_{14}H_8ClNO_2$): C, 65.26; H, 3.13; N, 5.44. Found: C, 65.73; H, 3.89; N, 5.03

^{1}HNMR (300 MHz, $CDCl_3$): δ 8.20 (5-H); δ 8.18 (7-H); δ 8.15 (8-H); δ 7.96 (6-H); δ 7.74 & δ 7.70 (2'-Hs); δ 7.66 (3'-H) & δ 7.64 (3'-Hs);

^{13}CNMR (300 MHz, $CDCl_3$): 158.61 (C-4); 155.51 (C-2); 146.02 (C-8b); 137.47 (C-4'); 136.83 (C-7); 129.50 (C-3'); 129.11 (C-2'); 128.91 (C-1'); 128.69 (C-5); 128.02 (C-6); 126.86 (C-8) and 116.90(C-5a).

m/z found for ($C_{14}H_8ClNO_2$): 258 (M+1), 280 (M+Na), 537 (2M+Na).

1.2.1.4 Synthesis of 2-methyl benzo[d] [1, 3] oxazin-4-one (1d)

A solution of anthranilic acid and acetic anhydride (1mole in 0.5L) was refluxed for 2hrs. The excess solvent was removed by distillation. The residual brown gummy slurry when subjected to vacuum distillation in the range of 120^{o}C-130^{o}C at about 8mmHg pressure; the slurry melted and white needle shaped crystals are deposited throughout the condenser and the receiving flask. Yield was about 85%.The solid was recrystallized from dry hexane as long white dense needle. In a separate batch of

preparation it was resublimed in vacuum to get the needle shaped crystals (m.p- 81.9^{o}C, lit mp-81-82^{o}C).

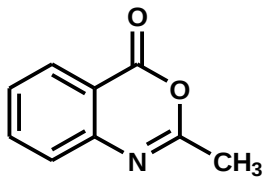

(4)

Yield 84%; White solid; m.p.- 81.9^{o}C

Anal. Calcd for ($C_9H_7NO_2$): C, 67.07; H, 4.38; N, 8.69. Found: C, 67.56; H, 3.98; N, 8.33.

^{1}HNMR (300 MHz, $CDCl_3$): δ 8.73 (5-H); δ 8.12 (7-H); δ 7.60 (8-H); δ 7.14 (6-H); δ 2.27(CH_3);

^{13}CNMR (300 MHz, $CDCl_3$): 171.47 (C-2); 169.43 (C-4); 142.04 (C-8b); 135.64 (C-7); 131.72 (C-5); 122.73 (C-6); 120.53 (C-8); 113.78 (C-5a) and 25.52 (-CH_3).

m/z found for ($C_9H_7NO_2$): 160(M), 161(M+1), 162(M+2), 180(M+H_2O+H^+), 359(2M+2H_2O+H^+).

1.2.2 Synthesis of 3-amino-2-phenyl-quinazoline-4(3H)-one (2a):

To an ethanolic solution of 2-phenyl-3,1-benzoxazin-4-(3H)-one (1gm, 4.22 mmole), hydrazine hydrate 98% (1.5ml) was added and the mixture was heated in a water bath for about 3 hours. The flask containing the reaction mixture was cooled and the solid thus formed was filtered and washed with water. The air dried product was recrystallized from ethanol. Purity of the compound was checked by TLC using benzene and ethyl acetate as mobile phase in ratio of 7:3.

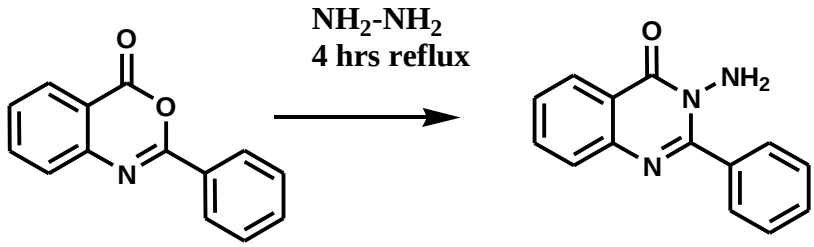

Scheme 1.2: Synthesis of 3-amino-2-phenyl-quinazoline-4(3H)-one

Yield 76%; Brownish Yellow solid; m.p.- 220 °C;

Anal. Calcd for ($C_{20}H_{16}N_2O_4$): C, 68.96; H, 4.63; N, 8.04. Found: C, 68.44; H, 4.92; N, 7.89.

^{1}HNMR (300 MHz, $CDCl_3$): δ 8.73 (5-H); δ 8.12 (7-H); δ 7.60 (8-H); δ 7.14 (6-H); δ 2.27(CH_3);

^{13}CNMR (300 MHz, $CDCl_3$): 171.47 (C-2); 169.43 (C-4); 142.04 (C-8b); 135.64 (C-7); 131.72 (C-5); 122.73 (C-6); 120.53 (C-8); 113.78 (C-5a) and 25.52 (-CH_3).

IR (KBr, cm^{-1}): 2944, 1760, 1750, 1645, 1605, 1472, 1464, 1320, and 1008

m/z found for ($C_{20}H_{16}N_2O_4$): 349(M+1), 350(M+2), 407(M+2H_2O+Na).

1.2.3 Synthesis of 3-(Arylideneamino)-2-phenylquinazoline-4(3*H*)-ones (3a-j):

A mixture of 3-amino-2-phenylquinazolin-4(3H)-one (0.01 mole), appropriate aromatic aldehyde (0.01 mole) and ethanol (20 mL) was refluxed for 4-6 hours. The resulting mixture was cooled and poured into ice water. The separated solid was filtered, washed with water and recrystallized from ethanol.

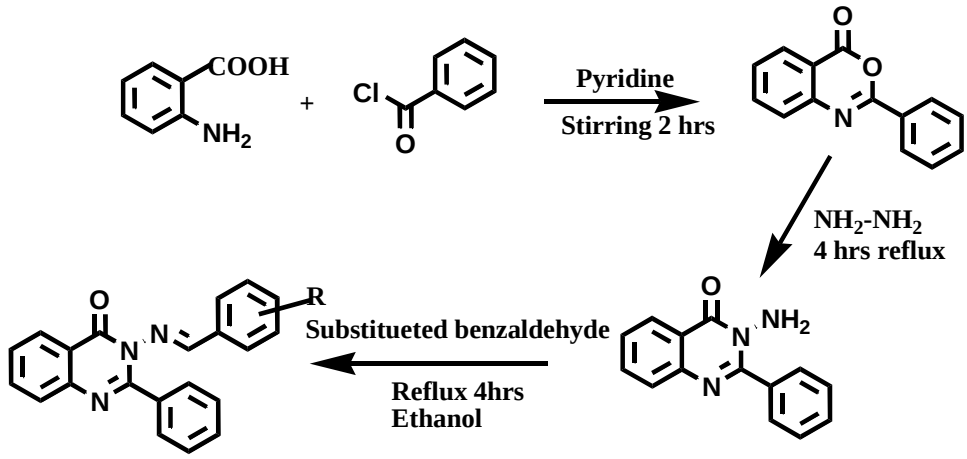

Scheme 1.3: Synthesis of the 3-(Arylideneamino)-2-phenylquinazoline-4(3H)-ones

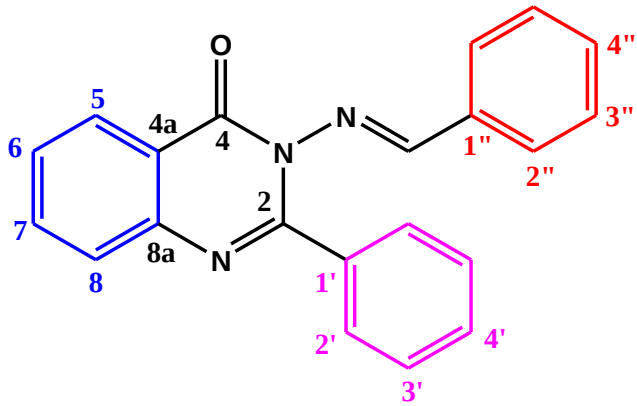

3-(Arylideneamino)-2-phenylquinazoline-4(3H)-one

(5)

3-{[(2-Hydroxyphenyl)methylene]amino}-2-phenylquinazolin-4(3H)-one **(3a)**

Yield 76%; mp- 144 ^{o}C; R_f 0.77;

^{1}**H-NMR:** 6.69 (H- 5”), 6.9 (H-3”), 7.35 (H-4”), 7.35 (H-6”), 7.4 (H-4’), 7.48 (H-3’), 7.56 (H-6), 7.6 (H-8), 7.6 (H-7), 7.81 (H-2’), 8.36 (H-5), 9.19 (s, 1H, H-C=N), 9.99 (OH, H-bonded), 7.8 Hz (J_{56});

^{13}**C-NMR:** 116.42 (C-1”), 117.50 (C-3’’), 119.69 (C-5”), 121.46 (C-4a), 127.32 (C-8), 127.39 (C-6), 128.00 (C-2’),128.97 (C-5), 130.34 (C-3’), 132.5 (C-6”), 133.33 (C-4’), 134.19 (C-4”), 134.84 (C-7), 146.37 (C-8a), 153.63 (C-2), 159.14 (C-4), 159.74 (=C(OH)-, C-2”), 164.75 (H-C=N), C-1’ quaternary peak not observed;

IR (KBr, cm^{-1}) : 3200-3100, 1681.8, 1604.7, 1467.7;

m/z found for ($C_{21}H_{15}N_3O_2$): 342 (M+1);

Anal. Calcd. for $C_{21}H_{15}N_3O_2$: C, 73.89%; H, 4.45%; N, 12.31%; found: C, 74.10%; H, 4.45%; N, 12.28%.

3-{[(4-Methoxyphenyl)methylene]amino}-2-phenylquinazolin-4(3H)-one **(3b)**

Yield 75%; m.p. 140°C; R_f 0.75;

^{1}HNMR: 3.84 (s, 3H, methoxy protons), 7.37 (H-3'/ H-4'), 7.40 (H-3"), 7.46 (H-8), 7.53 (H-6), 7.78 (H- 2"), 7.80 (H-7), 7.84 (H-2'), 8.36 (H-5), 8.87 (1H, s, H-C=N-N);

^{13}C-NMR: 55.40 (-O-CH_3), 114.34 (C-3"), 121.48 (C-4a), 125.89 (C-1"), 126.90 (C-8), 127.26 (C-2'), 127.70 (C-6), 127.88 (C-5), 129.89 (C-2"), 129.90 (C-4'), 130.75 (C-3'), 134.39 (C-7), 134.67 (C-1'), 146.50 (C-8a), 159.40 (C-4), 163.08 (=C(OCH_3)-,C-4"), 164.0 (C-2), 166.55 (H-C=N);

m/z found for ($C_{22}H_{17}N_3O_2$): 356(M+1)

IR (KBr, cm^{-1}): 1679.9, 1602.7, 1448.4, 1494.7, 1257.5, 1170.7

Anal. Calcd. for $C_{22}H_{17}N_3O_2$: C, 74.35%, H, 4.82%, N, 11.82%; found: C, 74.40%, H, 4.90%, N, 11.78%.

3-{[(4-Fluorophenyl)methylene]amino}-2-phenylquinazolin-4(3H)-one **(3c)**

Yield 68%; m.p. 166°C; R_f0.73;

^{1}H-NMR: 7.1 (H-4"), 7.41 (H-3'), 7.45 (H-4'), 7.49 (H-6), 7.53 (H-8), 7.54 (H-2"), 7.7 (H- 2'), 7.8 (H-7), 8.3 (H-5), 9.04 (s, 1H, H-C=N); 7.8 Hz (J_{56}), 0.9 Hz (J_{57}), 0Hz (J_{58}), 6.3 Hz (J_{67}), 1.8 Hz (J_{68}), 8.7 Hz ($J_{2"3"}$);

^{13}C-NMR: 166.30 (=C(F)-, C-4"), 164.84 (H-C=N), 153.97 (C-4), 153.90 (C-2), 146.60 (C-8a), 134.55 (C-1'), 134.15 (C-7), 131.00 (C-2"), 130.89 (C-4'), 130.50 (C-1"), 129.30 (C- 2'), 128.98 (C-3'), 127.68 (C-6), 127.20 (C-5), 126.79 (C-8), 121.50 (C-4a), 116.33 (C-3");

m/z found for *($C_{21}H_{14}N_3OF$):* 344(M+1);

IR (KBr, cm^{-1}): 1674.1, 1614.3, 1593.1, 1554.5, 1537.2, 1469.7, 1373.2, 1184.2;

Anal. Calcd. for $C_{21}H_{14}N_3OF$: C, 73.46%, H, 4.11%, N, 12.24%; found: C, 73.50%, H, 4.10%, N, 12.18%.

3-{[4-Dimethylaminophenyl)methylene]amino}-2-phenylquinazolin-4(3H)-one **(3d)**

Yield 70%; m.p. 178°C; R_f 0.8;

^{1}H-NMR: 3.04 (-N-CH_3), 6.66 (H-3"), 7.40 (H-3' and H-4'), 7.58 (H-6 and H-2"), 7.79 (H-8 and H-2'), 7.80 (H-7), 8.36 (H-5), 8.67 (s, 1H. H-C=N); 8.7 Hz (J_{56}), 0.9 Hz (J_{57}), 0 Hz (J_{58}), 7.5 Hz (J_{67}), 9.0 Hz ($J_{2"3"}$);

^{13}C-NMR: 187.65 (H-C=N), 159.80 (C-4), 154.07 (C-2), 153.06 (=C($N(CH_3)_2$), C-4"), 146.66 (C-8a), 134.80 (C-1'), 134.15 (C-7), 130.72 (C-2"), 129.70 (C-4'), 129.30 (C-2'), 127.89 (C-3'), 127.68 (C-3), 127.20 (C-5), 126.79 (C-8), 121.58 (C-1"), 120.30 (C-4a), 111.52 (C-3"), 40.13 (-N-CH3);

IR (KBr, cm^{-1}): 1681.8, 1589.2, 1556.4, 1508.2, 1456.2, 1375.2, 1328.9, 1313.4;

m/z found for (*$C_{23}H_{20}N_4O$*): 344(M+1)

Anal. Calcd. for C23H20N4O: C, 74.98%, H, 5.47%, N, 15.2%; found: C, 74.99%, H, 5.50%, N, 15.13%.

3-{[4-Chloroyphenyl)methylene]amino}-2-phenylquinazolin-4(3H)-one **(3e)**

Yield 72%; m.p. 162°C; R_f 0.81;

^{1}H-NMR: 7.37 (H-3'), 7.42 (H-4'), 7.49 (H-6), 7.53 (H-8), 7.54 (H-3"), 7.68 (H-2"), 7.80 (H-7), 7.82 (H-2'), 8.36 (H-5), 9.10 (s, 1H, H-C=N);

^{13}C-NMR: 121.47 (C-4a), 127.16 (C-8), 127.33 (C-2'), 127.88 (C-6), 127.93 (C-5), 129.24 (C-3'), 129.77 (C-3"), 129.92 (C-4'), 130.00 (C-2"), 131.36 (C-1"), 134.36 (C-1"), 134.78 (C 7), 138.46 (=C(Cl)-, C-4"), 146.47 (C-8a), 154.00 (C-2), 159.22 (C-4), 164.40 (H-C=N);

IR (KBr, cm^{-1}): 1679.9, 1591.2, 1554.5, 1377.1;

m/z found for (*$C_{21}H_{14}N_3OCl$*): 360(M+1);

Anal. Calcd. for $C_{21}H_{14}N_3OCl$: C, 70.10%; H, 3.92%; N, 11.68%; found: C, 70.20%; H, 4.10%; N, 11.62%.

3-{[3-Methoxyphenyl)methylene]amino}-2-phenylquinazolin-4(3H)-one **(3f)**

Yield 75%; m.p. 134°C; Rf 0.67;

Anal. Calcd. for $C_{22}H_{17}N_3O_2$: C, 74.35%; H, 4.28%; N, 11.82%; found: C, 74.45%; H, 4.35%; N, 11.78%.

^{1}HNMR: 3.74 (s, 3H, methoxy protons), 7.30 (H-4"), 7.40 (H-2"), 7.43 (H-3'), 7.45 (H-4'), 7.55 (H-5"/ H-6"), 7.62 (H-6), 7.69 (H-8), 7.72 (H-7), 7.82 (H-2'), 8.37 (H-5), 9.09 (s, 1H, H-C=N-N);
^{13}C-NMR: 111.74 (C-2"), 119.15 (C-4"), 121.56 (C-4a), 121.76 (C-6"), 122.33 (C-8), 127.08 (C-6), 127.31 (C- 5), 127.87 (C-2'), 128.17 (C-5"), 128.18 (C-3'), 129.84 (C-4'), 134.22 (C-1'), 134.51 (C-7), 134.88 (C-1"), 146.51 (C-8a), 154.13 (C-2), 159.27 (C-4), 159.86 (=C(OCH3), C-3"), 165.52 (H-C=N);
IR (KBr, cm^{-1}): 1679.9, 1575.7, 1465.8, 1367.4, 1317.3, 1276.8;
m/z found for ($C_{22}H_{17}N_3O_2$): 356(M+1);

3-{[(4-Hydroxyphenyl)methylene]amino}-2-phenylquinazolin-4(3H)-one **(3g)**
Yield 76%; m.p. 167°C; Rf 0.63;
Anal. Calcd. For $C_{21}H_{15}N_3O_2$: C, 73.89%; H, 4.43%; N, 12.31%; found: C, 73.99%; H, 4.49%; N, 12.30%.
^{1}H-NMR: 5.03 (-OH), 7.42 (H-3"/H-5"), 7.50 (H-3'/H-4'), 7.52 (H-6), 7.68 (H-2"/H-6"), 7.78 (H-7), 7.80 (H-8), 7.82 (H-2'), 8.29 (m, H-5), 9.16 (s, 1H, H-C=N-N);
^{13}C-NMR: 110.00 (C- 3"), 120.10 (C-4a), 126.61 (C-8), 127.08 (C-6), 127.79 (C-5), 128.20 (C-2'), 129.28 (C-3'), 130.29 (C-4'), 133.94 (C-2"), 134.50 (C-7), 134.52 (C-1"), 143.12 (C-8a), 149.00 (C-2), 149.88 (-CH=N-), 155.00 (C-4), 161.54 (=C(OH)-, C-4"), C-1' quaternary peak not observed;
IR (KBr, cm^{-1}): 3307.7, 3213.2, 1668.2, 1645.2, 1604.7, 1554.5, 1375.2, 1338.5;
m/z found for ($C_{21}H_{15}N_3O_2$) : 342(M+1)

3-{[(4-Hydroxy-3-methoxyphenyl)methylene]amino}-2-phenylquinazolin-4(3H)-one **(3h).** Yield 74%; m.p. 155°C; Rf 0.62;
Anal. Calcd. for $C_{22}H_{17}N_3O_3$: C, 71.15%; H, 4.61%; N, 11.31%; found: C, 71.25%; H, 4.65%; N, 11.26%.

^{1}H-NMR: 3.81 (s, 3H, methoxy protons), 5.03 (-OH), 6.92 (H-5"), 7.20 (H- 2"), 7.32 (H-6"), 7.50 (H-3'/H-4'), 7.52 (H-6), 7.76 (H-7), 7.78 (H-8), 7.83 (H-2'), 8.3 (m, H-5), 8.90 (s,1H, H-C=N-N);

^{13}C-NMR: 55.95 (-O-CH3), 108.67 (C-2"), 114.46 (C-5"), 125.40 (C-6"), 126.40 (C-4a), 126.63 (C-8), 127.08 (C-1"), 127.27 (C-2'), 127.77 (C-6), 128.20 (C-5), 129.31 (C-1'), 129.93 (C-3'), 130.32 (C-4'), 134.50 (C-7), 143.23 (C-8a), 146.72 (=C(OH)-, C-4"), 147.28 (=C(OCH3)-, C- 3"), 154.40 (C-4), 159.82 (-CH=N-);

IR (KBr, cm^{-1}): 3305.8, 3215.1, 1749.3, 1712.7, 1664.5, 1575.7, 1467.7, 1377.1;

m/z found for ($C_{22}H_{17}N_3O_3$): 372 (M+1);

***3-{[(3-Nitrophenyl)methylene]amino}-2-phenylquinazolin-4(3H)-one* (3i).**

Yield 78%; m.p. 248°C; Rf 0.53;

Anal. Calcd. for $C_{21}H_{14}N_4O_3$: C, 68.10%; H, 3.84%; N, 15.15%; found: C, 68.15%; H, 3.81%; N, 15.13%

^{1}H-NMR ($CDCl_3$ + DMSO-d6): 7.22 (H-7), 7.30 (H-3'), 7.62 (H-6), 7.63 (H-4'/ H-4"), 7.9 (H-8), 8.02 (H-2'), 8.26 (H- 5"/ H-6"), 8.54 (H-5), 9.58 (H-2"), 8.59 (s, 1H, H-C=N);

^{13}C-NMR ($CDCl_3$ + DMSO-d6): 118.29 (C- 4a), 120.65 (C-4"), 122.30 (C-8), 122.33 (C-2"), 126.90 (C-5"), 127.27 (C-5), 127.97 (C-6"), 128.17 (C-2'), 128.28 (C-6), 130.00 (C-7), 131.50 (C-3'), 132.40 (C-4'), 133.47 (C-1"), 134.09 (=C(NO3)-, C- 3"), 139.82 (C-8a), 161.65 (-CH=N-), 164.88 (C-2), 165.50 (C-4), C-1' quaternary peak not observed;

IR (KBr, cm^{-1}): 1674.1, 1641.3, 1500, 1456.2, 1344.3;

m/z found for *($C_{21}H_{14}N_4O_3$)* : 371(M+1);

***3-{[(Pheny)lmethylene]amino}-2-phenylquinazolin-4(3H)-one* (3j)**

Yield 80%; m.p. 196°C; R_f 0.68;

Anal. Calcd. for $C_{21}H_{15}N_3O$: C, 77.52%; H, 4.65%; N, 12.91%; found: C, 77.54%; H, 4.71%; N, 12.85%.

^{1}H-NMR ($CDCl_3$ + DMSO-d6): 6.98 (H-7), 7.40 (H-3'), 7.41 (H-4'), 7.45 (H-6), 7.49 (H-3"), 7.55 (H-4"), 7.67 (H-8), 7.81 (H-2'), 8.05 (H-2"), 8.47 (s, 1H, H-C=N), 8.62 (H-5);

^{13}C-NMR ($CDCl_3$ + DMSO-d_6): 119.83 (C- 4a), 121.62 (C-5), 122.82 (C-2"), 127.47 (C-2'), 127.72 (C-6), 127.84 (C-8), 128.66 (C-3'), 128.82 (C- 3"), 130.62 (C-4"), 132.10 (C-4'), 132.72 (C-7), 133.65 (C-1'), 134.31 (C-1"), 139.79 (C-8a), 149.98 (-CH=N-), 165.77 (C-4), 166.03 (C-2);

IR (KBr, cm^{-1}): 1662.52, 1647.1, 1645.2, 1556.4, 1454.2;

m/z found for ($C_{21}H_{15}N_3O$): 326(M+1);

Chapter 2

Characterization of dimers of 2-substituted-benzo[d][1,3]oxazin-4-ones

Chapter 2

Characterization of dimers of 2-substituted-benzo[d][1,3]oxazin-4-ones

2.1 Introduction

The study of inter molecular interaction is a frontier topic because of its prolific role in a wide variety of chemical and biological phenomena (Karger *et al.*, 1999). This intermolecular interaction plays important roles in the biological activities possessed by medicinally important compounds. One such interaction, the hydrogen bonding, gives rise to the hydrogen bonded molecular assemblies is the major building blocks of supramolecules. The hydrogen bond represents one of the modern frontiers of scientific venture because of its role in the structure stabilizing, or even structure-directing role. The hydrogen bonded structures are studied in various disciplines of science including self-organized and biologically relevant molecules. The hydrogen bond is a unique phenomenon in structural chemistry and biology (Desiraju & Steiner, 2001). In spite of various studies, the role of hydrogen bond in structure stabilizing is yet not fully explored. Here, a brief review of hydrogen bond is presented to understand its arrangement and importance.

2.1.1 Definition of hydrogen bond

The term "Hydrogen bond" was brought into the mainstream by Pauling (1939). Pauling's definition of a hydrogen bond is that '*Under certain conditions, an atom of hydrogen is attracted by rather strong forces to two atoms instead*". It is clear from this definition that the strength of the hydrogen bond depends upon the relative electro negativity of the donor and acceptor atoms (Pauling, 1939).

In 1960, Pimentel and McClellan further refined the definition of hydrogen bond like this- " *A hydrogen bond is said to exist when (1) there is evidence of a bond, and (2)*

there is evidence that this bond specifically involves a hydrogen atom already bonded to another atom" (Pimente & McClellan, 1960). It is indeed surprising than that most authors felt the need for a universal definition of 'hydrogen bond'. However IUPAC defines it as follows: The hydrogen bond is an attractive interaction between a hydrogen atom from a molecule or a molecular fragment X–H in which X is more electronegative than H, and an atom or a group of atoms in the same or a different molecule, in which there is evidence of bond formation (Arunan *et al.*, 2011).

2.1.2 Type of hydrogen bond

The O-H and N-H groups are considered as the most general proton donor groups that form strong hydrogen bonds. Similarly, the most conventional proton acceptors are the O-atom and the N-atom. The C-H group acts as a proton donor even though the polarity of C-H group is apparently less than that of O-H and N-H groups (Bonchev & Cremaschi, 1974). The capacity of *n* electronic clouds of -OC- bonds and aromatic rings to act as hydrogen bond acceptors was recognized (Levitt & Perutz, 1988).

Although the strength of a hydrogen bond is not as big as a covalent bond, it is able to control a molecular ensemble due to its directionality and cooperative effects. Jeffrey and Saenger (1991) (Jeffrey & Saenger, 1991) has classified hydrogen bond as "strong" and "weak". According to Desiraju, hydrogen bonds that are able to control crystal and supramolecular structure effectively are stronger e.g. O-H-O=C, N-H-O=C and O-H-O-H, while weak hydrogen bond has variable influence on crystal structure and packing (Desiraju & Steiner, 2001). The type of interactions mentioned elaborately involves *conventional* hydrogen bonds such as O-H...O and N-H...O, that are in contact, where the acceptor and donor atoms are electronegative. Fascinatingly, researchers at present emphasizes on another sort of hydrogen bonds where the donor is an atom with low or moderate electronegativity, and which possess strength weaker than that observed in *conventional* hydrogen bonds (Desiraju & Steiner, 1999).

Many of the evidences of these *weak* hydrogen bonds can be found in biomolecules, organic molecules, organometallic compounds and inclusion complexes; and many were characterized with the aid of several diffraction methods. Particular cases of such interactions are the C-H...O and the C-H...N hydrogen bonds, where the acceptor

atom can be oxygen or nitrogen, and the donor is the carbon atom. The role of such interaction on the structural stabilization in molecular systems is still unclear and also a debatable issue. Yet, the number of such studies exploring the importance of this interaction is increasing with time.

2.1.3 C-H-O interaction

In 1937, C–H···O interaction was first hinted by Samuel Glasstone. He established the concept of C–H···O interactions in mixtures of acetone with different halogenated derivatives of hydrocarbons. Though C-H- O hydrogen bond is well-established in structural chemistry and physical organic chemistry but existence of a C-H...O interaction itself is still debated amongst the authors. Over the past decade the concept of supramolecular chemistry was envisaged as an 'emergent phenomena'. (Stoddart, 2009). The fact remains that most of the studies are limited to the systems in which hydrogen is attached to some hetero-atom. The importance of newer motifs for molecular assemblies framed with much weaker hydrogen bonded systems like C-H---O=C H-bond hitherto remained largely unexplored. Sutor (Sutor, 1963) and Ramachandran (Ramachandran *et al.,* 1963) believed that these interactions contribute significantly to crystal stability and Sutor proposed the existence of this type of hydrogen bond in the early 1960s. Today many crystallographers and structural chemists accept that these interactions are of significance. A landmark study was done by Taylor and Kennard in 1982 (Taylor & Kennard, 1982), providing conclusive evidence about the existence of C-H-0 hydrogen bonds in crystals. Subsequently, G. R. Desiraju asserts in his published text as- 'It certainly is'. (Desiraju, 1991; Desiraju, 2002). Since then, several articles were published on this type of hydrogen bonded system; but the subsistence of such H-bonds in solution state still remained in the probing stage of - 'may be' because of the inherent feebler nature compared to other H-bonds.

Although C-H-O interactions are much weaker than the conventional O-H- O bonds, it is now well established that it plays an important role in a wide variety of chemical and biochemical phenomena. The energy of C-H-O hydrogen bonds rarely exceeds 8 kJ mol^{-1} while it significantly contributes in crystal packing and

supramolecular design (Desiraju, 1996; Steiner 1997). Interestingly, in past decade, literatures have suggested that C-H-O hydrogen bonds are also key interacting bonds in the structure and activity of biological systems. The occurrence of C-H-O hydrogen bonds was also reported in the active sites of enzymes such as serine hydrolases (Derewenda *et al.,* 1994) and kinase inhibitors (Talylor & Kennard, 1982). Despite the intrinsic weakness in strength, these types of bonds are being recognized to have certain roles in many aspects of chemistry and biology (Harumi & yukihiro, 2005). Formation of aryl -CH---O hydrogen bond in certain kind of Kinase inhibition studies is established in crystal structure of protein complex of pyrazol-3-quinazolin-4-ylamine (Pierce *et al.,* 2005).

Additionally, theoretical methods also used to estimate the binding energies of these non-conventional hydrogen bonds. Theoretical studies proved that this is a very important stabilizing force in some systems (Louit *et al.,* 2002; Ruiz *et al.,* 2004; Graza *et al.,* 2005; Navarrete-lopez *et al.,* 2007). Previous authors estimated the strength (2.1 kcal/mol) of the C-H interaction, with the C=O group in four conformers of the *N,N*-dimethylformamide dimer in approximately 2.1 kcal/mol (Vargas *et al.,* 2000). They have also reported that by using a linear correlation between C-H...O bond energies and gas-phase proton affinities, the ΔH for the C-H...O=C hydrogen bond in around 3.0 kcal/mol, about 2.3 kcal/mol less than the N-H...O=C hydrogen bond strength. This fact reveals that the C-H...O=C hydrogen bonds involved in proteins are strong enough to play an important role in the stabilization of secondary and ternary structure of these systems (Ramírez *et al.,* 2008). Although most of the experimental results reported refer to the crystalline state, what remains yet to be known or established are the small molecular assemblies with C-H---O bonds which can exist in protic solvents as well. Though it is reported that cooperative interactions of the weak forces enhances the stability of the molecular assembly (Prins *et al.,* 2001). It is a general chemical intuition that this zipper effect should be insufficient to stabilize the system particularly in water or methanol solution.

2.2 Materials and methods

The curve fitting for the studies were done using ORIGIN 6.1, owned by Department of Physics, North Bengal University. Quantum mechanical calculations were carried out on a Desk Top PC with an intel Pentium IV Core 2 Duo processor. The semi empirical program package MOPAC 2000 (Fujitsu) program, in Chem 3D Ultra 8.0 Graphic interface under CambridgeSoft software Chem Office 3D Ultra 8.0 Graphic interface under CsmbridgeSoft software Chem Office Ultra 2004 was used for visualization. For each compound, computations were carried out with the PM3 method. The semi-empirical (MOPAC) method for the quantum mechanical calculations was. The molecular structures obtained in this were used in a configurational interaction calculation to compute dipole moments, bond orders, and electronic transition energy.

The other spectroscopic methods were written in the Chapter-1.

2.3 Results and Discussion

2.3.1 UV-spectrometric study:

The absorption spectra of the 2-substituted-bezo[d][1,3]oxazin-4-one were observed in the range of 250-400 nm in various solvents, the corresponding λ_{max} with molar extinction coefficients are tabulated in the in the Table 2.1. A typical UV-spectral graph in different concentrations is shown in the Figure 2.1 the peaks with higher intensity in the range of wave lengths 250 nm to 270 nm were for π-π^* transitions and the peaks of lower intensity in the range of 270 nm to 340 nm were due to n- π^* transitions. It is apparent from the graph that with increasing concentrations there was a shift of λ_{max} values to higher wave length which is more prominent in the 250 nm to 270 nm range but not so prominent in the peaks at 270 nm to 340 nm range which originated due to forbidden n- π^* transition. Another interesting point is that the spectra have an explicit isosbestic point 340 nm. The occurrence of the isosbestic point signifies that the substance under study is converted to another that has very close molar absorption

Table 2.1- UV-spectrometric study of the compound 1a, 1b, 1c and 1d.

Compound(s)	Solvent(s)	Lambda max (nm) (λ_{max})	Molar Extinction coefficients
1a	Water + 35% methanol	232 265 307	20443 11182 6955
	n-octanol	215 239.5 290.5 317	20505.5 20406.5 16700.2 11598
1b	Water +35% methanol	237.5 267.5 306.5	18282 11776 7406
	n-octanol	217.5 243.5 293.5 320	34012 26603.5 28723 21527.5
1c	Water +35% methanol	239 279	18328 11180
	n-octanol	222	31256
1d	Water + 35% ethanol	252	27374.5
	n-octanol	236	21362
1a = 2-phenylbezo[d][1,3]oxazin-4-one, 1b = 2-(4-methyphenyl)bezo[d][1,3]oxazin-4-one , 1c = 2-(4-chlorophenyl)bezo[d][1,3]oxazin-4-one, 1d = 2-methyl-4H-bezo[d][1,3]oxazin-4-one			

of UV radiations and are in equilibrium. This converted product should be a dimer as we have also seen in the DART method of Mass spectra one peak corresponded to $2M^{+}$.

The UV-spectral property was also studied in water, chloroform and toluene, wherein all the spectra indicated involvement of carbonyl in the dimer formation**.** The stock solution of all derivatives of 1 X 10^{-4} was prepared in different solvents (methanol, toluene, chloroform and water) and each solution was diluted with same solvents up to concentrations 1 X 10^{-5}. However, in case of dilution with water, the stock solution was prepared in methanol.

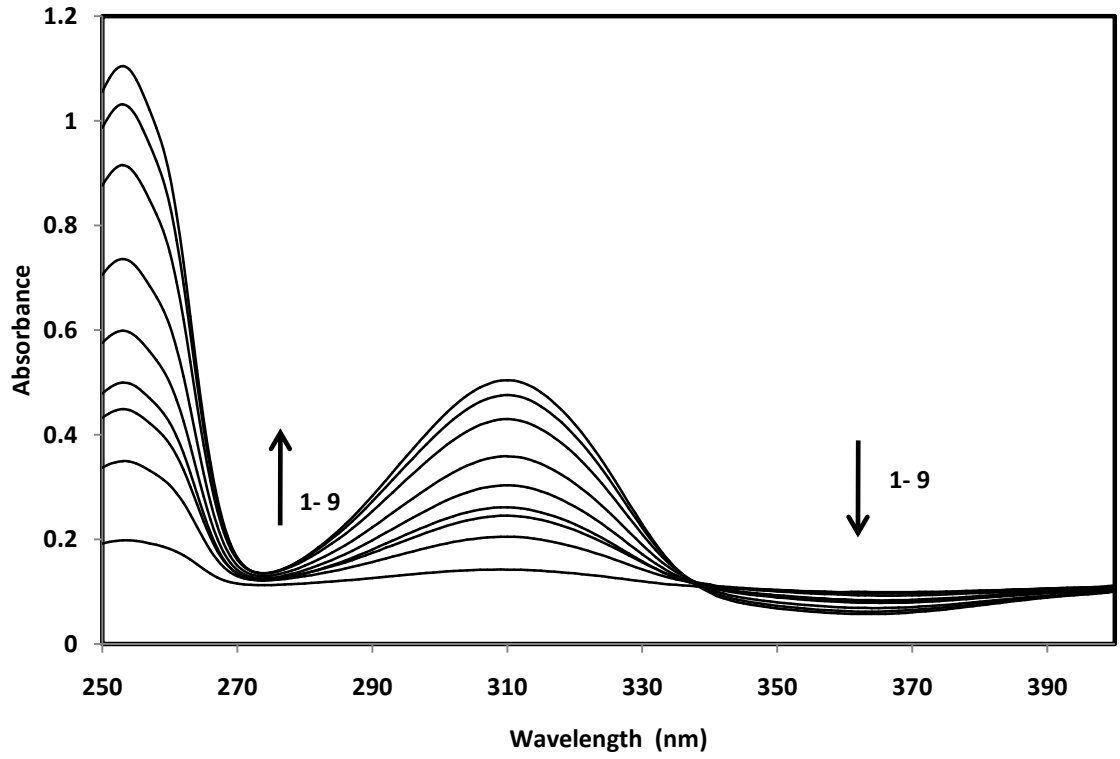

Figure 2.1: UV-spectra of compound 2-methyl-4H-bezo[d][1,3]oxazin-4-one at different molar conc. in methanol (1) 1X 10^{-5} (2) 2X 10^{-5} (3) 3X 10^{-5} (4) 4X 10^{-5} (5) 5 10^{-5} (6) 6 X 10^{-5} (7) 7 X 10^{-5} (8) 8 X 10^{-5} (9) 1X 10^{-4} .

2.3.2 Determination of the Dimerization Constant

To analyze the association feature of these compounds, we have used a simple association model in which associate constant will indicate about their association strength. The average extinction coefficients in the wavelength within 250-350 nm were plotted by various concentrations within range of 10^{-4} to 10^{-5} molar.

The dimerization constant was determined using following equations where M is monomer, [M] is molar concentrations of monomer, D is dimer, [D] is molar concentration of dimer and P is observed property (average molar extinction coefficient, OD)

$$K = \frac{[D]}{[M]^2} \qquad (1)$$

$$C = [M] + 2[D] \qquad (2)$$

$$\frac{C - M}{2} = K[M]^2$$

$$C - M = 2K[M]^2$$

$$2K[M]^2 + M - C = 0$$

$$M = \frac{-1 \pm \sqrt{1 + 8KC}}{4K}$$

$$D = \frac{4KC + 1 - \sqrt{1 + 8KC}}{2a}$$

$$P = [M]P_M + [D]P_D \qquad (3)$$

$$P = \alpha P_\alpha + \beta P_\beta \qquad (4)$$

The observed optical density OD_{obs} can be formulated by the solution of equations (1) to (3) which is given by

$$\mathrm{OD_{obs}} = OD_{[M]}.\frac{-1+\sqrt{1+8\mathrm{K_a}C}}{4\mathrm{K_a}} + OD_{[D]}.\frac{1+4\mathrm{K_a}C-\sqrt{1+8\mathrm{K_a}C}}{8\mathrm{K_a}}$$

C is the monomer concentration and [M] and [D] are calculated in terms of C because it is measurable.

The curve fitting for the studies were done using ORIGIN 6.1. The "best-fit" curve was fitted by a minimum sum of squares method to the plot of average properties against concentration C to obtain the dimerization constant (K_a) value in different solvents. Average extinction coefficients case equation (4) gave better curve-fit results. Some curve fit data along with the predicted cum observed values are presented. The dimerization constants are determined within the dilution range 10^{-5} to 10^{-4} molar in UV spectroscopic method.

UV spectra of 2-methyl-4H-bezo[d][1,3]oxazin-4-one and 2-methyl-4H-bezo[d][1,3]oxazin-4-one showing average absorbance of calculated vs. observed in different concentration in different solvents and their curve fitted graph. Some of the data used in curve fittings and the nature of the fit is shown in following Figure 2.2 and 2.3 respectively.

Diluted with water

Conc	Av OD observed	Av OD predicted
1.00E-05	0.12995	0.12724
2.00E-05	0.21845	0.21396
3.00E-05	0.27149	0.29188
5.00E-05	0.45623	0.43555
6.00E-05	0.50603	0.50382
7.00E-05	0.56088	0.57048

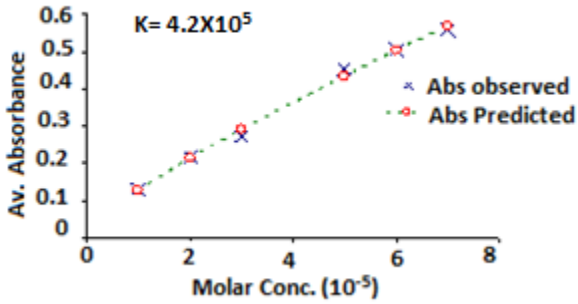

R^2 = 0.9968; K=4.2E+05

Figure 2.2 (a): UV spectra of 2-phenyl-4H-bezo[d][1,3]oxazin-4-one showing average absorbance of calculated vs. observed in different concentration in water and their curve fitted graph

Diluted with chloroform

Conc	Av OD observed	Av OD predicted
1.00E-05	0.09058	0.09299
2.00E-05	0.21808	0.21075
3.00E-05	0.35901	0.35328
4.00E-05	0.53488	0.52057
5.00E-05	0.69625	0.71265
6.00E-05	0.91008	0.92949
7.00E-05	1.15689	1.1711
8.00E-05	1.48096	1.43748
9.00E-05	1.71963	1.72863
1.00E-04	2.039	2.04456

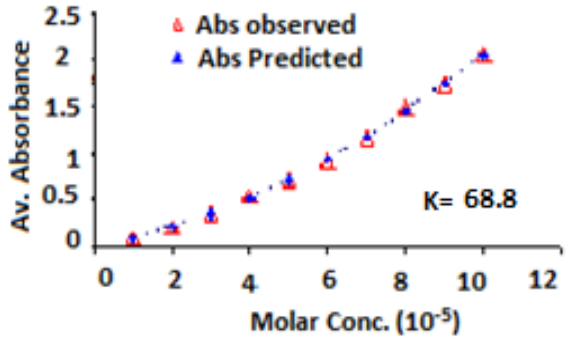

R^2 = 0.9992; k = 68.76; p = 7914.721; q =1884949.28.

Figure 2.2 (b): UV spectra of 2-phenyl-4H-bezo[d][1,3]oxazin-4-one showing average absorbance of calculated vs. observed in different concentration in chloroform and their curve fitted graph.

Diluted with methanol

Conc	Av OD observed	Av OD predicted
1.00E-05	0.09582	0.09724
2.00E-05	0.2181	0.21828
3.00E-05	0.35904	0.36128
4.00E-05	0.53487	0.52462
5.00E-05	0.69617	0.70686
6.00E-05	0.91022	0.90673

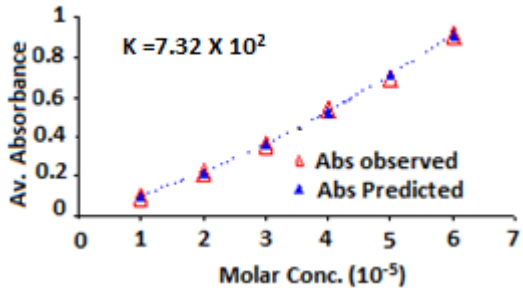

R^2 = 0.99949; k =732.52; p=8464.80; q= 193763.75.

Figure 2.2 (c): UV spectra of 2-phenyl-4H-bezo[d][1,3]oxazin-4-one showing average absorbance of calculated vs. observed in different concentration in methanol and their curve fitted graph.

Diluted with toluene

Conc	Observed Av. Ext. Coeff	Predicted Av. Ext Coeff
1.00E-05	6923.224	6809.78
2.00E-05	8418.2	
2.13E-05		8564.85
3.00E-05	9177.314	
3.25E-05		9913.74
4.00E-05	10872.38	
4.38E-05		11000.37
5.00E-05	11134.98	
5.50E-05		11904.38
6.00E-05	12765.5	
6.63E-05		12674.38
7.75E-05		13342.16
8.00E-05	14067.6	
8.88E-05		13929.59
9.00E-05	13702	
1.00E-04	14148.49	14452.36

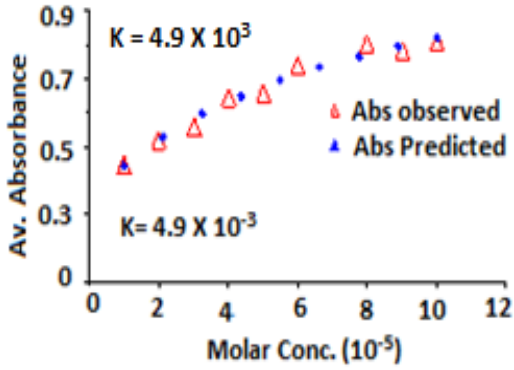

R^2 = 0.9785; k=4937.1; p= 4671;q= 60847.

Figure 2.2 (d) : UV spectra of 2-phenyl-4H-bezo[d][1,3]oxazin-4-one showing average absorbance of calculated vs. observed in different concentration in toluene and their curve fitted graph.

Diluted with water

Conc	Av ext observed/ 10E+05	Av ext predicted/ 10E+05
1 E-05	0.08389	0.0673
2 E-05	0.1231	0.12179
3 E-05	0.17196	0.17416
4 E-05	0.22468	0.22542
5 E-05	0.27	0.27599
6 E-05	0.3171	0.32605
7 E-05	0.37359	0.37574
8 E-05	0.42352	0.42512
9 E-05	0.47556	0.47426

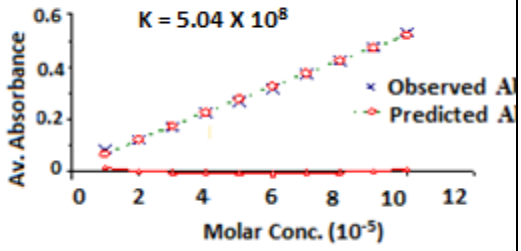

R^2= 0.99764; k=504139167.76; p=22591933780.29; q=907181796.89

Figure 2.3 (a) : UV spectra of 2-methyl-4H-bezo[d][1,3]oxazin-4-one showing average absorbance of calculated vs. observed in different concentration in water and their curve fitted graph.

Diluted with chloroform

Conc	Av Ext coeff observed	Av Ext coeff Predicted
2.00E-05	2664.74	2667.914
3.60E-05		2564.306
4.00E-05	2557.7	
5.00E-05	2495.78	
5.20E-05		2489.207
6.00E-05	2445.23	
6.80E-05		2431.055
8.00E-05	2394.25	
8.40E-05		2384.056
1.00E-04	2349.52	2344.91

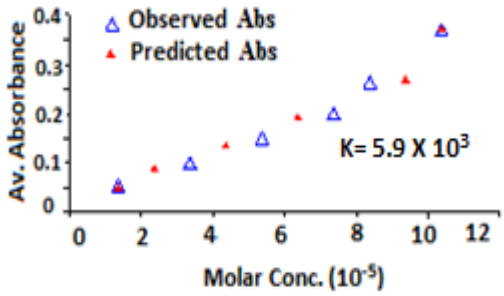

R^2= 0.99374; k=5994.74481; p= 2886.18199; q=3151.51164.

Figure 2.3 (b): UV spectra of 2-methyl-4H-bezo[d][1,3]oxazin-4-one showing average absorbance of calculated vs. observed in different concentration in chloroform and their curve fitted graph.

Diluted with methanol

Conc	Av Ext. observed	Av Ext predicted
2.00E-05	5332	5733.7
3.00E-05	7656	8280.522
4.00E-05	10232	10650.86
5.00E-05	12480	12866.09
6.00E-05	14670	14943.97
7.00E-05	17458	16899.41
8.00E-05	19152	18745.03

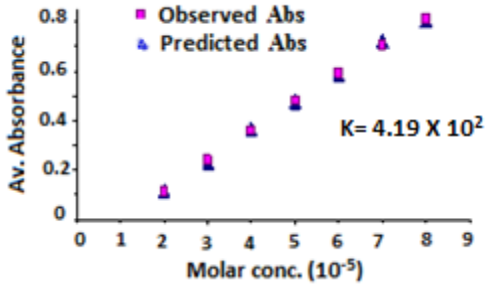

R^2= 0.9986 ; k =419.7; p=0.1; q =577707

Figure 2.3 (c): UV spectra of 2-methyl-4H-bezo[d][1,3]oxazin-4-one showing average absorbance of calculated vs. observed in different concentration in methanol and their curve fitted graph.

Diluted with toluene

Conc	Av Ext. observed	Av Ext predicted
1.00E-05	6347	6063.977
2.00E-05	7358	7434.357
3.00E-05	8772	8795.027
4.00E-05	10088	10146.12
5.00E-05	11505	11487.75
6.00E-05	12504	12820.05
7.00E-05	13979	14143.14
8.00E-05	15632	15457.13
9.00E-05	16623	16762.15
10.00E-05	18360	18058.3

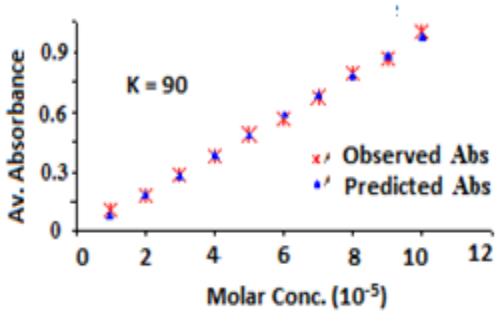

R^2 = 0.99756; k =90; p=4683.75; q=1548461.62

Figure 2.3(d) : UV spectra of 2-methyl-4H-bezo[d][1,3]oxazin-4-one showing average absorbance of calculated vs. observed in different concentration in toluene and their curve fitted graph.

Different workers have used to determine dimerization constants, assuming the only existence of dimers and monomers of the compounds in solution, the formation of the dimer is expressed by the equations $K_a = [D]/[M]^2$ (eqn-1) and $C = [M] + 2[D]$ (eqn-2) (Matsumoto *et al.,* 2003) and observed property (P) as in equation-(3); when P is expressed in mole-fraction equation-(3) is used for the determination of dimerization constant in Self-Association model (Martin, 1996).

The approximation used in mole fraction calculation in eqn (3), is the use of C with the consideration that the dimer concentration is very low and the average extinction coefficient is calculated in terms of monomer concentration, it should not impair significantly the value of dimerization constant since the existence of isosbestic point signifies comparable molar ODs for both the monomer and dimer and as a consequence the average value would not be dominated preferentially by monomer or dimer.

Table 2.2. Dimerization constants of compounds 1a, 1b, 1c and 1d in different solvents.

Compound	Methanol	Chloroform	Water	Toluene
2-phenyl-4H-bezo[d][1,3]oxazin-4-one (R=phenyl)	7.3E+02	6.8E+01	4.2E+05	4.9E+03
1b (R=p-Me-phenyl)	7.1E+05	1.0E+04	1.4E+09	-------
1c (R=p-Cl-phenyl)	1.8E+03	3.0E+03	1E+07	-------
2-methyl-4H-bezo[d][1,3]oxazin-4-one (R=methyl)	4.2E+02	5.9E+03	5.0E+08	9E+01

The changes observed in the association constants in different solvents (Table-2.2) can be attributed to the ability of the solvent to engage in hydrogen bonding which can compete with self-association and to differential solution of the different dipoles of the associated and unassociated species. It is observed that the value of dimerization constant is lesser in protic polarisable solvents like methanol and chloroform (0.1M to 1E-05M range). But in polar protic solvent water the dimerization constants are comparatively much higher. As water is the least polarizable among the solvents studied we can say that solvent polarizability has significant role in dissolving the monomer. The self-association of daunorubicin (anthracycline antibiotic) in aqueous solution was examined using visible absorption (Martin, 1980). Similarly, they have also interpreted Spectral changes in the concentration range 10^{-6} to 1.5 X 10^{-3}M in terms of a monomer-dimer equilibrium for daunorubicin and data were analyzed using a nonlinear curve-fitting technique.

2.3.3 Analysis of NMR Spectra

NMR spectroscopy is an important tool to study the weak interaction such as C-H-O in solution state. On the basis of the importance of NMR, we initiated NMR spectroscopic characterization. The spectra were taken in $CDCl_3$.The proton and carbon peaks in NMR spectra are assigned unequivocally by proton homonucler and proton

carbon heteronuclear correlation spectra. After proper assignment of all the peaks the effect of dilution on the peak positions was investigated; it is revealed that in $CDCl_3$ all the proton peaks shifts regularly to higher δ-values with dilution. The changes in chemical shift values of all the protons with dilution for 2-methyl-4H-bezo[d][1,3]oxazin-4-one is depicted in Figure 2.4.

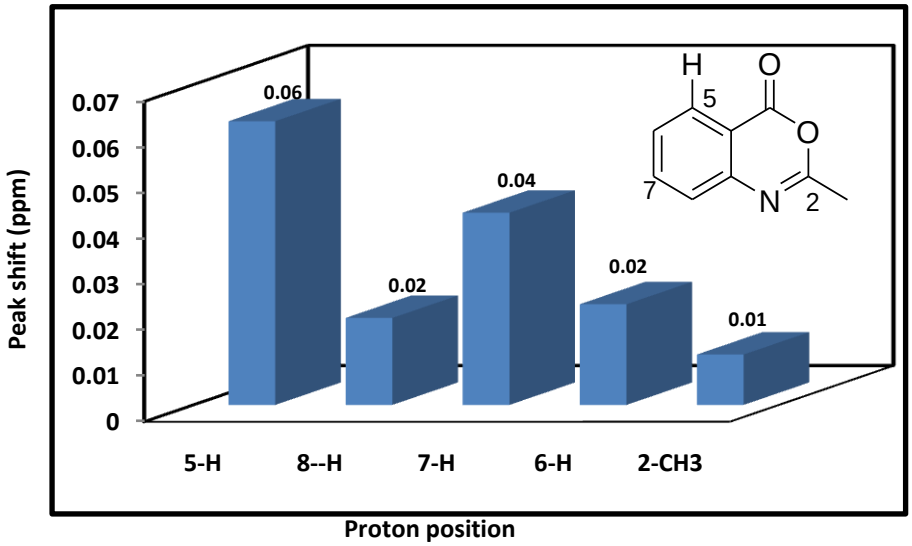

Figure. 2.4: Change of proton chemical shift within the dilution range

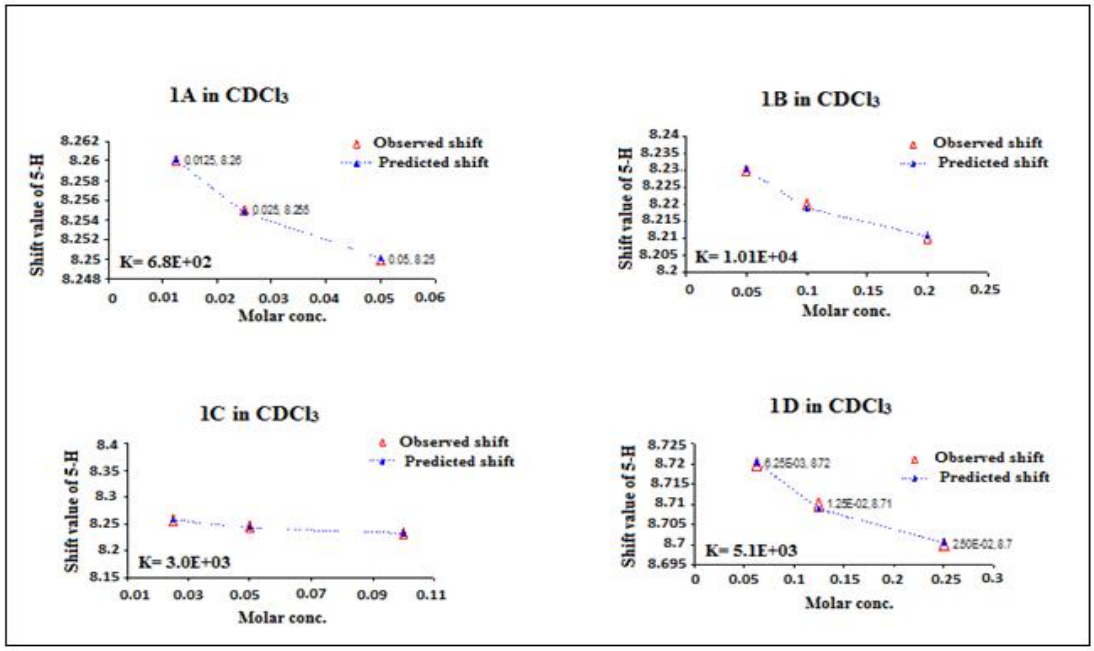

Figure 2.5: Shift of peaks at 5-H in different concentrations in 1a-1d.

Using similar equations used for the calculation of dimerizatipon constants in UV-spectra, here we also found good fit. Curves which corresponded to the values in chloroform in UV-method. Some curve fit tables are shown in Figure 2.5.

Previous author has reported the presence of unusual N-H-O hydrogen bond in benzoxazine dimer by using solid state NMR (Schnell *et al.,* 1998; Goward *et al.,* 2001). Thilagavathy *et al* (2009) recently reported that 2-phenylbenzo[d] [1, 3] oxazin-4-one is stabilized by weak intermolecular C-H---O interaction and pi-pi stacking held responsible for stabilization of the crystal packing (Thilagavathy *et al.,* 2009). So far, various studies reported the presence of weak interaction having C-H-O H-bond in solid state but in liquid it is still unanswered and need more investigation or study. Interestingly, the occurrence of C–H-O hydrogen bonds in liquids has aroused much interest recently (Jedlovszky & Turi, 1997; Yukhnevich & Tarakanova, , 1998; Gil *et al.,* 1995; Ribeiro-Claro *et al.,* 1997; Karger *et al.,* 1999; Marques *et al.,* 2001). Moreover, various authors focused on the exploring the presence of weak hydrogen bonds in dimer in solid state (Brown *et al.,* 2001; Brown & Spiess, 2001; Aliev & Kenneth, 2004). In this study we have tried to detect and explore the role of C-H-O hydrogen bond in dimer of the said moiety in solution state. Generally two of the criteria supposed to suggest presence of C-H-O hydrogen bond in compound if, the deshielding of H in HX observes in NMR and a shift toward lower field in the spectra. It is also reported that proton donating ability of a C-H bond can only be observed by 1H NMR (Dingley & Grzesiek, 1998; Pecul 2000).

After careful observation we found that proton at the ortho position i.e. H5 shows slightly high values of peak shift of 0.06, while proton at para position i.e H-7 shows peak shifts of 0.04 to the carbonyl. It was reported that downfield shift is ca 1-2 ppm in case when interaction occurs with proton acceptors in sterically favourable conditions and it becomes insignificant in case of weak interaction. The same pattern of slight peak shift was also observed in case of 4-methoxybenzaldehyde (Karger *et al.,* 1999; Marques *et al.,* 2001). Therefore, the higher value of the peak shifts may be because they are deshielded due to the pull of electron from carbony oxygen, due to salvation of monomer in $CDCl_3$. So, here we are in a position to satisfy both criteria (above mentioned) to claim

the presence of hydrogen bond. As well as, at this point we may safely say that monomer is found to be better solvated than monomer

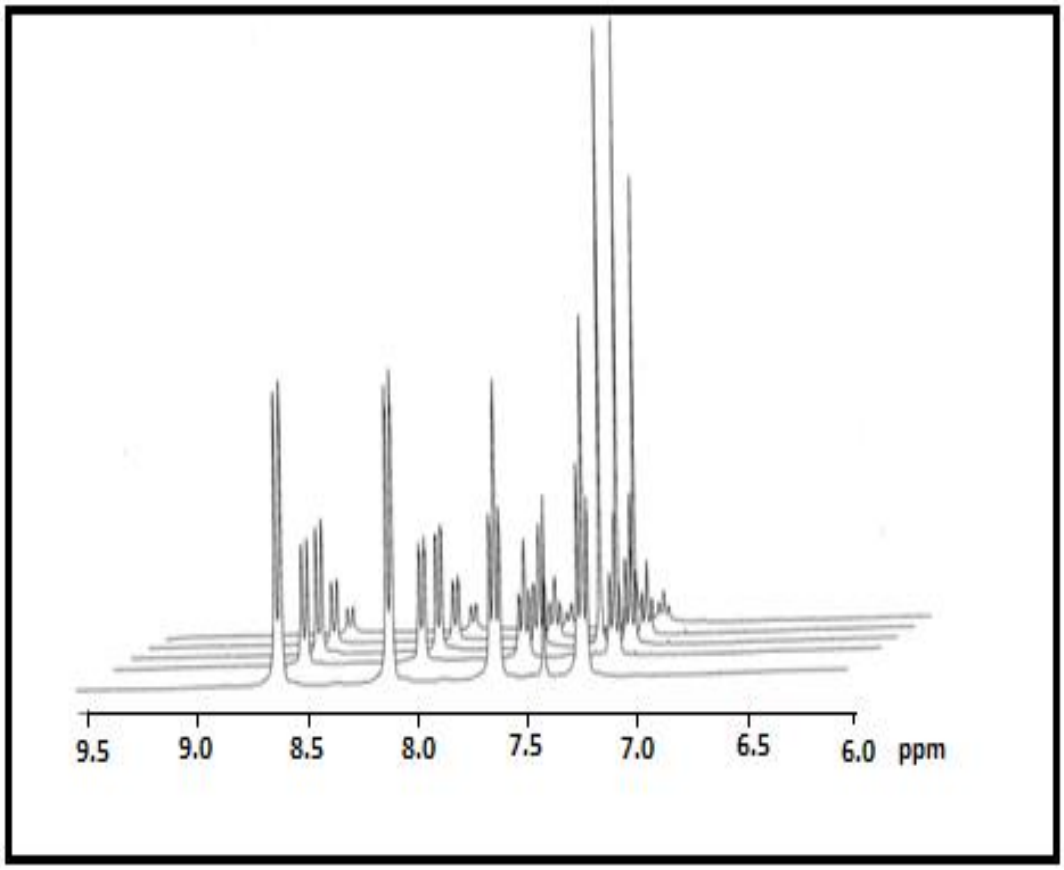

Figure 2.6: Stacked H^1-NMR of 2-methyl-4H-bezo[d][1,3]oxazin-4-one in $CDCl_3$ in different dilutions.

This spectrum also revealed that major salvation effect is observed on the carbonyl group, as seen from the NMR shift pattern of the H-5 and H-7 protons. This pattern was observed most prominent in compound 2-methyl-4H-bezo[d][1,3]oxazin-4-one which do not bear any substituted aryl group. The shift in proton peaks at different position easily seen in the stacking plot of NMR spectra of 2-methyl-4H-bezo[d][1,3]oxazin-4-one in different dilution ranges. In the other compounds 1a, 1b and 1c), the effect was masked to a certain extent for 2-aryl derivatives due to pi- electron polarization of the aromatic ring.

2.3.4 Vibrational spectral analysis

In vibrational spectral analysis we have used both the IR and Raman-spectral analysis. The analysis was supplemented by DFT as well as lower level PM3 method wherever necessary. The vibrational ranges are split into carbonyl range and aromatic proton range.

2.3.4.1 The C=O region

Evidence of the prescence of C–H---O=C hydrogen bonds in the solution phase was gathered from the observed changes in the $\nu_{C=O}$ region of the vibrational spectra with dilution. The vibrational spectral analysis of the compound 2-phenyl-4H-bezo[d][1,3]oxazin-4-one (in KBr) is reported by us; the absorption peaks at 1783 cm^{-1} (DFT) 1763 cm^{-1} (IR) and the 1757 cm^{-1} (Raman) was assigned to the $\nu_{C=O}$ stretching mode, the C(=O)-O asymmetric stretching band at 1258cm^{-1} in IR and 1259cm^{-1} in Raman and the C=N stretching band at 1692cm^{-1} in IR were also almost unequivocally assigned. The observed deviation from the calculated and observed value of the C=O stretching bands only suggested possible existence of H-bonding. A priori IR studies by Marques *et al* (2001) have shown the existence of C-H---O=C hydrogen bond in 4-ethoxybenzaldehyde where 1700cm^{-1} and 1690cm^{-1} bands were assigned to as stretching band for free HC=O and for H-bonded HC=O respectively; the increase in intensity of the free carbonyl stretching with the increase of dilution in carbon tetrachloride was reported. Similar observation was also reported by Ribeiro-Claro *et al* (1997) and Matsumoto *et al* (2003) in which the carbonyl absorption band at the higher frequency was assigned to the free carbonyl and the relative intensity of this peak increases with dilution in non hydrogen bonding solvents.

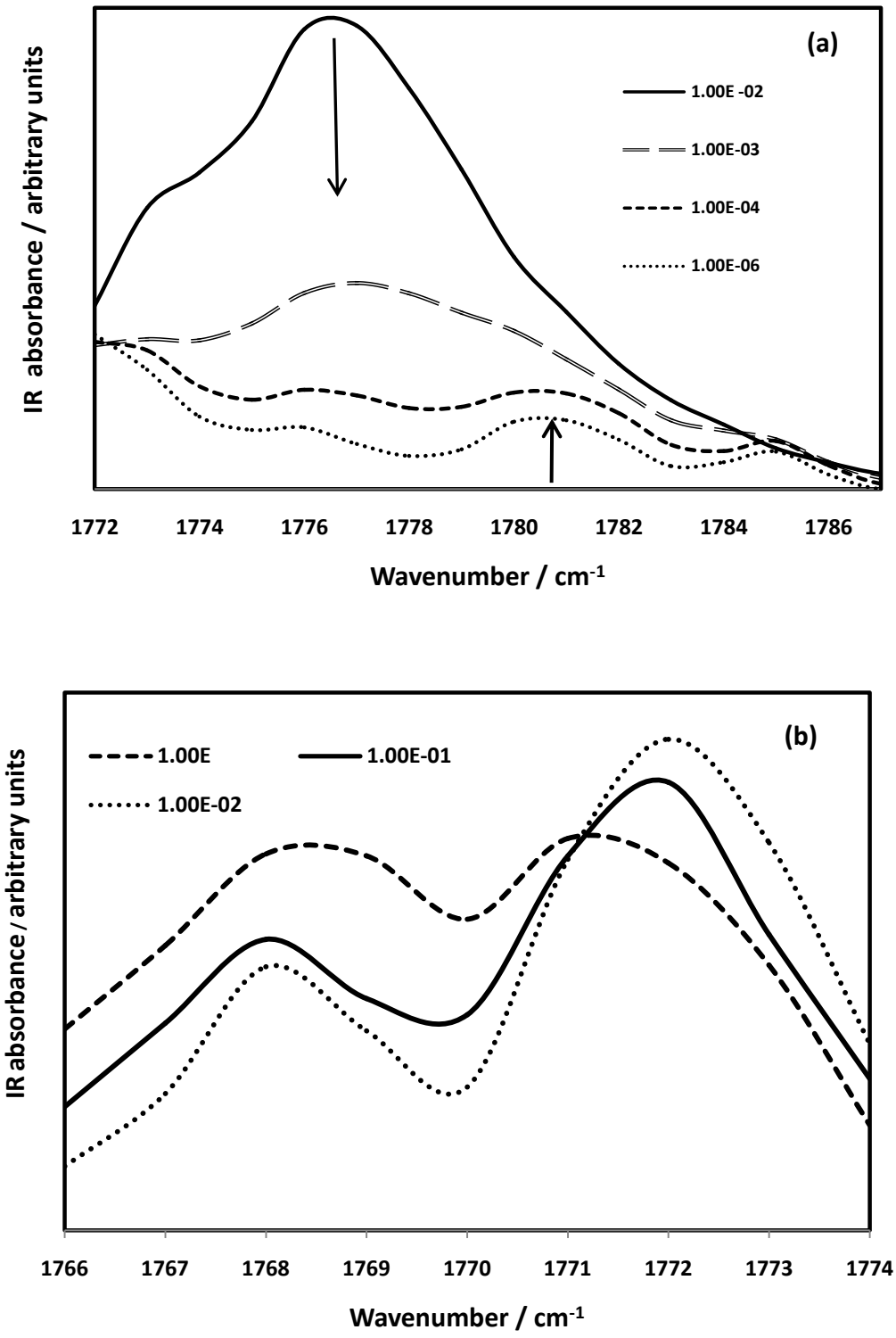

Figure 2.7: IR-spectra of compound 2-phenyl-4H-benzo[d][1,3]oxazin-4-one in (a) hexane and (b) CCl_4 in the region of C=O stretching modes at different concentration.

The FTIR spectra of the compound 2-phenyl-4H-benzo[d][1,3]oxazin-4-one in a non donor solvent hexane at different concentration in the region of the C=O stretching modes is shown in Figure 2.7a. The higher wave number component (1781cm^{-1}, more close to the DFT-calculated value with respect to that observed in KBr) corresponds to the free C=O group and the lower wave number component (1776 cm^{-1}, close to the observed value in KBr) to the hydrogen-bonded C=O group. The relative intensity of the peak near 1781cm^{-1} increased with dilution which signifies that the compound exists as mostly C=O---H-C bonded dimer in KBr. In CCl_4 (Figure 2.7b) a similar change in the intensity is observed for the free C=O at 1772cm^{-1} and hydrogen bonded C=O at 1768cm^{-1}. The sample dilution leads to an increase in the free (monomer) $\nu_{C=O}$ band intensity relative to the bonded (dimer) $\nu_{C=O}$ band.

In the compound 2-methyl-4H-benzo[d][1,3]oxazin-4-one, an intense band for the carbonyl was found to be visible at 1757cm^{-1}(KBr), while the same compound diluted in hexane displayed the band at 1774.4cm^{-1} (Figure 2.8). In H-bonding solvent chloroform the intensity of the C=O band was greatly reduced and bifurcated into two bands at 1749.3cm^{-1} and 1751.2cm^{-1}; the intensity of the band at 1751.2cm^{-1} increased with progressive dilution (Figure 2.9). These observations can be related to the presence of two C–H---O interactions. The C=N stretching band for the compound 2-methyl-4H-benzo[d][1,3]oxazin-4-one appeared at 1649cm^{-1}, 1653cm^{-1}, and 1684cm^{-1} in nujol, dilute solution in hexane and chloroform respectively. Thus, the H-bonded and free carbonyl absorption bands are visible in solvents of different polarizability and new bands appeared in chloroform solution which can form new H-bond with the carbonyl. It can be safely noted that two molecules can approach each other as DA-AD pair only if the C5-H proton participate in the H-bonding in the dimer.

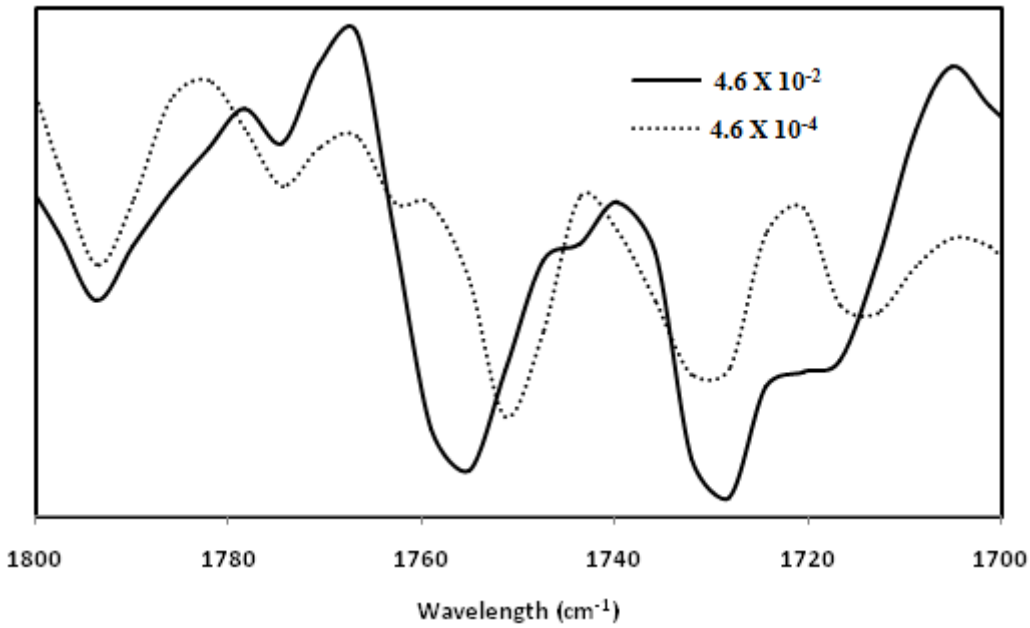

Figure 2.8: The expanded band of Raman spectra of 2-methyl-4H-benzo[d][1,3]oxazin-4-one in $CHCl_3$.

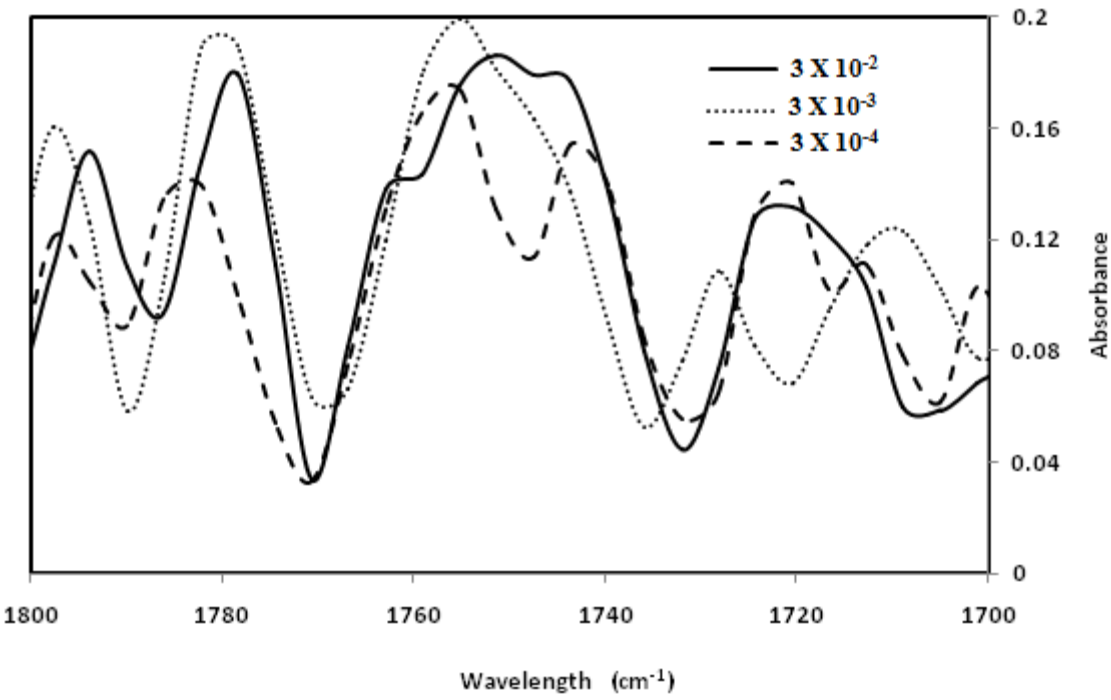

Figure 2.9: The expanded band of IR spectra of 2-methyl-4H-benzo[d][1,3]oxazin-4-one in hexane.

2.3.4.2 C-H stretching region

The C-H stretching occurs above 3000 cm^{-1} and is typically exhibited as a multiplicity of weak to moderate bands, compared with the aliphatic C-H stretch. In solid KBr the bands observed at 3040, 3050 and 3060 cm^{-1} in the IR spectrum were assigned as ν*C-H modes of the benzene ring. In the Raman spectrum two bands are observed at 3022 and 3070 cm^{-1}. Proper assignment of this bands are reported by us in a priori work (Ambujakshan *et al.,* 2008) for the compound 2-phenyl-4H-benzo[d][1,3]oxazin-4-one. In solution the spectra being more sharp a complex pattern of more bands were observed. In order to make the matter simple we like to confine our discussion with the compound 2-methyl-4H-benzo[d][1,3]oxazin-4-one where the aromatic hydrogen is least in number. Still the spectra are complex as shown in Figure. 2.10 and 2.11.

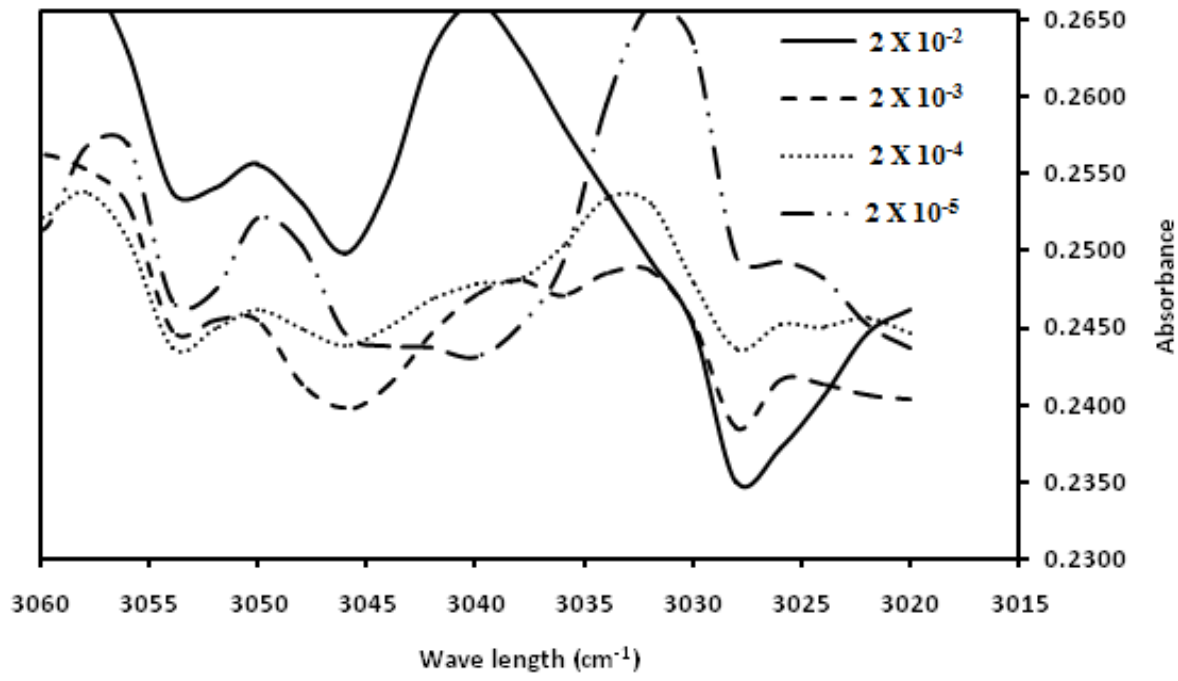

Figure 2.10: IR spectra of 2-methyl-4H-benzo[d][1,3]oxazin-4-one in CCl_4.

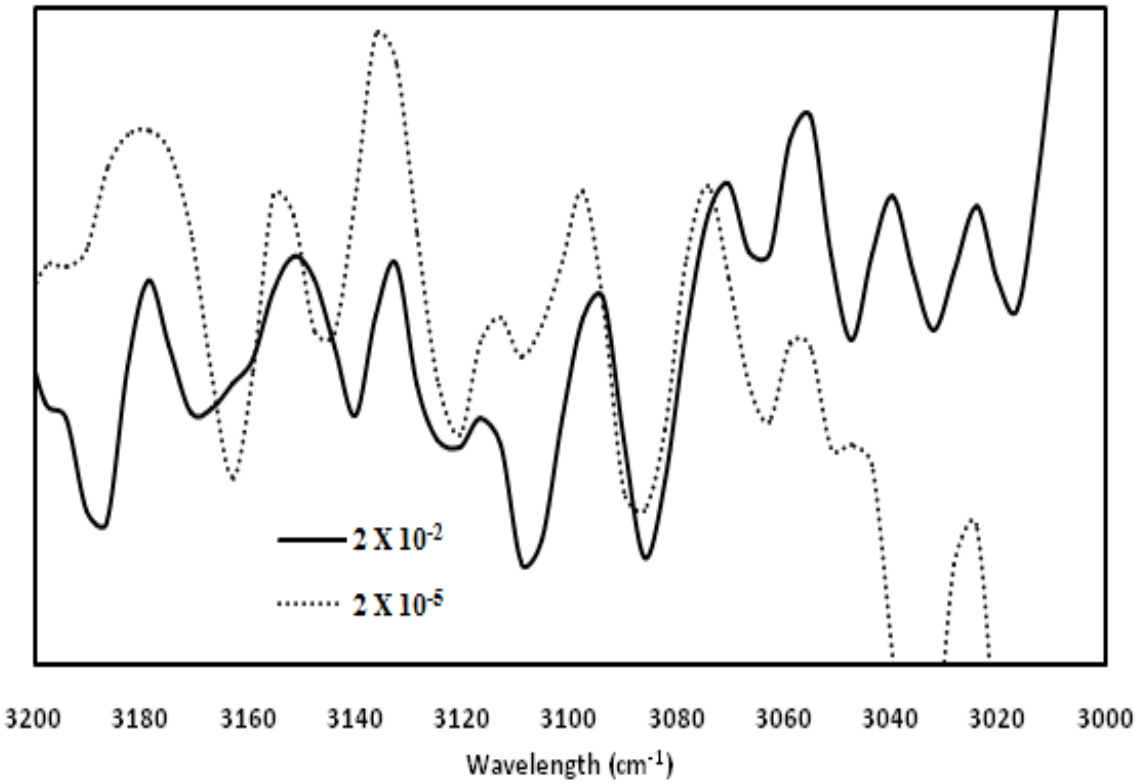

Figure 2.11: Raman spectra of 2-methyl-4H-benzo[d][1,3]oxazin-4-one in THF.

In these above figures we tried to keep the spectral range in comparable intensity so that the relative changes in frequency as well as intensity become easily visible. Now we computed the vibration frequencies for both the monomer and H-bonded dimers. The calculated frequencies with their respective intensity for the C-H bond stretching range are plotted in a radial plot (Figure- 2.12). The band shift is associated with intensity; however we used the monomer frequency in radial axes.

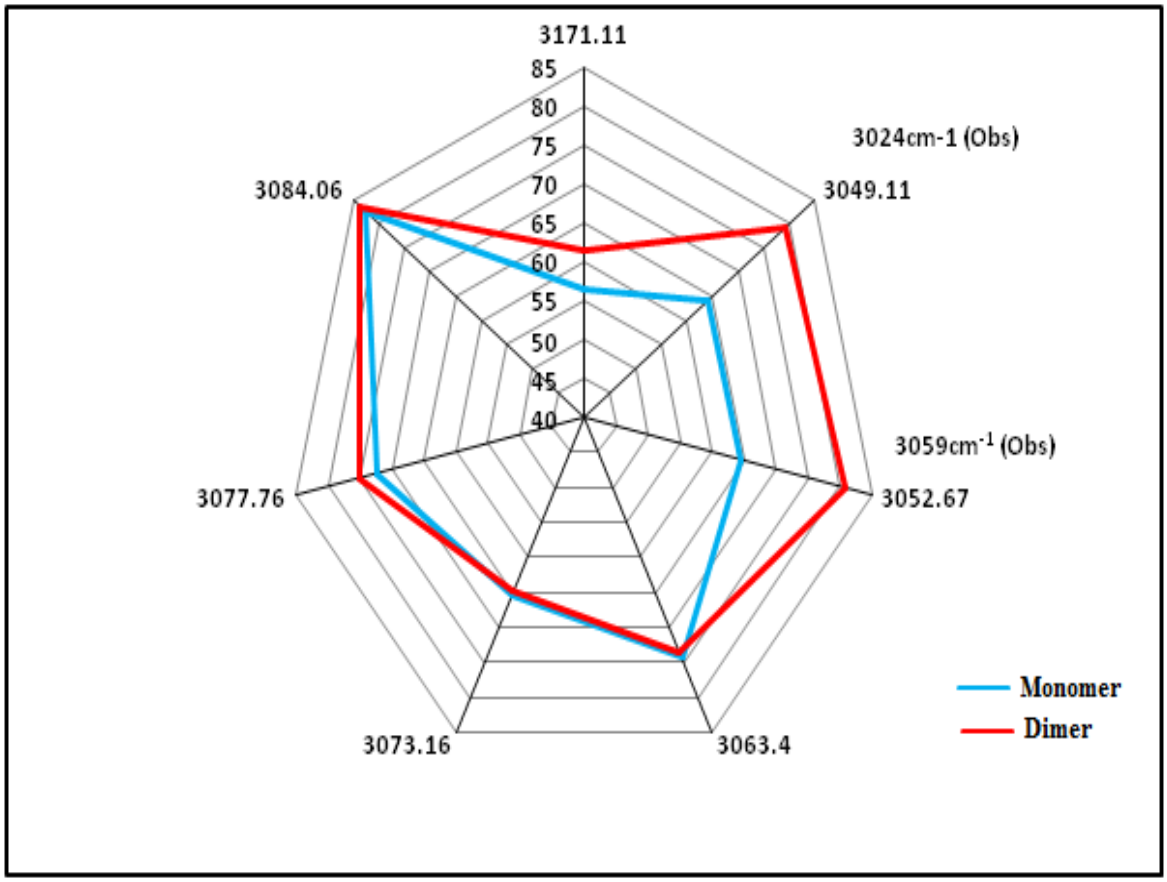

Figure 2.12: Radial plot for frquency in cm^{-1} vs intensity of 2-methyl-4H-benzo[d][1,3]oxazin-4-one.

Moreover, from this radial plot it is imperative that change in intensity as well as band shift of two specified peaks must be there in our observed spectra if our proposition is correct (Figure 2.12). Thus, from the experimental IR- spectra we have chosen the most concentrated solution where dimer concentration should be higher and the most dilute solution where the monomer concentration should be higher. Now the calculated frequencies corresponded with the observed frequencies for the stated solution since intensity is arbitrary. Thus we got a plot as shown in Figure.2.13.

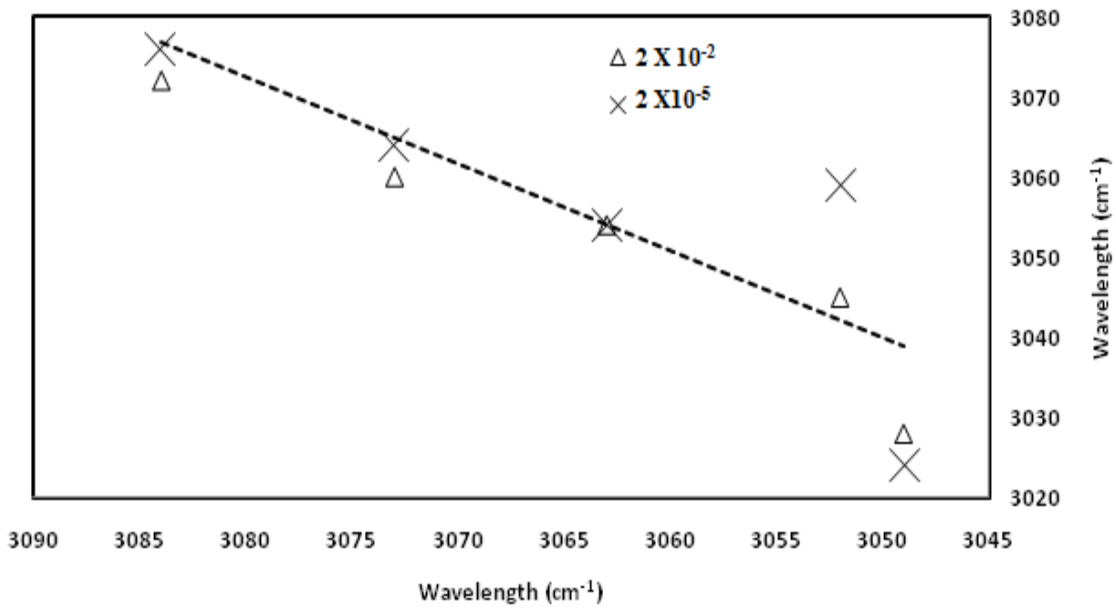

Figure 2.13: IR absorption bands of calculated monomer vs. observed in Dilute sol.(X) and in Conc. Sol. (Δ) 2-methyl-4H-benzo[d][1,3]oxazin-4-one.

The graph clearly suggested that two points have deviated from the trend line and this deviation is greater for the concentrated solution compared to that in the dilute solution. Thus the spectral analyses unequivocally prove the existence of monomer dimer equilibrium in the solution state and the dimer is H-bonded dimer.

Chapter 3

Morphology of 2-substituted-benzo[d][1,3]oxazin-4-ones

Chapter 3

Morphology of 2-substituted-benzo[d][1,3]oxazin-4-ones

3.1 Introduction

3.1.1 Importance of weak interaction in polymorphism

In many areas of chemistry, researchers are continuously working on the interrelationships between molecules in the solid state polymorphism. Subsequently, it is of great concern to improve our understanding regarding the structures of crystalline materials and the involvement of different forces. Generally, the hydrogen bonds are considered as the highest energy interactions in molecular crystals and thus emerge to be the most important attractive force. It is well documented that multiple H-bonding sites promote polymorphism in multifunctional molecules (e.g. pharmaceuticals). The polymorphism exhibited by these molecules could be recognized with respect to the different H-bonding topologies. Moreover, polymorphism also occurs in systems without strong hydrogen bonds (N – H ··· X, O – H ··· X, S – H ··· X; X = N, O, S, F, Cl, Br, I). Even in these cases, H-bonding may still be present in the form of weaker interactions such as C – H ··· X and C – H ··· Π

3.1.2 Definition of Polymorphism

The term “Polymorphism” is taken from Greek word, *Polus* = many and *morph* = shape. Thus, it is defined as the ability of a substance to exist in two or more crystalline phases that have different arrangements or conformations of the molecules in the crystal lattice (Haleblian & McCrone, 1969; Haliblian, 1975; Bym, 1982). It is supposed that polymorphism depends on the communities and associated with the structure of solid (Desiraju, 1987). The polymorphism is defined in different ways in different disciplines; for example, in Biology, it is defined as species with different phenotypes, designating even sexual dimorphism, nuclear dimorphism and lipid polymorphism. While in

chemistry, it refers to a solid compound that can adopt different forms/crystal structures and also involve different packing of the same molecule (Brog *et al.*, 2013).

Historically, for the first time, polymorphism in an organic compound, benzamide, was brought to light by Wohler & Liebig (1832), but the first crystal structure of polymorphism was determined in 1938 when Robertson & Ubbelohde discovered the first X-ray diffraction structure of polymorphs with resorcinol (Desiraju *et al.*, 2011).

Polymorphism can now be explained as the ability of a substance to exist in two or more crystalline phases that have different arrangements of the molecules in the crystal lattice or simply defined as the ability of a molecule to crystallize in more than one form, exhibiting different crystals of the same substance with different unit cells and crystal packing arrangements.

3.1.3 Significance of Polymorphism

Polymorphs are studied in many disciplines, chemistry, material science, pharmaceutical science etc. Polymorphs often possess differing physical and thermodynamic properties (density, refractive index, melting points, solubility, thermal stability etc), chemical (chemical reactivity) spectroscopic properties and kinetic properties (Raw, 1999; Hilfiker, 2006). Various reviews, book chapters, and literatures related to pharmaceutical polymorphism were reported within the past two decades which affirmed the growing importance of pharmaceutical polymorphism within the scientific community and industry as well as regulatory agencies (Byrnel *et al.*, 1999; Rod *et al.*, 2004; Colin *et al.*, 2004, Dharmendra & William, 2004; Hilfiker, 2006; Harry, 2009; Braga *et al.*, 2010; Lee *et al.*, 2011; Desiraju, 2013). Different polymorphic forms of drugs may show differences in bioavailabilities (Bym, 1982). This has major implications in the pharmaceutical industry'. This may manifest itself in varying reactivity, solubility and transportation rates in living body. It is now widely appreciated that the occurrence of polymorphism in molecular crystalline solids impacts on the production of fine chemical products such as pharmaceuticals and pigments. (Susich, 1950; Kendall, 1952;

Ebert & Gottlieb, 1952; Warwicker, 1959; Thomas & Ghode, 1989; Whitaker, 1992; Rodrı´guez-Spong *et al.,* 2004)

After a period of continuing investigation of polymorphism, more than half a century, the Innsbruck school has found that under normal pressure conditions around one-third of organic substances show crystalline polymorphism (Burger, 1979; Kuhnert-Brandstatter & Riedmann 1987). Since differences in polymorphism affect both chemical properties (shelf-life, solubility, density, etc.) and the pharmaceutical performance (bioavailability, stability, etc.) of the drug substance, the characterization of polymorphs acquired key importance in pharmaceutical industry (Martin, 2006). Now-a-days, study of polymorphism in molecular crystals has renewed interest as it bears importance in the industrial application related to its occurrence (Bernstein 2007; Brittain, 2102). Since different polymorphs have different energies, the solubility is dependent on the polymorphic state. In addition to other major factors, the inherent solubility and rate of dissolution of the drug substance itself plays important role in bioavailability of finished products. The researchers have started to take very interest in polymorphism to satisfy the regulations imposed regarding bioavailability of formulations of new chemical entities by regulatory authorities in various countries (Bakar *et al.,* 2010). However, Burger has pointed out that, only in rare cases, the difference in solubility between polymorphs is expected to result in significant bioavailability differences. There are only few marketed products (chloramphenicol palmitate, novobiocin etc) which show major bioavailability differences because of polymorphism (Burger, 1982; Mullins & Macek, 1960). Nowadays, durability on products has become tighter in the pharmaceutical industry. Therefore, polymorphic behaviour should be identified at an early stage of development as a means of ensuring reliable and robust processes and conventionality with good industrialized practice (Bavin, 1989). These practices help to avoid the occurrence of unlikeable conditions, the control of quality in manufacture and product reliability in any industry by ensuring that the processes are well understood and under control.

In short, the very existence of polymorphism reveals something about the solid-state. The study of polymorphic system enabled us to understand solid-state molecular behavior, intermolecular interactions and the relationship between crystal structure,

crystal growth and crystal habits and also their impact on bulk properties. It has immense importance in the development of appropriate organic compound and its application for humankind.

3.1.4 Methods to characterize Polymorphism

Due to major role in solubility of products, nowadays the characterization of polymorphism becomes an important concern in research. However, plenty of analytical techniques are available to characterize and determine polymorphism in organic compounds for a long time. The commonest methods depend upon the some extent on the area of interest. But in most of the research fields , microscopy (McCrone, 1957; Teetsov & McCrone, 1965) , IR (Davis *et al.,* 2004), UV (Leites *et al.,* 1998) and NMR (Remenar *et al.,* 2004) spectroscopy, DSC (Auer *et al.,* 2003; Davis *et al.,* 2004; Albertinia *et al.,* 2003; Remenar *et al.,* 2004) and X-ray powder diffraction (Auer *et al.,* 2003; Albertinia *et al.,* 2003; Davis *et al.,* 2004; Airaksinen *et al.,* 2004) were most widely used.

The preliminary examination can be done by a binocular microscope which enables the overall characteristics of the sample to be established. The hot stage microscopy allows determining the transition temperature coupled with a microscope and allows recognising changes in crystal habit as well as in light transmission. The changes in crystal habits indicate the solid state phase transition (Marthi *et al.,* 1992). The differentiation of monotropic and enantiotropic relationship, the estimation of tendency of melts and individual phases to supercool, the generation of stable and unstable polymorphs and also recording of their optical properties can be studied by hot stage microscopy (Bloss, 1971; Jordan, 1993).

The main thermal techniques considered for polymorphic forms of organic compounds are differential scanning calorimetry (DSC), differential thermal analysis (DTA) and thermogravimetric analysis (TGA) (Perrenot & Widman, 1994). DSC and DTA are alternative ways of measuring heat capacity changes in a sample (Wiedemann & Bayer, 1985; Voress, 1994) In DSC, melting points are measured but also the

transformation of metastable forms and determining the relation between the different polymorphic forms can be studied (Hino *et al.,* 2001; Park *et al.,* 2003). The working principle of DTA is similar to DSC, but quantitative study cannot be done by DTA. The weight changes in polymorphism can be monitored by TGA as a function of the temperature and is therefore particularly valuable in examining solvent loss from crystals and in identifying sublimation and decomposition processes (Reading & Crag, 2007).

The third technique is spectroscopy, including very classical techniques like infrared and Raman spectroscopy to study the vibrational modes of the compound (Takasuka *et al.,* 1982; Skrdla *et al.,,* 2001; Paulechka *et al.,* 2009), NMR (Remenar, 2004) can be used for measuring the difference in magnetically non equivalent nuclei in two different polymorphs and also UV to monitor the change in intensity of polymorphs on heating. However, Infrared spectroscopy has had, of course, enormous exposure in the literature through reviews and research papers but there are surprisingly few descriptions of the precautions to be taken when recording or interpreting the IR spectra of polymorphs. For example, in the case of non-matching spectra, a wide variety of causes might be suspected, including mis-labeling of a homologue, (Rosenkrantz & Zablow, 1953) sample purity, crystal size, (Baker, 1957), crystal habit and orientation, (Griesser & Burger, 1993; Kobayashi *et al.,* 1994) formation or partial decomposition of a salt, solubility in the mulling medium, hydration, (Kuhnert-Brandstatter & Riedmann, 1989) dehydration (Burger & Ramberger, 1979) or other solvent loss under vacuum, level of impurities in the mulling or disk medium and instrumental variables (Free & Miller 1994) including the inadequate elimination of background peaks.

The literature suggests that the polymorph identification is a leading application of single crystal diffraction analysis. As Dorothy Crowfoot Hodgkin argued in her Nobel lecture of 1964: ‘‘The great advantage of X-ray analysis as a method of chemical structure analysis is its power to show totally unexpected and surprising structure with, at the same time, complete certainty’ (Brog *et al.,* 2013). In the study of different crystalline structures, within a compound, one polymorph is distinguished from another by a unique powder diffraction pattern associated with that specific crystal structure.

3.1.5 Role of weak interactions in Polymorphism in organic compounds

The role of intermolecular interactions like van der Waals interactions, coulombic interactions, hydrogen bonding, and steric repulsions in determining the arrangement of molecules in a crystal were documented by various authors. Even the cooperative action of very weak interactions like C-H…O hydrogen bonding, π…π, X…X (X = halogen), and C-H…π interactions can significantly contribute towards stabilizing a specific molecular arrangement in a crystal (Desiraju, 2002; Desiraju, 1999). These weak interactions are strong enough to cause changes in torsion angles, thereby giving different conformations and a particular molecular conformation which is near the most stable equilibrium conformation is often stabilized. As these interactions are weak and various molecular conformations can have nearly the same energy, the molecules can crystallize in different crystal forms. Molecules capable of possessing torsional degrees of freedom give rise to different conformations that may be preserved in different crystal forms. (Borka & Haleblian, 1990).

In 1897, Acetylsalicylic acid, aspirin, was first synthesized and isolated by Hoffman and first crystal structure was reported by Wheatley in 1964 (Wheatley, 1964; Sneader, 2000). Interestingly, Peterson and Zaworotko reported a new structure for this compound in 2005 (Vishweshwar, 2005). On the basis of crystal data of Desiraju, authors have reported that the two polymorphs have the same groups but clearly different unit cells. Moreover, slight differences in terms of torsions angles were also observed in molecular geometry of the two forms. The difference in hydrogen bond made differences in hydrogen bonded sheet structure, which causes the occurrence of two different polymorphs (Bond *et al.,* 2007).

The preceding text will reveal the dimension of molecule-molecule interaction of the synthesized compounds that may in future guide the researchers to increase the efficacy of drug. A number of quinazoline derivatives are already available in market as medicine against various diseases as reviewed by earlier authors (Selvam & Kumar, 2011). Most of the published literatures have commented on the limitation and mentioned only about the efficacy limit of biological activities. Consequently, it would be also of

great concern for the researchers to think about the quinazoline derivatives which are unable to expose their biological activities, in spite of the fact that they contain medicinally important skeleton. By intervening the said problem, some more quinazoline derivatives could be added to the list of marketed drugs. This study focused on uncovering the reason for low antibacterial activity in 2-substituted-benzo[d][1, 3] oxazin-4-one derivatives. With the conviction that CHO plays role in crystal packing of 2-phenyl- benzoxazine, we tried to explore the existence of CHO hydrogen bond in dimer and its impact on their antibacterial activity.

3.2 Materials and Methods

3.2.1 Characterization of polymorphism in solid state

3.2.1.1 Differential Scanning Calorimetry

Differential scanning calorimetry (DSC) was carried out with a Shimadzu DSC-60 instrument (Shimadzu, Kyoto, Japan). Samples weighing 3–5 mg were heated in opened aluminum pans at a rate of 10 K/min under nitrogen gas flow of 35 mL/min.

3.2.1.2 Microscopy

3.2.1.2.1 Phase contrast Microscopy

The primary morphological changes of polymorphic forms were compared by visual monitoring with phase contrast inverted microscope (Olympus, CK40-SLP) at 200X magnification.

3.2.1.2.2 Atomic Fluorescent Microscopy

AFM measurements were performed using IIIa MultiMode AFM (Digital Instruments, USA).

3.2.1.2.3 Scanning Electron Microscopy

A Jeol JSM-6100 scanning electron microscope was used to obtain photomicrographs of compound 2-methyl-4H-benzo[d][1,3]oxazin-4-one polymorphs. Samples were mounted on a metal stub with an adhesive tape and coated under vacuum with gold.

3.2.1.3 Powder X-Ray Diffraction

X-ray Powder Diffraction (XRPD) patterns were recorded on a X'Pert Philips PW3020 diffractometer (Philips, The Netherlands) over the 2y range of 58–408, using

graphite monochromatized Cu Ka radiation (1.54184 A °), in aluminum sample holders, at room temperature.

3.2.1.4 UV Spectroscopy

The compound 2-methyl-4H-benzo[d][1,3]oxazin-4-one was synthesized by the scheme mentioned in chapter 1. UV-Visible absorbance was measured using a Shimadzu UV-160A spectrophotometer (Shimadzu, Kyoto, Japan) in the range 200–900 nm using a quartz recipient with an optical pathway of 1 cm.

Saturated water solutions- Saturated solutions of form I and II were generated by placing an excess amount of sample (7 mg) in 100 mL of water. The suspension was stirred during 24 h at room temperature and the final solutions were filtered using 0.2 mm Millipore filter (final measured pH:5). No extra dilution was necessary.

Saturated methanol solutions- Saturated solutions of form I and II were obtained by placing an excess amount of sample (0.1 g) in 0.5 mL of absolute ethanol. The suspension was stirred for 4 h at room temperature in capped glass vials. The solutions were filtered using 0.2 mm Millipore filter and analyzed after appropriate dilution.

A saturated solution of compound 2-methyl-4H-benzo[d][1,3]oxazin-4-one was prepared in water, methanol and chloroform. The UV scan was taken for each of the solutions and then allowed to reflux for two hours. After two hours of reflux, a repeat UV scan was taken. In another experiment, 4.5E-04, 9.16E-04, 1.83E-03, 2.75E-03 and 4.58E-03 M solutions were prepared in methanol. UV scan was taken before and after the reflux of two hours.

3.2.1.5 Vibrational spectroscopy

Saturated solutions of 2-methyl-4H-benzo[d][1,3]oxazin-4-one was prepared in CCl_4 and hexane. Different dilutions were made from the saturated solution. Infrared spectra were recorded on a FTIR-8300 SHIMADZU spectrophotometer in the 4000-400 cm^{-1} region for each dilution.

3.3 Results and Discussion

3.3.1 Study of Polymorphism in solid state

In this study we have chosen 2-methyl-4H-benzo[d][1,3]oxazin-4-one as the model compound to explore its possible polymorphic behavior because of its simple structure, containing CH_3 at 2^{nd} position of Quinazolone ring. The crystals of 2-methyl-4H-benzo[d][1,3]oxazin-4-one on keeping gradually turned into powder and some sublimates made a layer on the wall of the container. On keeping for 15-20 days, the entire powdered mass turned into an agglomerate having mp 188.2 ^{o}C (Form II). This substance showed lower solubility in hexane; but a little amount of the 2-methyl-4H-bezo[d][1,3]oxazin-4-one with mp 81.9 ^{o}C (Form I) was crystallized in this procedure. The metamorphic form of 2-methyl-4H-benzo[d][1,3]oxazin-4-one with mp 81.9 ^{o}C (Form I), was effectively recovered by vacuum sublimation at below 125-130 ^{o}C. The compound on recrystallization from hexane and ether mixture gave mica like laminar crystal with mp 188.2 ^{o}C (Form II) (Figure 3.1). The crystal polymorphism of 2-acetamidobenzamide was first indicated by difference in the reported melting points of material obtained from these routes (Errede, 1980; Buttar 1998). Errede (1980) found that super-cooling solutions of acetone or methanol gave fine crystals of the α form and that larger crystals of the β form could be grown from acetone, methanol or aqueous solutions; while Barnett *et al* (2006) found that the α form could be obtained by slow cooling of hot saturated solutions of water, ethanol, methanol or ethyl acetate. Barnett *et al* (2006) also found that the β form initially proved difficult to obtain, but that once the β form had been obtained it was the form that resulted from many crystallization conditions which had previously given the α form. The α form has a melting point of 179−180 °C and a density of 1.325 g cm^{-3}; while the β form has a melting point of 189−190 ^{o}C and a density of 1.345 cm^{-3}.

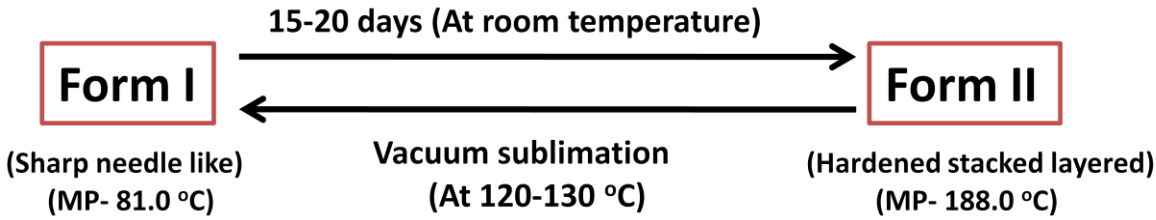

Figure 3.1: Schematic representation of the changes in morpholgy of 2-methyl-4H-benzo[d][1,3]oxazin-4-one .

3.3.1.1 Morhology study

The Phase contrast microscopic (Figure 3.2) SEM (Figure 3.3) and AFM (Figure 3.4) images of the two forms were also provided. So far as our knowledge is concerned from the published literatures, no information on X-ray structural data is available for this compound (2-methyl-4H-bezo[d][1,3]oxazin-4-one).

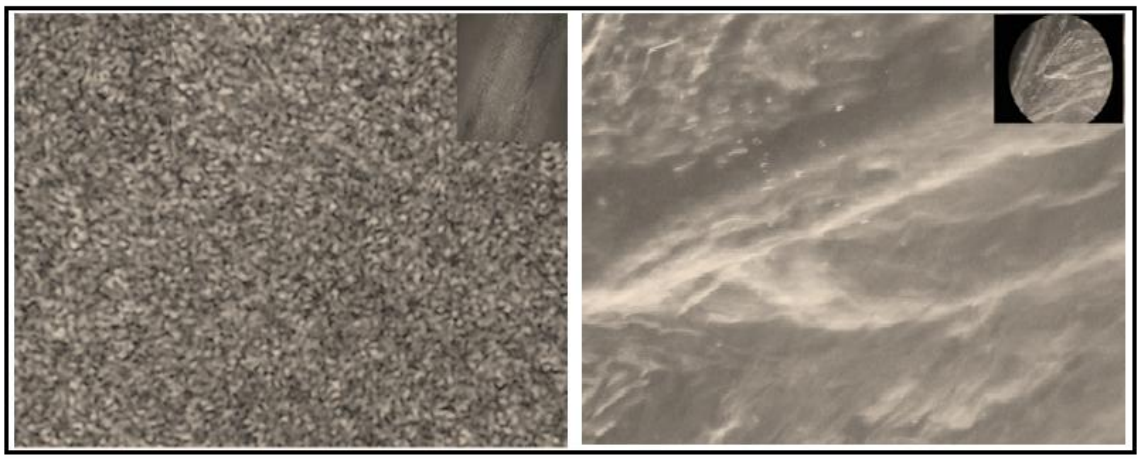

Figure 3.2: Phase contrast microscopic image (200X magnification) of Form I and Form II.

The image obtained from both sources revealed significant diffrences in the morphology of two polymorphic forms. As two lone pairs in the carbonyl plane flank the carbonyl oxygen, we theorize some change in direction of H-bond may be responsible for the metamorphism.

The different morphology was observed for different polymorphs in phase contrast microscopy (Figure 3.2). Additionally, the SEM (Figure 3.3) image also indicated the presence of two different morphologies for two different polymorphs. Despite their similarity and peak overlap, peaks specific for each of the polymorphs was considered and used to confirm that Form I is not detected in form II and vice-versa.

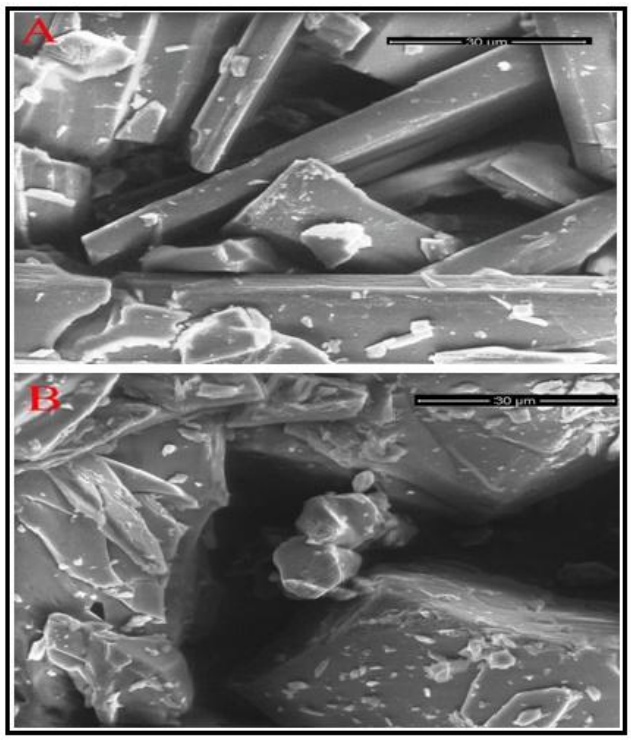

Figure 3.3 : - SEM image of (A) 2-methyl-4H-benzo[d][1,3]oxazin-4-one Form I (mp 81 ^{o}C) and (B) 2-methyl-4H-benzo[d][1,3]oxazin-4-one Form II (mp 188 ^{o}C)

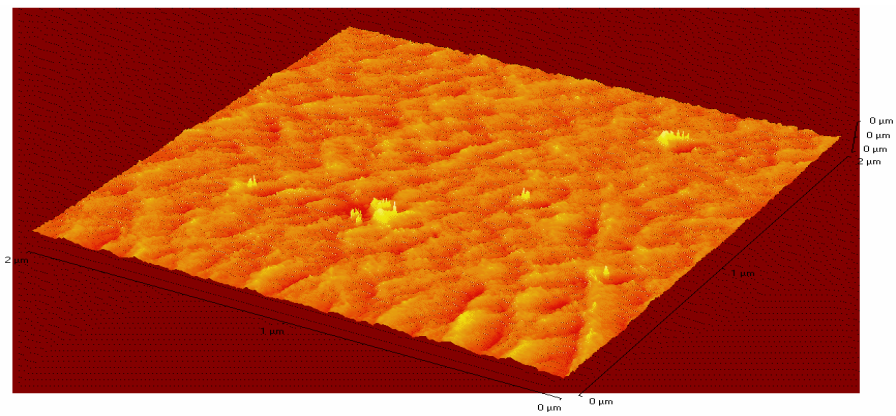

Figure 3.4: AFM image of 2-methyl-4H-benzo[d][1,3]oxazin-4-one Form II.

3.3.1.2 Differential Scanning Calorimetry study

In order to obtain the evidence for the existence of two polymorphs, a Differential Scanning Calorimetry (DSC) study was done. A DSC run of a powdered mixture of two polymorphs shows significant peaks at 81 and 188.91 corresponding to the melting point of form I (81 ^{o}C) and form II (188.9 ^{o}C) respectively (Figure 3.5). The heat of fusion (ΔHf_{FormI} = 20.1729kJ/mol and ΔHf_{FormII} = 20.4257kJ/mol) of each metamorphoses and heat of sublimation (ΔHf = 25.641kJ/mol) of the second phase was calculated by differential scanning calorimetry (DSC).

In DSC study, the two polymorphs, I and II, show only a single peak due to melting at all heating rates, with onset temperatures of 82 and 188 ^{o}C, respectively. This indicated the presence of two polymorphs. The presence of the single intense peak in both polymorphs indicated the pure polymorphs.

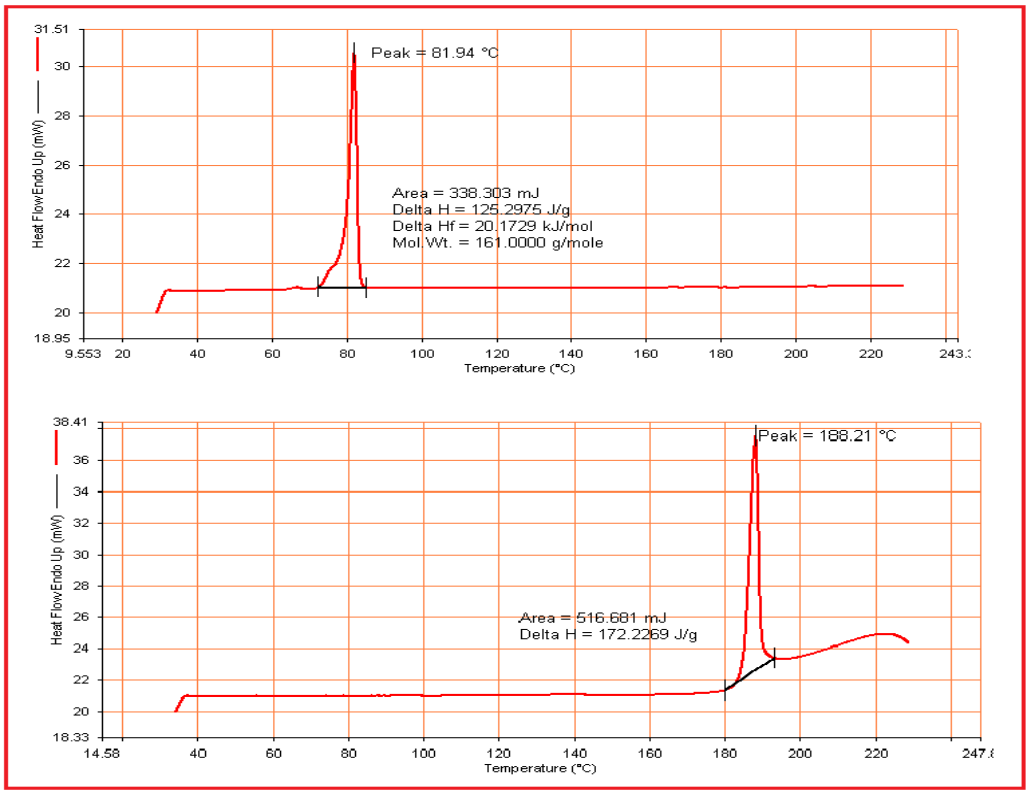

Figure 3.5: (a) DSC curve of form I with m.p.81.9 ^{o}C (b) form II with m.p 188.21

3.3.1.3 PXRD study

Compound 2-methyl-4H-benzo[d][1,3]oxazin-4-one existing in two distinct polymorphic forms was also ascertained from PXRD observations (Figure 3.6). The X-ray diffraction pattern measurement showed significant shift and variations in peaks of both the forms. Literature suggests that the two samples can be considered as un-identical; same peaks are not present and when the intensity variations of the same peaks those are larger than 20%. Small changes in the form of new peaks, additional shoulders, or shifts in the peak position often indicate the presence of a second polymorph (Brog *et al.*, 2013). The 2Θ vs. intensity plot of the powder X-ray diffraction (PXRD) data of the substances with 2-methyl-4H-benzo[d][1,3]oxazin-4-one mp- 81^{o}C and mp- 188 ^{o}C are shown in Figure 3.5. The steep nature of the peaks with a fairly straight base- lines are clear indication of their crystalline nature for both the forms. The similarity in the appearance of peaks is an indication of similar crystal packing and of same chemical composition. The variation of peak intensities and little shifts of some peaks suggest that they have different morphology.

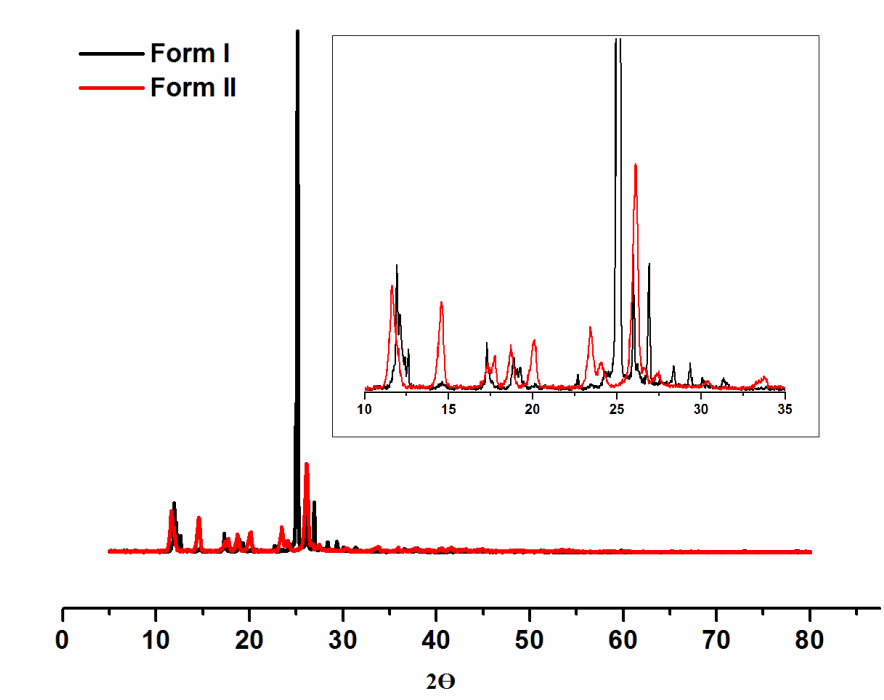

Figure 3.6 : PXRD patterns of the Form I (red) and Form II (black) polymorphs of compound 2-methyl-4H-benzo[d][1,3]oxazin-4-one .

The results of first hand analysis of the peaks and spacing distances are shown in Table 3.1 and Table 3.2. The assignment of the Millar indices for the major peaks in diffractogram is very essential. In the tables we tabulated the corresponding 2Θ -values for the most intense peaks and a serial number of peaks at first two rows. In the subsequent rows the 2Θ values are converted to the Θ values in radian and then they are transformed to sin Θ -values. In the sixth row all the $\sin^2 \Theta$ values are divided by the corresponding lowest value. In the next row the values are multiplied with two and in the subsequent row the nearest integers of these values are tabulated. These integers corresponded to the Miller indices as shown in the next row. Thus we assigned each tabulated peaks, in the first row, with the corresponding Millar planes of the crystals. Thus our apparent supposition about the crystalline nature of the substances is confirmed. The sequential appearance of the Miller Planes suggested the essential primitive nature of the crystals. Moreover, both the substances posses same kind of essentially Simple Cubic Crystal lattice (SCC). The ratio $\sin^2 \Theta$ values of the 6th and the 1st peak being 4 in both the cases imperative to our findings of correct designation of Miller indices. This result indicates similar stacking in both the morphological forms. The peak corresponding to 100- Millar indices is invisible for both the morphs in the diffractogram. The spacing between the similar planes ($d_{(hkl)}$) is tabulated in the last row in each table. Lattice length ($a = 2^{\wedge 0.5} * d_{(110)} = d_{(100)} = b = c$) for the Form I (mp-81.9 ^{o}C) and the Form II (mp-188 ^{o}C) are 10.492 Å and 10.766 Å respectively. In graphite c = 6.71 Å is reported and the sheets stacked in this orientations. For SCC unit cell a= b=c so in our system the stacking is less compact than that in graphite (Gray *et al.,* 2000). This is expected because graphite is homo-atomic planner, the molecule in our investigation expectedly did not favour such compact staking but it reflects from the data that there is a little bit similarity. The morphological forms for the second one, the unit cell is bigger than the first one though the second form is the thermodynamically more favoured. It implies that the dipole-dipole interaction is dominant over the pi-pi interaction; on the other hand pi-pi interaction governed the stacking pattern in graphite. The interplay of these two interactions is responsible for originating the polymorphism in the 2-methyl-4H-benzo[d][1,3]oxazin-4-one.

Refinement of crystal data analysis is a topic of the crystallographers. One of the great (pioneer) crystallographer of India, Kedareswar Banerjee worked with Sir William Lawrence Bragg, the father of crystallography and worked on anthracene, naphthalene, graphite etc., those data still being refined; of late (Wowe *et al.*, 2003**)** interlayer spacing of graphite is estimated to 3.355(1) Å. Being homo-atomic and due to favourable Pi-interactions, the layers should be more closer than that in our system. The findings for interlayer spacing of diagonal planes ($d_{(110)}$ /2 =3.71 Å and 3.82 Å), presented in the last rows of the table bears good accordance to corresponding data for graphite.

In conclusion, both the polymorphic forms are of same chemical structure, similar unit cell and similar staking pattern; only difference is the compactness of the stacking. And the striking finding is that less compactly pact form has higher melting point - which is due to excess favourable dipole-dipole interaction strength gained at little sacrifice of pi-pi stabilizing interaction. Single crystal X-Ray Diffraction Study of 2-phenyl-4H-benzo[d][1,3]oxazin-4-one is reported (Thilagavathy *et al.*, 2009) to have the structure shown in Figure 3.7.

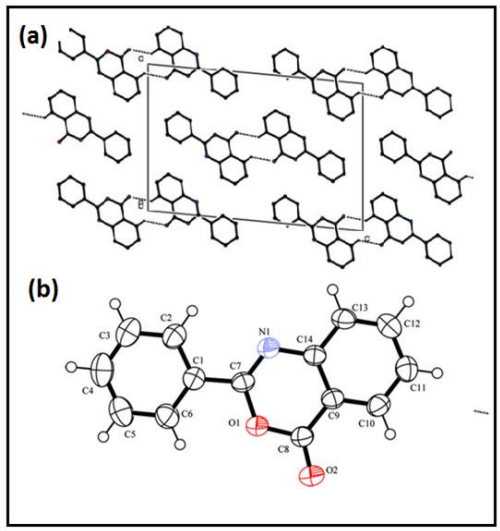

Figure 3.7: (a) The crystal packing viewed down the *b axis. C-H···O hydrogen bonds are shown as* dashed lines. (b) The molecular structure of the 2-phenyl-4H-benzo[d][1,3]oxazin-4-one, with atom labels and 50% probability displacement ellipsoids for non-H atoms.

Table 3.1- PXRD data analysis of Form I

	1	2	3	4	5	6	7	8	9	10	11	12	
2Θ deg	11.922	14.602	17.382	18.881	20.382	24.302	25.962	26.922	28.382	29.362	30.242	31.562	
Θ deg	5.961	7.301	8.691	9.4405	10.191	12.151	12.981	13.461	14.191	14.681	15.121	15.781	
Θ in radian	0.1040	0.1274	0.1517	0.1648	0.1779	0.2121	0.2266	0.2349	0.2477	0.2562	0.2639	0.2754	
sin Θ	0.1039	0.1271	0.1511	0.1640	0.1769	0.2105	0.2246	0.2328	0.2452	0.2534	0.2609	0.2720	
$Sin^2 Θ$	0.0108	0.0161	0.0228	0.0269	0.0313	0.0443	0.0505	0.0542	0.0601	0.0642	0.0680	0.0740	
$Sin^2 Θ_n$ / $Sin^2 Θ_1$	1	1.492	2.110	2.486	2.893	4.094	4.663	5.008	5.554	5.936	6.288	6.835	**$Sin^2 Θ_7$ / $Sin^2 Θ_2$ =4.108 here 7th and 2nd**
2*ratio	2	2.98	4.22	4.97	5.79	8.19	9.33	10.02	11.11	11.87	12.58	13.67	
Near integer	2	3	4	5	6	8	9	10	11	12	13	14	
Miller Planes	110	111	200	102	112	202	300	3,01,211	311	222	302	321	
d (hkl)	7.4232	6.0663	5.1018	4.7000	4.3572	3.6625	3.4320	3.3117	3.1446	3.0418	2.9553	2.8347	

Table 3.2- PXRD data analysis of Form II

Peak No.s	**1**	**2**	**3**	**4**	**5**	**6**	**7**	**8**	**9**	**10**	
2Θ deg	11.622	14.582	17.332	18.762	20.122	23.602	26.142	27.482	30.352	33.722	
Θ deg	5.811	7.291	8.666	9.381	10.061	11.801	13.071	13.741	15.181	16.861	
Θ in radian	0.1014	0.1273	0.1513	0.1637	0.1756	0.2060	0.2281	0.2398	0.2650	0.2943	
sin Θ	0.1012	0.1269	0.1507	0.1630	0.1747	0.2045	0.2262	0.2375	0.2619	0.2901	
$Sin^2 Θ$	0.0103	0.0161	0.0227	0.0266	0.0305	0.0418	0.0511	0.0564	0.0686	0.0841	**$Sin^2 Θ_7$ / $Sin^2 Θ_2$ =4.08 here 6th and 1st**
$Sin^2 Θ_n$ / $Sin^2 Θ_1$	1	1.488	2.098	2.455	2.820	3.865	4.727	5.214	6.337	7.775	
2*ratio	2	2.98	4.20	4.91	5.64	7.73	9.45	10.43	12.67	15.55	
Near integer	2	3	4	5	6	8	9	10	13	16	
Miller Planes	110	111	200	102	112	202	3,01,211	301	302	400	
d (hkl)	7.614	6.074	5.116	4.729	4.412	3.769	3.689	3.408	3.245	2.943	

3.3.2 Study of polymorphism in solution state

It was observed that the 2-substituted-4H-benzo[d][1,3]oxazin-4-ones remains as a mixture of monomer and dimer in equilibrium and the corresponding dimerization constants are also evaluated. The obtained data suggested considerable amount of dimers is present in the solutions. Apparently the obvious question rose how the dimers got such extra stability with the weak C=O--H bond. It is known that cooperative interaction of weak forces influences many physico-chemical properties. We thought it necessary to search some other reasons, if any, are responsible for the observed higher than expected concentration of dimers in the solution state. In the study of solid state morphology we found two polymorphic phases of almost similar crystalline nature. We intended to refine our search for dimer; in the following paragraphs we shall narrate details of our study with the findings.

3.3.2.1 UV Spectrometric Study

The solution of the compound 2-methyl-4H-benzo[d][1,3]oxazin-4-one in the stated solvents were refluxed for two hours. The UV-spectra of the solutions were recorded at room temperature along with the corresponding unrefluxed solutions. In Figure 3.8 the UV spectrum is shown in solvents, water, methanol and chloroform. It is observed that the spectra is exhibiting slight shift in λ_{max} to higher values concomitant to the change in OD. The differences are found to be prominent in methanol solution.

The change of the spectra is little bit more prominent in methanolic solution. Different concentrations of compound 2-methyl-4H-benzo[d][1,3]oxazin-4-one in methanol is subjected to the same process as stated above and the data were plotted together as shown in Figure. 3.9. The spectra indicated a hidden isosbestic point below 230nm and another one near 330nm to 350nm indicating that substances in the solution are in equilibrium and are convertable to one another.

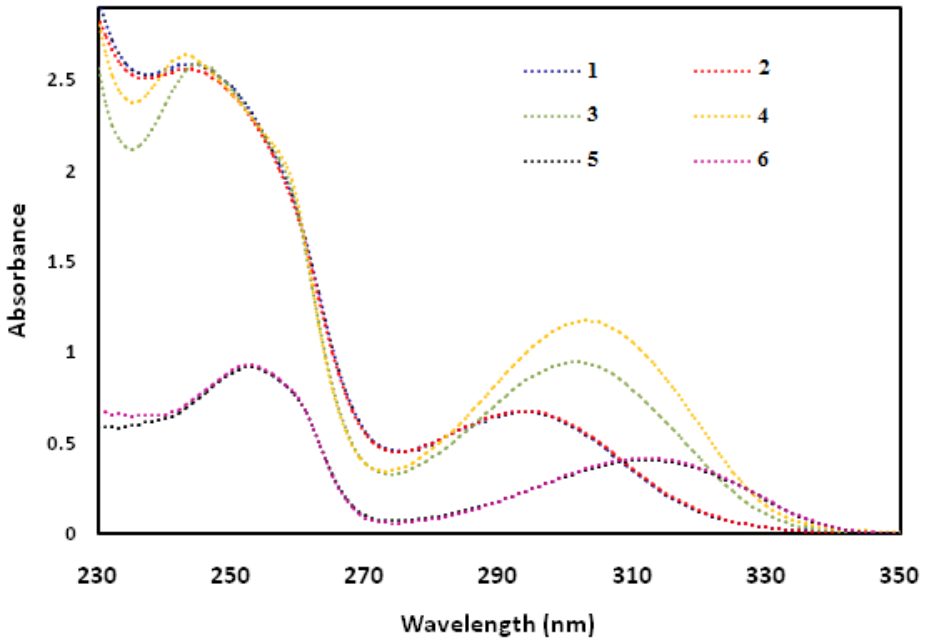

Figure 3.8: UV-spectra of 2-methyl-4H-benzo[d][1,3]oxazin-4-one before and after reflux in H_2O (1-before reflux & 2-after reflux), CH_3OH (3-before reflux & 4-after reflux) and $CHCl_3$(5-before reflux & 6-after reflux).

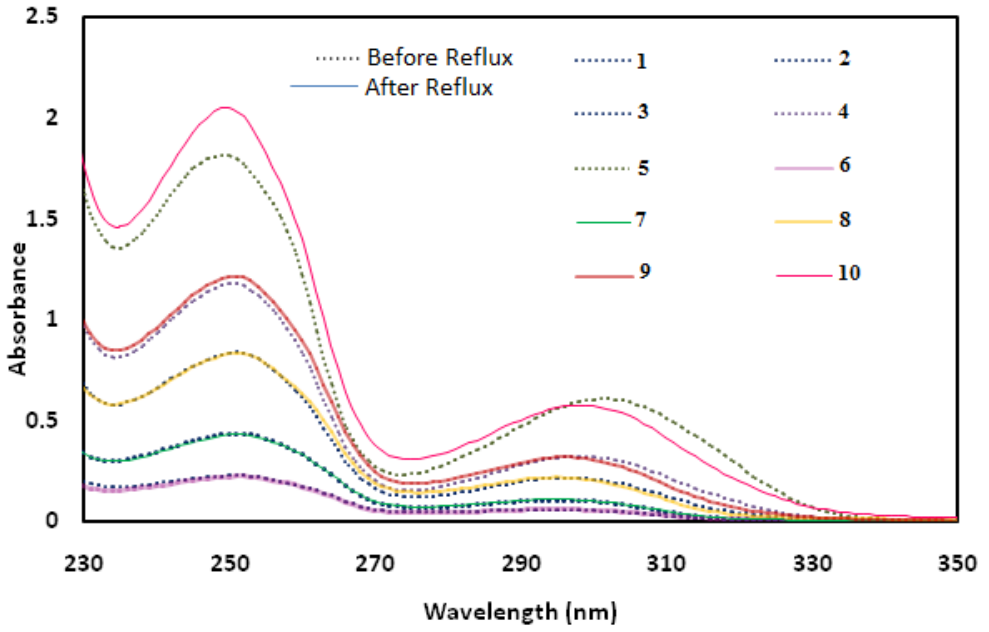

Figure 3.9: UV-spectra of 2-methyl-4H-benzo[d][1,3]oxazin-4-one in CH_3OH at concentrations 4.5E-04 (1-Before reflux, 6- After reflux), 9.16E-04 (2-Before reflux, 7- After reflux), 1.83E-03 (3-before reflux, 8- after reflux), 2.75E-03 (4-Before reflux, 9- After reflux) and 4.58E-03 (5-Before heating, 10- After heating) respectively (dotted line- without reflux and solid line- cooled after reflux).

To have more clearer indication of the existence of metamorphism, the average molar extinction coefficients, before and after reflux, of the spectra within 230 to 330nm were plotted against molar concentration (in terms of monomer) Figure 3.8. Two distinct set of values are found which when fitted in the dimer equation yielded two dimerization constants, 2.35E+03 and 4.32E+02 respectively (as shown in Figure 3.10). The monomer dimer equilibrium constant as calculated earlier is close to the second value which indicates the first is a kienetically formed dimer and the second is the thermodynamically formed dimer.

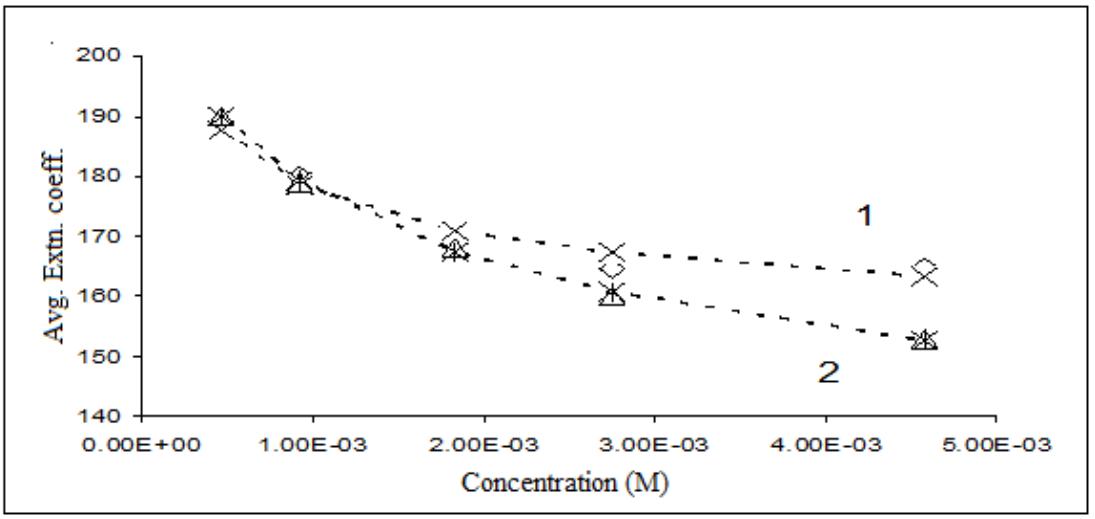

Figure. 3.10: Average extinction coefficient vs Molar Conc in terms of monomer of 2-methyl-4H-benzo[d][1,3]oxazin-4-one ; the trend line with K values (1) 2.35 X 10^3 and (2) 4.32 X 10^2 respectively.

Notably, the time scan Uv-spectra of the compound 2-methyl-4H-benzo[d][1,3]oxazin-4-one in methanol at 40^0C shows a gradual increase of OD from 0 to 60 minutes as depicted in Figure 3.11 . The time dependent change of OD of the spectra showed a linear relation (Figure 3.12) both of which are indicative of the presence of the monomer in some sort of equilibrium with two species of the dimer as D↔2M↔D* as presented in Figure 3.13. The average OD vs time plot in (Figure. 3.12) shows a linear relation which is similar to the zeroth order kinetics of conversion of one dimer to the other. This observation can be explained as both the dimers are linked via the monomers in between

(D↔2M↔D*). The time dependent change in OD is similar to that described by Barnett et al.

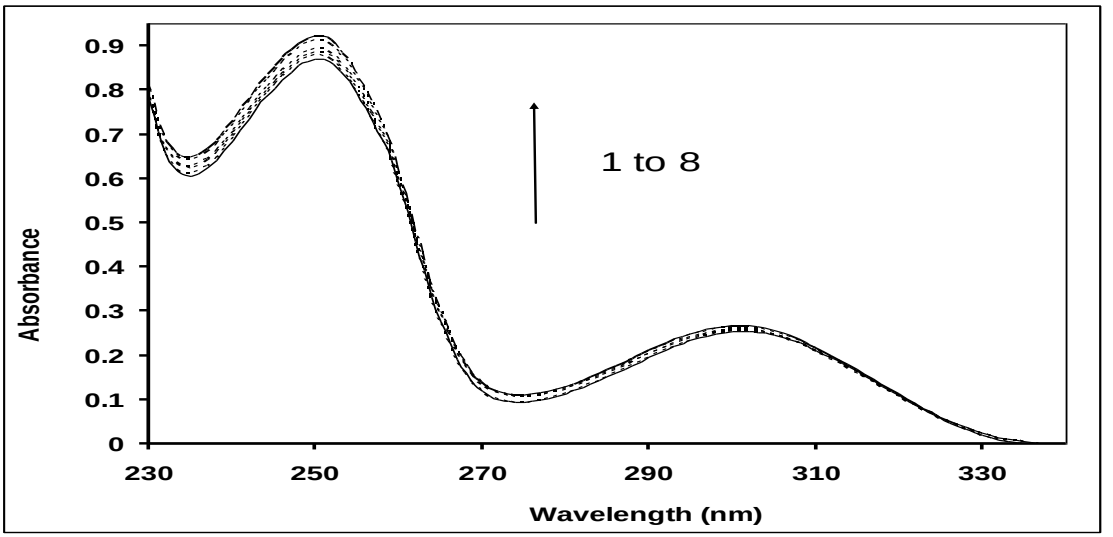

Figure 3.11- Time scan UV-spectra of 2-methyl-4H-benzo[d][1,3]oxazin-4-one in methanol at 40^0C at intervals 0,5,10,25,30,40,45 and 60 mins (1 to 8).

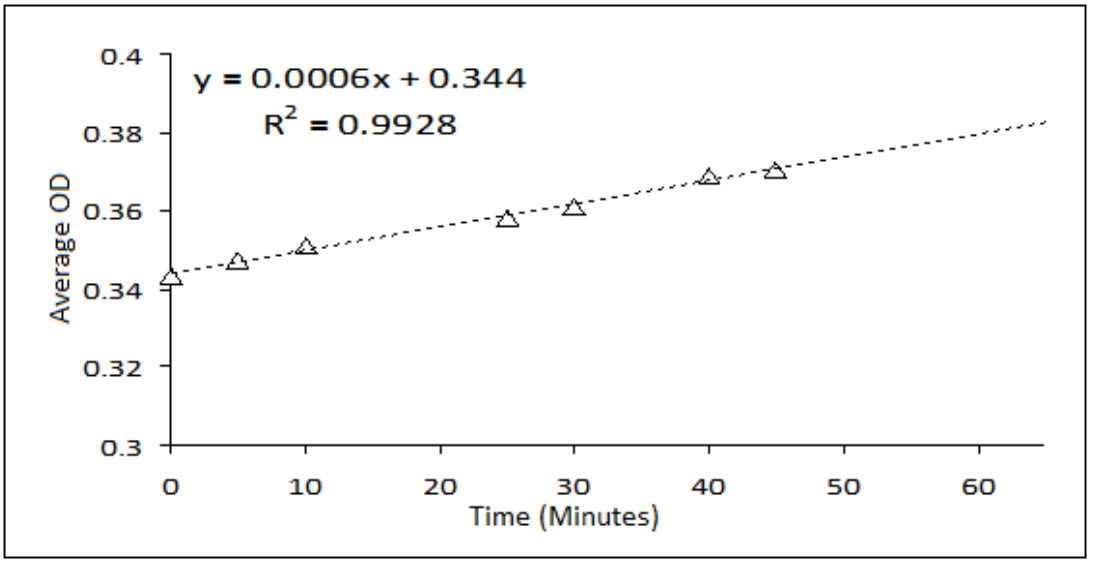

Figure 3.12- Average OD (230 to 330 nm) versus time (min) of 2-methyl-4H-benzo[d][1,3]oxazin-4-one in methanol

The concomitant polymorphs of 3-Acetylcoumarin was found to depend on the crystallization temperature in the 1:1 chloroform/hexane solvent system by Munshi et al. They also observed that one form in a *head to head* configuration was stabilized by C-H-O and C-H- interactions while other form in a *head to tail* configuration of the molecules in the crystal lattice was stabilized by only C-H-O interactions (Munshi *et al.*, 2004).

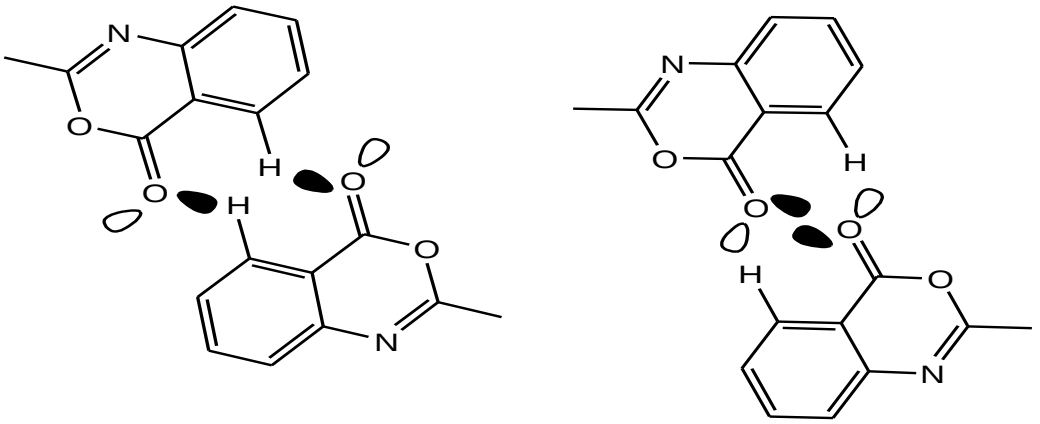

Figure 3.13: Predicted pattern of Dimeric association in 2-Substituted benzo[d] [1, 3] oxazin-4-ones.

These structures are drawn tentatively (Figure 3.13) since direct evidence is hard to gather. The unconventional hydrogen bond C-H$\cdots\pi$ interaction is also noticed because of its role as the driving force in determining crystal packing and molecular conformation (Desiraju, 1996; Steiner, 1997; Wahl & Sundaralingam, 1997, Morita *et al.*, 2006). So, it will be of genuine interest to highlight the observations as cited above suggesting the existence of C=O---H-C H-bonds in the dimers along with directional property of H-bond. Solvent induced self assembly and relative occurance of its polymorphic form in 2,6-dihydroxybenzoic acid is reported by Davey (Davey, 2001) In the present system the effect of solvent is prominent. However, the identification of two dimers was not possible by the HPLC.

3.3.2.2 NMR study

In diffusion-ordered NMR spectroscopy (DOSY), in which one dimension represents chemical shift data while the second dimension resolves species by their diffusion properties pseudo separation is possible depending on different diffusion properties of the constituent solutes in solution. This powerful tool for identifying individual

species in a multi-component solution—earned the nickname "chromatography by NMR." (Li *et al.*, 2009) Based on this belief, we extended our efforts to utilize DOSY techniques to characterize the presence of dimer in solution. Figure 3.14 shows a representative DOSY NMR spectrum which provides further evidence for the existence of the dimer along with the monomer.

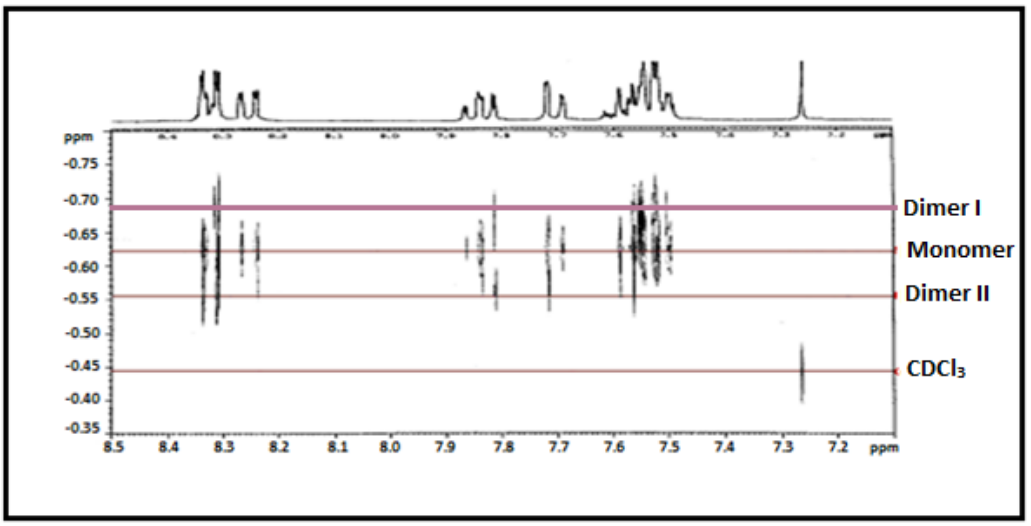

Figure 3.14: DOSY NMR spectra showing the existence of monomer and dimer species

In the DOSY spectra, in addion to the solvent and the monomer, two other species of slightly different diffusion coefficients were observed as we assumed these two species are there to prove the existence of two dimers.

The study of intermolecular interactions always has drawn fascination of the scientists in all fields of chemistry, physics and biology. During the last decades, lots of sophisticated instrumental methods were developed to monitor such phenomena. Of late, there is a paradigm shift in organic chemistry to ponder beyond the covalent bonds. The study of weak interactions becomes necessary to study the supra-molecular framework. The effect of very weak inter-molecular interaction in organic reactions also becomes a frontier topic of the organic chemistry.

Chapter 4

Impact of dimers of 2-substituted-benzo[d][1,3]oxazin-4-ones on Antibacterial activity

Chapter 4

Impact of dimers of 2-substituted-benzo[d][1,3]oxazin-4-ones on Antibacterial activity

---

4.1 Introduction

In the preceding chapter, the existence of dimers in solution state was discussed. In the present chapter, the effect of the dimers on antibacterial activities is explored. The importance of such study lay in the fact that most of the drug molecules are capable of forming self association, while the effect of self association on drug action is not properly investigated. However, the dimerization of semisynthetic eremomycin derivatives and their effect on antibacterial activity was studied by Mirgorodskaya *et al* (2000)**.** Many classes of cytotoxic agents that have the potential to become effective anticancer drugs are hydrophobic, a property that is typically associated with poor solubility in aqueous medium (Khan *et al.,* 2006). The limited water solubility of hydrophobic compounds results from their propensities to form self-association. The key factor toward achieving highest activity is bioavailability, a factor that is likely to be impacted by self-association properties of the drug. Hence, it was important to understand compound's self-association/dimerization behaviour in solution and examine how this behaviour correlates with antibacterial activity.

4.2 Materials and methods

4.2.1 Reagents and Chemicals

All the chemicals and reagents used in the experiment were of analytical grade (AR) and purchased from E. Merck, India. The growth media or its components used were purchased from HiMedia, India.

4.2.2 Maintenance of bacterial strain

For short-term preservation and routine use, stock bacterial culture were maintained on Nutrient agar (NA) slant containing peptone,10 g/l; yeast extract, 5 g/l; NaCl, 10 g/l; and agar 15g/l, at pH 7.0. LB agar medium was sterilized by autoclaving at 121 °C for 20 minutes and 4 ml was transferred into the test tubes to form LB agar slant. A loopful of bacterial cultures from the stock samples was streaked on LB agar slant and incubated at 37 °C for 24 h. The cultures were stored in the refrigerator at 4 °C. For long-term preservation, cultures in 10-15% glycerol were stored at -20 °C and sub-cultured after every 3 months.

Bacterial strains and growth experiments

All experiments were done using the strains *Escherichia coli K12, Bacillus subtilis, Staphylococcus aureus,* and *Pseudomonas aeruginosa* 2257. Fresh inoculum was prepared by transferring a single colony of 24 h old cultures into 10 ml sterile nutrient broth (pH 7.0) in 100 ml Erlenmeyer flask. The inoculated medium was incubated at 37°C for 4 h with agitation. The culture was harvested by centrifuging at 8000 rpm for 5 min at 4 °C and washed twice with sterile phosphate buffer saline (PBS) to remove traces of media if any. The washed pellet was finally suspended in 3 ml sterile PBS. Aliquots of approximately 10^4 cells were added to 10 ml of nutrient broth in Erlenmeyer flask. The flask was kept at 37°C (with shaking at 200 rpm) throughout the period of investigation. Survivability of cells in LB was assessed through dilution-plating of pure culture aliquots at different time intervals on fresh LB agar plates. The number of cells present on that particular colony was also enumerated using dilution-plating technique.

4.2.3 Determination of Minimum Inhibitory Concentration (MIC)

The antibacterial activity was assayed against different bacteria *Escherichia coli K12, Bacillus subtilis, Staphylococcus aureus, and Pseudomonas aeruginosa* 2257 by turbidometric method. The test compound was dissolved in DMSO (SRL Extra pure) to prepare the stock solution and aseptically used for experiments. The required volume of

stock solution was transferred to tubes containing a defined volume of nutrient broth to achieve a desired concentration of the compound. The concentrations of the tested compound were 100, 400, 600, 800 and 1000 µg/ml in comparison to the standard drug ampicillin. Control set was contained DMSO, respective of each experimental tubes. A loopfull of bacterial culture from 24 h old slant was transferred to 10 ml of nutrient broth (Himedia M502) and incubated at 37 ^{0}C for 4 h. The tubes in duplicate containing 5ml nutrient broth were inoculated with 0.1 ml of 4 h liquid culture. The tubes containing nutrient broth were incubated at 37 ^{0}C for 16 h and the relative growths in the tubes were determined turbidometrically in the spectrophotometer. Taking the growth in tubes without drug as 100% (X), the percent growth (Y) in presence of studied compounds at particular concentration was calculated by the formula: (OD_{540} of the tube with drug / OD_{540} of the tube without drug)* 100. The inhibition % was calculated as X-Y (Nanda *et al.,* 2007).

4.2.4 Growth curve and Growth Kinetic study of *E. coli* K12 in presence of 2-substituted-benzo[d][1,3]oxazin-4-ones

The overnight culture of *E. coli* K12 (in NB medium), that were inoculated with a freshly grown single colony, was diluted 100-fold into 10 ml NB medium and allowed to grow for 4h to obtain log phase cells. The culture was then inoculated into 1000 ml NB medium and divided into five portions (C1, E1, E2, E3 and E4). Further each portion was distributed in four separate sterilized Erlenmeyer flasks and labelled as 100, 400, 600 and 800 (numerical represented their concentrations in µg/ml). Then to each labelled flask appropriate volume of compound was added from stock solution to achieve the desired concentration, while in C1 portion flasks only respective volume of DMSO was added (control). All Erlenmeyer flasks were incubated at 37^{o}C with shaking. Growth of *E. coli* K12 was quantified in terms of optical density at different time interval. (Miller, 1972). Culture was prepared as mentioned above. At different time intervals, cultures were withdrawn from time-defined flasks (both control and test) for measuring optical density. The growth rate constant was determined in between 4 to 6 hours in each case.

4.2.5 Mathematical evaluation of Dimerization on antibacterial activity

In order to separate the activity of the monomer and dimer we used the following equations: 2M=D, $K=[D]/[M]^2$; M+S = MS, K'=[MS]/[M]*[S]; D+S=DS, K''=[DS]/[D]*[S]; I=p*[M]+q*[D]; C=[M]+[MS]+2[D]+2[DS]; where M, D and S are monomer, dimer and bacterial substrate respectively and K, K' and K'' are corresponding association constants; I is the observed bacterial growth inhibition per mole, p and q are the corresponding contributions by the monomer and dimer respectively and C is the concentration in terms of monomer. With the consideration that the mole fraction of the bacterial drug absorbing surface is supposed to be one, hence [S] is considered as unity in the equilibrium equation, [S]≈1. The mathematical model used for evaluation of bacterial inhibition for the monomer and dimer separately:

$$M + \mathrm{M} = \mathrm{D} \quad (1)$$

$$\mathrm{K} = \frac{[\mathrm{D}]}{[\mathrm{M}]^2} \quad (2)$$

$$M + \mathrm{S} = \mathrm{MS} \quad (3)$$

$$\mathrm{K}' = \frac{[\mathrm{MS}]}{[\mathrm{M}][\mathrm{S}]} \quad (4)$$

$$[\mathrm{D}] + [\mathrm{S}] = [\mathrm{DS}] \quad (5)$$

$$K'' = \frac{[\mathrm{DS}]}{[\mathrm{D}][\mathrm{S}]} \quad (6)$$

$$\mathrm{I} = \mathrm{p} * [\mathrm{M}] + \mathrm{q} * [\mathrm{D}] \quad (7)$$

$$\mathrm{C} = [\mathrm{M}] + [\mathrm{MS}] + 2[\mathrm{D}] + 2[\mathrm{DS}] \quad (8)$$

$$\mathrm{C} = [\mathrm{M}] + \mathrm{K}'[\mathrm{M}] + 2[\mathrm{D}] + 2\mathrm{K}''[\mathrm{D}]$$

$$\mathrm{C} = (1 + \mathrm{K}')[\mathrm{M}] + 2(1 + \mathrm{K}'')[\mathrm{D}]$$

$$= (1 + K')[M] + 2K(1 + K'')[M]^2$$

$$[\mathrm{S}] \approx 1 \text{(Considered)}$$

$$2K(1+K'')[M]^2 + (1+K')[M] - C = 0 \qquad (9)$$

By putting, $m = (1+K'')$ and $s = (1+K')$

The eqn 9 turns to, $2Km[M]^2 + s[M] - C = 0$

$$[M] = \frac{-s+\sqrt{s^2+8KmC}}{4Km} \qquad (10)$$

Substituting [M] in equation (7) we get -

$$I = \left[\left\{p + q.K\left(\frac{-s+\sqrt{s^2+8KmC}}{4Km}\right)\right\}.\left(\frac{-s+\sqrt{s^2+8KmC}}{4Km}\right)\right]$$

4.3 Results and Discussion

4.3.1 Determination of Minimum Inhibitory Concentration (MIC)

The antibacterial activities of the synthesized compounds were evaluated against four bacteria, *E. coli* K12, *Pseudomonas aeruginosa* 2257, *Staphylococcus aureus* and *Bacillus subtilis*. MIC value of each synthesized compounds against bacterial culture is given in Table 4.1. The obtained MIC of 3-aryl-deneamino-2-phenyl-quinazoline-4-(3H)-one was matched with the previous report. But, to assist interpretation of sensitivity of compounds 2-substituted-benzo[d][1,3]-oxazine-4-one (1a-1d), an in-vitro breakpoint *i.e.* > 1000 µg/ml for these compounds were assigned. From this data MIC breakpoint of > 1000 µg/ml has found for these compounds only against *E. coli* K12, however they did not show any inhibitory effect against other three bacteria.

4.3.2 Growth kinetics of *E. coli* K12 in the presence of compound 1a-1d

As it was intended to explore the effect of the dimers on antibacterial activities, growth kinetics was studied at different concentration of 2-substituted benzo[d][1,3]-oxazine-4-one against *E. coli* K12. The increase in OD at 540 nm, which represents growth of *E. coli* K12, was plotted against time at different concentrations (Figure 4.1).

Table 4.1 Antibacterial activity (MIC) of synthesized compounds 1a-1d, 2a and 3a-j.

Compound	**R**	**Gram-negative**		**Gram-positive**	
		E. coli K12 (µg/ml)	*P. aeruginosa* 2257(µg/ml)	*S. aureus* (µg/ml)	*B. subtilis* (µg/ml)
1a	-	> 1000	ND	ND	ND
1b	-	> 1000	ND	ND	ND
1c	-	> 1000	ND	ND	ND
1d	-	> 1000	ND	ND	ND
2a	-	400	800	ND	400
3a	2′′-OH	200	300	200	300
3b	4′′-OCH_3	200	200	200	100
3c	4′′-F	200	200	100	200
3d	4′′-$N(CH_3)_2$	100	200	100	100
3e	4′′-Cl	200	300	100	100
3f	3′′-OCH_3	400	200	200	100
3g	4’-OH	400	300	200	300
3h	3′′-OCH_3, 4′′-OH	100	500	200	200
3i	3′′-NO_2	200	200	300	200
3j	H	200	500	100	100

ND- Not Defined

The corresponding growth rate constants (µ) were determined within time interval of 4-6 hours (Figure 4.2). The results revealed that growth and growth rate constants decreased with increasing concentrations of the compound(s). The results revealed that 1a was the only compound which showed significant inhibition against *E. coli* K12. Lysis of bacterial cells is observed in the death-phase. The phase contrast microscopic image shows some morphological changes suggestive of distortion of bacterial cell as well. So, we have used *E. coli* K12 as model organism for further study.

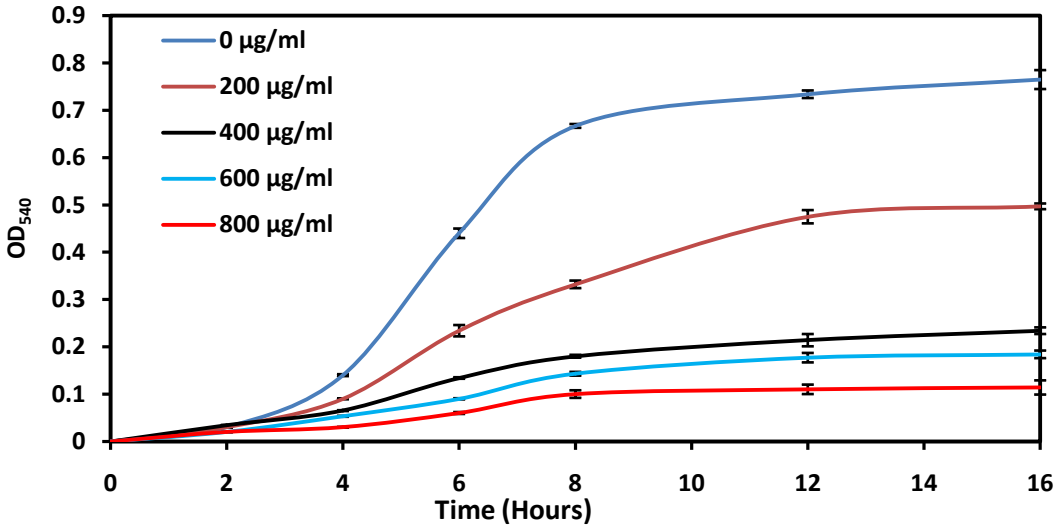

Figure 4.1(a): Growth curve of *E. coli* K12 in presence of 2-phenyl benzo[d] [1, 3] oxazin-4-one **(**1a).

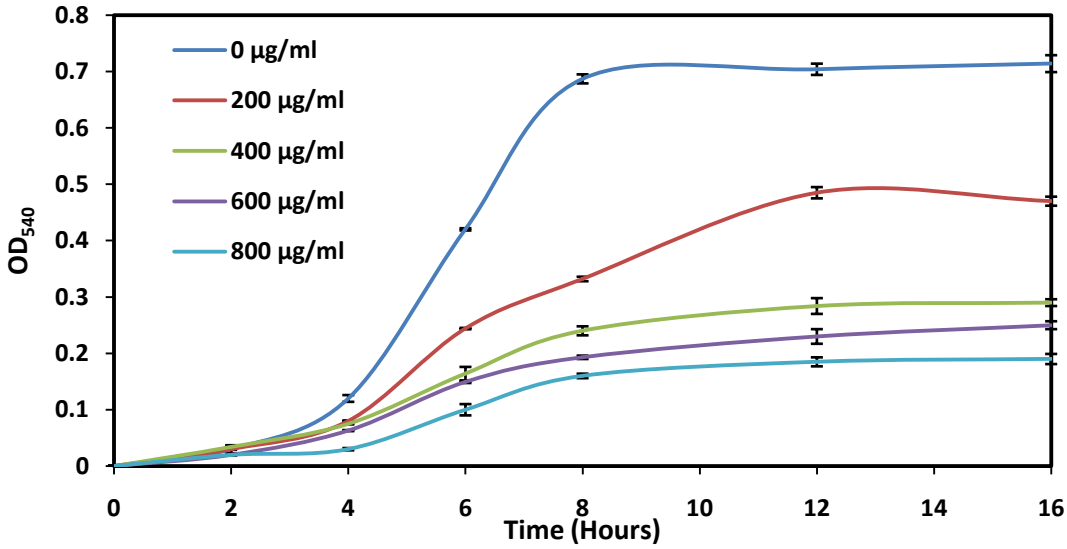

Figure 4.1(b): Growth curve of *E. coli* K12 in presence of 2-p-tolyl-benzo[d] [1, 3] oxazin-4-one **(**1b).

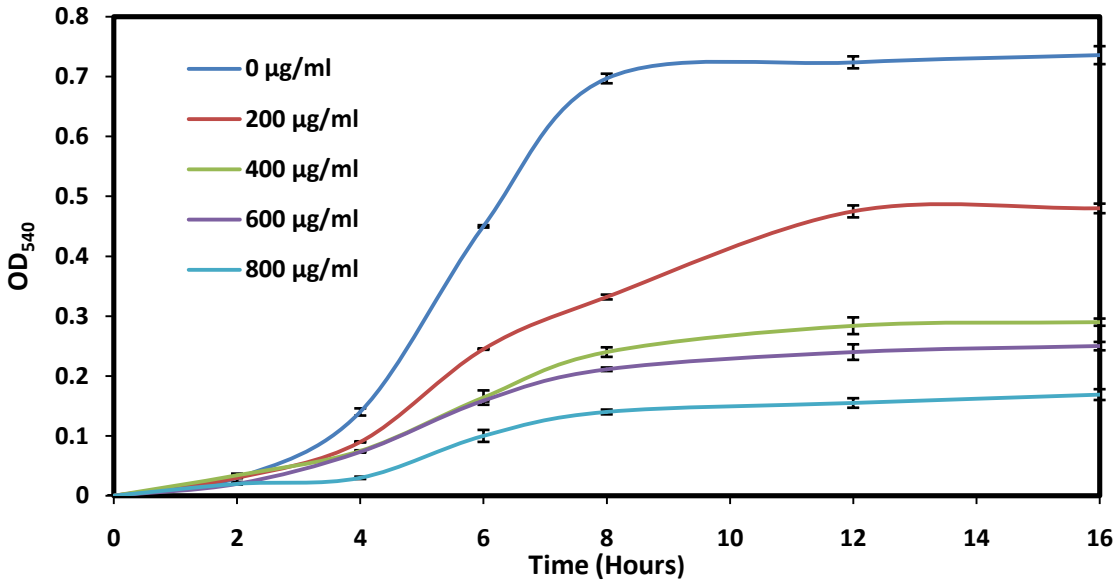

Figure 4.1(c): Growth curve of *E. coli* K12 in presence of 2-p-chlorophenyl-benzo[d] [1, 3] oxazin-4-one (1c).

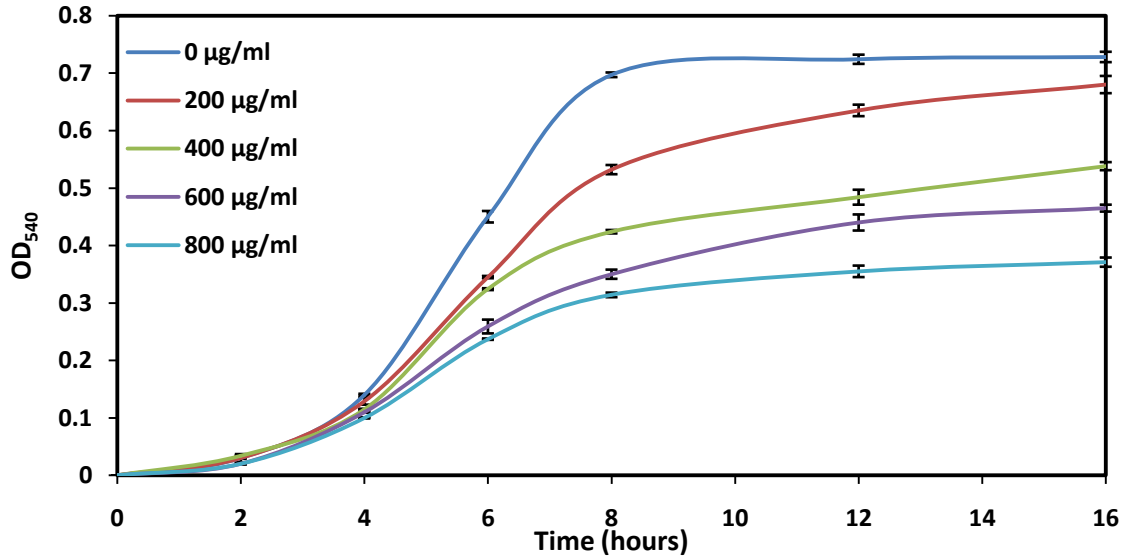

Figure 4.1(d): Growth curve of *E.coli* K12 in presence of 2-p-chlorophenyl-benzo[d] [1, 3] oxazin-4-one (1d).

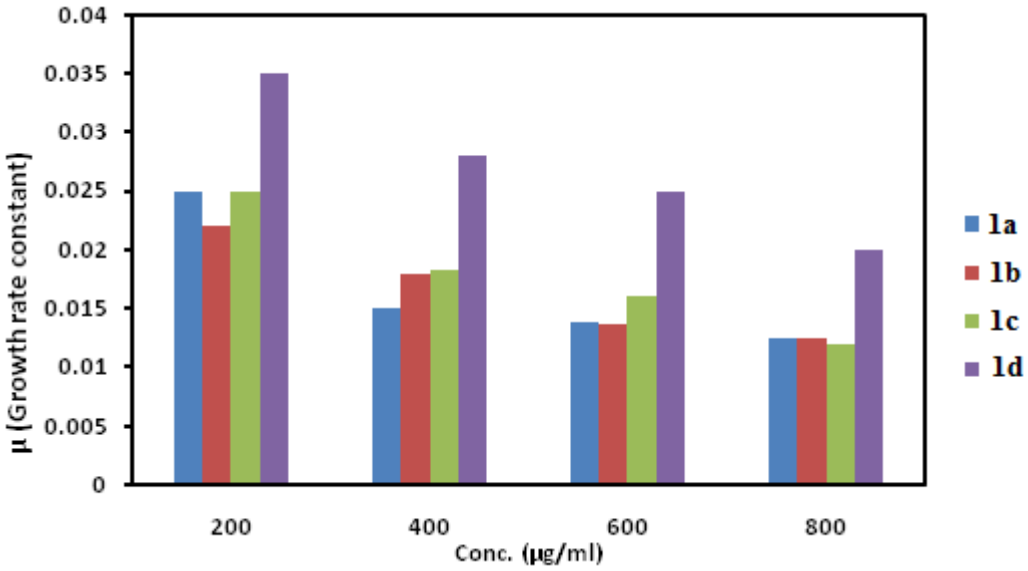

Figure 4.2: Representation of Growth rate constants of *E. coli* K12 in presence of compounds 1a, 1b, 1c and 1d

4.3.3 Impact of Dimerisation on Bacterial Inhibition

To study the effect of dimerization on antibacterial activity, the antibacterial activities of the compounds were assayed against the gram negative bacteria *E. coli* K12. Figure 4.3 shows the percent inhibition (percent of inhibition respective to control) of bacterial growth in presence of studied compounds at different concentrations.

It is apparent from the plot that the change of percent inhibition of the compound 1d at different concentration is minimal, while compound 1a and 1c have the higher values. The percent inhibition values used in this graph when converted to molar inhibition *i.e.* percent inhibition per mole of compound, as obtained by dividing the percent inhibition with the respective mole of compounds in 100, 400, 600 and 800 µg/ml to corresponding molar amount.

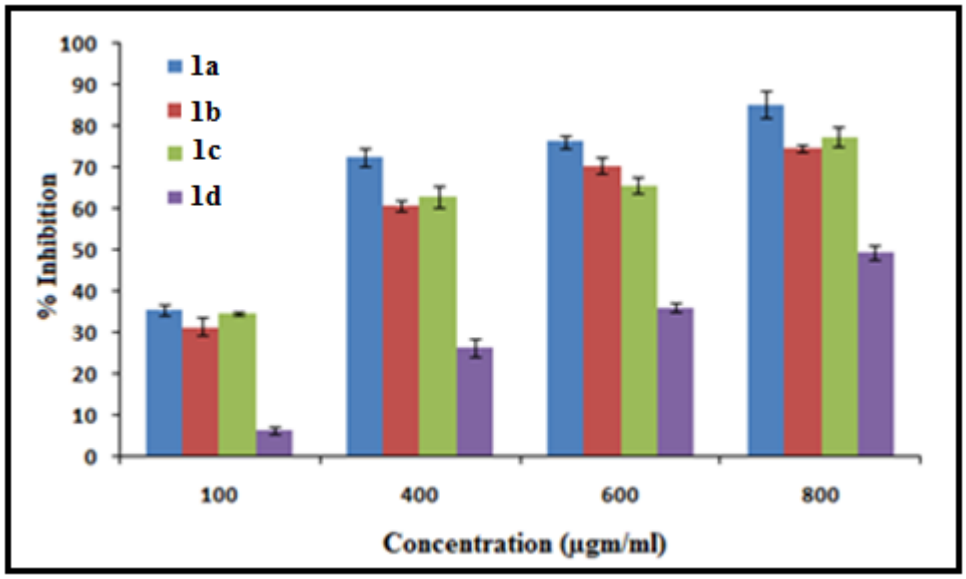

Figure 4.3: Percent Inhibition of bacterial growth against *E. coli* K 12 at different concentrations of compounds (1a-1d).

This chart is interesting because it tells that the compounds' potentiality to antibacterial effect is markedly higher at dilute solution and gradually decreased at higher concentrations. Though when expressed in micrograms the percent inhibition it is found to increase with the increase of the amount of the said compounds (Figure 4.4).

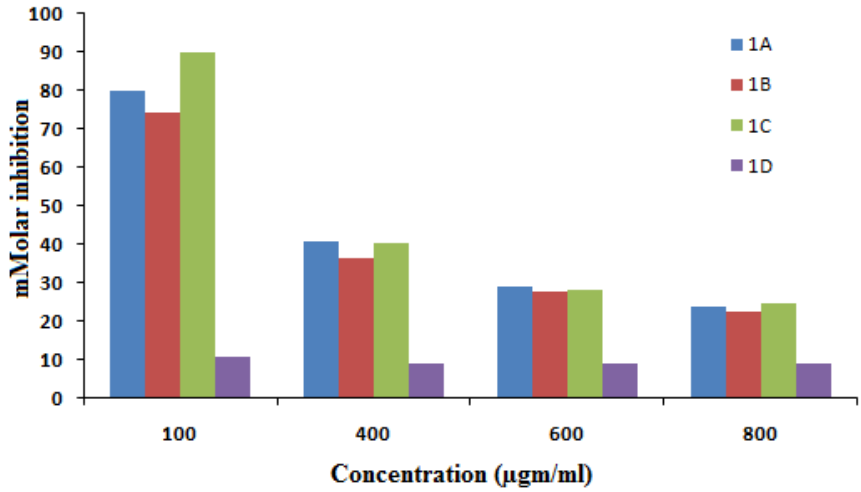

Figure 4.4: mMolar inhibition of bacterial growth (*E. coli* K12) at different concentrations of compound 1a - 1d.

To the best of our knowledge no other studies have expressed percent inhibition in molar terms. But we find it convenient to judge the antibacterial property at different concentrations in molar term. This term clearly states that the property per mole in different set of concentrations.

The apparently new phenomenon is similar to monomer dimer equilibrium in solution, where percent of monomer increases with dilution. Similar pattern was also observed in previous studies. Similar to the present study, earlier authors have found more monomer of antitumour agent novatrone (mitoxantrone) drug in higher dilution (Davies *et al.,* 2000). In fact this observation forced us to the search of monomer dimer equilibrium in solution for the studied compounds. For the sake of rational arrangement of the chapters we described such studies in the earlier part of the thesis.

The observed molar inhibition values are fitted in the derived equation at different concentrations. A good fit was observed in all cases.

Table 4.2: Association constants of monomer and dimer with bacteria (per molar) and coefficients p and q.

Compound	*p*	*q*	*k*	*m*	*s*
1a	1.4E+06	9.1E+03	0.24	1.03	9.4
1b	7.8E+05	0.00013	0.14	1.8	5.8
1c	1.7E+07	0.001	0.17	1.5	10.7
1d	1E+06	15.9	0.21	1.2	1.03

The contribution of monomer to the antibacterial activity, p, is always much higher than that of the dimer, q. These results are the clear mathematical indication that the monomer is mainly responsible for the antibacterial activity. And the expected preponderance of monomer proportion at dilute solution is responsible for the observed higher molar activity at dilute solutions. The electron withdrawing chlorine atom at 4' position in 2-phenyl-ring increased the antibacterial property and electron donating methyl group at this position reduced the property of the monomer.

The dimer activity indicted from the values of q, is negligible but non zero. The monomer – dimer equilibrium constant values (k X 10^4) in bacterial medium are expectedly low in the bacterial medium than that in water. The monomers bind better than the corresponding dimers as ″s″ values are found to be higher than the corresponding ″m″ values (Table 4.2). The nearly flat nature of the molar inhibition property (Figure 4.4) of the compound 1d can now be safely assigned to be due to the monomer buffering effect originating from the existence of two metamorphic dimers in solution state. The curve fit graph represented that the experimental inhibition has also matched with our observed inhibition percentage (Figure 4.5).

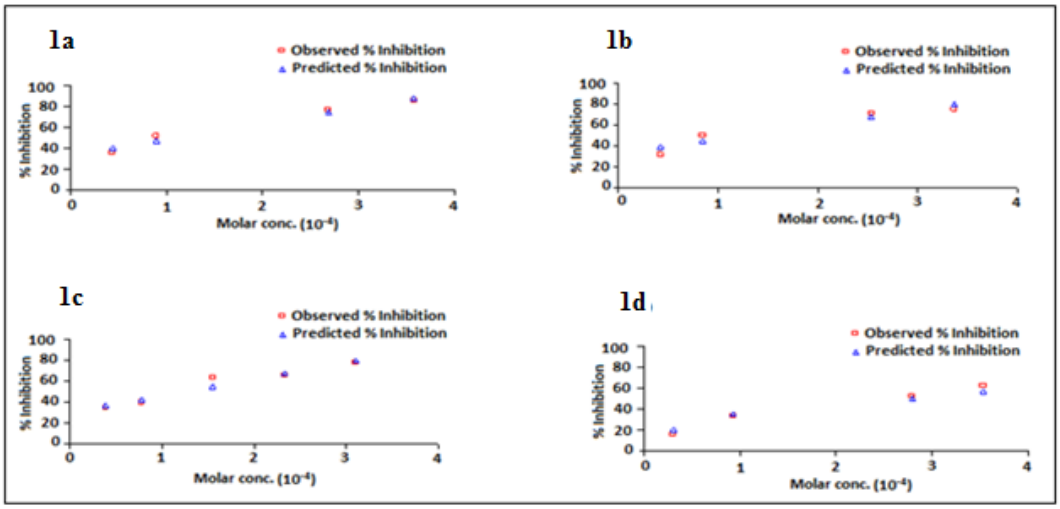

Figure 4.5: Curve fit plot of inhibition percentage against molar concentration of compound 1a, 1b, 1c and 1d.

We have pointed out that there is some intrinsic predicament for achieving much better antibacterial activity (Nanda *et al.*, 2007) of the molecules having this type of pharmacophore. Therefore, in the present study we have tried to address some reasons for that. No a priori work indicted the effect of self association of the drug molecules in their biological activity. In this sense, our method of SAR study is totally new of its kind.

Chapter 5

Anti-proliferative activity, Molecular Docking and inhibition of Human Dihydrofolate reductase enzyme shown by Quinazoline-4(3H)-ones

Chapter 5

Anti-proliferative activity, Molecular Docking and inhibition of Human Dihydrofolate reductase enzyme shown by Quinazoline-4(3H)-ones

5.1 Introduction

Cancer is considered as one of the major clinical and public health problem. Cancer may be defined in three phases (i) aggressive- cells can grow and divide without respect to normal restrictions, (ii) invasive - adjacent tissues can be invaded and destroyed and/or (iii) metastatic - spread to further locations in body (Baba *et al.*, 2007). Conversely, benign tumors are self-limited in their growth and do not invade or metastasize and differentiate them from malignant properties of cancer. Cancer is known to affect people at all ages, even fetuses, but possibilities for the more common varieties have a tendency to increase with age. At present, cancer is considered as a leading cause of death worldwide. It is reported that in 2008 about 13% of all deaths (accounted for 7.6 million deaths) occurred due to cancer and more than 70% of all deaths occurred in low and middle income countries. It is now counted among five leading causes of death (American Chemical society, 2007). Cancer morbidity reached upto nine million people worldwide by 2015. Furthermore, deaths from cancer worldwide are projected to rise over 11 million in 2030 as per WHO Cancer Fact sheet No 297 February 2011. It is well known that conventional anticancer drug discovery and development processes have selected agents that had significant cytostatic or cytotoxic activity on tumour cell lines. The drug discovery was mainly focused on development of cytotoxic agents. These agents play a vital role in inhibiting metabolic pathways critical to cell division (Florea *et al.*, 2011).

The advances in history of cancer chemotherapy are shown in Figure 5.1, where most popular and effective drug methotrexate and 5-flurouracil were invented in 1950-60. With the current chemotherapy, lack of selectivity of chemotherapeutic agents against

cancerous cells is a significant problem. However, advances in the fields of drug discovery and cell biology are facilitated by the developments of Computer-Aided Drug Design. To facilitate the discovery of novel therapeutic agents, Computer-Aided Drug Design (CADD) assist to discover novel chemical entities with the potential to be developed into novel therapeutic agents. Thus, modern computational-aided drug design established a novel platform by which researchers perform in-depth *in silico* simulation prior to labour-extensive wet-lab validation (Zhang, 2009).

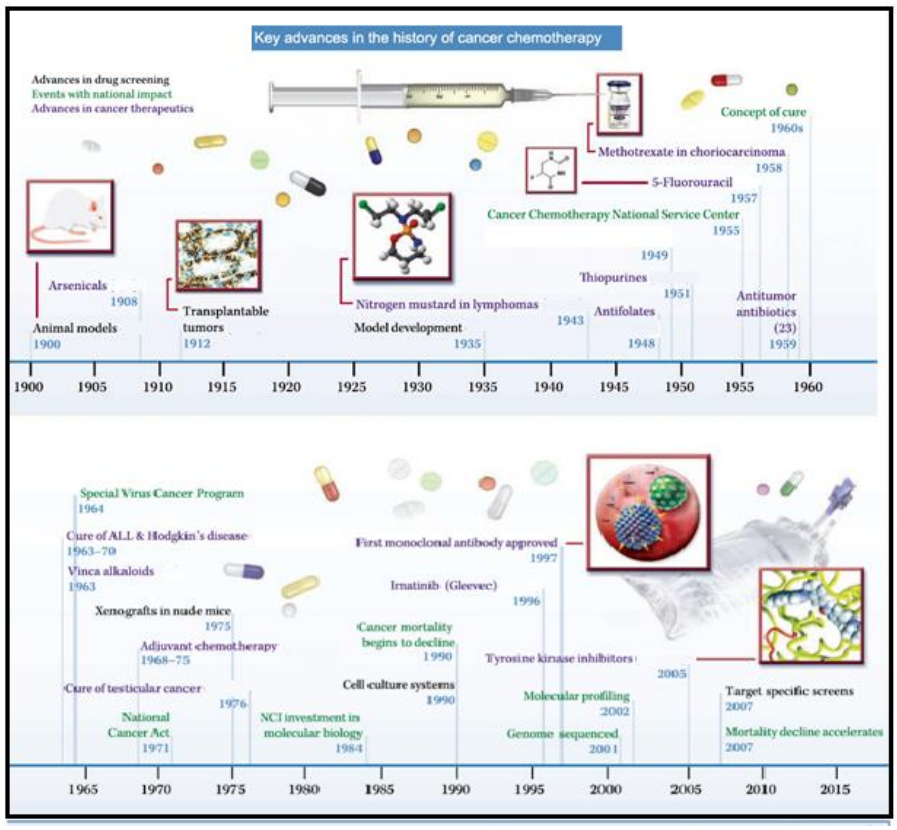

Figure 5.1: Representation of the key advances in the history of cancer chemotherapy.

5.1.1 Computer Aided Drug Design

5.1.1.1 Importance of computer-aided-drug design in medicinal chemistry

The strategy of medicinal chemists in their research is to discover new chemical entities which maximally resemble existing drugs with respect to key physicochemical and biological properties, with the knowledge that the quest for 'drug-like' properties may indeed help achieve good pharmacokinetic and pharmaco-dynamic properties **(**Hughes, 2011**).** In this regard, Computer-aided drug design plays a vital role in drug discovery and development and has become an indispensable tool in the pharmaceutical industry. Computational medicinal chemists can take advantage of all kinds of software and resources in the computer-aided drug design field for the purposes of discovering and optimizing biologically active compounds (Liao *et al.,* 2011). Thus, Computer-aided drug discovery/design methods have played a major role in the development of therapeutically important small molecules for over three decades.

5.1.1.2 Evaluation of Drug likeliness and ADME/Tox

In silico prediction of properties like, absorption, distribution, metabolism and excretion (ADME) by employing theoretical models play progressively more important roles in support of the drug development process (Hou & Wang, 2008). The importance of optimizing the ADME properties has been widely recognized in determining potential drug candidates. Generally, the evaluation of a drug is determined not only by good efficacy and specificity, but also by having acceptable ADME and toxicity properties (ADMET) (Tetko *et al.,* 2006). At the early stage , ADME predictions generally center on simple ADME or ADME-related properties, such as octanol-water partitioning coefficient (logP), apparent partition coefficient (log D), intrinsic solubility (logS), etc. and more complex ADME properties such as human intestinal absorption, blood-brain partitioning, oral bioavailability, clearance, volume of distribution and metabolism (Hou *et al.,* 2008). To exercise a pharmacological effect in tissues, a compound has to penetrate various physiological barriers, such as the blood–brain barrier, gastrointestinal barrier, and the microcirculatory barrier, to reach the blood circulation. Thereafter, it is

transported to its effectors site for distribution to tissues and organs, degraded by specialized enzymes, and finally removed from the body *via* excretion. The character of a pharmaceutical compound may be described by its pharmacokinetic or ADME properties (Tetko *et al.,* 2006). In addition, genetic variation in drug metabolizing enzymes implies that some compounds may undergo metabolic activation and cause adverse reactions or toxic in humans (Gardiner & Begg, 2006).

Accordingly, the ADME/Tox properties of a compound directly influence its usefulness and safety. The membrane permeability of a compound is determined by a combination of factors including compound size, aqueous solubility, ionizability (pKa) and lipophilicity (log P). The solubility of a neutral compound or of a compound in its non-ionized form is defined as the intrinsic solubility and normally represented as logs (Hou & Wang, 2008). In practice, about 85% of drugs have logs between -1 and -5. Christopher Lipinski carefully studied the physico-chemical properties of 2245 drugs from the World Drug Index (WDI) and found that poor absorption and permeation are more likely to occur when molecular weight <500 g/mol, Clog P< 5, hydrogen bond donors <5 and hydrogen bond acceptors <10 . A 'rule of five' was subsequently proposed with respect to drug likeness. He defined "drug-like" molecules as those that met 3 out of 4 of the following rules: a molecular weight ≤ 500 Da, ≤ 5 hydrogen bond donors, ≤ 10 hydrogen bond acceptors, the sum of N's and O's ≤10 and a ClogP ≤ 5 (MlogP ≤ 4.15) (Lipinski *et al.,* 1997). These rules were extended by other researchers, including Ghose *et al* (1999) and Oprea (2000). However, these rules could only serve as the minimal criteria for evaluating drug-likeness. It has been estimated that 68.7% of compounds in the Available Chemical Directory (ACD) Screening Database (2.4 million compounds) and 55% of compounds in ACD (240 000 compounds) do not violate the 'rule of five' (Hou *et al.,* 2006). It has been reported that the polar surface area (PSA) inversely correlates with the lipid penetration ability (Palm *et al.,* 1997). Compounds that are completely absorbed by humans tend to have PSA values of 60A˚, while compounds with PSA >140A˚ are less than 10% absorbed.

A molecular property is a complex balance of various structural features which determine whether a particular molecule is similar to the known drugs (Lilith *et al.,* 2010). It generally means "molecules which contain functional groups and/or have physical properties consistent with most of the known drugs". These properties, mainly hydrophobicity, molecular size, flexibility and presence of various pharmacophoric features influence the behavior of molecules in a living organism, including bioavailability. Computational chemists have a wide array of tools and approaches available for the assessment of molecular diversity. Diversity analysis has been shown to be an important ingredient in designing drugs. The computational sensitivity analysis and structural analysis have been used to study the drug-likeness of the candidate drug (Mohammed *et al.,* 2010; Mohammed *et al.,* 2011). Therefore, these drug-likeness filters or rules may be useful in the early stage of drug discovery to some extent while they should be used cautiously.

5.1.1.3 Evaluation of Interaction of Drug with target enzyme/receptor

Computer-Aided Drug Design (CADD) also included use of computational methods to simulate drug-receptor interactions. Molecular docking has become an increasingly important tool for drug discovery. Generally, docking is a computational technique that places a small molecule (ligand) in the binding site of its macromolecular target (receptor) and estimates its binding affinity (Yuriev *et al.,* 2011) (Figure 5.2). Many forces are involved in the intermolecular association: hydrophobic, dispersion, or van der Waals, hydrogen bonding, and electrostatic. The major force for binding appears to be hydrophobic interactions, but the specificity of the binding appears to be controlled by hydrogen bonding and electrostatic interactions (Ramesh *et al.,* 2012). The process of docking a ligand to a binding site tries to mimic the natural course of interaction of the ligand and its receptor *via* a lowest energy pathway (Ferreira *et al.,* 2015).

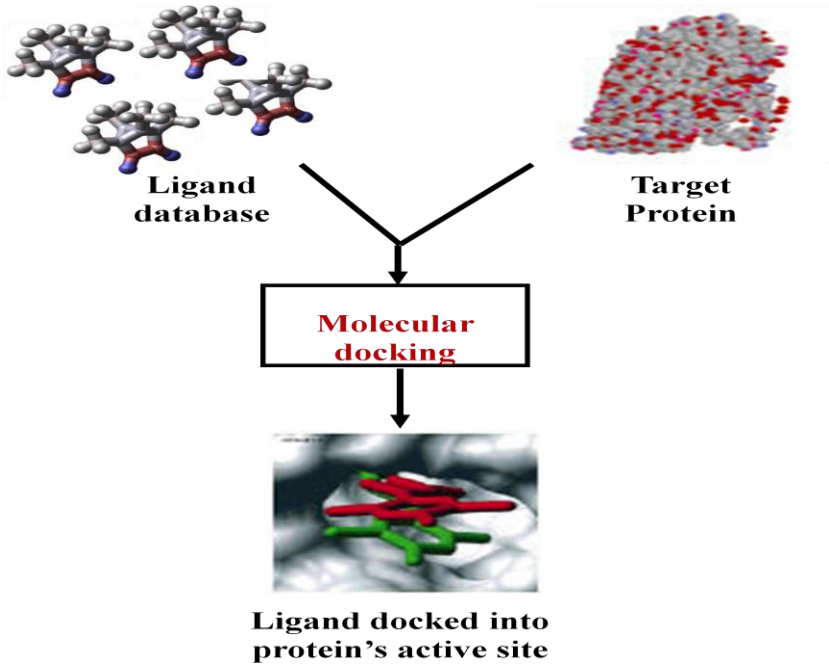

Figure 5. 2: Schematic representation of molecular docking.

5.1.2 Dihydrofolate reductase (DHFR)

Human dihydrofolate reductase (hDHFR) is one of the best therapeutic targets for the anticancer drug because of its metabolic importance. In the context of DHFR inhibitor, Farber used folate analogues for the treatment of acute lymphoblastic leukemia in 1948 (Farber, 1948). Further, in 1958, it was reported that folate analogues showed antitumor activity by inhibition of the dihydrofolate reductase (Osborn, 1958; Osborn & Huennekens, 1958).

Dihydrofolate reductase (DHFR; tetrahydrofolate dehydrogenase; 5, 6, 7, 8-tetra-hydrofolate-NADP$^+$ oxidoreductase; EC 1.5.1.3) is an enzyme of pivotal importance in biochemistry and medicinal chemistry. DHFR functions as a catalyst for the reduction of dihydrofolate to tetrahydrofolate. Reduced folates are carriers of one-carbon fragments; hence they are important cofactors in the biosynthesis of nucleic acids and amino acids (Roth, 1986). The inhibition of DHFR leads to partial depletion of intracellular reduced folates with subsequent limitation of cell growth (Nerkar *et al.*, 2009). DHFR has attracted attention of protein chemists as a model for the study of enzyme structure/

functional relationships. The species-differences among the DHFRs, **(**Falco *et al.,* 1949**)** were used to discover compounds with particular selectivity, e.g., that are lethal to bacteria but relatively harmless to mammals (Buchall & Hitchings, 1965). Such selective inhibitors are trimethoprim and pyrimethamine, which are used in therapy for their antibacterial and antiprotozoal properties, respectively. The enzymatic reduction involved in the inhibition of DHFR is a random process in which either the substrate (dihydrofolate) or the cofactor NADPH, forms a binary complex with the enzyme, with subsequent rapid binding of the inhibitor, to form ternary complex. Good amounts of work were done regarding inhibitors of DHFR (Blancey *et al.,* 1984).

Compounds that inhibit DHFR exhibit an important role in clinical medicine as exemplified by the use of methotrexate in neoplastic diseases (Jolivet *et al.,* 1983; Borst & Quellette, 1995), inflammatory bowel diseases (Kozarek *et al.,* 1989) and rheumatoid arthritis (Weinblatt *et al.,* 1985), as well as in psoriasis (Weinstein, 1971; Abu-Shakra, 1995) and in asthma (Mullarkey *et al.,* 1988) like that of trimethoprim in bacterial diseases (Green *et al.,* 1984). Lately, a new generation of potent lipophilic DHFR inhibitors such as trimetrexate (TMQ) and piritrexim (PTX) have shown antineoplastic (Maroun, 1988) and most importantly, antiprotozoal (Allegra *et al.,* 1987) activities. This is the exclusive *de novo* sources of dTMP, hence inhibition of DHFR or TS activity in the absence of salvage, leads to "thymine-less death **(**Masur, 1990; Berman, Werbel *et al.,* 1991). Thus DHFR inhibition has long been an attractive goal for the development of chemotherapeutic agents against bacterial and parasitic infections as well as cancer (Borst *et al.,* 1995).

5.1.3 Inhibitors of Dihydrofolate Reductase

Inhibitors of DHFR are classified as either classical or non-classical antifolates (Al-Rashood *et al.,* 2014). The classical antifolates are characterized by a *p*-aminobenzoylglutamic acid side-chain in the molecule and thus closely resemble folic acid itself. Methotrexate (MTX) is N-{4-[[(2, 4-diamino-6-pteridyl) methyl]-N^{10}-methyl-amino]} benzoyl-glutamic acid, the most well known drug among the classical antifolates. Compounds classified as non-classical inhibitors of DHFR do not possess the

p-aminobenzoylglutamic acid side-chain but rather have a lipophilic side-chain (Green *et al.*, 1984).

5.1.3.1 Classical DHFR Inhibitors

The classical inhibitor serves as an antimetabolite, which means that it has a similar structure to that of a cell metabolite, resulting in a compound with a biological activity that is antagonistic to the metabolite. In case of folic acid, MTX, most often used DHFR inhibitor in clinic today, is antagonistic to folic acid. The antibacterial drug trimethoprim is generally used together with the TMP (Al-Rashood, 2005). The most common use of MTX is as an anticancer drug. It inhibits the synthesis of metabolites involved in one-carbon unit transfer reactions such as the biosynthesis of the important nucleotides. Moreover, MTX is considered as a competitive and reversible inhibitor of DHFR that binds tightly to the hydrophobic folate-binding pocket of the enzyme. The affinity of MTX for DHFR increases considerably in the presence of the cofactor NADPH and have anti-inflammatory and immuno-suppressive properties with accompanied activity against autoimmune disorders (Graffner-Nordberg, 2001).

5.1.3.2 Non-classical DHFR Inhibitors

The clinically useful properties of MTX have stimulated the quest for a variety of new analogues with modifications within the molecule, without interfering too much with the pharmacophore of the original drug. Intrinsic and acquired resistance to MTX and other antifolate analogues limit their clinical efficacy. Thus, research is enduring for a more selective drug, most importantly, without the severe side-effects often associated with MTX (Jolivet *et al.*, 1983). New more lipophilic antifolates have been developed in an attempt to circumvent the mechanisms of resistance, such as decreased active transport, decreased polyglutamation, DHFR mutations etc (Urakawa *et al.*, 2000). These modified antifolates differ from the traditional classical analogues by increased potency, greater lipid solubility, or improved cellular uptake.

In this study we have tried to investigate the antiproliferative potential of some 3-(Aryldeneamino)-2-phenyl-quinazoline-4(3H)-ones via inhibition of hDHFR. Computational approaches have demonstrable capability to play an important role in this endeavour.

5.2 Materials and methods

5.2.1 Chemicals

Chemicals used are: Anthranilic acid (Sigma Aldrich India), pyridine, anisaldehyde, salicylaldehyde, 3-(4, 5- dimethylthiazol-2-yl)-2,5-diphenyltetrazolium bromide (MTT), p-nitro blue tetrazolium/5-bromo-4-chloro-3-indolyl phosphate system (NBT-BCIP) (SRL, India).

Cell lines were obtained from NCCS Pune, India. Dulbecco's Modified Eagle Medium (DMEM), fetal bovine serum (FBS), penicillin streptomycin neomycin (PSN) antibiotic, trypsin and ethylenediaminetetraaceticacid (EDTA) were obtained from Gibco BRL (Grand Island, NY, USA). Tissue culture plastic wares were obtained from NUNC (Roskidle, Denmark) and Bradford protein assay reagent from Fermentus, EU. DAPI (4', 6-diamidino-2-phenylindole dihydrochloride), acridine orange (AO), and ethidium bromide (EtBr) were procured from Invitrogen, California.

5.2.2 Maintenance of Cell culture

MCF-7 (Human breast adenocarcinoma), HepG2 (Human hepatocellular carcinoma), and HeLa (Human cervical cancer) cells were cultured in DMEM supplemented with 10% fetal bovine serum (FBS) and 1% antibiotic penicillin , streptomycin and Neomycin (PSN) at 37°C in a humidified atmosphere under 5% CO_2. After 75-80% confluency, cells were harvested with 0.025% trypsin and 0.52 mM EDTA in phosphate buffered saline (PBS), and seeded at desired density to allow them to re-equilibrate a day before the start of experiment.

5.2.3 Molecular Docking

The study comprised compounds belonging to quinazoline-4-(3H)-ones (Figure 5.3) along with one standard drug methotrexate. The selected compounds have different substituents as shown in Table 5.1.

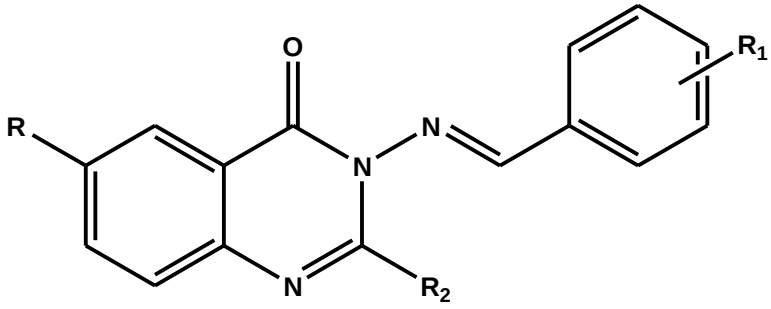

Figure 5.3. Structure of 3-amino-2-aryl-4(3H)-quinazolinone

Table 5.1- The substituents of the 3-amino-2-aryl-4(3H)-quinazolinone

Compounds	R	R^1	R^2
3a	H	2-OH	Ph
3b	H	4-OCH3	Ph
3c	H	4-F	Ph
3d	H	4-N(CH3)2	Ph
3e	H	4-Cl	Ph
3f	H	3-OCH3	Ph
3g	H	4-OH	Ph
3h	H	3-OCH3, 4-OH	Ph
3i	H	3-NO2	Ph
3j	H	H	Ph
4a	H	3,5-Cl	Ph
4b	H	3-NO2-4-Cl	Ph
4c	H	4-CF3	Ph
4d	H	3-Cl	Ph
4e	H	2,3-Cl	Ph
4f	H	2,6-Cl	Ph

4g	H	3,4-F	Ph
4h	H	3-CF3	Ph
4i	6-Br	2-F	Me
4j	6-Br	3-F	Me
4k	6-Br	4-F	Me
4l	6-Br	2-CF3	Me
4m	6-Br	3-Cl	Me
4n	6-Br	2,4-Cl	Me
4o	6-Br	2,6-Cl	Me
4p	6-Br	3,4-F	Me
4q	6-Br	2-Cl-5-NO2	Me
4r	6-Br	4-Cl-3-NO2	Me
4s	6-Br	2-F-3-CF3	Me
4t	6-Br	3,4-OMe	Me
4u	6-Br	2,3-OMe	Me
4v	6-Br	2,5-OMe	Me
4w	6-Br	3-NO2	Me
4x	6-Br	2-OH	Me
4y	6-Br	2,4-OMe	Me
4z	6-Br	5-Cl-3-OH	Me
4	H	2,3-Cl	Me

5.2.3.1 Chemical Drawing

The structure of the compounds was drawn by software ACDLabs Chemsketch 12.0. The created structures were energy minimized by 3D viewer in ACDLabs and the corresponding structures were saved as MDL.mol file format.

These files were opened in ArgusLab 4.0 software and energy minimization of each of the structure was done by using UFF calculation. The respective structures were then saved as the .pdb file format for the further study.

5.2.3.2 Molecular Docking

In order to carry out the molecular docking study, we used the AutoDock 4.0 suite as molecular-docking tool (Morris *et al.,* 1998). It is suitable software for performing automated docking of ligands to their macromolecular receptors. Protein- ligand softwares were widely used to support the drug design process.

5.2.3.3 Preparation of Human DHFR

The basic requirement of the docking is the identification of appropriate target protein. We have chosen Human Dihydrofolate Reductase (PDB ID 1DHF) which fulfills all the requirements of this study. It was retrieved from the PDB structural database site (http://www.rcsb.org/pdb). The .pdb file format of protein was taken as input of Autodock program. All water molecules and ligands were removed from the proteins before the docking procedure. The protein was modified using the AutoDock program through which all missing hydrogen, side chain atoms added and residues repairing were done by using the graphic user interface of AutoDock tools (ADT).

5.2.3.4 Preparation of Ligands

The .pdb file format of ligands was used for the docking. The docking input files of ligands were also prepared using ADT package. Similarly ‘‘.pdb’’ file of ligand was given as input to modify ligand file which allowed the program to calculate its parameters such as non-polar hydrogen, aromatic carbons and rotatable bonds along with the ligand torsions. The Torsion count option was used to adjust the number of rotatable and non-rotatable bonds. For all the ligands Torsions were defined by the use of Torsion Tree option from the AutoDock software. The Torsion Tree option was used to Choose Torsions, Set Number of Torsions to most atoms and to Detect Root which is the rigid part of the ligand. The number of active

torsions was set to the maximum number of atoms. Ligands were saved as .pdbqt file format.

5.2.3.5 Grid box preparation

AutoDock requires pre-calculated grid maps, one for each atom type, present in the ligand being docked and its stores the potential energy arising from the interaction with macromolecule. This grid must surround the region of interest in the macromolecule. In the present study, the binding site was selected based on the amino acid residues, which are involved in folate binding. . Therefore, the grid was centered in the active region of hDHFR motif and includes all amino acid residues that surround active site. The grid box size was set at 90, 90, and 90 A° (x, y, and z), though it was changed depending on the ligand size. AutoGrid 4.0 Program, supplied with AutoDock 4.0 was used to produce grid maps. The preparation steps were started by using .pdb file of human DHFR as the receptor, and its ligand. Grid Box is the coordinate area determination for the docking process. It is configured in AutoDock Tools. Using MGLTools 1.5.1., the grid was centered on the active site of the enzyme for docking. The grid box was saved in a grid parameter file (.gpf) format.

5.2.3.6 Docking simulation

During the docking process, a maximum of 10 conformers was considered for each compound. Docking for 10 number of GA run was carried out using Lamarckian Genetic Algorithm (LGA) and all other parameters set to default. The top ranked model in the lowest energy cluster with maximum cluster size was considered for all further interaction studies. This process was done using AutoGrid 4.0 and Autodock 4.0. The following data are necessary for conducting the docking: enzyme file in .pdbqt format, ligand in .pdbqt format, .gpf files, and .dpf files.

5.2.3.7 Analysis and visualization of docking simulation results

The docking result of AutoDock 4.0 is in the docking log file (.dlg) format. Then, by using python script, the docking results were converted to .pdb format. Out

of 10-model result, one best model was picked up, based on the free energy bonding data, in order to analyze its interaction.

5.2.4 *In silico* Physicochemical and Drug likeliness Tests

Drug-likeliness is mostly a statistics of descriptors derived from databases of compounds used to evaluate the drug-likeliness of other compounds. The web server which predicted the (1) CMC like rule which is based on databases contain more than 7000 compounds, used or tested as medicinal agents in humans. (2) MDDR contained more than 10000 drugs launched or under development (3) The WDI 1997 contains 51596 compounds for comparing the drug-likeliness and also by the Lipinski rule of five. Drug likeliness was calculated using OSIRIS server, which is based on a list of about 5,300 distinct substructure fragments created by 3,300 traded drugs as well as 15,000 commercially available chemicals yielding a complete list of all available fragments with associated drug likeliness.

The physical characteristics of all the molecules were determined because the biological properties could be predicted by their physicochemical property. Molinspiration supported internet benefitted the chemistry community by offering free on-line services for calculation of important molecular properties (LogP, polar surface area, number of hydrogen bond donors and acceptors and others). Any compound to be considered as a lead must possess acceptable scores for all of the descriptors and Osiris Property explorer http://www. organic-chemistry.org/prog/peo/ were used to calculate - logP, solubility, drug likeliness, polar surface area, molecular weight, number of atoms, number of rotatable bonds, volume, drug score and number of violations to Lipinski's rule The cLogP, solubility, drug likeness and drug Score of each molecule were also determined by OSIRIS server.

Computer aided method is an easy platform to search such kinds of biologically active compounds with favorable ADMET (Absorption, Distribution, Metabolism, Excretion and Toxicity) and drug-likeness properties**.** The ADME are the most important part of pharmacological studies of the concerned molecule required for drug based discovery. Pre ADMET is the tool that provides drug-

likeliness, ADME profile and toxicity analysis for the ligand. It uses Caco2-cell (heterogeneous human epithelial colorectal adenocarcinoma cell lines) and MDCK (Madin-Darby Canine Kidney) cell models for oral drug absorption prediction and skin permeability, and human intestinal absorption model for oral and trans-dermal drug absorption prediction. Distribution is predicted using BBB (blood brain barrier) penetration and plasma protein binding.

5.2.5 Inhibitory toxicity prediction

The Osiris program was used to predict the overall toxicity of the most active derivatives as it may point to the presence of some fragments generally responsible for the irritant, mutagenic, tumorigenic, or reproductive effects in these molecules.

5.2.6 Pharmacophore generation

The compounds were structurally aligned to get a ligand based pharmacophore using PharmaGist tool (Schneidman-Duhovny et al, 2008). A ligand-based pharmacophore modeling was performed using PharmaGist webserver. The method consists of four major steps: (i) ligand representation, (ii) pairwise alignment, (iii) multiple alignments and (iv) solution clustering and output as shown in Figure 5.4. In a common pharmacophore development approach, large number of possible conformations for each ligand were generated, whereas PharmaGist uses the most active compound as 'the pivot' that is considered within the search for the common pharmacophore. The benefit of this approach lies in the fact that when there is no information on the binding conformation of any of the ligands, a set of conformations for only one of them (the pivot) needs to be computed. Unless a pivot is specified by the user, the algorithm iteratively tries each input ligand as a pivot. The algorithm identifies pharmacophores by computing multiple flexible alignments between the input ligands. The resulting multiple alignments reveal spatial arrangements of consensus features shared by different subsets of input ligands. The highest-scoring ones are potential pharmacophores (Dror *et al.,* 2009). Ten active compounds (Table 5.1) from the series were selected to generate pharmacophore models. Compound 11 was assigned as the pivot molecule and default values were used for other settings. Models with all the 10 ligands with contribution to

the pharmacophoric features were considered. Generated models were ranked with the scores and the one with highest score was selected as the best pharmacophore model.

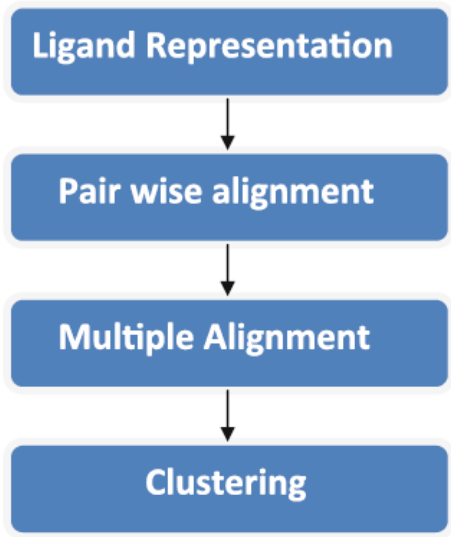

Figure 5.4: Flow-chart of PharmaGist method

5.2.7 hDHFR activity assay

hDHFR activity was measured using the DHFR assay kit (Sigma-Aldrich-CS0340) as per the manufacturer's instructions. Typically, DHFR activity is measured using a Jasco V spectrophotometer to quantify the decrease in absorbance at 340 nm for every 5 s over 2.5 min. The stock solutions for the reaction mixture was Methotrexate (1×10^{-6}M) , NADPH (1×10^{-3}M), DHF (1×10^{-3}M) and synthesized compounds (10^{-6}M). DHFR activity was determined by measuring the decrease of absorbance at 340 nm characteristic of dihydrofolate as it is reduced to tetrahydrofolate (THF). The activity calculation measures the decrease in OD obtained during 2.5 min. The output of the kinetics program was ΔOD/min.

$$Inhibition\ \% = \frac{Activity\ of\ DHFR\ in\ presence\ of\ inhibitor}{100} \text{X}\ Activity\ of\ DHFR\ in\ presence\ of\ inhibitor$$

The % inhibition values were plotted versus drug concentration (log scale). The 50% inhibitory concentration (IC_{50}) of each compound was obtained.

5.2.8 MTT assay

Stock solutions of synthesized compounds and standard compounds (methotrexate and curcumin) at a concentration of 10 mg/ml were prepared in dimethyl sulfoxide (DMSO, Hi-Media). The cytotoxic effect of each of compound was evaluated by tetrazolium- dye, MTT, assay (Mosmann, 1983; Denizot & Lang, 1986) with slight modifications. Briefly, the cancerous cells (MCF 7, $HepG_2$ and HeLa) were seeded in 96-well plates at a density of $5x10^3$ cells/well in 200 µl culture medium. Following 24 h incubation and attachment, the cells were treated with different concentrations of compounds and similar concentration of diluents (DMSO) for further 24 h. After treatment, media was replaced with MTT solution (10 µl of 5 mg/ml per well) prepared in PBS and incubated for 3 h at 37 ^oC in a humidified incubator with 5% CO_2. The yellow MTT dye was reduced by succinate dehydrogenase in the mitochondria of viable cells to purple formazan crystals. To solubilize the formazan, 50 µl of isopropanol was added to each well. The plates were gently shaken for 1 min and absorbance was measured at 600 nm, with reference 490 nm, by microtiter plate reader (MIOS Junior, Merck). The percentage of cytotoxicity was calculated as (Y-X)/Y x 100, where Y is the mean optical density of control (DMSO treated cells) and X is the mean optical density of treated cells with compounds.

5.2.9 Assessment of cell morphology

Cells (3×10^4/well) grown in 6-well plates in DMEM supplemented with 10% FBS for 24 h were treated with or without derivatives. Cells were seeded in 35 mm polyvinyl coated cell culture plates and allowed to attach at 37 ^0C for 24 h in CO_2 incubator. The following day, cells were treated with either 75 µg/ml of compounds or DMSO alone, serving as control, and incubated again at the same conditions. The morphological changes of cancerous cells under treatment and control conditions were compared by monitoring with phase contrast inverted microscope (Olympus, CK40-SLP) at 200X magnification. The images were photographed at 24 h of incubation.

5.2.10 Trypan blue exclusion assay

After morphological assessment, the cell viability was simultaneously assessed by Trypan blue dye exclusion assay (Strober, 1992). For this, the cells were trypsinized with 0.25% trypsin-EDTA solution, resuspended in phosphate buffer saline (PBS) and stained with 0.4% Trypan bluedye solution (v/v in PBS). Within two minutes, the cells were loaded in a Neubauer chamber and the number of viable and non-viable cells per 1 x 1 mm square was counted under phase contrast microscope. The dead cells, because of losing the semi permeability of membrane, retained the blue dye and hence are colored whereas viable or live cells remained unstained. The cells/ml was calculated as average cell count x dilution factor x 10^4 cells/ml. The % cell viability was determined as [(no. of viable cells/ total no. of viable + non-viable cells) x 100. The percentage of growth inhibition was represented as {cell viability (control) – cell viability (with test compound).

5.2.11 Statistical analysis

All values are expressed as mean ± SD. Statistical significance was compared between various treatment groups and controls using the one-way analysis of variance (ANOVA). Data were considered statistically significant when P values were <0.01.

5.3 Results and Discussion

In the last few years, the attention was oriented towards the synthesis and biological evaluation of quinazolinone derivatives as they exhibit a broad spectrum of biological activities. Moreover, there is an increasing interest in finding novel field of applicability for Quinazoline-4(3H)-one compounds as anticancer drugs. Importantly, FDA has approved several quinazoline derivatives as anticancer drugs from the past 15 years, such as gefitinib, erlotinib and lapatinib (Roskoski *et al.*, 2014).

5.3.1 Drug likeliness of compounds

Apart from advances in technology and understanding of biological systems, drug discovery is still a long process with low rate of new therapeutic discovery. Fortunately, modern computational-aided drug design established a novel platform by which researchers perform in-depth *in silico* simulation prior to labor-extensive wet-lab validation. Hence we have chosen first to perform *in silico* evaluation of compounds' drug likeliness behaviour (physicochemical properties, interaction with target protein, ADMET and drug score) and their possibility to become a drug in future

All the ten compounds used in this study were allowed to pass through different parameters required to fulfill the candidature of these compounds as future drug. In addition to these ten 3-(Aryldeneamino)-2-phenyl-quinazolin-4(3H)-one, we have computationally constructed twenty seven more quinazolinone compounds, which are reported for their biological activity (Xingwen *et al.*, 2007). This approach was also taken to verify dependability of the applied tools and softwares. All compounds (synthesized and computationally constructed) have successfully qualified Lipinski's Rules, CMC like rule (except 4a and 4f), MDDR like rule and WDI like rule (Table 5.2). Compounds tested in this study were predicted to have good oral bioavailability. Some of the compounds (4e, 4f and 4) have shown excellent permeability, while others have relatively less or poor (in some cases) permeability. The drug likeliness and drug score were found significant for all tested compounds.

The suitability of a promising drug also depends on its toxicity. The therapeutic index of a drug would be higher when it shows low toxicity/side effects. Based on this we have performed toxicity prediction using Osiris Property Explorer. Results revealed that the compounds have low toxicity. The prediction using Osiris Property Explorer was shown in color codes. Green color represents low toxicity, yellow represents the mediocre toxicity, and red represents high toxicity (Table 5.3).

Table 5.2- Data representing the qualification of the substituents for drug likeliness using CMC like rule, MDDR like rule and WDI like rule along with Rule of Five as predicted using OSIRIS server

Compound	CMC like rule	MDDR like rule	Rule of five	WDI like rule
1a	Qualified	Mid structure	Suitable	90%
2a	Qualified	Mid structure	Suitable	90%
3a	Qualified	Mid structure	Suitable	90%
3b	Qualified	Mid structure	Suitable	90%
3c	Qualified	Mid structure	Suitable	90%
3d	Qualified	Mid structure	Suitable	90%
3e	Qualified	Mid structure	Suitable	90%
3f	Qualified	Mid structure	Suitable	90%
3g	Qualified	Mid structure	Suitable	90%
3h	Qualified	Mid structure	Suitable	90%
3i	Qualified	Mid structure	Suitable	90%
3j	Qualified	Mid structure	Suitable	90%
4a	Not qualified	Mid structure	Suitable	90%
4b	Qualified	Mid structure	Suitable	90%
4c	Qualified	Mid structure	Suitable	90%
4d	Qualified	Mid structure	Suitable	90%
4e	Qualified	Mid structure	Suitable	90%
4f	Not qualified	Mid structure	Suitable	90%
4g	Qualified	Mid structure	Suitable	90%
4h	Qualified	Mid structure	Suitable	90%
4i	Qualified	Mid structure	Suitable	90%
4j	Qualified	Mid structure	Suitable	90%
4k	Qualified	Mid structure	Suitable	90%
4l	Qualified	Mid structure	Suitable	90%

4m	Qualified	Mid structure	Suitable	90%
4n	Qualified	Mid structure	Suitable	90%
4o	Qualified	Mid structure	Suitable	90%
4p	Qualified	Mid structure	Suitable	90%
4q	Qualified	Mid structure	Suitable	90%
4r	Qualified	Mid structure	Suitable	90%
4s	Qualified	Mid structure	Suitable	90%
4t	Qualified	Mid structure	Suitable	90%
4u	Qualified	Mid structure	Suitable	90%
4v	Qualified	Mid structure	Suitable	90%
4w	Qualified	Mid structure	Suitable	90%
4x	Qualified	Mid structure	Suitable	90%
4y	Qualified	Mid structure	Suitable	90%
4z	Qualified	Mid structure	Suitable	90%
4	Qualified	Mid structure	Suitable	90%

Table 5.3: Toxicity prediction as per output of Orisis programme

Compound	**Mutagenic**	**Tumorogenic**	**Irritant**	**Reproductive effect**
1a	Green	Green	Green	Yellow
2a	Green	Green	Green	Yellow
3a	Green	Green	Green	Green
3b	Green	Green	Green	Green
3c	Green	Green	Green	Green
3d	Green	Green	Green	Green
3f	Green	Green	Green	Green
3g	Green	Green	Green	Yellow
3h	Green	Green	Green	Green
3i	Green	Green	Green	Green
3g	Green	Green	Green	Green
4a	Green	Green	Green	Yellow
4b	Green	Green	Green	Yellow
4c	Green	Green	Green	Yellow

4d	Green	Green	Green	Yellow
4e	Green	Green	Green	Yellow
4f	Green	Green	Green	Yellow
4g	Green	Green	Green	Yellow
4h	Green	Green	Green	Yellow
4i	Green	Green	Green	Green
4j	Green	Green	Green	Yellow
4k	Green	Green	Green	Green
4l	Green	Green	Green	Green
4m	Green	Green	Green	Green
4n	Green	Green	Green	Green
4o	Green	Green	Green	Green
4p	Green	Green	Green	Green
4q	Green	Green	Green	Green
4r	Green	Green	Green	Green
4s	Green	Green	Green	Green
4t	Green	Green	Green	Green
4u	Green	Green	Green	Green
4v	Green	Green	Green	Green
4w	Green	Green	Green	Green
4x	Green	Green	Green	Green
4y	Green	Green	Green	Green
4z	Green	Green	Green	Green
4	Green	Green	Green	Green

5.3.1.1 Molecular descriptor properties

The oral bioavailability of the compounds projected as potential drugs were evaluated by determining the molecular weight, number of rotatable bonds (nrotb), number of hydrogen bonds (nON and nOHNH), and drug's polar surface (TPSA) as shown in Table 5.4. Since the individual molecular weights of all the compounds were less than 500, the numbers of rotatable bond were <10, the number of hydrogen bond donors and acceptors were < 12, and TPSA values being <140, they qualified to be an ideal oral drug. Compounds tested in this study were also predicted to have good oral bioavailability.

Table 5.4. Molecular descriptor properties of compounds.

Compounds	miLogP	TPSA	nON	nOHNH	Nviolations	nrotb	volume	natoms
1a	3.2	43.10	4	0	0	1	195.84	17.0
2a	3.1	45.75	4	0	0	1	199.76	17.0
3a	5.7	65.26	4	0	0	1	327.87	25.0
3b	6.7	57.89	4	0	0	1	294.72	25.0
3c	3.9	45.03	4	0	0	3	315.87	23.0
3d	4.8	48.87	4	0	0	3	287.67	22.0
3e	4.5	45.03	4	0	0	2	298.0	26.0
3f	5.6	48.54	4	0	1	2	321.8	23.0
3g	5.8	49.87	4	0	0	3	318.9	24.0
3h	6.9	65.26	4	0	0	3	307.0	22.0
3i	5.2	58.92	4	0	0	3	305.0	25.0
3j	6.2	45.03	7	0	0	2	312.65	26.0
4a	5.887	47.26	4	0	1	3	321.37	27.0
4b	5.16	93.08	4	0	0	3	317.53	27.0
4c	4.25	47.26	4	0	0	3	288.64	25.0
4d	5.25	47.26	4	0	1	3	307.84	26.0
4e	5.863	47.26	4	0	1	3	321.37	27.0
4f	5.86	47.26	4	0	1	3	321.37	27.0
4g	4.85	47.26	4	0	0	3	304.17	27.0
4h	5.47	47.26	4	0	1	4	325.60	29.0
4i	3.47	47.26	4	0	0	2	262.27	22.0
4j	3.5	47.26	4	0	0	2	262.27	22.0
4k	3.52	47.26	4	0	0	2	262.27	22.0
4l	4.20	47.26	4	0	0	3	288.64	25.0
4m	4.01	47.26	4	0	0	2	270.88	22.0
4n	4.64	47.26	4	0	0	2	284.41	23.0
4o	4.62	47.26	4	0	0	2	284.41	23.0
4p	3.61	47.26	4	0	0	2	267.20	23.0

4q	3.92	93.08	7	0	0	3	294.21	25.0
4r	3.52	47.26	4	0	0	2	262.27	22.0
4s	4.32	47.26	4	0	0	3	293.57	26.0
4t	3.00	65.72	6	0	0	4	308.43	25.0
4u	3.18	65.72	6	0	0	4	308.43	25.0
4v	3.40	65.72	6	0	0	4	308.43	25.0
4w	3.2	93.08	7	0	0	3	280.67	24.0
4x	3.3	67.48	5	1	0	2	265.36	22.0
4y	3.40	65.72	6	0	0	4	308.43	25.0
4z	3.95	67.48	5	1	0	2	278.898	23.0
4	4.62	47.26	4	0	0	2	284.41	23.0

Calculation of the fragment based drug-likeliness of the compounds signifies that the compounds have the same fragments as compared to the existing drugs. The drug-likeliness values of all the compounds are reasonably acceptable (except 4h,4i and 4s) as shown in Table 5.5. The higher drug-likeliness values are found in case of compounds 4c, 4d, 4e and 4f. Results indicated that these four compounds have the most fragments similar to existing potent drugs to fulfill the content of drugs. The drug score values (Table 5.5) were also calculated which took into account the effect of drug-likeliness, LogP, solubility, molecular weight, and toxicity risk together.

Table 5.5. Fragment based drug-likeliness of the compounds.

Compound	cLogP	Solubility	MW	Drug likeness	Drug Score
1a	2.35	-3.34	223	1.84	0.51
2a	3.93	-3.06	237	1.11	0.6
3a	3.74	-4.5	341.0	5.27	0.67
3b	4.05	-4.82	355	5.04	0.61
3c	4.22	-5.11	343	2.59	0.56

3d	4.01	-4.84	368	5.99	0.61
3e	4.72	-5.54	359	6.03	0.43
3f	4.05	-4.82	355	5.4	0.61
3g	3.77	-4.6	341	5.37	0.66
3h	3.77	-4.5	371	5.27	0.67
3i	3.44	-4.88	370	5.39	0.65
3j	4.12	-4.8	325	5.21	0.62
4a	5.26	-6.27	393	1.71	0.23
4b	3.77	-5.44	404	5.07	0.45
4c	4.65	-5.44	393	5.19	0.4
4d	5.26	-5.54	359	5.51	0.31
4e	5.26	-6.27	394	5.59	0.4
4f	4.65	-6.27	394	6.1	0.31
4g	4.16	-5.43	361	2.68	0.42
4h	4.8	-5.58	393	-1.84	0.21
4i	3.42	-4.78	362	1.44	0.59
4j	3.42	-4.78	360	0.12	0.4
4k	3.42	-4.78	360	1.91	0.61
4l	4.12	-5.24	410	-6.99	0.27
4m	3.97	-5.2	376	2.72	0.55
4n	4.59	-5.2	411	3.17	0.44
4o	3.97	-5.94	411	3.76	0.56
4p	3.48	-5.09	378	0.19	0.47
4q	3.71	-5.84	421	1.5	0.45
4r	3.71	-5.84	428	3.16	0.49
4s	4.18	-5.56	402	-4.45	0.25
4t	3.15	-4.5	402	4.56	0.66
4u	3.15	-4.5	402	3.02	0.65
4v	3.15	-4.5	402	3.23	0.66
4w	3.09	-5.1	387	2.57	0.6

4x	3.06	-4.17	358	2.7	0.71
4y	3.15	-4.5	402	1.57	0.61
4z	3.67	-4.9	392	3.41	0.6
4	3.89	-5.1	332	4.94	0.49

Any compound that is considered to be a better drug candidate should exhibit better drug score. Our data showed that compound 4x has the best score (0.71), compounds (2a, 3b, 3c, 3d, 3f, 3g, 3i, 3j, 4t, 4v,4k,4i,4m,4o and 4y) in the range of 0.5-0.66 and rest of the compound in range of 0.2-0.5. The hydrophobicity of drugs could be inferred from LogP values (Table 5.5). It was found that hydrophobicity and retention time of drug inside the host are directly related *i.e.* higher the hydrophobicity, higher the retention time of the drug inside the body (Tambunan *et al.,* 2011).

5.3.1.2 ADME prediction

In modern drug designing process, computational approaches like preADMET prediction; MDCK and Caco-2 cell permeability, etc. serve as computational screening model for the prediction of intestinal drug absorption. All the compounds under study have qualified HIA%, *in vitro* plasma% (>90% in all the cases) and Caco-2 cell permeability (>25 nm/sec) to be good drug candidate. Some of the compounds have shown excellent permeability, while others have relatively less or poor (in some cases) permeability in relation to qualify as CNS drug and MDCK permeability as shown in Table 5.6. Less permeability may have been predicted because of the solubility which depends to a certain degree on arrangement of molecules in the crystal and these topological aspects cannot be predicted via atom types or substructure fragments.

Table 5.6 preADME prediction of compounds.

Compound name	HIA%	Caco-2 nm/sec	MDCK nm/sec	In vitro plasma%	In vitro blood barrier
1a	96.73	25.98	0.04	93.29	0.135
2a	97.68	27.54	0.05	92.28	0.198
3a	98.06	37.28	35.19	96.43	1.137
3b	98.66	42.28	34.16	95.64	2.05
3c	96.94	45.54	0.053	96.39	2.34
3d	98.38	44.77	0.046	93.71	1.12
3e	98.53	44.77	0.020	96.49	2.31
3f	96.72	34.45	26.32	96.63	1.76
3g	97.68	36.43	26.46	97.18	1.96
3h	97.89	36.49	0.020	98.6	1.45
3i	97.589	36.55	32.52	99.18	2.28
3j	96.34	42.27	0.04	98.42	2.41
4a	98.06	38.752	15.94	96.47	0.84
4b	99.142	42.6359	0.044	93.484	0.027
4c	97.68	47.7122	0.044	92.11	0.135
4d	97.84	35.998	44.058	93.244	2.07
4e	98.06	17.55	25.09	96.07	1.107
4f	98.06	17.34	34.26	95.998	2.05
4g	97.62	43.077	0.182	93.022	0.269
4h	97.668	37.517	0.044	93.718	0.127
4i	97.589	37.62	0.0958	96.408	2.31
4j	97.589	37.62	0.053	100	1.39
4k	97.589	18.775	0.046	99.18	0.996
4l	97.63	42.27	0.020	100	0.1945
4m	97.809	38.752	0.094	100	1.319
4n	98.003	42.6359	0.0412	100	0.79

4o	98.033	47.7122	0.125	100	1.38
4p	97.592	35.998	0.025	98.44	0.491
4q	99.14	17.55	0.023	100	0.292
4r	99.143	17.34	0.0208	100	0.201
4s	97.64	43.077	0.021	98.35	0.159
4t	97.485	37.517	0.024	95.31	0.241
4u	97.485	37.62	0.026	92.21	1.88
4v	97.485	37.62	0.028	92.71	1.93
4w	99.38	18.775	0.0323	100	0.194
4x	96.169	21.197	0.138	94.513	0.623
4y	97.48	37.06	0.028	89.708	0.358
4z	96.56	22.355	0.037	98.24	0.49
4	97.64	39.17	75.66	91.17	1.67

5.3.2 Molecular Docking and Pharmacophore study

In order to evaluate the candidature of compounds as inhibitor of hDHFR, in terms of their binding affinity to hDHFR active site, we have performed molecular docking of these compounds with hDHFR. The protein-ligand complex structures were suitable for the docking study, since the ligand pockets were clearly determined.The docked complexes of receptor and compounds have been compared with the original PDB structure (1DHF:A) in terms of the occupancy of the active site by the compounds. The molecular alignment results (Figure 5.5) have shown that all the compounds under study along with the standard drug methotrexate have occupied the same cavity as is occupied by the natural ligand folate.

The active site of the human dihydrofolate reductase (hDHFR) is represented by Ile-7, Ala-9, Trp-24, Glu-30, Gln-35, Asn-64, Arg-70, Val-115, Tyr-121 and Thr-136 (Yamini *et al.,* 2011) as shown in Figure 5.6. It can be inferred that the compounds have affinity for the active site and can act as competitive inhibitors to the natural ligand.

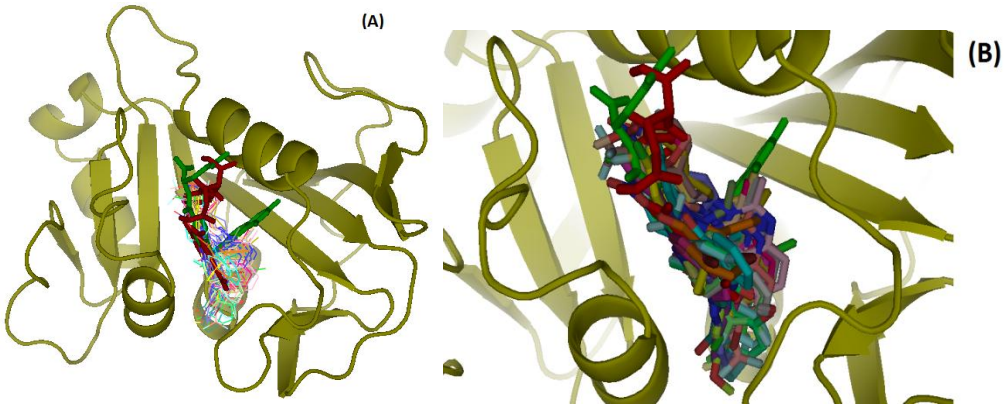

Figure 5.5: Docking model of compounds with hDHFR (PDB ID- 1DHF) protein (Folic Acid and methotrexate are represented in green and red sticks respectively, and the other molecules are shown in line representation) (B) Zoomed view of the active site showing all the docked molecules (ligands are represented in different color sticks including folic acid and methotrexate represented in green and red sticks respectively)

The compounds were evaluated in terms of their binding mode to hDHFR. Based on the Binding Free Energy (ΔG binding) of the protein-ligand interaction and Inhibition constant (Ki), one of 10 models was chosen to be the best one (Table 5.7). The docking result showed that all compounds have low binding energy and inhibition constant as compared to the standard drug methotrexate. The minimum binding energy (maximum stability) was found for compound 4e (-12.38 Kcal/mol). The N1 of 4e forms hydrogen bond with the Ser-59 with a distance of 2.71Å. The amino acids Val-115, Phe-31, Phe-34, Tyr-121, Thr-136 and Asp-21 are found to be involved in making hydrophobic interactions with 4e. Interestingly, all these amino acids are also present in active site of hDHFR, which infers that 4e binds in the active site region of enzyme. 4b molecule also formed significantly stable complex on docking. Similar to 4e, the N1 atom of 4b formed hydrogen bond with the Ser-59. It was reported that the tested quinazoline's recognition with the key amino acid Glu-30 and Ser-59 is essential for binding and biological activity (Al-Rashood *et*

al., 2006) The maximum binding energy was found in 4p (-10.05 Kcal/mol) which did not form hydrogen bond with the residues of the receptor.

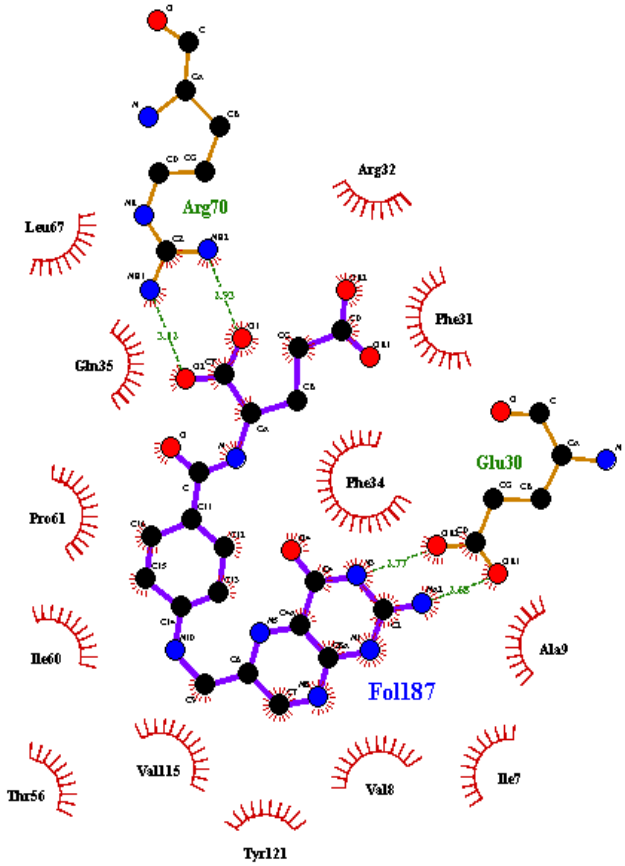

Figure 5.6: LigPlot generated snapshot of the residues in the active site of 1DHF interacting with the natural ligand Folate.

‘

It was observed from the calculated binding energies that incorporation of phenyl at 2-C increased the interaction with the enzyme in comparison to compounds substituted with methyl at 2-C. The compounds 4a- 4h have binding energies in range of -11.28 to -12.38 Kcal/mol. The inhibition constant is directly proportional to the binding energy as shown in Table 5.7. The docking model of compounds and hDHFR are shown in Figure. 5.7.

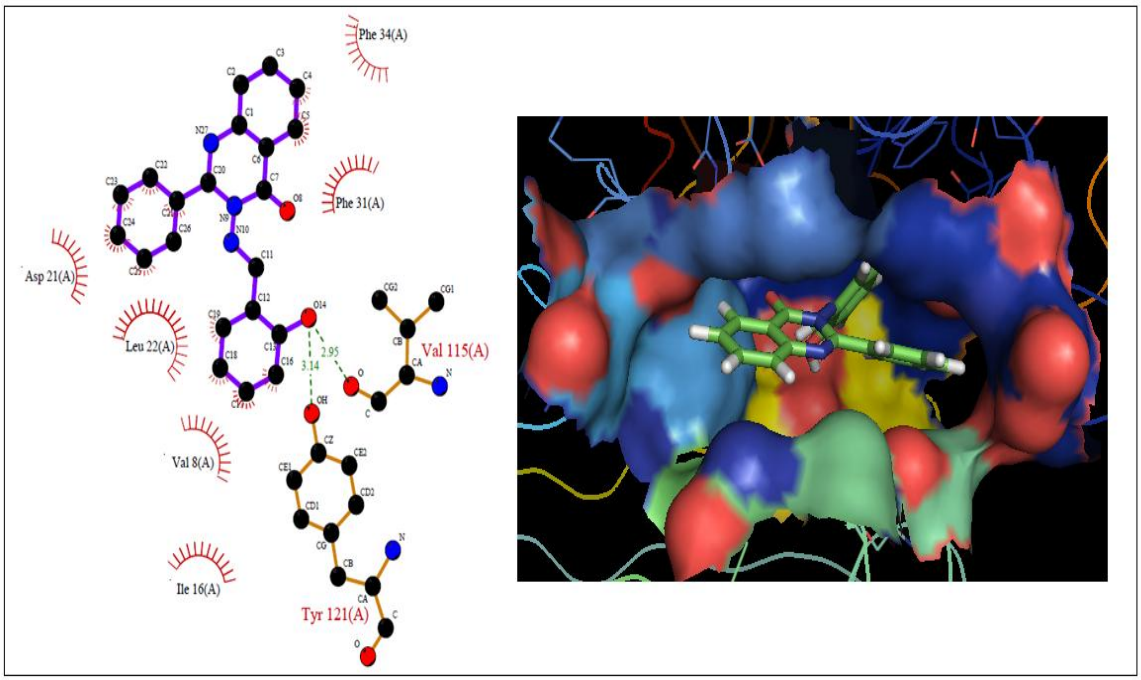

Figure 5.7 (a): Interaction of compound 3a docked with hDHFR

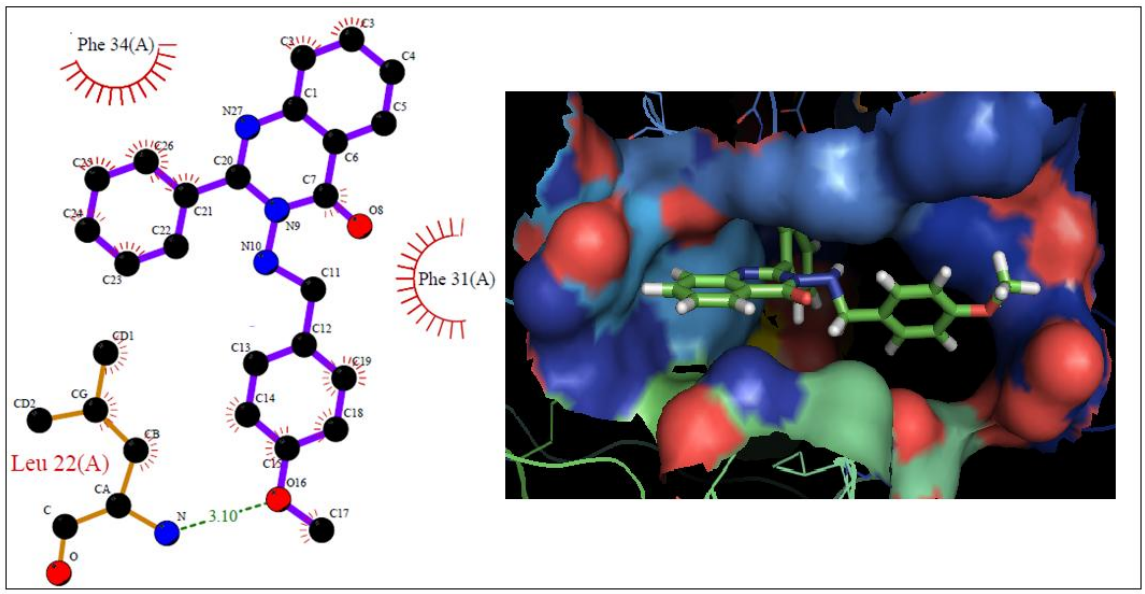

Figure 5.7 (b): Interaction of compound 3b docked with hDHFR

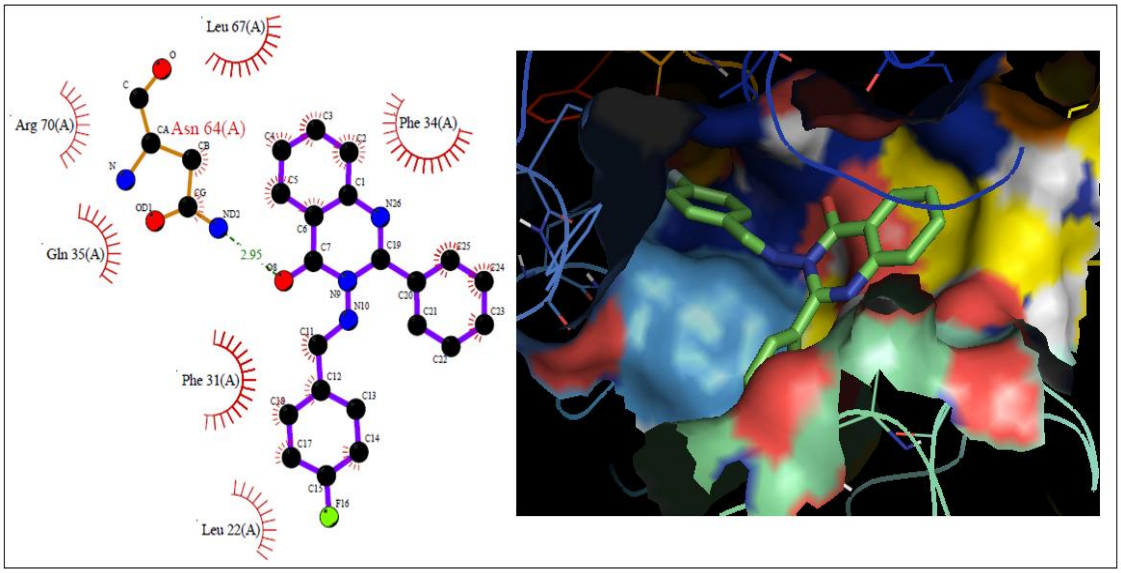

Figure 5.7 (c): Interaction of compound 3c docked with hDHFR

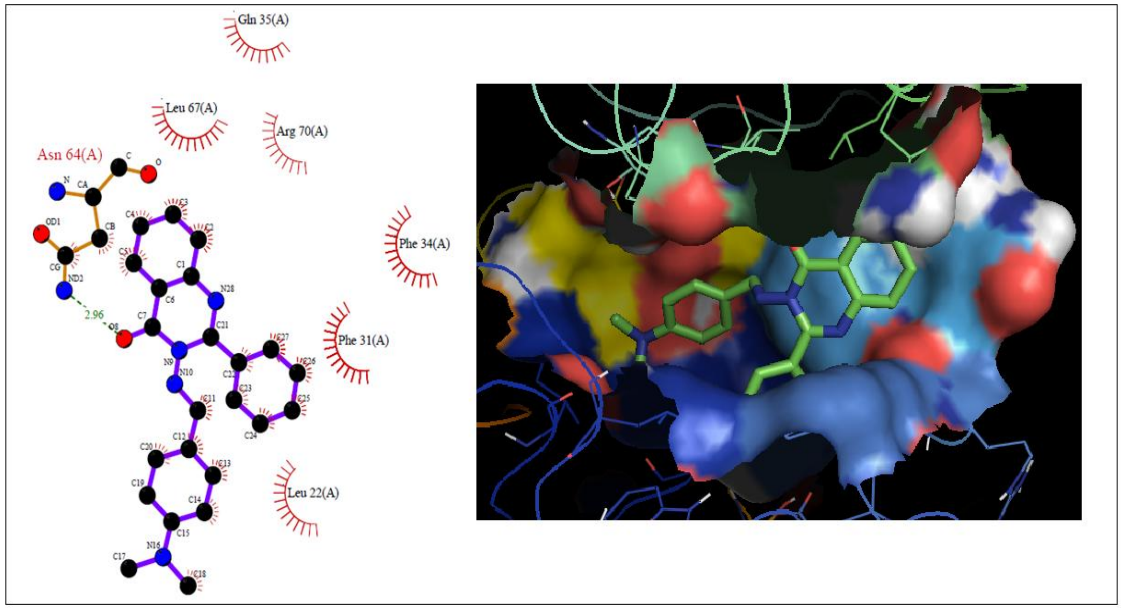

Figure 5.7 (d): Interaction of compound 3d docked with hDHFR

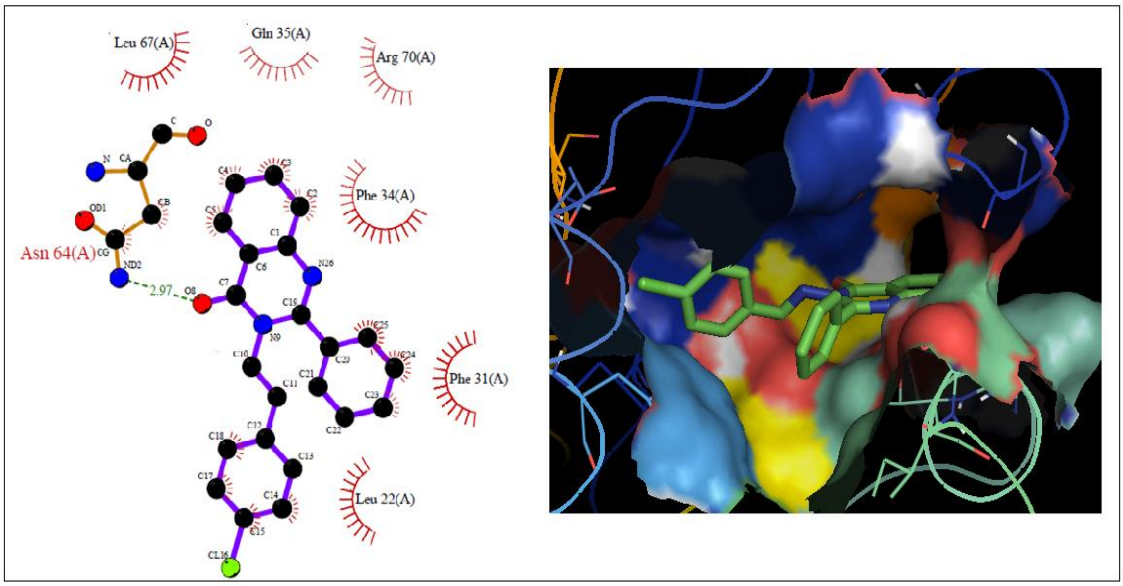

Figure 5.7 (e): Interaction of compound 3e docked with hDHFR

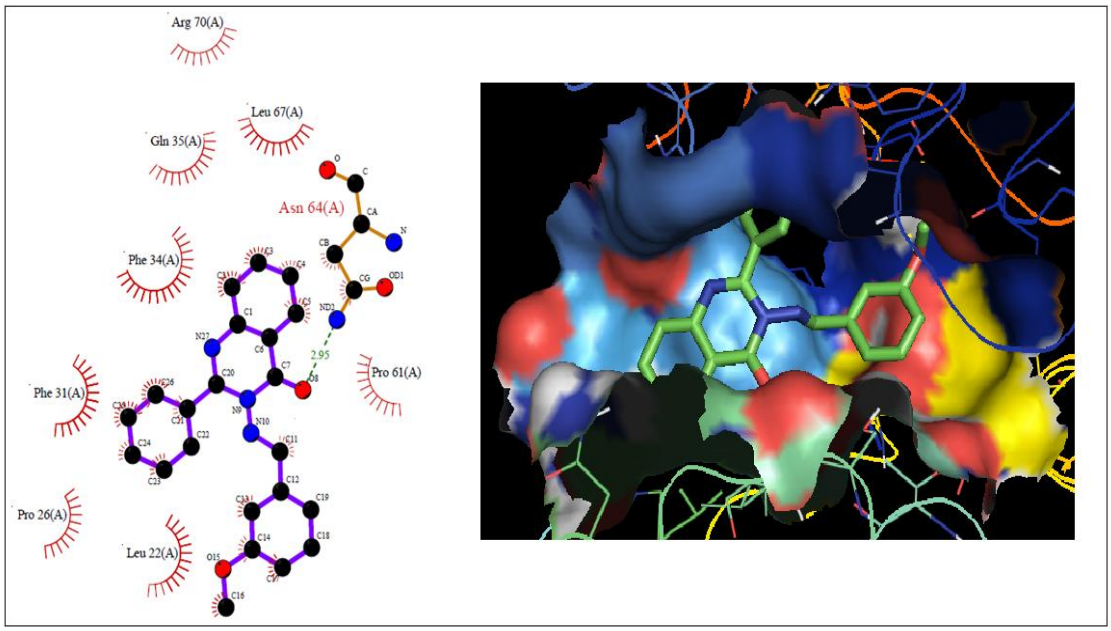

Figure 5.7 (f): Interaction of compound 3f docked with hDHFR

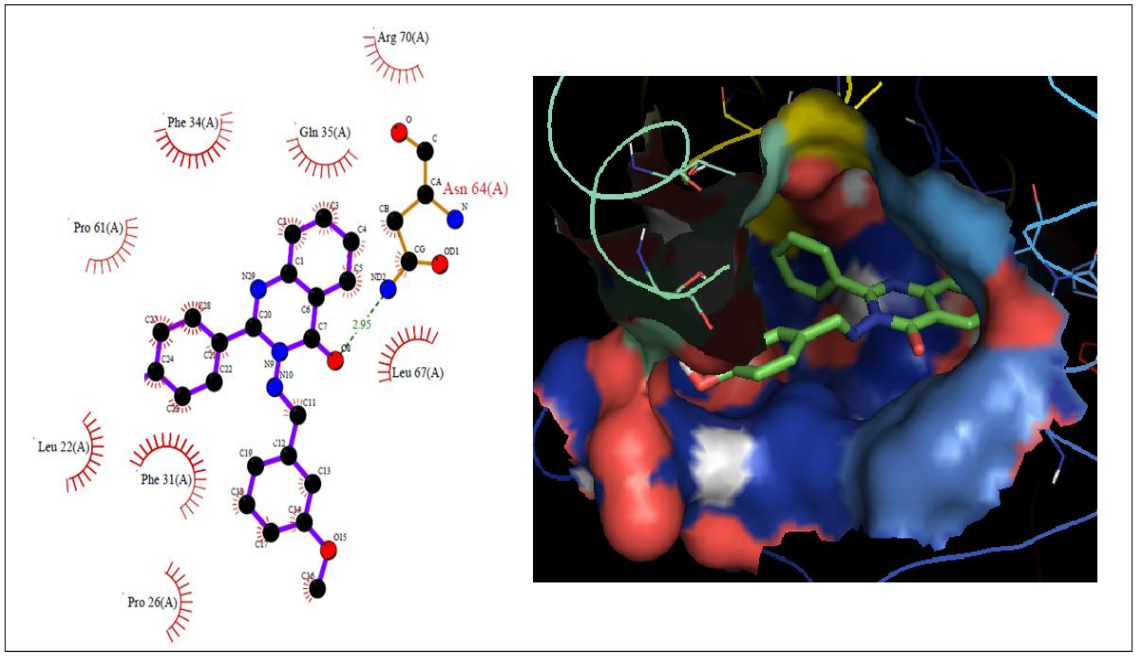

Figure 5.7 (g): Interaction of compound 3g docked with hDHFR

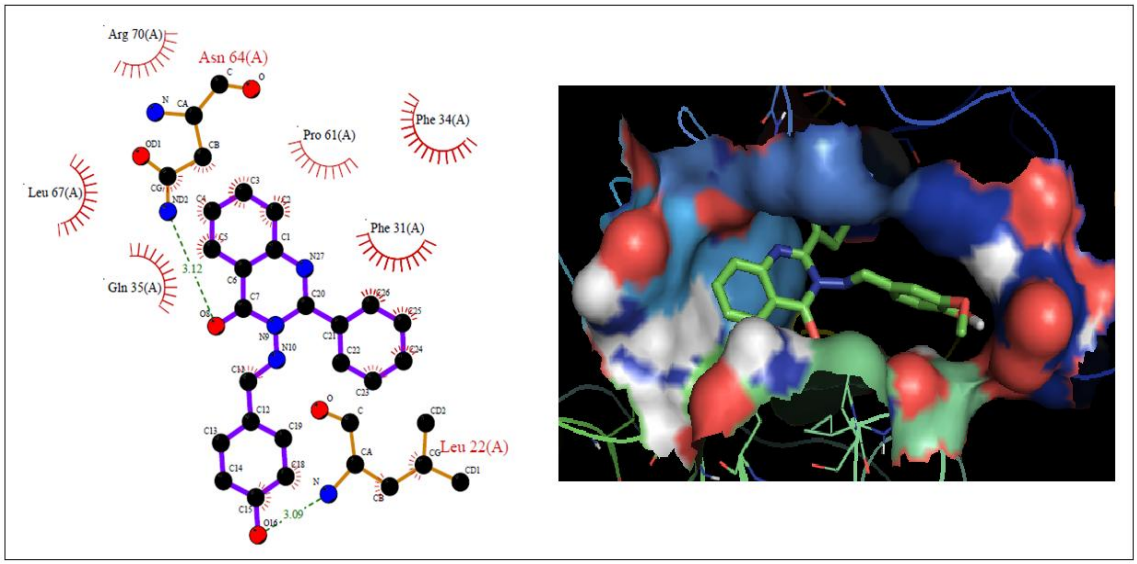

Figure 5.7 (h): Interaction of compound 3h docked with hDHFR

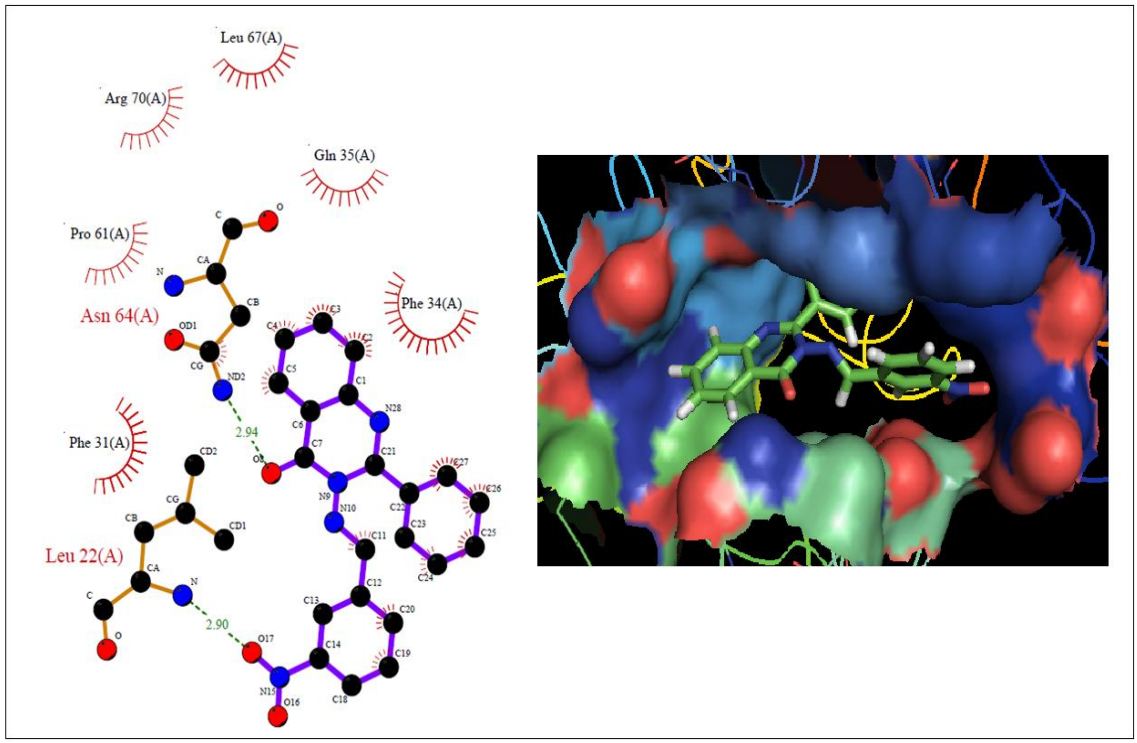

Figure 5.7 (i): Interaction of compound 3i docked with hDHFR

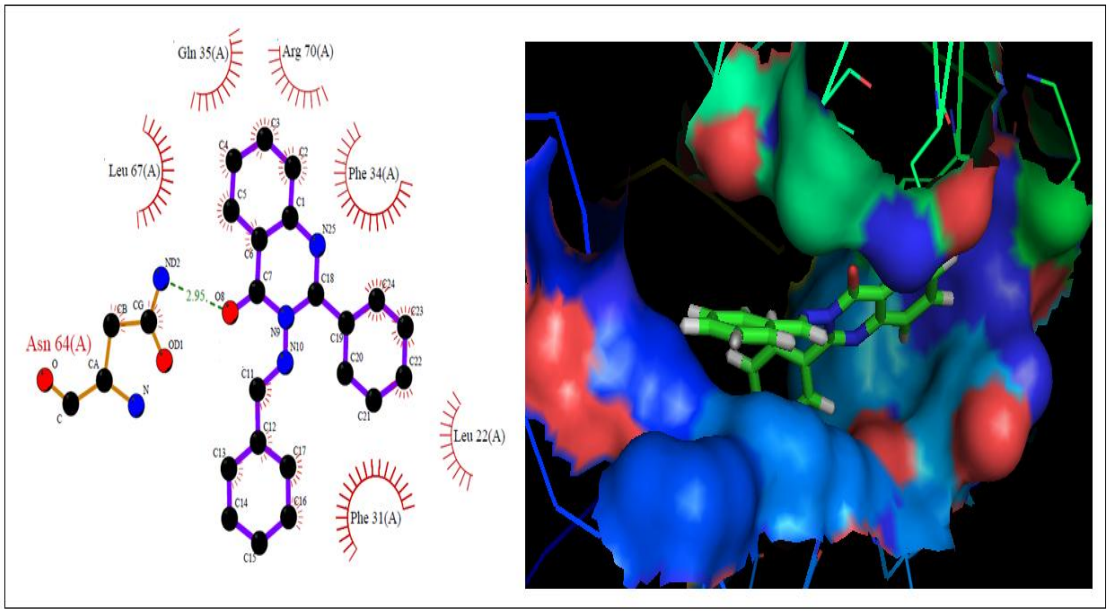

Figure 5.7 (j): Interaction of compound 3j docked with hDHFR

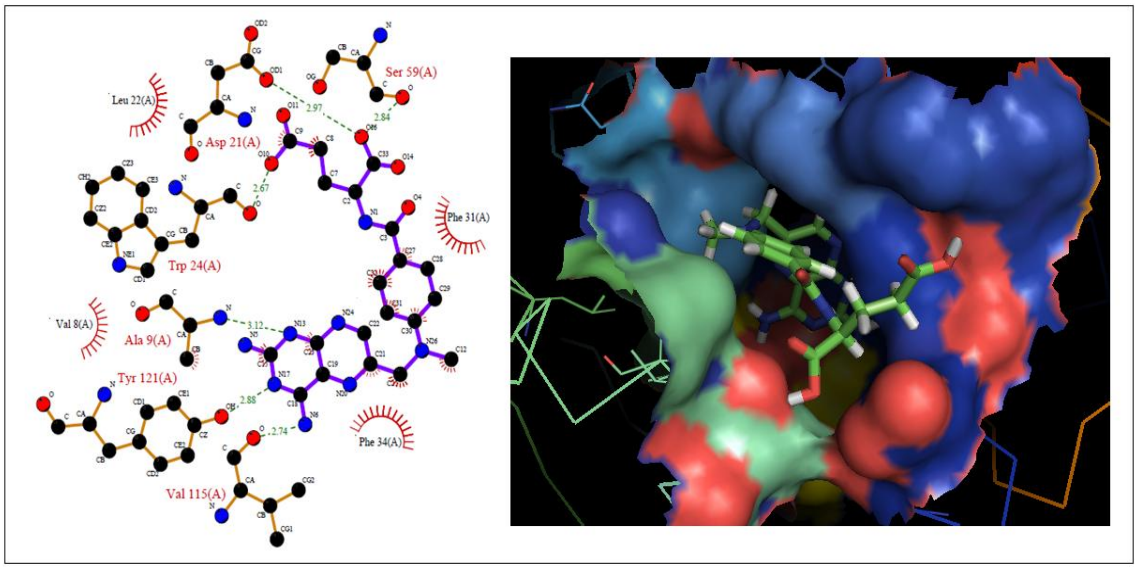

Figure 5.7 (k): Interaction of methotrexate docked with hDHFR

Table 5.7 Binding energy and Inhibition constant of ligand -human DHFR interaction for each test compound.

Compound	Binding energy Kcal/Mol	Inhibition constant (nM)
1a	-6.43	234µM
2a	-7.23	178 µM
3a	-10.62	16.38
3b	-10.79	12.28
3c	-10.43	22.64
3d	-11.17	6.42
3e	-10.89	13.96
3f	-10.72	10.13
3g	-10.91	31.21
3h	-10.24	10.21
3i	-11.62	3.2

3j	-11.37	4.64
4a	-11.73	2.5
4b	-12.33	0.91
4c	-11.2	6.61
4d	-11.7	2.35
4e	-12.38	0.846
4f	-11.88	1.96
4g	-11.26	5.55
4h	-11.28	5.43
4i	-10.45	21.82
4j	-10.65	15.49
4k	-10.62	16.23
4l	-10.96	9.26
4m	-11.14	6.79
4n	-11.39	4.44
4o	-10.76	13.0
4p	-10.05	42.94
4q	-11.52	3.59
4r	-11.5	3.72
4s	-10.56	18.06
4t	-10.41	10.09
4u	-10.92	9.91
4v	-10.56	18.18
4w	-12.15	1.23
4x	-10.79	12.35
4y	-10.62	16.35
4z	-10.38	24.81
4	-10.47	21.25
MTX	-8.62.	479.78

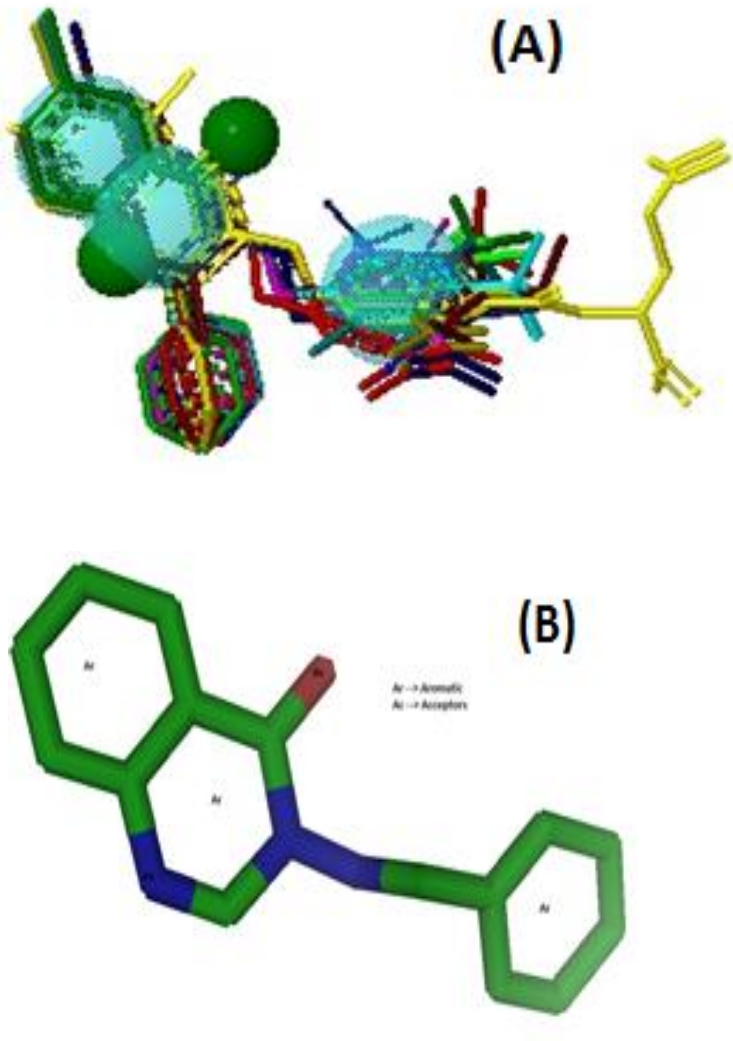

Figure 5.8: (A) Structural Alignment of molecules. (B) Pharmacophore having characteristics: Score(66.813)

The synthesized compounds have been comparatively evaluated in terms of their binding mode to hDHFR pocket. The substitution of 4th position with oxygen plays a vital role in binding with hDHFR. The most active compounds among 3 series 3i, in addition to Asp 64, it also forms hydrogen bond with Arg 70. The overall outcome of this molecular study revealed that: (1) the quinazoline ring is a satisfactory backbone for inhibition of mammalian DHFR, establishing contact with the key amino acids residues

in the enzyme pocket. The oxygen present at the 4th position formed hydrogen bond with the Asp 64 of hDHFR.

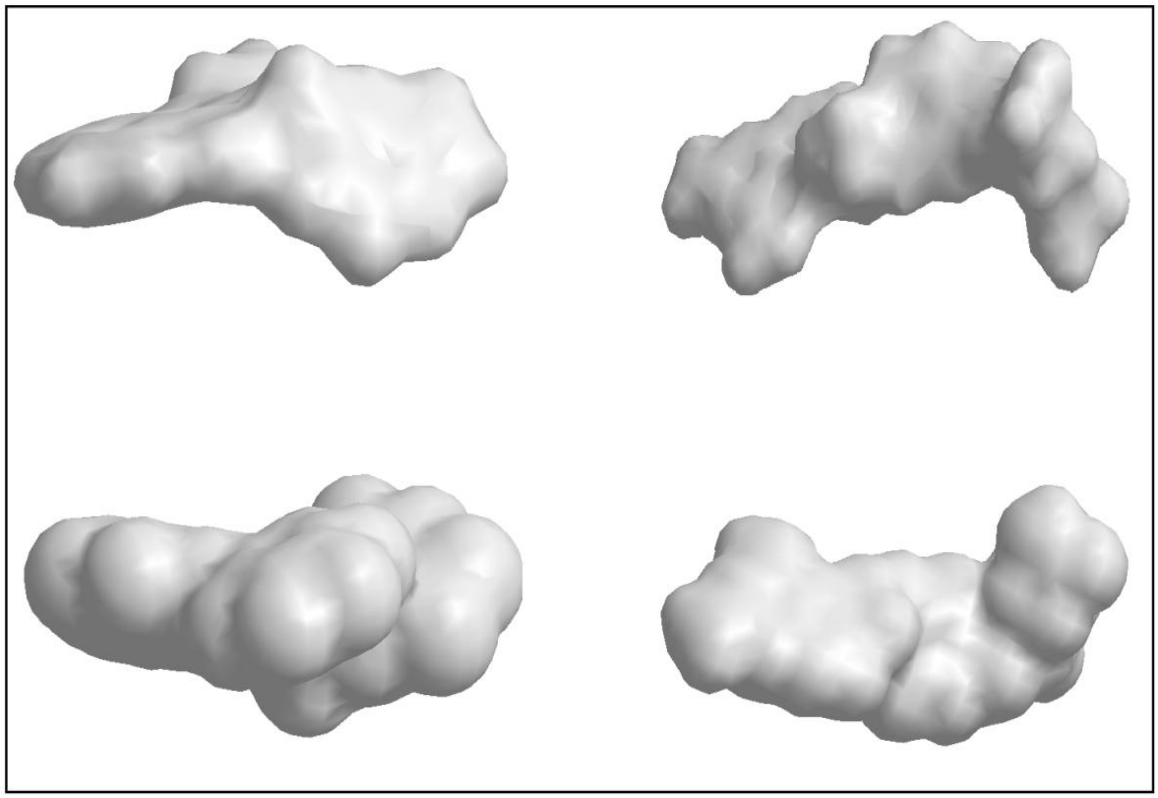

Figure 5.9: Connolly molecular surface (upper panel) and solvent accessible surface (lower panel) of MTX, 1 (left) and the active compound 3a (right).

Many authors have used ligand-based approach for pharmacophore modeling of species-specific DHFR inhibitors. Moreover, a pharmacophore model for hDHFR (human) inhibitors has also been modeled (Al-Omary *et al.,* 2010). All the studied compounds were used to develop a ligand based pharmacophore (Figure 5.8) using PharmaGist tool, which could be used further for the development of new, improved and optimized drug acting as inhibitor to hDHFR. The aligned binding conformation of the docked complexes clearly revealed that they can bind at the site quite well where natural ligand Dihydrofolate (Dhf) and inhibitor Methotrexate bound.

The pharmacophore has 3 aromatic rings and two hydrogen bond acceptors which enables in making several non covalent interactions like hydrophobic-hydrophobic interactions, hydrogen bonding, pi cloud interactions, etc.

This pharmacophore is qualifying all the four parameters of Lipinski's rule of five and thus could be considered as a lead molecule to generate new conformations for virtual screening library along with more modifications which could enhance its therapeutic index by enhancing the kind of interactions it could possibly make with the target protein. Furthermore, Connolly molecular surface, solvent accessible surface demonstrated their closely related molecular surface, charge distribution and electrostatic potential (Figure 5.9).

5.3.3 *In vitro* Inhibtion of Human Dihdrofolate reductase

The above section has shown that these compounds have possible properties and fragments to develop into a drug in future. We also found in molecular docking that these compounds have strong affinity for hDHFR. Hence, we thought to test the efficacy of these compounds as hDHFR inhibitors. Moreover, it is well known that amongst various methods of cancer treatment, inhibition of human dihydrofolate reductase plays a key role in cancer chemotherapy. Literature supports candidature of Quinazoline and quinazolinone to be potent hDHFR enzyme inhibitor hence chosen for this study. The synthesized compounds (3a-3j) were evaluated as inhibitors of human DHFR using instruction provided in assay kit. The human DHFR inhibition activities were reported as IC_{50} values (Tables 5. 8). Compounds 3a, 3d, 3g, 3h and 3i, proved to be the most active hDHFR inhibitors with IC_{50} values range of 0.3 to 5µM, while compounds 3b, 3c, 3e and 3f were considered of moderate activity with IC_{50} range of 6 to 10 µM, the rest of the tested compounds were considered poorly active with IC_{50} > 10 µM. Methotrexate (IC_{50} = 8 µM) was used as a positive control.

The inhibition in hDHFR activity indicated the inhibition of purine biosynthesis. The reference compound methotrexate showed IC_{50} value of 8±1.34, which is similar with the previous reports. The compounds 3a, 3b, 3c, 3d, 3f, 3g, 3h and 3i showed IC_{50} value less than methotrexate. Among these compounds, 3d and 3g showed four times less IC_{50} value than methotrexate.

Table 5.8- IC_{50} value of quinazoline-4(3H) against the hDHFR.

Compounds	hDHFR IC_{50} (μM)
3a	6.57±1.23
3b	8.0±0.53
3c	5.7±0.37
3d	2.4±0.41
3e	13.18±1.63
3f	7.87±0.82
3g	2.8±0.36
3h	5.95±1.53
3i	3.84±0.29
3j	17.21±0.64
MTX	8±1.34

5.3.4 Antiproliferative activity

As we have mentioned that our main focus of this chapter was to propose the antiproliferative activity of 3-(Aryldeneamino)-2-phenyl-quinazoline-4(3H)-one. Generally, for an agent to be useful as an anti-cancer drug, it must show preferential anti-proliferative activity against tumor cell lines. All the synthesized compounds (1a, 2a and 3a-3j) along with Methotrexate and curcumin (as a reference drug) were screened for their antitumour activity against three cancerous cell lines; HepG2 (human liver cancer cell line), MCF-7 (human breast cancer cell line) and HeLa (human cervical cancer cell line) using MTT assay as described previously with slight modification. Each cell line was incubated with five concentrations (0–100 μg/mL) of each compound and the results were used to create compound concentration versus survival fraction curves. Three experiments with test compounds were performed in triplicate for each assay and the percent inhibition of cell viability was determined and compared with the data available for standard Methotrexate and Curcumin. The data were subjected to linear regression analysis and the regression lines were plotted for the best fit straight line. The IC_{50} (50%

inhibition of cell viability) concentrations were calculated based on the regression equation. The IC_{50} of each compound against cell lines are shown in Table 5.9.

The results represented in Figures 5.10, 5.11 and 5.12 clearly show the growth inhibitory effect in HeLa , HepG2 and MCF7 cell lines in the presence of synthesized compound at concentration of 75µg/mL .

Table 5.9: IC_{50} value of quinazoline-4(3H) against the growth of HeLa, HepG2 and MCF7 cancer cell lines.

Compounds	HeLa (µg/ml)	MCF 7 (µg/ml)	HepG2 (µg/ml)
1a	ND	ND	ND
2a	ND	ND	ND
3a	22±2	21±6	23±3
3b	97±5	ND	28±5
3c	ND	95±5	45±3
3d	54±3	68±3	ND
3e	87±6	ND	ND
3f	ND	ND	30±4
3g	ND	52±5	64±6
3h	ND	ND	27±4
3i	23±4	28±5	46±4
3j	ND	ND	ND
Curcumin	17±1	22 ±3	9±3
Methotrexate	27±2	29±2	42±3.7

ND- Not Defined

So, concerning sensitivity of cell lines to the synthesized compounds, HepG2 cell line was shown to be the most sensitive toward the tested compounds followed by MCF7 and HeLa cell lines. Out of the 12 compounds, 7 showed activity against HepG2 cell lines, 5 showed against MCF7 cell line and 5 showed against HeLa cell lines. So, the tested compounds showed a distinctive pattern of selectivity. Based on the IC_{50} values, we have categorized the active compounds in three groups; highly active compounds

whose IC_{50} ranges from 0-30 μg/mL, moderate active compounds whose IC_{50} ranges from 31-70 μg/mL and poor active compounds whose IC_{50} ranges from 71-100 μg/mL.

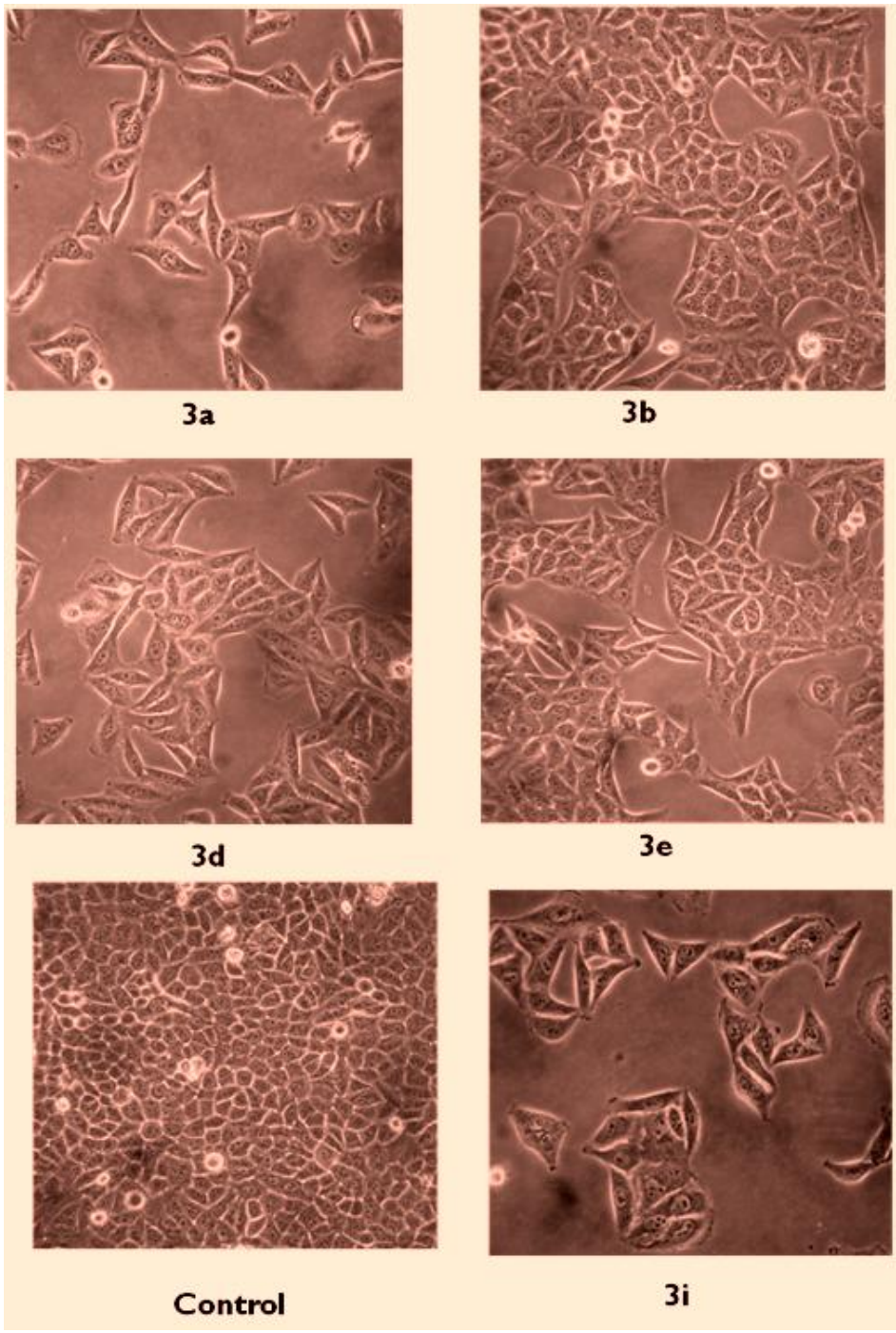

Figure 5.10: Effect of 75μg/ml of quinazoline-4(3H)-one on the proliferation of HeLa cell line (observed under phase contrast microscope).

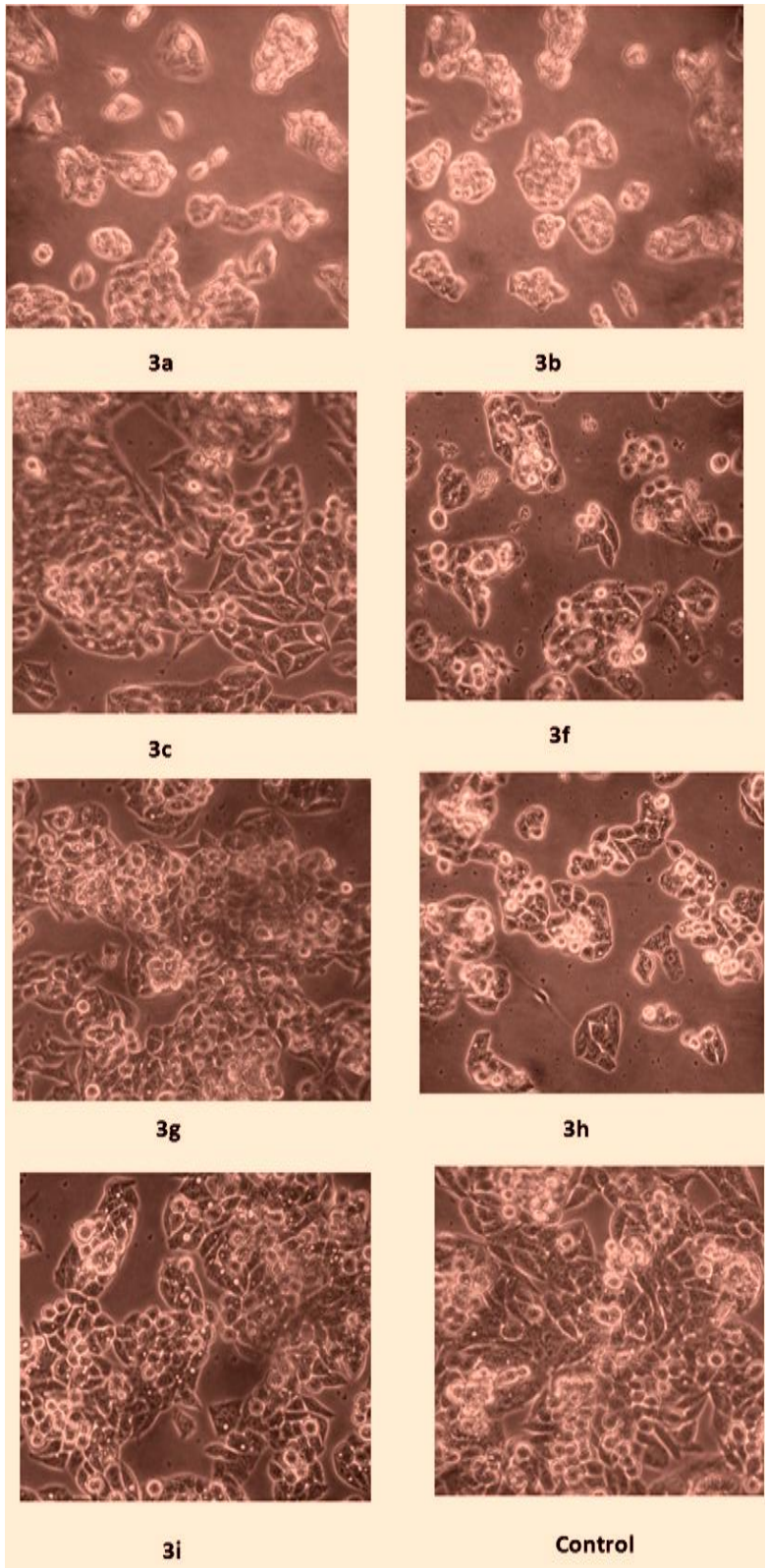

Figure 5.11: Effect of 75µg/ml of quinazoline-4(3H)-one on the proliferation of HepG2 cell line (observed under phase contrast microscope).

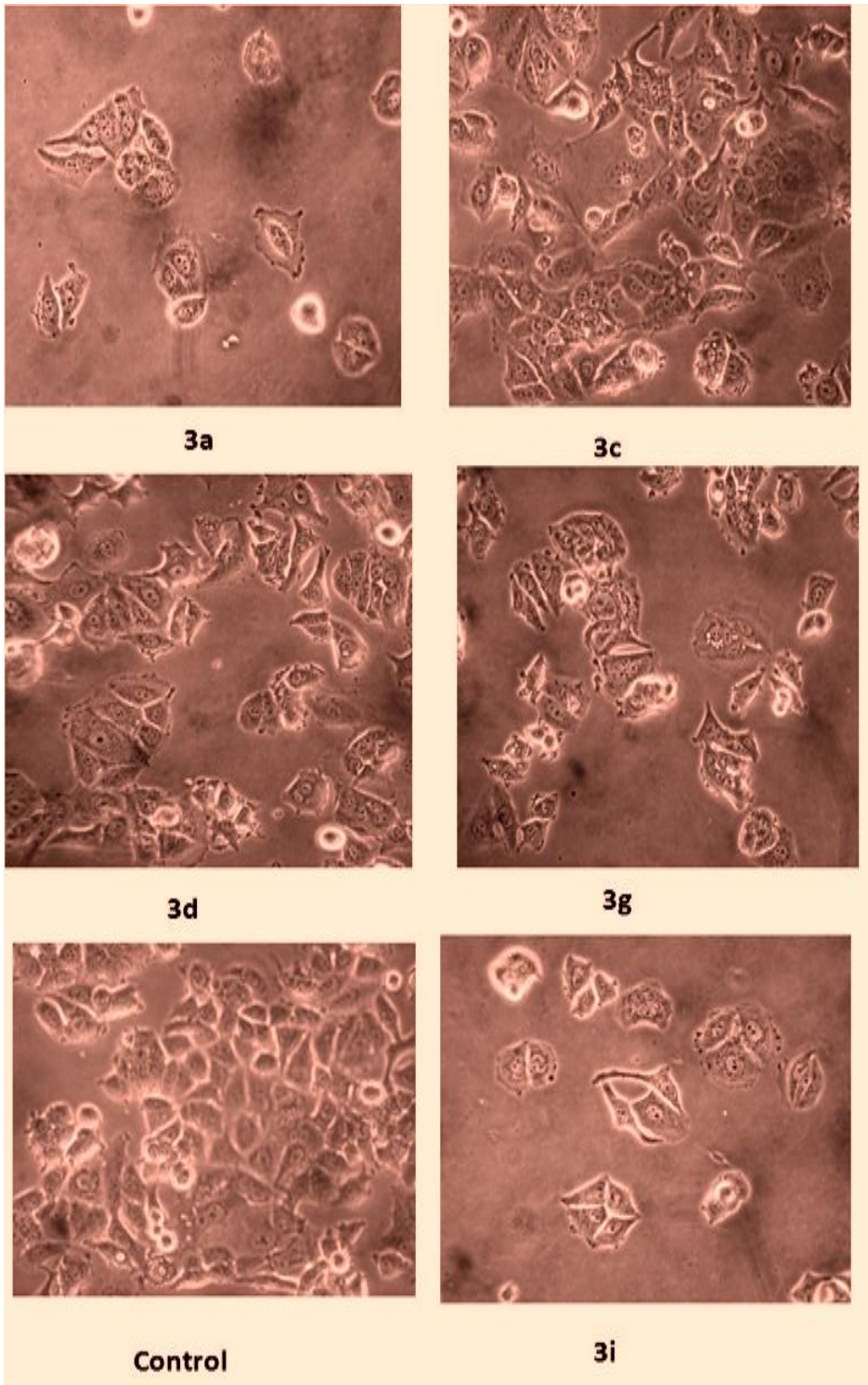

Figure 5.12: Effect of 75µg/ml of quinazoline-4(3H)-one on the proliferation of MCF7 cell line (observed under phase contrast microscope).

Considering HepG2 cell line, compound 3a (IC_{50} = 23±3) showed highest activity, along with 3a, 3b, 3f and 3h showed high activity, 3c and 3i showed moderate activity while 3g (IC_{50} = 64±6) shows poor activity. Against MCF7 cell line, compound 3a (IC_{50} = 21±6), 3i (IC_{50}= 28±5) showed high activity, 3d and 3g showed moderate activity whereas, 3c (IC_{50}= 95±5) showed poor activity. In view of HeLa cell line, compound 3a and 3i showed high activity, 3d showed moderate activity while 3b and 3e showed poor activity. Results revealed that 3a and 3i showed broad spectrum activity by inhibiting the proliferation of three studied cell lines. The broad spectrum activity of compound 3i could be related to presence of a nitro-aromatic group in the 2- phenylquinazolinone ring system. Various literatures supported that nitro group containing compounds showed various biological activities like antibacterial, antihelmentic, anticancer etc. Previous author reported that presence of nitro group enhanced the cytotoxicity activity in human melanoma cell (Sk *et al.,* 2011). The nitro-aromatic compound, 1-chloro-2,4-dinitrobenzene (dinitrochlorobenzene, DNCB) has been reported to induce apoptosis in HeLa and A549 cells (Cennas *et al.,* 2006). The nitro group containing aromatic compound, Flutamide, is also used in metastatic prostate cancer (Coe *et al.,* 2007). Aromatic compounds containing hydroxyl group is reported to regulate biological activities. The methoxy group present in the aromatic ring was also reported to possess vital role in growth inhibition activity (Nagarajan *et al.*, 2004). Curcumin containing hydroxy and methoxy groups were shown to possess higher cytotoxic activity on different cell lines (Naama *et al.*, 2010). Compound 3g contains both hydroxyl and methoxy groups in its quinazolinone ring, the presence of these two groups may be responsible for its effect on the cancer cell lines used. The hydroxyl group present in the compound in 3a may be attributed to its higher activity. So, we can hypothesize that the high activity of compounds 3a and 3i against three cancer cells may be attributed to the occurrence of OH and NO_2 moieties which may be important for hydrogen bonding at the receptor site. The results obtained from trypan blue test were similar to those obtained by the MTT test and reveal a clear cytotoxic effect of these compounds. Morphological alterations, such as rounded cells were not visible after 24 of incubation. Interestingly, the extent of the cytotoxic effects of the compounds depended on the tumour cell line.

These compounds also exhibited several interactions with human dihydrofolate reductase enzyme, giving rise to the conclusion that they might exert their action through inhibition of hDHFR enzyme. However, the same pattern of inhibition was not observed in antiproliferative activity. This may be due to the hindrance in entrance and bioavailability of compounds. We have addressed the way out of low solubility in the next chapter.

Chapter 6

Preparation and Characterization of β-Cyclodextrin inclusion complex of Quinazoline-4(3H)-ones

Chapter 6

Preparation and Characterization of β-Cyclodextrin inclusion complex of Quinazoline-4(3H)-ones

6.1 Introduction

Quinazoline-4-(3H)-one derivatives have gained extensive research interest due to their wide range of biological activity. It is reported that they exhibit antitubercular, antihypertensive, anticancer, anti-HIV, antiviral, anti-inflammatory and antifungal activities (Waisser *et al.,* 2010; Li *et al.,* 2010). Despite their great medicinal value to emerge as successful drugs, aqueous solubility is one of the key limiting determinants (Nanjwade *et al.,* 2011). Cyclodextrins (CDs) are water-soluble, homochiral, cyclic oligosaccharides containing six, seven, or eight α-1, 4-linked D-glucopyranose units (α, β, and γ cyclodextrins), and have pore sizes ranging from 4.9 to 7.9 Å (Figure 6.1) (Asanuma *et al.,* 2000; Singh *et al.,* 2002; Wulff *et al.,* 2002; Ogoshi *et al.,* 2003). The hydrophobic nature inside its cavity with an outside hydrophilic part enables β-CD (Figure 6.2) to encapsulate hydrophobic molecules to form thermodynamically favored molecular microcapsules, namely inclusion complexes or host–guest complexes. This binding between the guest molecules and host β -CDs is not permanent, but rather it remained in a dynamic equilibrium. The strength of binding mainly depends on specific local interactions between the surface atoms and the extent of how ‘‘host–guest’’ complex fits together. In recent times, this approach of complexion with β-Cyclodextrins (Figure 6.3) has been frequently used to increase oral bioavailability (Basson *et al.,* 1996; Buvari & Barcza, 2000; Nasonglela *et al.,* 2003). In this approach some drugs gain shelf life (Amma *et al.,* 2006) to a certain extent, and additionally it contributes to controlled drug release rate, improved organoleptic properties and maximized gastrointestinal tolerance (Loftsson & Brenster, 1996). Thus, increased solubility of a drug plays a very important role in absorption, which ultimately affects its bioavailability (Ghodkea *et al.,* 2009).

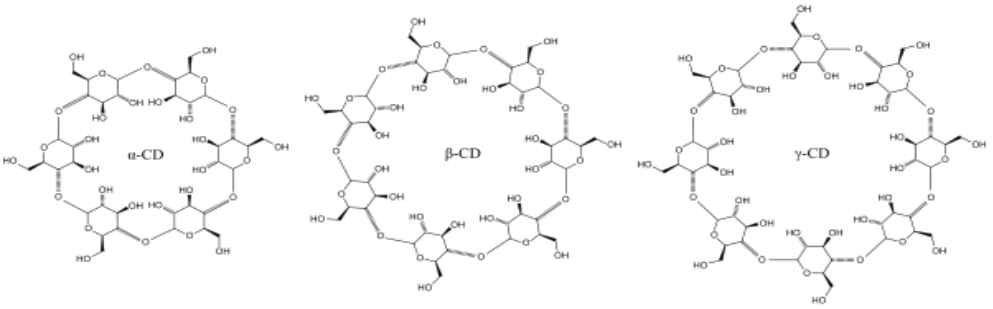

Figure 6.1: Representing the α-CD, β-CD and γ-CD.

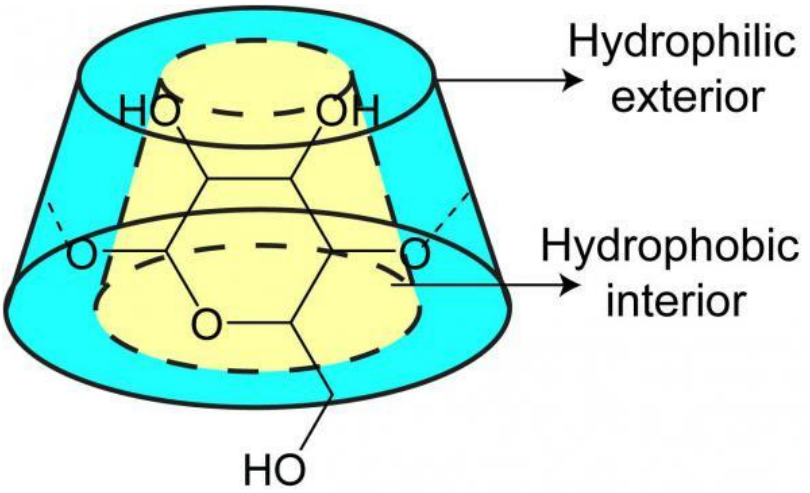

Figure 6.2: Interior Hydrophobic region and Exterior Hydrophilic region of β-cyclodextrin

A number of quinazoline products based upon cyclodextrins complex were reported. Most of the studies however remained confined to established drugs while very few emphasized to increase the solubility of potentially biologically active quinazoline-4(3H)-ones which may help developing new drugs in the future. Recently, a protocol for synthesis of 2, 3-dihydroquinazoline-4(1H)-one derivatives, where a prior formation of an inclusion complex of isatoic anhydride with β -cyclodextrin was reported (Patel & Dalal, 2011). The host–guest complexation between 5-aminoisoquinoline and β-CD was also studied (Rajamohan *et al.*, 2012). It is therefore important to develop methods which can be applied to enhance the solubility.

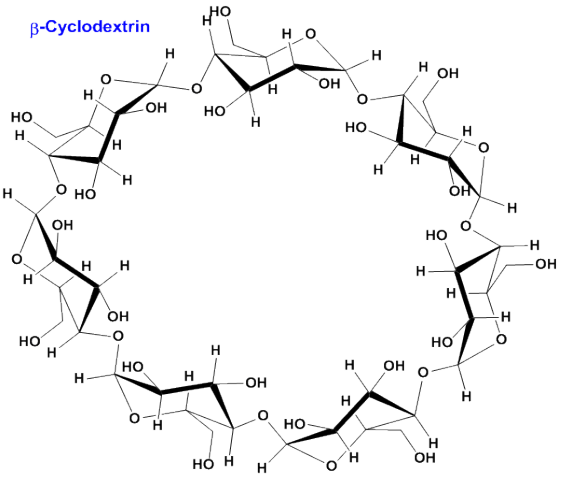

Figure 6.3: Structure of β-cyclodextrin

6.1.2 Techniques for solubility enhancement

There are various techniques available to improve the solubility of hydrophobic drugs. Some traditional and novel approaches to improve the solubility are:

a. *Particle Size Reduction*

The solubility of drug is often intrinsically related to drug particle size. As particle becomes smaller, the surface area to volume ratio increases. The larger surface area allows a greater interaction with the solvent which cause increase in solubility.

b. *Solid Dispersion*

Solid dispersions represent a useful pharmaceutical technique for increasing the dissolution, absorption and therapeutic efficacy of drugs in dosage forms. The concept of solid dispersions was originally proposed by Sekiguchi and Obi, who investigated the generation and dissolution performance of eutectic melts of a sulphonamide drug and a water-soluble carrier in the early 1960s **(**Obi & Sekiguchi, 1961**)**. The term solid dispersion refers to a group of solid products consisting of at least two different components, generally a hydrophilic matrix and a hydrophobic drug.

c. *Solvent Evaporation Method*

Solvent Evaporation Method is also useful for improvement and stability of solid dispersions of poor water soluble drugs. Tachibana and Nakumara **(**Tachibana & Nakamura, 1965**)** were the first to dissolve both the drug and the carrier in a common solvent and then evaporate the solvent under vacuum to produce a solid solution. This enabled them to produce a solid solution of the highly lipophilic β-carotene in the highly water soluble carrier polyvinylpyrrolidone. Many investigators studied solid dispersion of meloxicam naproxen and nimesulide using solvent evaporation technique (Chaumeli, 1998; Blagden *et al.,* 2007; Vogt *et al.,* 2008)

.

d. *Nanosuspension*

Nanosuspension technology was developed as a promising candidate for efficient delivery of hydrophobic drugs. This technology is applied to poorly soluble drugs that are insoluble in both water and oils. A pharmaceutical nanosuspension may be called as biphasic system consisting of nano sized (average particle size ranging between 200 and 600 nm.) drug particles stabilized by surfactants for either oral and topical use or parenteral and pulmonary administration (Muller *et al.,* 2000).

e. *Precipitation Techniques*

In the precipitation technique, drug is dissolved in a solvent, which is then added to nonsolvent to precipitate the crystals. The basic advantage of precipitation technique is the use of simple and low cost equipment. The basic challenge of this technique is that during the precipitation procedure the growing of the drug crystals needs to be controlled by addition of surfactant to avoid formation of microparticles. The limitation of this precipitation technique is that the drug needs to be soluble in at least one solvent and this solvent needs to be miscible with the non-solvent. Moreover precipitation technique is not applicable to drugs, which are simultaneously poorly soluble in aqueous and non-aqueous media (Riegelman, 1971).

f. *Inclusion Complex Formation Based Techniques*

Lipophilic drug-cyclodextrin complexes, commonly known as inclusion complexes, can be formed simply by adding the drug and excipients together, resulting in enhanced drug solubilization. Among all the solubility enhancement

techniques, inclusion complex formation technique was employed more precisely to improve the aqueous solubility, dissolution rate, and bioavailability of poorly-water soluble drugs.

In this chapter, the inclusion complexes were prepared and characterized by different spectroscopy and PXRD. It was observed that the effects of complexation by β-CD showing enhancement of the aqueous solubility of the compound.

6.2 Materials and method

6.2.1 Chemicals*:* β- cyclodextrin (HiMedia) was used in this study. All other reagents were of analytical grade

6.2.2 Preparation of inclusion complex

***Preparation of complexes Preparation of Physical mixture (PM*)**: The physical mixtures of the compound 2-phenyl-4H-benzo[d][1,3]oxazin-4-one and β-CD [1:1 molar ratio] were made by mixing together in a mortar and pestle.

Preparation of the complex by Kneading method (KND): The physical mixture was triturated in a mortar with a small volume of water-ethanol solution. The thick slurry was kneaded for 45 min and then dried at 40 ^{o}C. Dried mass was pulverized and sieved through a 100 micron mesh.

Preparation of the complex by Co-evaporation method (COE) **:**The aqueous solution of β-CD was added to an alcoholic solution of 2-phenyl-4H-benzo[d][1,3]oxazin-4-one. The resulting mixture was stirred for 1 hr and was evaporated at a temp of 45^{o}C until dry. The dried mass was pulverized and sieved through a 100 micron mesh.

Preparation of the complex by Freeze–Drying Method (FD) **:**The physical mixtures in 500 ml double distilled water were stirred for 2 days. The suspension was freeze-dried and the freeze-dried complex thus produced was pulverized and sieved through a mesh.

6.2.3 Optimization of the complex formation

The standard curve was prepared by dissolving the 2-phenyl-4H-benzo[d][1,3]oxazin-4-one in the water. The complexes formed in different methods were quantified in solution by comparing OD at 280 nm from this standard curve.

6.2.4 Molecular modelling

The geometry optimization of the compound and β-CD inclusion complexes was performed in gas phase and in the Cosmo-solvation sphere using MM2 and PM3 semi empirical quantum methods and the minimized energy molecular models were found to be docked properly when water was set as a solvent as a cosmo-solvation sphere (in different methods).

6.2.5 Characterization of inclusion complex

Thin Layer Chromatography: The compound, CD and complex dissolved in distilled water. TLC was done using the solvent system ethyl acetate: butanol (5:4) in F549 TLC plates. The spots were identified in UV.

UV spectroscopic study: All spectra were recorded in the wavelength range 200–500 nm at room temperature (UV-1700 Spectrometer, Jasco, Tokyo, Japan). The complex of the compound was solubilized in distilled water by stirring for ten minutes and thereafter the total solution was filtered. UV spectra were studied with this filtered solution without delay.

Fourier Transform Infrared spectrophotometry: IR spectra of stated compound, β-CD, physical mixture of compounds and the inclusion complex were monitored by mulling in nujol. All the samples were scanned in the region 4000-400 cm^{-1}.

Raman Spectroscopy: Raman spectra of the stated compounds, β-CD, physical mixture of compounds and the inclusion complex were recorded on Varian FT-Raman and Varian 600 UMA. All the samples were scanned in the region 4000-400 cm^{-1}.

Differential Scanning Calorimetry

Differential scanning calorimetry (DSC) was carried out with a Shimadzu DSC-60 instrument (Shimadzu, Kyoto, Japan). Samples weighing 3–5 mg were heated in opened aluminum pans at a rate of 10 K/min under nitrogen gas flow of 35 mL/min.

Powder X-Ray Diffraction

X-ray Powder Diffraction (XRPD) patterns were recorded on a X'Pert Philips PW3020 diffractometer (Philips, The Netherlands) over the 2y range of 58–408, using graphite monochromatized Cu Ka radiation (1.54184 A °), in aluminum sample holders, at room temperature.

6.3 Results and Discussion

6.3.1. Standardization of methods and mulling time

Before switching on to the formation of inclusion complex, we have performed simple computational study to get scheme/suggestion for best way to form inclusion complex. In this context, molecular modelling was carried out in the gas phase, and in cosmosolvation in water as a solvent. The energies calculated for the stoichiometric systems 1:1 and 1:2 (compound: cyclodextrin) are described. In all cases, the more stable conformations were attained in the presence of water. The 1:1 stoichiometry was the one which presented the higher stability. The possible structure of the inclusion complex produced is shown in the Figure 6.4**.** It was found that water played a pivotal role in the formation of the complex. In the absence of any water in the system, the inclusion complex did not form *i.e*. compound 2-phenyl-4H-benzo[d][1,3]oxazin-4-one did not enter into the cavity of cyclodextrin, but with the addition of water, it readily entered into the cavity and formed an inclusion complex.

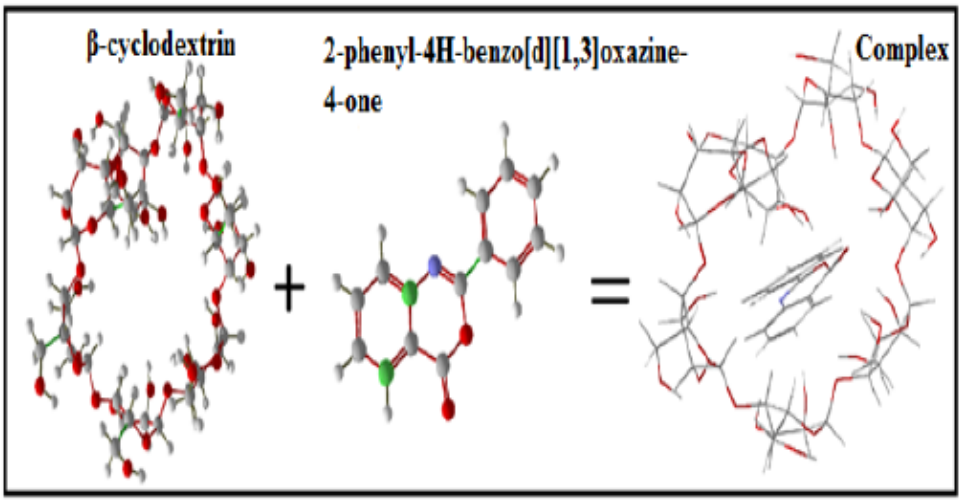

Figure 6.4: The probable structure of inclusion complex

The inclusion complexes formed by different methods were primarily characterized by the degree of transparency of the solution made in water. In 5.0 ml of distilled water, β- CD [34 mg (6 mM)] solubilized to clear solution, the physical mixture [17 mg β- CD + 3.34 mg stated compound (3 mM : 3 mM)] formed a turbid suspension, and the complex [17 mg β- CD + 3.34 mg stated compound (3 mM : 3 mM)] was found to be faintly turbid as shown in Figure 6.5A, B, & C respectively. A comparative TLC study was done on pre-coated silica-gel plates using the solvent mixture [ethyl acetate: butanol (5:4 v/v)]. The compound showed Rf. value of 0.8 while β- CD did not move with the solvent system. The spots corresponding to β- CD and the compound was visible with little trailing of the compound spot in the physical mixture (PM) while in the complex a large trailing was observed with faint spot of the free compound. The occurrence of the faint spot along with the trailing is the indication of the slow diffusion of the compound in the eluting solvent mixture used in TLC study.

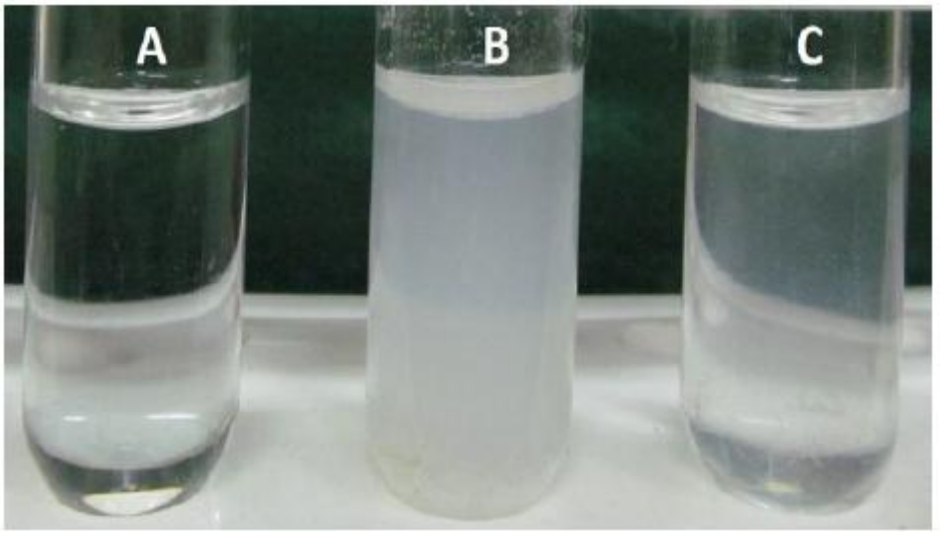

Figure 6.5: Solution in water (A) β-CD (B) Physical mixture (C) Inclusion Complex

In order to design the best formulation of inclusion complexes, we have used the information obtained by molecular modelling. The β -cyclodextrin was mixed with a small amount of warm water to make slurry and then kept at the 50 ^{o}C for 12 h. We allowed extra time so that the dry β- CD swells to full. The slurry was maintained for 12 h with occasional mauling. After 12 h, equimolar amount of the 2-phenyl-4H-benzo[d][1,3]oxazin-4-one and the β -cyclodextrin slurry was mixed by triturating in a mortar with a small volume of water-ethanol solution. The thick slurry was kneaded

for 45 min and air dried at 50 ^{o}C. The crushing time for the complex preparation was varied as follows: 0 min, 20 min, 30min, 40 min and 60 min. The 1:1 mixture of compounds and β-cyclodextrin was used in every preparation. Dried mass was sieved through a 100 micron mesh. It is found that after 40 min crushing, the product yield was optimized. It is observed that crushing time has also played an important role in the complexation process. With the increase in the time of crushing during making a complex, the absorbance of aqueous solution increased. It was found that upto 40 minutes the UV absorption in water solution increases. This serves to be a very basic and simple novel experiment that shows how the complex formation depends upon the crushing time. It showed no further enhancements of the peaks beyond that time *i.e.* a plateau after 40 minutes of crushing of the compound, which revealed that 40 minute crushing time is the optimum. The time for optimization of inclusion complex is shown in Figure 6.6.

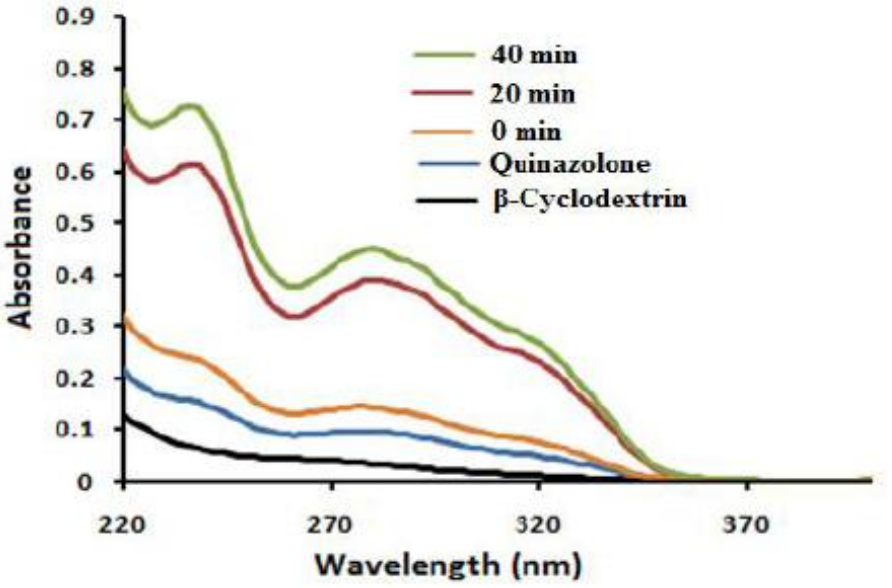

Figure 6.6: Effect of crushing time on inclusion complex formation

We used UV-absorption as an indicator for the formation of inclusion complex; since the compounds under study possessed chromophores which display appreciable UV-absorption; but they are insoluble in water. After formation of inclusion complex, expectedly the water solution displayed versus absorption and the amount of absorption was used as a good indicator of the complex formation. In the UV spectra, the relative absorbance of the compound was changed due to the complex

formation as shown in Figure. 6.7. It was found that the complex produced in the physical mixture (PM) without the addition of the water was very low in comparison to the complex produced by the kneaded (KND) method which involved the addition of water during crushing. The study shows that the dissolution rate of 2-phenyl-4H-benzo[d][1,3]oxazin-4-one (Quinazolone) was enhanced to a great extent by complex formation using the kneading method as compared to other methods.

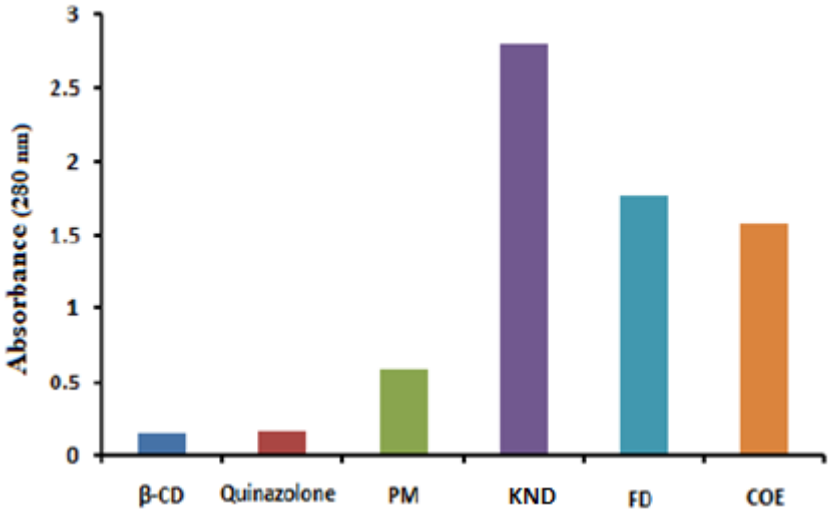

Figure 6.7: Efficiency of different methods for formation of inclusion complex.

Vibrational spectroscopic studies with theoretical calculation of the 2-phenyl-4H-3,1- benzoxazine-4-one is reported earlier. This helped us to conclusively report the formation of the complex from its IR studies. The most intense IR-band of the compound is the C=O stretching band which occurs at 1760-1763 cm^{-1} in IR KBr and 1760.9 cm^{-1} in Nujol. The slight shift in lower wave number in nujol is the indication that in non-polar environment the carbonyl stretching frequency can shift slightly to lower frequency. In the complex, the band appeared at 1762.8 cm^{-1} which can be easily characterized. This indicates that in spite of the hydrophobic environment inside the β- cyclodextrin, the stretching of the band is highly restricted due to the encagement into the cyclodextrins cavity. In PM, this band appeared at 1772.5 cm^{-1} indicating more polar environment which has dampened the frequency to about 10 cm^{-1}. Hence, it indicates the fact that the compound remained outside the β-cyclodextrin. The asymmetric stretching of C-O generally appears in the range of 1255±10 cm^{-1}. This band was identified in IR at 1258 cm^{-1} (KBr), at 1257.5 cm^{-1} (Nujol) in PM and in the complex, and remained unchanged in all the cases. Another

strong band of the titled compound is the C=N stretching which occurred at 1692 cm^{-1} as a sharp band in nujol. This band for the complex appeared at 1607 cm^{-1} which shows that the band is very sensitive to environmental change; in fact, we have identified the band as weak in the PM and very weak in the complex. The related band, phenyl carbon-nitrogen band, identified at 1319 cm^{-1} in KBr, 1313 cm^{-1} in nujol is also sensitive to the change in polarity of the environment that appears at 1319 cm^{-1} in the complex and 1309.6 cm^{-1} in the PM. The out of plane deformation band of phenyl ring at around 755±15 cm^{-1} is also a characteristic band. In the compound, the band is identified in KBr at 765 cm^{-1}, in nujol at 763 cm^{-1}. This band appeared for the complex at 763.8 cm^{-1} and for PM at 769.5 cm^{-1}. This band is characteristic of mono substituted benzene ring derivatives. The observed changes in their occurrence indicate that this ring also encaged inside the β- cyclodextrins ring (Figure 6.8).

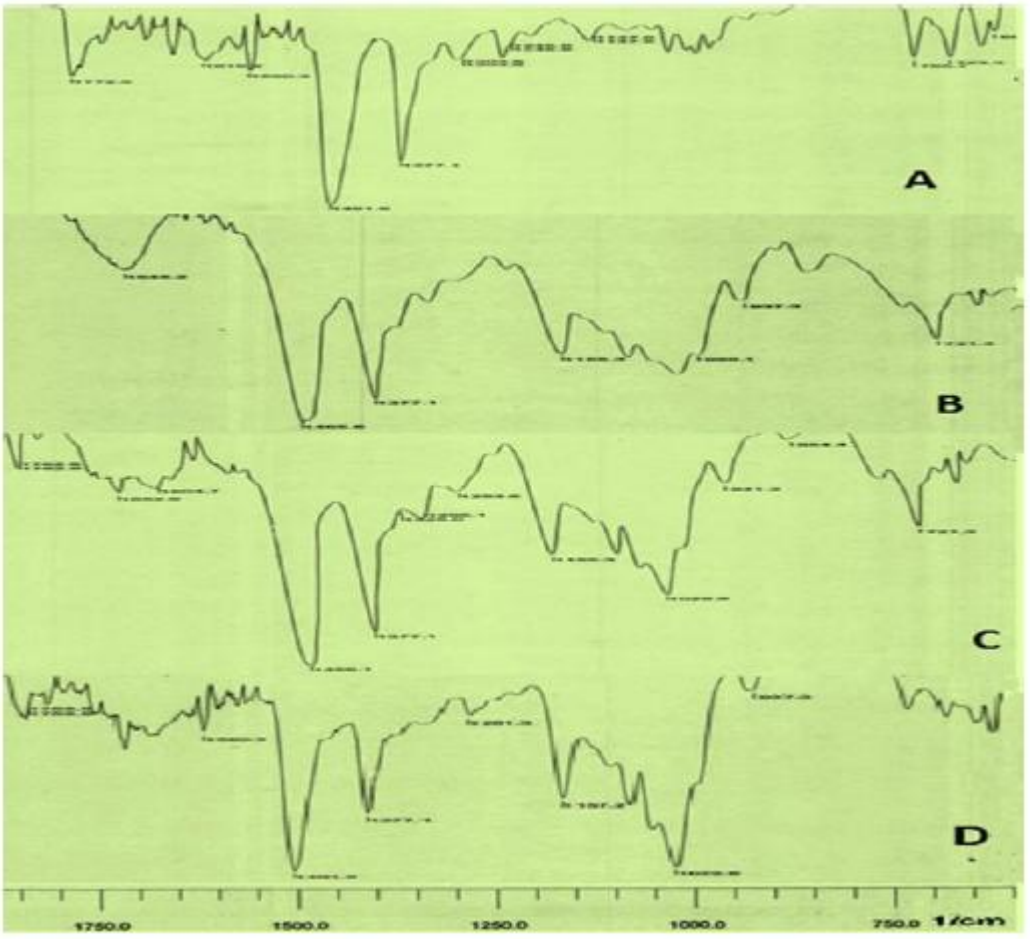

Figure 6.8: IR spectra of (A) 2-phenyl-4H-3,1- benzoxazine-4-one (B) β-cyclodextrin (C) Physical mixture (PM) and (D) Inclusion complex (KND).

Thus, in a nutshell the observed changes in trivial bands clearly designates that the full molecule is encaged inside the cavity of β- cyclodextrins ring in the complex and residing outside in PM.

After getting a clear indication of the complex formation of 2-phenyl-4H-benzo[d][1,3]oxazin-4-one with CD, we have tried for more biologically active synthesized compounds (3a, 3b and 3c) for inclusion complex study in more detail. In our previous studies, we have reported the vibrational spectroscopy and respective DFT calculation of these three compounds. So, we have chosen them for inclusion complex study. The inclusion complexes were prepared with same methods used for 2-phenyl-4H-3,1- benzoxazine-4-one.

6.3.2 Vibrational spectroscopy study of inclusion complex

Infrared and Raman spectra of the compounds (3a, 3b and 3c) and inclusion complex and physical mixture of compunds with β- CD are shown in Figure 6.9a, b and c and 6.10a, b and c respectively. An infrared spectrum was used to evaluate the functional groups of compounds involved in the complexation. Infrared and raman spectra of compounds are characterized by identification of the carbonyl (C=O), methyl. In the spectra of the inclusion complex, these bands were shifted towards higher frequencies and the asymmetrically vibration peak of C=O band was obtained as three intensity peaks increases, suggesting formation of the inclusion complex. The IR spectrum of β-CD is characterized by intense bands at 3000–3600 cm^{-1} that are associated with the absorption of the hydrogen bonded –OH groups of β-CD. The vibrations of the CH-CH groups appear in the 2897– 3250 cm^{-1} region. Thus, spectral changes were always concerned with COOH, -CH_3 and CH groups of the β- CD.

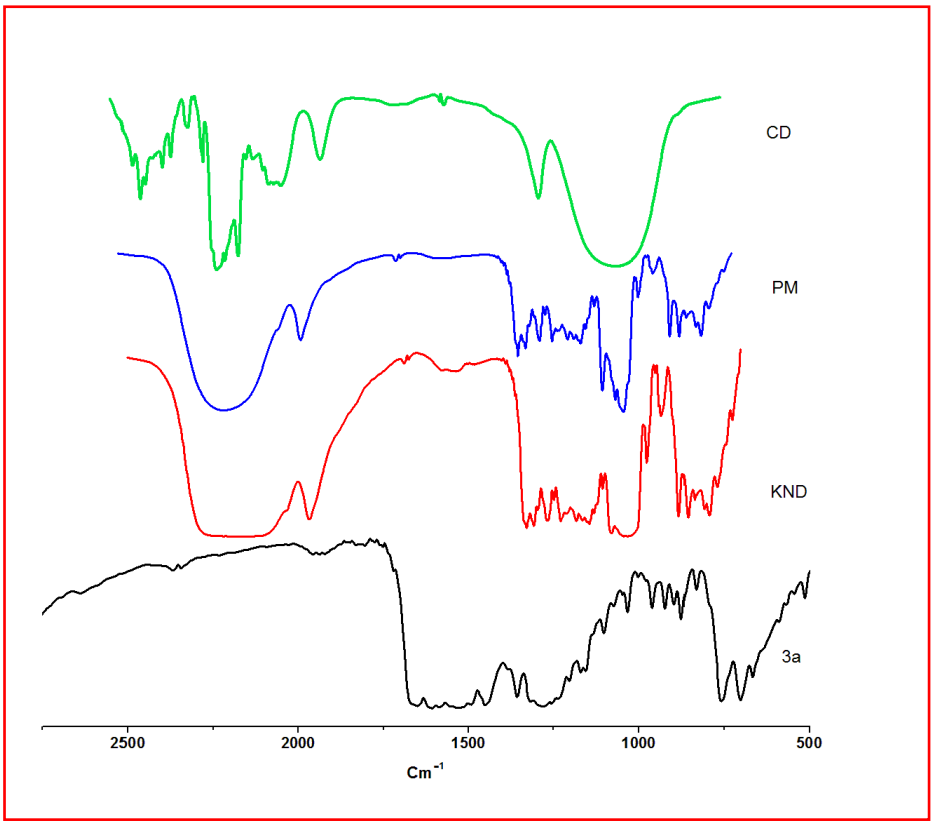

Figure 6.9(a) : FTIR spectra (KBr pellets): Compound 3a; Physical mixture (PM) of 3a and β-CD; 3a/β-CD inclusion complex by kneaded method (KND) and β-Cyclodextrin (CD).

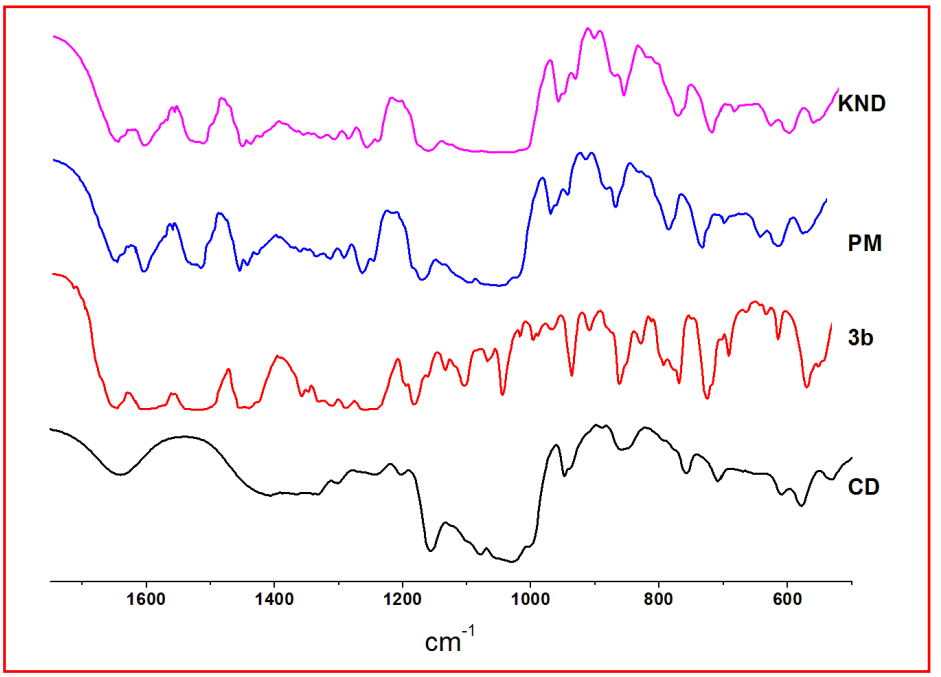

Figure 6.9(b): FTIR spectra (KBr pellets): Compound 3b; Physical mixture (PM) of 3b and β-CD; 3b/ β-CD inclusion complex by kneaded method (KND) and β-Cyclodextrin (CD).

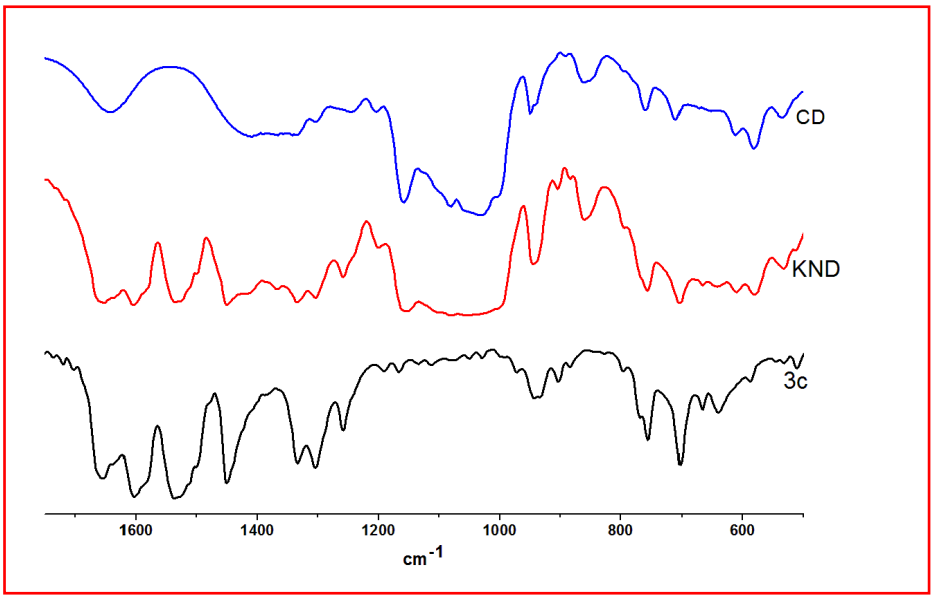

Figure 6.9(c): FTIR spectra (KBr pellets): Compound 3c; Physical mixture (PM) of 3c and β-CD; 3c/ β-CD inclusion complex by kneaded method (KND) and β-Cyclodextrin (CD).

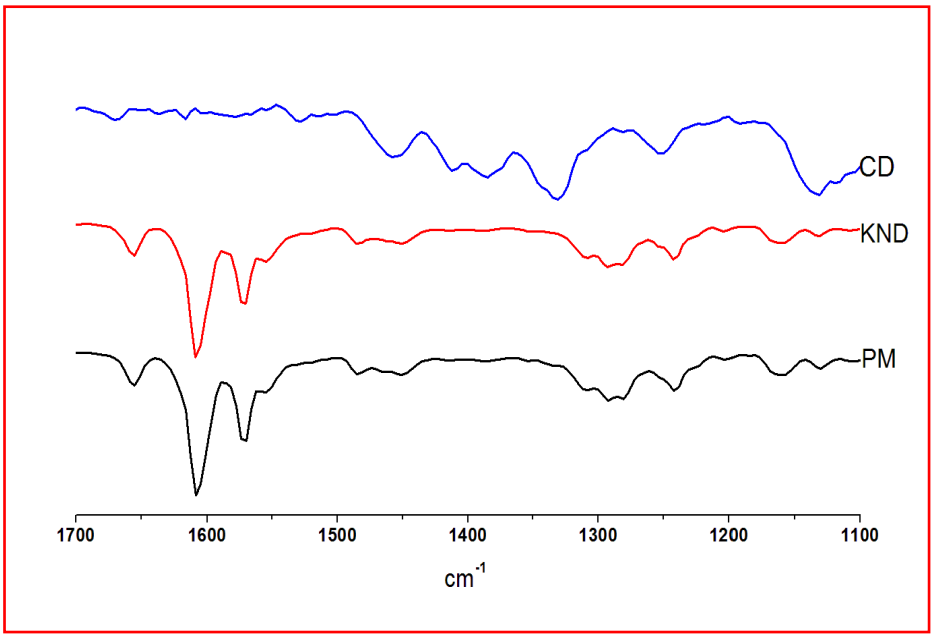

Figure 6.10(a): Raman spectra: Compound 3a; 3a/ β-CD inclusion complex (KND) and β-Cyclodextrin (CD).

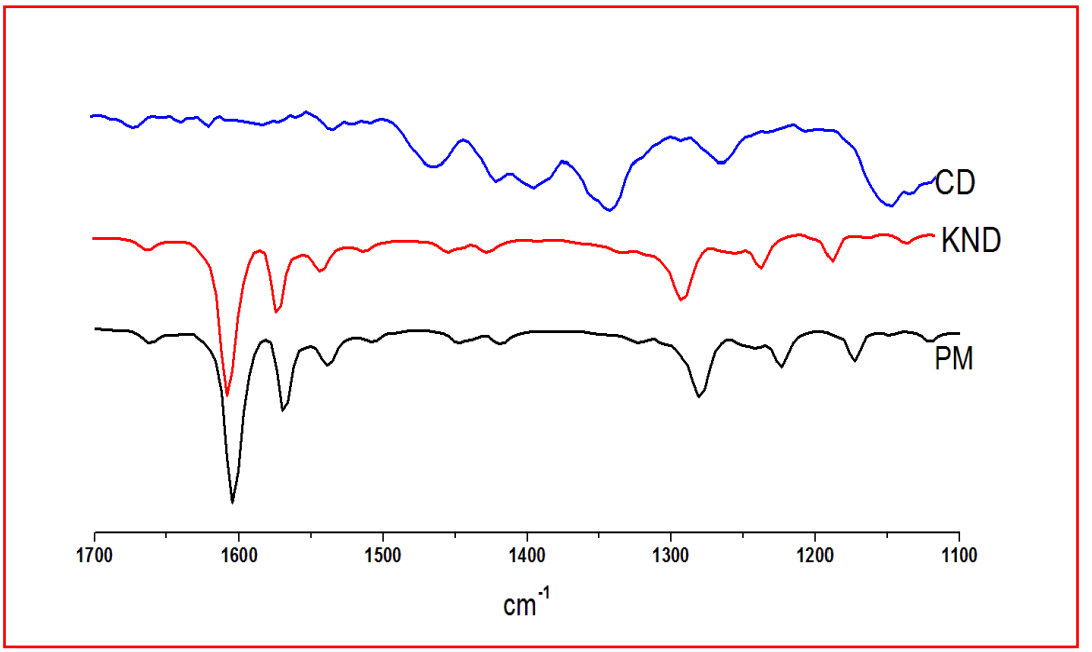

Figure 6. 10 (b): Raman spectra: Compound 3b; 3b/ β-CD inclusion complex (KND) and β-Cyclodextrin (CD).

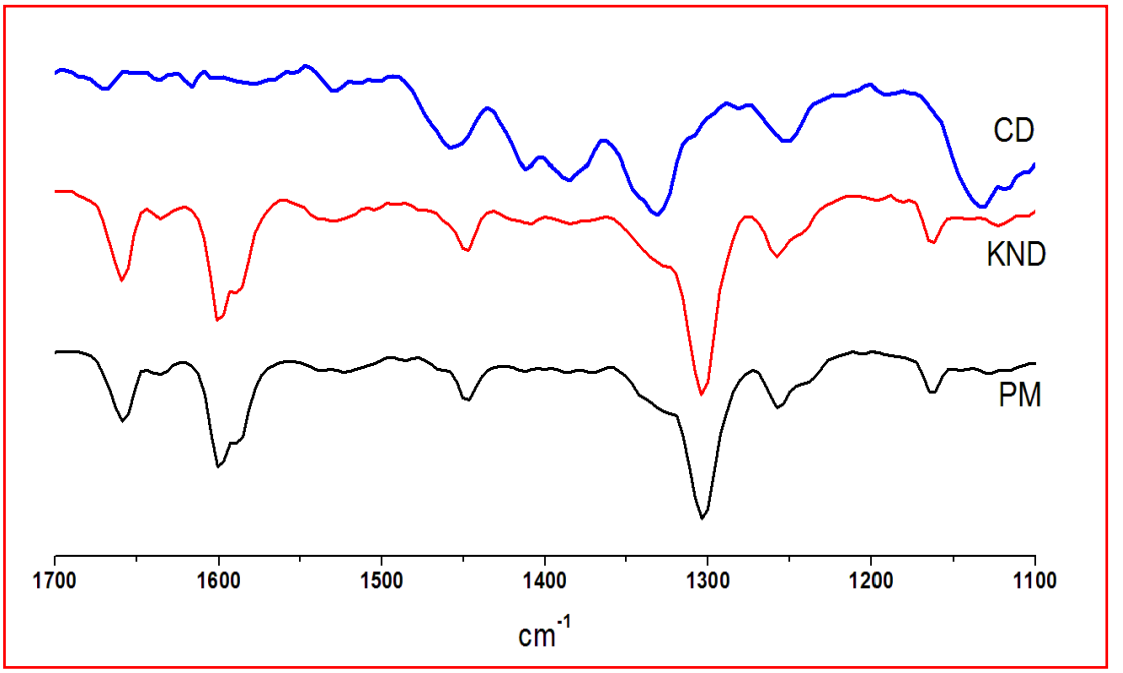

Figure 6. 10(c) Raman spectra: Compound 3c; 3c/ β-CD inclusion complex (KND) and β-Cyclodextrin (CD).

6.3.3 Powder X-ray diffraction study of inclusion complex

True inclusion complexes have its diffraction pattern altered from those of pure components. The powder X-ray pattern for individual components, complex and physical mixture is shown in Figure 6.11a, b and c. The diffraction pattern of complex was found to be different than diffraction pattern of pure β-CD and compounds. Comparing the pattern for β- CD-compounds complex with that of physical mixture reveals mark differences. In complex, new peaks were found and shift in the peak positions were also found where as the physical mixture has peaks which are superimposition of two individuals. The intensity of certain peaks in the complex are also enhanced thereby confirming complex formation.

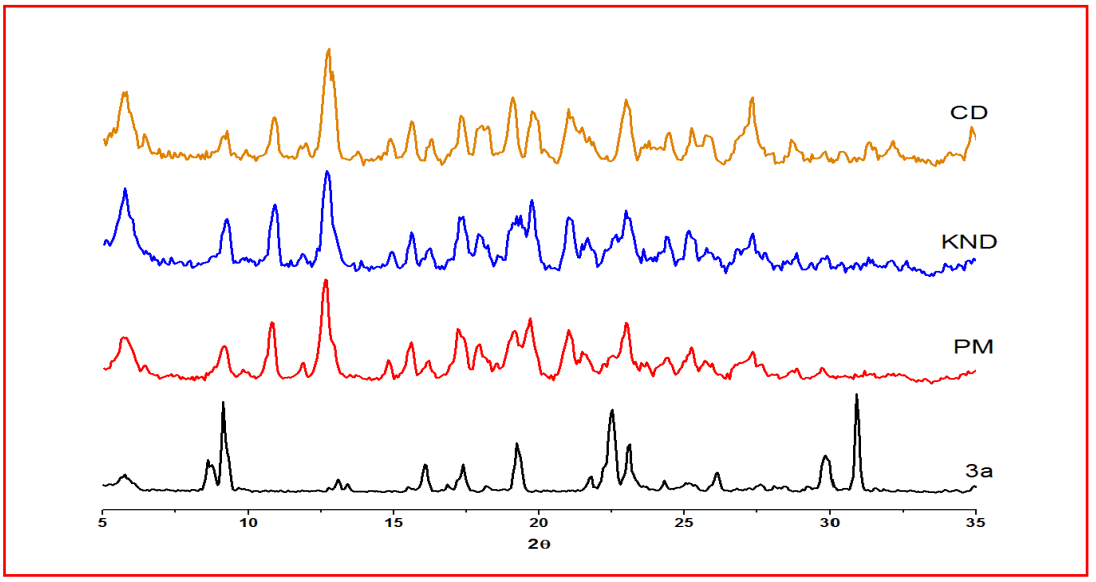

Figure 6.11(a): PXRD patterns: 3a; Physical mixture (PM) ; 3a/ β-CD inclusion complex (KND) and β- CD

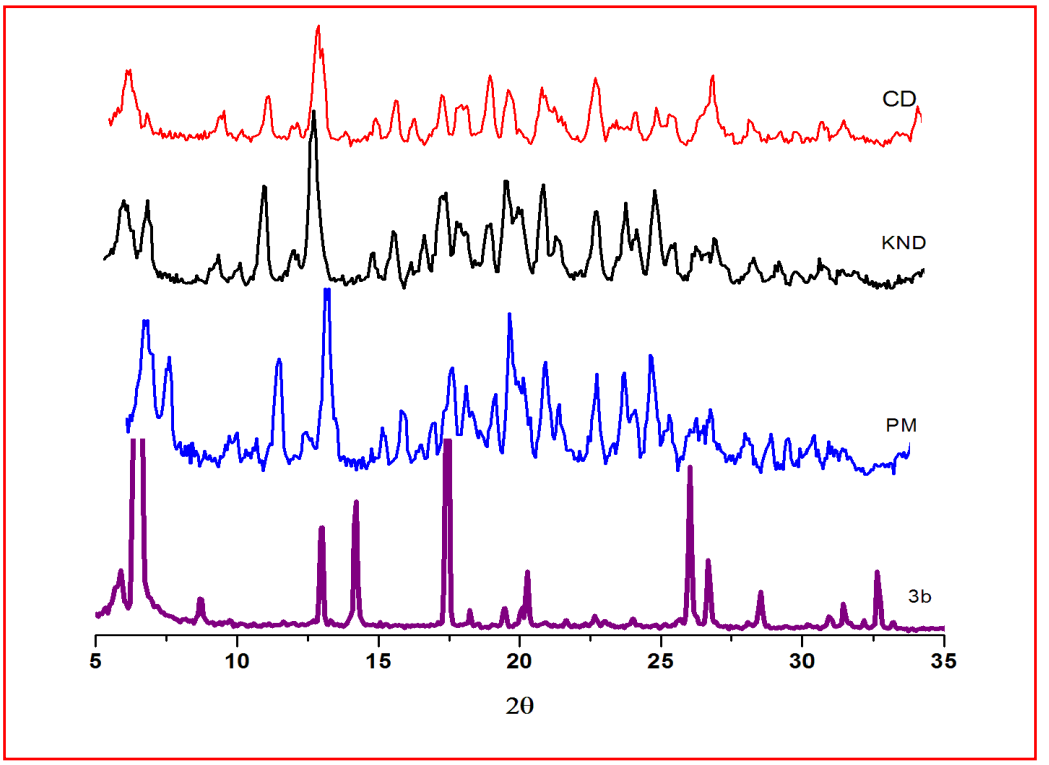

Figure 6. 11 (b): PXRD patterns: 3b; Physical mixture (PM) ; 3b/ β-CD inclusion complex (KND) and β-CD

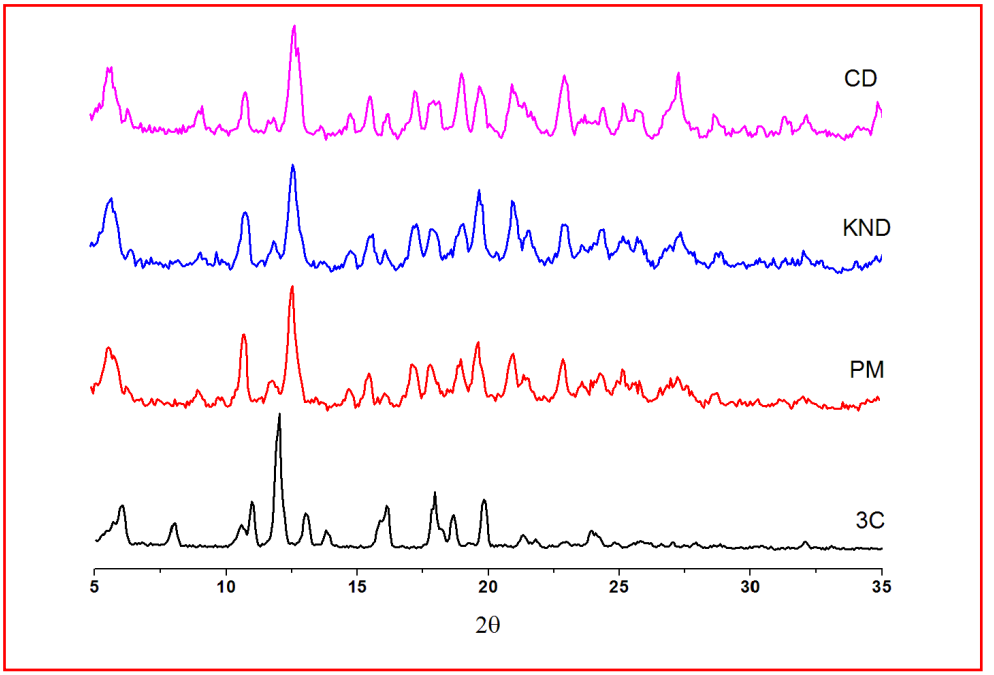

Figure 6. 11 (c): PXRD patterns: 3c; Physical mixture (PM) ; 3c/ β-CD inclusion complex (KND) and β- CD

6.3.4 Differential scanning calorimetry study of inclusion complex

DSC is a fast technique to examine and verify the drugs that form inclusion complex with β-CD and to confirm the absence of the drug melting endotherm. The thermal analysis has been reported as an important method for recognition and characterization of CDs complexes. When guest molecules were embedded in CDs cavities or in the crystal lattice, their melting point is generally shifted to a different temperature and the intensity decrease or disappears. The results of DSC thermograms for given samples are shown in Figure 6.12a, b and c. The DSC curve of compounds showed an endothermic reaction and its melting peak was at the respective onset temperature. The thermal behaviour of β-CD exhibited a sharp endothermic peak due to its melting. Physical mixture showed a sharp endothermic peak. Therefore it was concluded that some part of the compound is complexes with β-CD but some part remained outside of the complex.

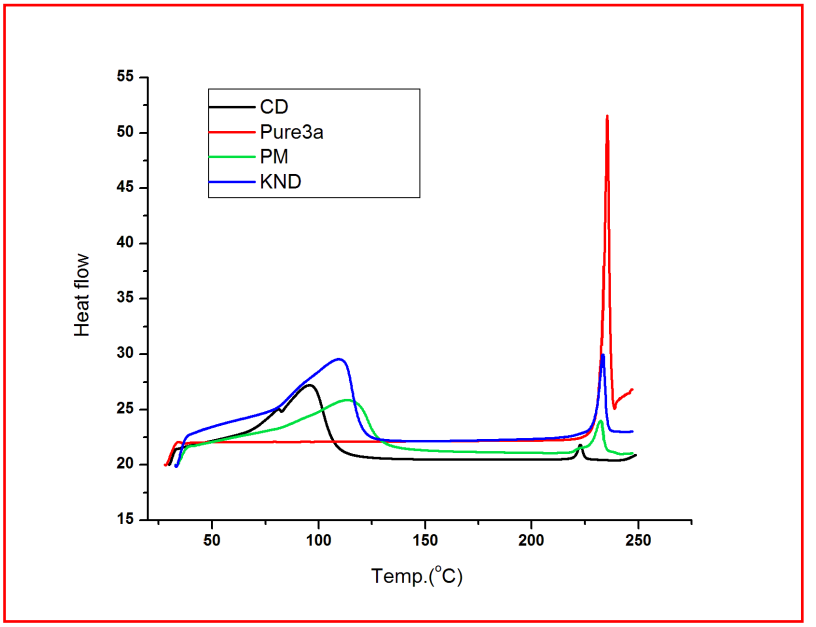

Figure 6.12(a): DSC curves for: β-CD; 3a; physical mixture (PM) and inclusin complex (KND)

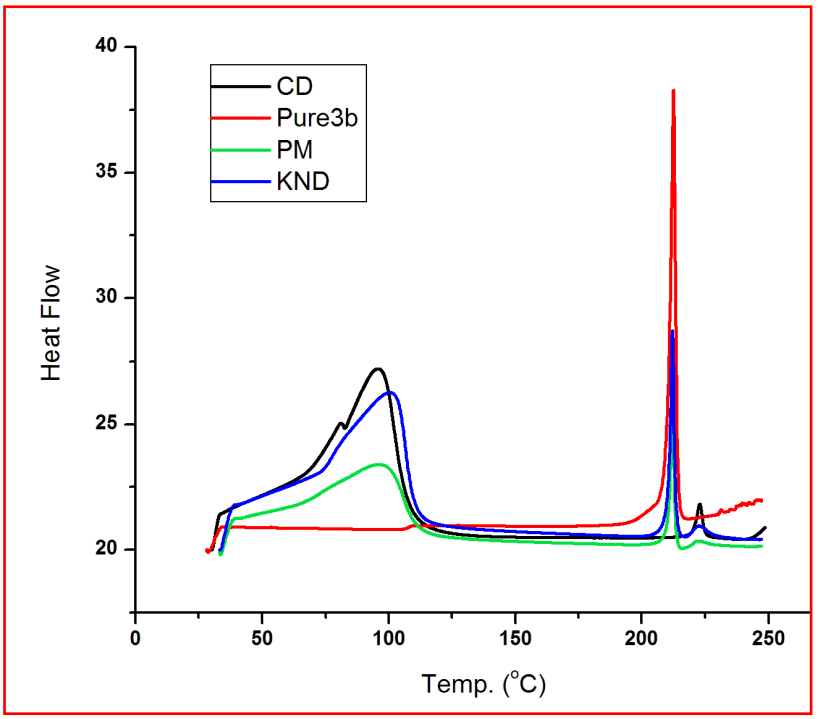

Figure 6.12(b): DSC curves for: β-CD; 3b; physical mixture; and inclusion complex.

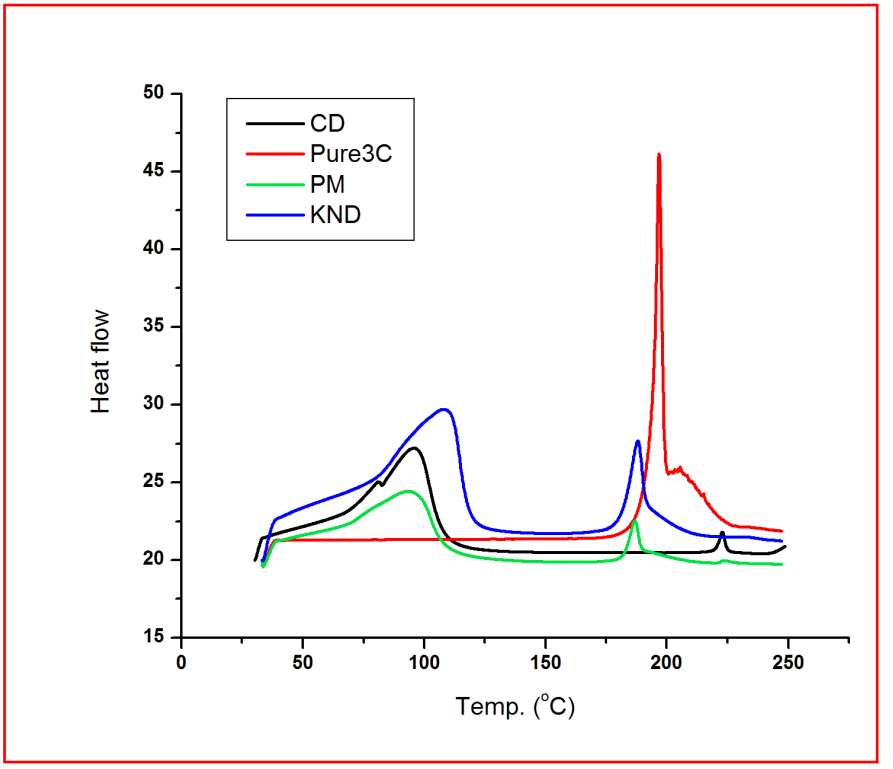

Figure 6.12(c): DSC curves for: CD; 3c; physical mixture (PM); and inclusion complex (KND).

The FT-IR, FT-Raman, DSC and PXRD results produced important evidences in support of compounds-CD inclusion complex formation. The solubility of the stated compounds was successfully enhanced with water by the formation of their inclusion complexes with β-cyclodextrin. These results have supported our approach to enhance the solubility of quinazoline compounds by β-Cyclodextrin which is an easy and economical method. The method may consequently increase the bioavailability of the drug molecule to improve its pharmaceutical potential.

General Discussion and Summary

The stability of the quinazoline nucleus (fused heterocyclic compound) has inspired researchers to introduce many bioactive moieties to this nucleus to synthesize new potential medicinal agents. The quinazolinone skeleton is a frequently encountered heterocycle in medicinal chemistry literature with applications including antibacterial, analgesic anti-inflammatory, antifungal, antimalarial, antihypertensive, CNS depressant, anticonvulsant**,** antihistaminic**,** antiviral and anticancer activities (Asif, 2014)**.**

Chapter 1 dealt with the synthesis of 2-substituted-benzo[d][1,3]oxazin-4-one and 3-(Aryldeneamino)-2-phenyl-quinazoline-4(3H)-ones by reported methods and the synthesized compounds were characterized by ESI-MS, UV and vibrational spectroscopy. All characteristic peaks have been observed in the spectroscopic data.

Chapter 2 addressed the characterization of dimeric association in 2-substituted-benzo[d][1,3]oxazine-4-one. The dimeric association was characterized with the help of mass spectroscopy, UV-Vis spectroscopy, vibrational spectroscopy and NMR spectroscopy. All techniques provided clear indication of the presence of dimeric association. Visible changes were observed in the association constants in different solvents. This may be attributed to the ability of the solvent to engage in hydrogen bonding which can compete with self-association and to differential solution of the different dipoles of the associated and unassociated species. It is observed that the value of dimerization constant is lesser in protic polarisable solvents like methanol and chloroform (0.1M to 1E-05M range). But in the polar protic solvent, water, the dimerization constants was comparatively much higher. As water is the least polarisable among the solvents studied, it can be explained that solvent polarizability has significant role in dissolving the monomer. So far, various studies have reported the presence of weak interactions having C-H-O H-bond in solid state but as far as the liquid state is concerned, it still remains unanswered and needs further investigation or study. The hydrogen bonded dimer of dimethyl ether, with three C-H...O-C improper, blue-shifting H-Bond interactions, has been reported by Tatamitani *et al* (2002). Their experimental

data combined with high-level *ab initio* calculations showed this kind of interaction to be improper, blue-shifted hydrogen bonding, with an average shortening of the C-H bonds involved in the hydrogen bonding of 0.0014 Å. They proposed that this kind of interaction is not very strong, but very common, and for this reason is expected to play an important role in biology and in chemistry. Interestingly, the occurrence of C–H-O hydrogen bonds in liquids has aroused much interest recently (Gil *et al.,* 1995; Jedlovszky & Turi, 1997; Ribeiro-Claro *et al.,* 1997;Yukhnevich & Tarakanova, , 1998; Karger *et al.,* 1999; Marques *et al.,* 2001)

Chapter 3 dealt with the study of morphology of 2-methyl-4H-benzo[d][1,3]oxazin-4-one. Polymorphism, the existence of more than one crystalline form of a compound, is a well known and widely studied phenomenon (Davey, 2003). It is now widely accepted that the occurrence of polymorphism in molecular crystalline solids has a huge impact on the production of fine pharmaceuticals products (Rodriguez-Spong *et al.,* 2004). The crystals of 2-methyl-4H-benzo[d][1,3]oxazin-4-one on keeping, gradually turned into powder and some sublimates made a layer on the wall of the container. On keeping for 15-20 days, the entire powdered mass turned into an agglomeration having mp 188.2^{o}C (Form II). Previous authors have reported that acetamidobenzamide exists in two crystal polymorphic forms: α and β having different melting temperature (Barnett *et al.,* 2006; Kelleher *et al.,* 2007). They also reported that α form features an approximately planar molecular conformation and an intramolecular N−H...O hydrogen bond. In present study, both the polymorphic forms are of same chemical structure, similar unit cell and similar stacking pattern; only difference is the compactness of the stacking. We have also analyzed that less compactly packed form has a higher melting point - which is due to excess favorable dipole-dipole interaction strength gained through sacrifice of pi-pi stabilizing interaction. The 2-substituted-4H-benzo[d][1,3]oxazin-4-ones remain as a mixture of monomer and dimer in equilibrium and the corresponding dimerization constants were also evaluated. The obtained data suggested that the amount of dimers in solutions is considerable. The monomer dimer equilibrium constant as calculated indicates that the first is a kinetically formed dimer and the second is the thermodynamically formed dimer.

In Chapter 4 we have tried to investigate the impact of the above mentioned dimerization on their antibacterial activity. MIC was determined for each compound. From this data, MIC breakpoint of > 1000 µg/ml has been found for each 2-substituted-benzo[d][1,3]-oxazine-4-one against *E.coli* K12. When expressed in micrograms the percent inhibition is found to increase with the increase of the concentration of the studied compounds. Interestingly, the compounds have shown higher antibacterial activity in dilute solution which gradually decreased at higher concentrations, when expressed in per molar inhibition. It was proposed that the antibacterial activity was largely contributed by the monomer rather than the corresponding dimer. Previous authors have also reported self association propensity and aggregate size leading to reduced cellular bioavailability (Khan *et al.,* 2006). Perhaps, this is the first report of antibacterial property at different concentrations in molar term *i.e*. percent inhibition in molar term. Therefore, in the present study, we have tried to deal with the effect of self association of the molecules in their biological activity.

In Chapter 5, *In silico* and *In vitro* studies were carried out to establish the drug likeliness behavior and antiproliferative activity of Quinazoline-4(3H)-one via inhibition of hDHFR activity. Drug likeliness, molecular descriptor property, ADME and drug score of compounds were evaluated by using different bioinformatic tools and softwares. Molecular docking was also carried out to explore the binding affinity of synthesized compounds with human DHFR. The docking result showed that all ten synthesized compounds have low binding energy and inhibition constant as compared to the standard drug methotrexate. Results also revealed that Asp 64 also plays a vital role in binding of these quinazoline derivatives with hDHFR. Interestingly, all these amino acids are also present in the active site of hDHFR. In hDHFR inhibition assay, the reference compound methotrexate showed IC_{50} value of 8±1.34, while compounds 3a, 3b, 3c, 3d, 3f, 3g, 3h and 3i showed IC_{50} value comparable with Methotrexate. The generated pharmacophore has 3 aromatic rings and two hydrogen bond acceptors and qualified for all the four parameters of Lipinski's rule of five. In the last few years, the attention was oriented towards the synthesis and biological evaluation of quinazoline derivatives as they exhibit a broad spectrum of biological activities. Moreover, there is an increasing interest in finding novel field of applicability for quinazoline compounds as anticancer drugs (Marzaro *et al.,* 2012; Ravez *et al.,* 2015). Importantly, FDA has approved several

quinazoline derivatives as anticancer drugs since the past 15 years, such as gefitinib , erlotinib and lapatinib (Roskoski et al, 2014). The synthesized compounds (1a, 2a and 3a-3j) and reference compounds (curcumin and methotrexate) were tested for their antiproliferative activity against three cancerous cell lines; HepG2 (human liver cancer cell line), MCF-7 (human breast cancer cell line) and HeLa (human cervical cancer cell line) using MTT assay. Results revealed that, among tested compounds 7 showed activity against HepG2 cell lines, 5 showed against MCF7 cell line and 5 showed against HeLa cell lines. HepG2 cell line was shown to be the most sensitive toward the tested compounds.

Chapter 6 addressed the low solubility of Quinazoline-4(3H)-one under the venture to increase their medicinal application. β-Cyclodextrin (β-CD) was used for formation of inclusion complexes, since, CDs offer advantages over other materials because they possess a hydrophobic cavity in which a wide variety of lipophilic guest molecules can be hosted (Gomes *et al.,* 2014). A number of descriptive studies on CD complexation have been published that characterize the solubility and/or dissolution increase of various poorly soluble compounds (Sinha *et al.,* 2005; Uzqueda *et al.,* 2006; Lee *et al.,* 2009; Kou *et al.,* 2011, Mangolim *et al.,* 2014). The aim of this chapter was to compare different methods of Quinazoline-4(3H)-one complexation with β-CD and to evaluate the formation of the complexes using FT-IR, FT-Raman, DSC and Powder X-ray diffraction techniques. Infrared and raman spectra of inclusion complexes were analysed by identification of the carbonyl (C=O), methyl and C-H stretching. In the spectra of the inclusion complex, these bands were shifted towards higher frequencies and the asymmetric vibration peak of C=O band with increased intensity was obtained. The diffraction pattern of the complex was found to be different from the diffraction pattern of pure β-CD and the pure compounds. In the inclusion complexes, new peaks as well as shifting of peak positions were observed. DSC results revealed that melting point of compounds were slightly shifted and furthermore there was a reduction in intensity. The FT-IR, FT-Raman, DSC and PXRD results produced important evidence of Quinazoline-4(3H)-ones and β-CD inclusion complex formation. The solubility of the stated compounds was effectively enhanced in water by the formation of their inclusion complexes by using an easy and economical method.

Bibliography

Abdel Gawad NM, Georgey HH, Youssef RM, El-Sayed NA (2010) Synthesis and antitumor activity of some 2, 3-disubstituted quinazolin-4(3H)-ones and 4, 6-disubstituted-1,2,3,4- tetrahydroquinazolin-2H-ones. Eur J Med Chem 45(12): 6058-6067.

Abu-Shakra M, Gladman DD, Thorne JC, Long J, Gough J, Faresell VT (1995) Long term methotrexate therapy in psoriatic arthritis: clinical and radiological outcome. J Rheumatol 22: 241-245.

Akbari VK, Kahar RG, Patel KC (2013) Synthesis, characterization and antimicrobial studies of novel quinazoline derivatives of syndon 52B: 1462-1467.

Alagarsamy V, Saravanan G (2013) Synthesis and anticonvulsant activity of novel quinazolin-4(3*H*)-one derived pyrazole analogs. Med Chem Res 22: 1711-1722.

Alagarsamy V, Thangathiruppathy A, Mandal SC, Rajasekaran S (2006) Pharmacological evaluation of 2-substituted (1,3,4) thiadiazolo quinazolines. Indian J Pharm Sci 68: 108-111.

Aliev A E, Harris Kenneth DM (2004) Probing Hydrogen Bonding in Solids Using Solid State NMR Spectroscopy, Supramolecular Assembly via Hydrogen Bonds I. Struct Bonding 108:1-53.

Allegra CJ, Chanber BA, Tuazon CU, Ogata Arakaki D, Baird B, Darke JC, Simmons JT, Lack EE, Shelhamer JH, Balis F, Walker R, Kovacs JA, Cliffordlane H, Masur H (1987) Activity of antifolate against Pneumocystis carinii dihydrofolate reductase and identification of a potent new agent. N Engl J Med 317: 978−985.

Al-Omary FA, Abou-Zeid LA, Nagi MN, Habib el-SE, AbdelAziz AA, El-Azab AS, Abdel-Hamide SG, Al-Omar MA, AlObaid AM, El-Subbagh HI (2010) Non-classical antifolates. Part 2: synthesis, biological evaluation, and molecular modeling study of some new 2,6-substituted-quinazolin-4-ones. Bioorg Med Chem 18(8): 2849-2863.

Al-Rashood Sarah T, Aboldahab IA, Nagi Mahmoud N, Laila A. Alaa Abouzeid A, Abdel-Aziz M., Sami G, Abdel-hamide, M. Youssef Khairia, M. Al-

Obaid AI. El-Subbagh H (2006) Synthesis, dihydrofolate reductase inhibition, antitumor testing, and molecular modeling study of some new 4(3H)-quinazolinone analogs. Bioorg Med Chem 14: 8608-8621.

Al-Rashood ST, Hassan GS, El-Messery SM, Nagi MN, Habib E-SE, Al-Omary FAM, El-Subbagh HI (2014) Synthesis, biological evaluation and molecular modeling study of 2-(1,3,4-thiadiazolyl-thio and 4-methyl-thiazolyl-thio)-quinazolin-4-ones as a new class of DHFR inhibitors. Bioorg Med Chem Lett 24 (18): 4557-4567.

Al-Rashood, ST (2005) Synthesis and evaluation of some new compounds of 2-methylthio-6-amino-4(3H)-quinazolinones as dihydrofolate reductase inhibitors. M.Sc. Thesis, College of Pharmacy, King Soud University, Riyadh, KSA.

Ambujakshan KR, Tresavarghese H, Mathew S, Ganguli S, Nanda AK, Panicker CY (2008) Vibrational spectroscopic studies and theoretical calculations of 2-phenyl-4H-3,1-benzoxazin-4-one. Orien J Chem 24: 865-874.

American Cancer Society. Global Cancer Facts & Figures (2007). Atlanta, GA: American Cancer Society; 2007.

Ammar HO, Salama HA, Gharab M, Mahmoud AA (2006) Implication of inclusion complexation of glimepiride in cyclodextrin–polymer systems on its dissolution, stability and therapeutic efficacy. Int J Pharm 320: 53-57.

Armarego WLF, (1963) A Text Book of Quinazolines.

Armarego, WLF. (1961) Quinazolines. Part 11 .I 1,4- and 3,4-Dihydropuinazoline. J Chem Soc 2697-2701.

Arunan E, Desiraju G R, Klein RA, Sadlej J, Scheiner S, Alkorta I, Clary DC, Crabtree RH., Dannenberg JJ, Hobza P, Kjaergaard HG, Legon AC, Mennucci B, Nesbitt DJ (2011) Defining the hydrogen bond: An account (IUPAC Technical Report), Pure Appl Chem ASAP Article .

Asanuma HA, Hishiya T, Komiyama M (2000) Tailor-Made Receptors by Molecular Imprinting. Adv Mater 12: 1019-1030.

Asif M (2014) Chemical characteristics, synthetic methods, and biological potential of quinazoline and quinazolinone derivatives. Int J Med Chem 395637.

Audeval B, Bouchacourt P, Rondier J (1988) Comparative study of diproqualone-ethenzamide versus glafenine for the treatment of rheumatic pain of gonarthrosis and coxarthrosis. (French) Gazette médicale de France 95: 70-72.

Baba AI, Catoi C (2007) Tumor Cell Morphology. In: Baba AI, Catoi C, editors. Comparative Oncology. Bucharest, Romania: The Publishing House of the Romanian Academy. 119–125.

Bain DI, Smalley RK (1968) Synthesis of 2-Substituted-4H-3,I -benzoxazin-4-ones. J Chem Soc (C): 1593-1597.

Bakar MRA, Nagy ZK, Rielly CD (2010) A combined approach of differential scanning calorimetry and hot-stage microscopy with image analysis in the investigation of sulfathiazole polymorphism J Ther Anal Calorim 99(2): 609-619.

Barnett SA, Tocher DA, Vickers M (2006) The solvates of *o*-acetamidobenzamide. Cryst Eng Comm 8: 313-319.

Bassani, VL, Krieger D, Duchene D, Woue D (1996) Enhanced water-solubility of albendazole by hydroxypropyl-b-cyclodextrin complexation. J Incl Phenom Macrocycl Chem 25: 149-152.

Bavin, M (1989) Polymorphism in process development. Chem Ind 527-529.

Berman EM, Werbel LM (1991) The renewed potential for folate antagonists in contemporary cancer chemotherapy. J Med Chem 34: 479-485.

Blagden N, de Matas M, Gavan PT, York P (2007) Crystal engineering of active pharmaceutical ingredients to improve solubility and dissolution rates. Adv Drug Deliv Rev 59(7): 617-630.

Blagden SP, Molife LR, Seebaran A, Payne M, Reid AH, Protheroe AS, Vasist LS, Williams DD, Bowen C, Kathman SJ, Hodge JP, Dar MM, de Bono JS, Middleton MR (2008) A phase I trial of ispinesib, a kinesin spindle protein inhibitor, with docetaxel in patients with advanced solid tumours. Br J Cancer 98: 894-899.

Blancey JM, Hansch C, Silipo C, Vittoria A (1984) Structure-activity relationship of dihydrofolate reductase inhibitors. Chem Rev 84: 333-407.

Bloss FD (1971) Crystallography and Crystal Chemistry, Holt, Reinhart and Winston, New York.

Bogert MT, May CE (1909) Researches on quinazolines (twenty-first paper). on certain quinazoline oxygen ethers of the type —n:c(or)— and the isomeric —nr.co— compounds J Am Chem Soc 31: 507-513.

Bogert MY, Seil HA (1907) Researches on Quinazolines (eighteenth paper), on 2, 3-dialkyl-4-quinazolones and the products obtained by alkylating 2-Alkyl- 4-Quinazolones (2-Alkyl-4-Hydroxy Quinazolones). J Am Chem Soc 29: 517-536

Bonchev D. Cremaschi P (1974) C-H Group as proton donor by formation of a weak hydrogen bond, Theoretica chimica acta, 30. VIII. 35(1): 69-80

Bond AD, Boese R, Desiraju GR (2007) On the polymorphism of aspirin**.** Angew Chem Int Ed 46(4): 615-617.

Bond AD, Boese R, Desiraju GR (2007) On the polymorphism of aspirin: Crystalline aspirin as intergrowth of two polymorphic domains. Angew Chem Int Ed 46(4): 618-622.

Borst P, Ouellette M (1995) New Mechanisms of Drug Resistance in Parasitic Protozoa. Annu Rev Microbiol (49): 427-460.

Borst P, Quellette M (1995) New mechanism of drug resistance in parasitic protozoa. Annu Rev Microbiol 49: 427-460.

Braga D, Grepioni F, Maini L, Polito M (2009) Molecular Networks, ed. M. W. Hosseini, Springer Berlin Heidelberg, Berlin, Heidelberg, 25.

Brittain HG (2010) Polymorphism and Solvatomorphism. J Pharm Sci 101: 464–484.

Brog J-P, Chanez C-L, Crochet A, From K M (2013) Polymorphism, what it is and how to identify it: a systematic review". RSC Adv 3: 16905-16931.

Brown SP, Spiess HW (2001) Advanced Solid-State NMR Methods for the Elucidation of Structure and Dynamics of Molecular, Macromolecular, and Supramolecular Systems. Chem Rev 101(12): 4125-4156.

Brunovska Z, Lyon R, Ishida H (2000) Thermal properties of phthalonitrile functional polybenzoxazines. Thermochim Acta 357: 195–203.

Buchall, JJ, Hitchings GH (1965) Inhibitor binding analysis of dihydrofolate reductases from various species. Mol Pharmacol 1: 126−136.

Burger A, Ramberger R (1979) Polymorphism of pharmaceuticals and other molecular crystals. II. Applicability of thermodynamic rules. Mikrochim Acta 2: 273-316.

Burger A, Ramberger R (1979) Polymorphism of pharmaceuticals and other molecular crystals. I. Theory of thermodynamic rules. Mikrochim Acta 72(3): 259-271.

Buttar D, Charlton D, Docherty MH, Starbuck R (1998) Theoretical investigations of conformational aspects of polymorphism. Part 1: *o*-acetamidobenzamide. J Chem Soc Perkin Trans 2: 763-772.

Buvari-Barcza A, Barcza L (2000) Changes in the solubility of bcyclodextrin on complex formation: guest enforced solubility of b-cyclodextrin inclusion complexes. J Incl Phenom Macrocycl Chem 36: 355–370.

Bym, S R (1982) Solid State Chemistry of Drugs. Academic Press, New York

Cao SL, Feng YP, Jiang YY (2005) Synthesis and *in vitro* antitumor activity of 4(3H)- quinazolinone derivatives with dithiocarbamate side chains. Bio Org Med Chem 15: 1915-1917.

Cavalli A, Lizzi F, Bongarzone S, Brun R, Luise Krauth-Siegel R, Bolognesi ML (2009) Privileged structure-guided synthesis of quinazoline derivatives as inhibitors of trypanothione reductase. Bioorg Med Chem Lett 19: 3031-3035.

Cenas N, Prast S, Nivinskas H, Sarlauskas J, Arner ESJ (2006) Interactions of nitroaromatic compounds with the mammalian selenoprotein thioredoxin reductase and the relation to induction of apoptosis in human cancer cells. J Biol Chem 281: 5593–5603.

Chandregowda V, Kush AK, Chandrasekara RG (2009) Synthesis and in-vitro antitumor activities of novel 4-anilinoquinazoline derivatives. Eur J Org Chem 44: 3046-3055.

Chandrika PM, Yakaiah T, Raghu Ram Rao A, Narsaiah B, Reddy NC, Sridhar V, Rao JV (2009) Synthesis of novel 4,6 disubstituted quinazoline derivatives

their anti-inflammatory and anticancer activity against U937 leukemia cell lines. Eur J Org Chem 43: 846-852.

Chauhan K, Sharma M, Shivahare R, Debnath U, Gupta, S, Prabhakar YS, Chauhan PMS (2013) Discovery of Triazine Mimetics As Potent Antileishmanial Agents . J Med Chem 56: 4374–4392.

Chaumeil JC (1998) Micronization: a method of improving the bioavailability of poorly soluble drugs. Methods Find Exp Clin Pharmacol 20(3): 211–215.

Chen K, Wang K, Kirichian AM, Al Aowad AF, Iyer LK, Adelstein SJ, Kassis AI (2006) *In silico* design, synthesis, and biological evaluation of radioiodinated quinazolinone derivatives for alkaline phosphatase-mediated cancer diagnosis and therapy. Mol Cancer Ther 5: 3001-3013.

Chinigo GM, Paige M, Grindrod S, Hamel E, Dakshanamurthy S, Chruszcz M, Minor W, Brown ML (2008) Asymmetric synthesis of 2,3-dihydro-2-arylquinazolin-4- ones: methodology and application to a potent fluorescent tubulin inhibitor with anticancer activity. J Med Chem 51(15): 4620-4631.

Chiou WL, Riegelman S (1971) Pharmaceutical applications of solid dispersion systems. J Pharm Sci 60(9): 1281–1302.

Coe KJ, Jia Y, Ho HK, Rademacher P, Bammler TK, Beyer RP, Farin FM, Woodke L, Plymate SR, Fausto N, Nelson SD (2007) Comparison of the cytotoxicity of the nitroaromatic drug flutamide to its cyano analogue in the hepatocyte cell line TAMH: Evidence for Complex I inhibition and mitochondrial dysfunction using toxicogenomic screening. Chem Res Toxicol 20: 1277–1290.

Cohen E, Klarberg E, James VR Jr (1960) Quinazolinone sulfonamides. A new class of diuretic agents. J Am Chem Soc 82: 2731–2735.

Colin RG, Christopher TW, O¨ rn A (2004) Drugs as materials: valuing physical form in drug discovery. Nat Rev 3: 926-934

Coppola GM (1999) The chemistry of 4H-3,1-benzoxazin-4-ones. J Heterocycl Chem 36: 563-588.

Davey RJ (2003) Pizzas, polymorphs and pills. Chem Commun 1463–1467.

Davey RJ, Blagden N, Righini S, Alison H, Quayle MJ, Fuller S. (2001) Crystal Polymorphism as a Probe for Molecular Self-Assembly during Nucleation from Solutions: The Case of 2,6-Dihydroxybenzoic Acid. Cryst Growth and Des. 1(1): 59-65.

Davoll J, Johnson AM (1970) Quinazoline analogues of folic acid. J Chem Soc Perkin 8: 997-1002.

Decker M (2005) Novel inhibitors of acetyl- and butyrylcholinesterase derived from the alkaloids dehydroevodiamine and rutaecarpine. Eur J Med Chem 40: 305-313.

Dempcy RO, Skibo EB (1991) Rational design of quinazoline-based irreversible inhibitors of human erythrocyte purine nucleoside phosphorylase. Biochemistry 30: 8480-8487.

Denizot F, Lang R (1986) Rapid colorimetric assay for cell growth and survival: modification to the tetrazolium dye procedure giving improved sensitivity and reliability. J Immunol Methods 89: 271–277.

Derewenda, ZS, Derewenda U, Kobos PM (1994) (His)C epsilon-H...O=C < hydrogen bond in the active sites of serine hydrolases. J Mol Biol 241(1): 83-93.

Desiraju GR, Steiner T (1999) The weak hydrogen bond in structural chemistry and biology. International Union of Crystallography, Monographs on Crystallography, Oxford Science Publications, New York,

Desiraju GR (1991) The C-H-O hydrogen bond in crystals: what is it?. Acc Chem Res 24: 290-296.

Desiraju GR (1996) The C−H···O Hydrogen Bond: Structural Implications and Supramolecular Design Acc Chem Res 29: 441-449.

Desiraju GR (2002) Hydrogen Bridges in Crystal Engineering: Interactions without Borders. Acc Chem Res 35: 565-573.

Dharmendra S, William C (2004) Drug polymorphism and dosage form design: a practical perspective. Adv Drug Deliv Rev 56: 335-347.

Dingley AJ, Grzesiek S (1998) Direct Observation of Hydrogen Bonds in Nucleic Acid Base Pairs by Internucleotide 2 JNN Couplings. J Am Chem Soc 120: 8293-8297.

Ebert AA, Gottlieb HB (1952) Infrared Spectra of Organic Compounds Exhibiting Polymorphism. J Am Chem Soc 74: 2806-2810.

El-Azab AS, Abdel-Hamide SG, Sayed-Ahmed MM, Hassan GS, El-Hadiyah TM, Al-Shabanah OA, Al-Deeb OA, El-Subbagh HI (2013) Novel 4(3H)-quinazolinone analogs: synthesis and anticonvulsant activity. Med Chem Res 22: 2815-2827.

El-Azab AS, Al-Omar MA, Abdel-Aziz AA, Abdel-Aziz NI, elSayed MA, Aleisa AM, Sayed-Ahmed MM, Abdel-Hamide SG (2010) Design, synthesis and biological evaluation of novel quinazoline derivatives as potential antitumor agents: molecular docking study. Eur J Med Chem, 45(9): 4188-4198.

El-Hashash, Maher A, Rizk Sameh A, El-Bassiouny Fakhry A (2012) Use of 2-Ethoxy(4H)-3,1-benzoxazin-4-one as a Precursor for Synthesis of Quinazoline and Quinazolinone Starting Materials. Chem Pro Eng Res 2: 17-32.

El-Helby AG, Wahab MH (2003) Design and synthesis of some new derivatives of 3H- quinazolin-4-one with promising anticonvulsant activity. Acta Pharma 53: 127–138.

El-Mekabaty A (2013) Chemistry of 4H-3, 1-Benzoxazin-4-Ones. International J of Modern Organic Chemistry 2: 81−121.

Errede LA, McBrady JJ, Tiers GVD (1980) Acylanthranils. 10. Influence of hydrogen bonding on hydrolysis of acetylanthranil in organic solvents J Org Chem 45(19): 3868–3875.

Eweas AF, El-Nezhawy AOH, Baiuomy AR, Awad MM (2013) Design, synthesis, anti-inflammatory, analgesic screening, and molecular docking of some novel 2-pyridyl (3*H*)-quinazolin-4-one derivatives. Med Chem Res 22: 1011-1020.

Falco EA, Hitchings GH, Russell PB, VanderWert H (1949) Antimalarial as antagonists of purines and pteroylglutamic acid. Nature 164: 107-108.

Farber S, Louis K, Sylvester RF, Wolff JA (1948) Temporary remissions in acute leukemia in children produced by folic acidantagonist, 4-aminopteroylglutamic acid (aminopterin). N Engl J Med 238: 787-793.

Ferone R, Burchall JJ, Hitchings GH (1969) *Plasmodium berghei* dihydrofolate reductase.Isolation, properties, and inhibition by antifolates. Mol Pharmacol 5: 49-59.

Florea AM, Büsselberg D (2011) Cisplatin as an anti-tumor drug: Cellular mechanisms of activity, drug resistance and induced side effects. Cancers 3: 1351-1371.

Friedlander P, Wleugel S (1883) Zur Constitution des Anthranils. Ber Disch Chem Ges 16: 2227–2229.

Garofalo A, Goossens L, Baldeyrou B, Lemoine A, Ravez S, Six P, David Cordonnier MH, Bonte JP, Depreux P, Lansiaux A, Goossens JF (2010) Design, synthesis and DNA binding of N-alkyl(anilino)quinazoline derivatives. J Med Chem 53(22): 8089-8103.

Garza J, Ramírez J-Z, Vargas R (2005) Role of Hartree−Fock and Kohn−Sham Orbitals in the Basis Set Superposition Error for Systems Linked by Hydrogen Bonds Phys Chem A 109(4): 643-651.

Ghodkea DS, Nakhatb PD, Yeole PG, Naikwade NS, Magduma CS, Shaha RR (2009) Preparation and Characterization of domperidone Inclusion Complexes with Cyclodextrin: Influence of Preparation method. Iran J Pharm Res 8(3): 145-151.

Ghose AK, Viswanadhan VN, Wendoloski JJ (1999) A knowledge- based approach in designingcombinatorial or medicinal chemistry libraries for drug discovery: Part 1. A qualitative and quantitativecharacterization of known drug databases. J Comb Chem 1: 55-68.

Gil FPSC, da Costa AM, Amorim Teixeira-Dias JJC (1995) Conformational Analysis of CmHh+10CH2CH20H (m = 1-4): The Role of CH-O Intramolecular Interactions. J Phys Chem 99: 8066-8070.

Giri RS, Thaker HM, Giordano T, Williams J, Rogers D, Sudersanam V, Vasu KK (2009) Design, synthesis and characterization of novel 2-(2,4-disubstituted-thiazole-5-yl)- 3-aryl-3*H*-quinazoline-4-one derivatives as inhibitors of NF-*κ*B and AP-1 mediated transcription activation and as potential anti-inflammatory agents. Eur J Med Chem 44: 2184–2189.

Goward GR, Schnell I, Brown SP, Spiess HW, Kim H-D, Ishida H (2001) Investigation of an N···H hydrogen bond in a solid benzoxazine dimer by 1H–15N NMR correlation techniques under fast magic-angle spinning. Magn Reson Chem 39: S5–S17

Graffner-Nordberg M (2001) Approaches to soft drug analogues of dihydrofolate reductase inhibitors: Design and synthesis. Acta Universitatis Upsaliensis.Comprehensive summaries of Uppsala dissertations from the Faculty of Pharmacy 252. Uppsala: Tryck and Medier, Uppsala.

Gray D, McCaughan A, Mookerji B (2009) Crystal Structure of Graphite, Graphene and Silicon. Physics for Solid State Applications. 6: 730-732.

Green E, Demos CH (1984) In Folate Antagonists as Therapeutic Agents. 2 Sirotnak FM, Burchall JJ, Ensminger WB, Montgomery JA, Eds Academic Press: Orlando, 191: 249.

Grover G, Suvarna GK (2006) Synthesis and evaluation of new quinazolone derivatives of nalidixic acid as potential antibacterial and antifungal agents. Eur J Med Chem 41: 256–262.

Gupta D, Kumar R, Roy RK, Sharma A, Ali I, Shamsuzzaman M (2013) Synthesis and biological evaluation of some new quinazolin-4(3H)ones derivatives as anticonvulsants. Med Chem Res 22: 3282-3288.

He L, Li H , Chen J, Wu X-F (2014) Recent advances in 4(3H)-quinazolinone syntheses. RSC Adv 4: 12065-12077.

Henriksen K, Byrjalsen I, Nielsen RH, Madsen AN, Larsen LK, Christiansen C, Beck-Nielsen H, Karsdal MA (2009) A comparison of glycemic control, water retention, and musculoskeletal effects of balaglitazone and pioglitazone in diet-induced obese rats. Eur J Pharmacol 616: 340-345.

Hilfiker R, Blatter F, von Raumer M (2006) Relevance of solid-state properties for pharmaceutical products. In: Hilfiker R, editor. Polymorphism in the pharmaceutical industry. Weinheim: Wiley- VCH Verlag GmbH & Co 1–18.

Hofman J, Hofmanova´ O (1969) 1,4-Benzoxazine derivatives in plants: Sephadex fractionation and identification of a new glucoside. Eur J Biochem 8: 109-112.

Hou T, Wang J (2008) Structure-ADME relationship: still a long way to go? Expert Opin Drug Metab Toxicol 4: 759–70.

Hou T, Wang J, Zhang W, Wang W, Xu X (2006) Recent advances in computational prediction of drug absorption and permeability in drug discovery. Curr Med Chem 13: 2653–2667.

Howe JY, Rawn CJ, Jones LE, Ow H (2003) Improved crystallographic data for graphite. Powder Diffraction 18: 150−154.

Jantová S, Letasiová S, Repický A, Ovádeková R, Lakatos B (2006) The effect of 3-(5-nitro-2-thienyl)-9-chloro-5-morpholin- 4-yl[1,2,4]triazolo[4,3-c] quinazoline on cell growth, cell cycle, induction of DNA fragmentation and activity of caspase 3 in murine leukemia L1210 cells and fibroblast NIH-3T3 cells. Cell Biochem Funct 24(6): 519-30.

Jantova S, Repicky A, Cipak L (2009) 3-(5-Nitro-2-thienyl)-9- chloro-5-morpholin-4-yl[1,2,4]triazolo[4,3-c]quinazoline induces ROS-mitochondrial mediated death signaling and activation of p38 MAPK in murine L1210 leukemia cells. Neoplasma 56(6): 494-499.

Jantova S, Repicky A, Paulovicova E, Letasiova S, Cipak L (2008) Antiproliferative activity and apoptosis induced by 6- bromo-2-(morpholin-1-yl)-4-anilinoquinazoline on cells of leukemia lines. Exp Oncol 30(2): 139-142.

Jatav V, Mishra P, Kashaw S (2008) CNS depressant and anticonvulsant activities of some novel 3-[5-substituted 1,3,4-thiadiazole-2-yl]-2-styryl quinazoline-4(3H)- ones. European J Med Chem 43: 1945-1951.

Jedlovszky P, Turi L (1997) Role of the C-H,,,O Hydrogen Bonds in Liquids: A Monte Carlo Simulation Study of Liquid Formic Acid Using a Newly Developed Pair-Potential. J Phys Chem 101: 5429-5436.

Jeffrey GA, Saenger W (1991) Hydrogen Bonding in Biological Structures. Berlin Springer

Jessy EM, Sambanthan AT, Alex J, Sridevi CH, Srinivasan KK (2007) Synthesis and biological evaluation of some novel quinazolones. Indian J Pharm Sci 69: 476-478.

Jolivet J, Cowan KH, Curt GA, Clendninn NJ, Chabner BA (1983) The pharmacology and clinical use of methotrexate. N Engl J Med 309: 1094−1104.

Jordan DD (1993) Optical crystallographic characteristics of some USP drugs J Pharm Sci 82(12): 1269- 1271.

Joseph A, Pai A, Srinivasan KK, Tukaram Kedar, Thomas AT, Jessy EM, Singla R (2010) Synthesis and anticancer activity of some novel 3-(1, 3, 4-thiadiazol-2-yl)-quinazolin-4-(3H)-ones. The Electronic J Chem (Orbital) 2(2):158-167.

Jung SY, Lee SH, Kang HB, Park HA, Chang SK, Kim J, Choo DJ, Oh CR, Kim YD, Seo JH, Lee KT, Lee JY (2010) Antitumor activity of 3,4-dihydroquinazoline dihydrochloride in A549 xenograft nude mice. Bioorg Med Chem Lett 20(22): 6633-6636.

Kadi AA, Azab AS, Alafeefy AM, Abdel SG (2006) Synthesis and biological screening of some new substituted 2-mercapto-4(3H)quinazolinone analogues as anticonvulsant agents. J Pharma Sci 34: 147-158.

Kamal A, Bharathi EV, Reddy JS, Ramaiah MJ, Dastagiri D, Reddy MK, Viswanath A, Reddy TL, Shaik TB, Pushpavalli SN, Bhadra MP (2011) Synthesis and biological evaluation of 3,5-diaryl isoxazoline/isoxazole linked 2,3-dihydroquinazolinone hybrids as anticancer agents. Eur J Med Chem, 46(2): 691-703.

Kan SC, Siddiqui WA (1979) Comparative studies on dihydrofolate reductases from Plasmodium falciparum and Aotus trivirgatus. J Protozool 26: 660−664.

Kandale A, Ohlyan R, Kumar G (2014) Synthesis and in-vitro antiproliferative activity of 2, 3-aryl substituted 1, 3-benzoxazin-4-one derivatives. Int J Pharm Pharma Sci 6(7): 68-71.

Karger N, Amorim da Costa AM and Ribeiro-Claro Paulo JA (1999) C-H-O Bonded Dimers in Liquid 4-Methoxybenzaldehyde: A Study by NMR, Vibrational Spectroscopy, and ab Initio Calculations. J Phys Chem A 103: 8672-8677

Kelleher JM, McAuliffe MT, Moynihan HA, Mullins ND (2007) Studies on the preparation and crystal polymorphism of 2-acetamidobenzamide and related compounds. ARKIVOC (xvi): 209-226.

Kendall D N (1952) Identification of Polymorphic Forms of Crystals by Infrared Spectroscopy. Anal Chem 25: 382-389.

Khan QA, Barbieri CM, Srinivasan AR, Wang YH, LaVoie EJ, Pilch DS (2006) Drug self-association modulates the cellular bioavailability of DNA minor groove-directed terbenzimidazoles. J Med Chem 49: 5245–5251.

Kim HJ, Brunovska Z, Ishida H (1999) Molecular characterization of the polymerization of acetylene-functional benzoxazine resins. Polymer 40: 1815–1822.

Kou W, Cai CF, Xu SY, Wang H, Liu J, Yang D, Zhang TH (2011) *In vitro* and *in vivo* evaluation of novel immediate release carbamazepine tablets: complexation with hydroxypropyl-beta-cyclodextrin in the presence of HPMC. Int J Pharm 409: 75–80.

Kozarek RA, Patterson DJ, Gelfand M D, Botoman VA, Ball TJ, Wilske KR (1989) Methotrexate induces clinical and histologic remission in patients with refractory inflammatory bowel disease Ann Intern Med 110: 353–356.

Kuhnert-Brandstatter M, Riedmann M (1987) Thermal analytical and infrared spectroscopic investigations on polymorphic organic compounds-1. Mikrochim. Acta, 11: 107-120.

Kuhnert-Brandsttter M, Riedmann M (1989) Thermal analytical and infrared spectroscopic investigations on polymorphic organic compounds—V. Mikrochim Acta 99: 125-136.

Lee AY, Erdemir D, Myerson AS (2011) Crystal polymorphism in chemical process development. Annu Rev Chem Biomol Eng 2: 259-280.

Lee YH, Sathigari S, Lin YJ, Ravis WR, Chadha G, Parsons DL, Rangari VK, Wright N, Babu RJ (2009) Gefitinib-cyclodextrin inclusion complexes: physico-

chemical characterization and dissolution studies. Drug Dev Ind Pharm 35:1113–1120.

Levitt M, Perutz Max F (1988) Aromatic rings act as hydrogen bond acceptors. J Mol Biol 201: 751-754

Li D, Keresztes I, Hopson R, Williard PG (2009) Characterization of Reactive Intermediates by Multinuclear Diffusion-Ordered NMR Spectroscopy (DOSY) Acc Chem Res 42: 270–280.

Li HZ, He HY, Han YY, Gu X, He L, Qi QR, Zhao YL, Yang L (2010) A general synthetic procedure for 2-chloromethyl-4(3H)- quinazolinone derivatives and their utilization in the preparation of novel anticancer agents with 4-anilinoquinazoline scaffolds. Molecules 15(12): 9473-85.

Li X, Liu N, Zhang H, Knudson SE, Slayden RA, Tonge PJ (2010) Synthesis and SAR studies of 1,4-benzoxazine MenB inhibitors: Novel antibacterial agents against *Mycobacterium tuberculosis.* Bioorg Med Chem Lett 20: 6306-6309.

Lipinski CA (2000) Drug-like properties and the causes of poor solubility and poot permeability. J Pharmacol Toxicol 44: 235–49.

Lipinski CA, Lombardo F, Dominy BW, Feeney PJ (1997) Experimental and computational approaches to estimate solubility and permeability in drug discovery and development settings. Adv Drug Deliv Rev 23: 3-25.

Loftsson T, Brewster ME (1996) Pharmaceutical applications of cyclodextrins. 1. Drug solubilization and stabilization. J Pharm Sci 85(10): 1017-1025.

Louit G, Hocquet A, Ghomi M (2002) Intramolecular hydrogen bonding in ribonucleosides: an AIM topological study of the electronic density. Phys Chem Chem Phys 4: 3843-3848.

Macias FA, Marin D, Oliveros-Bastidas A, Chinchilla D, Simonet AM & Molinillo JMG (2006). Isolation and Synthesis of Allelochemicals from Gramineae: Benzoxazinones and Related Compounds. J Agric Food Chem 54: 991–1000.

Madkour HMF (2004) Reactivity of 4H-3,1-benzoxazin-4-ones towards nitrogen and carbon nucleophilic reagents: applications to the synthesis of new heterocycles. ARKIVOC (i): 36-54.

Mahato AK, Srivastava B, and Nithya S (2011) Chemistry structure activity relationship and biological activity of quinazoline- 4(3H)-one derivatives. Inventi Rapid: Med Chem, 2:1.

Malik S, Khan SA (2014) Design and evaluation of new hybrid pharmacophore quinazolino-tetrazoles as anticonvulsant strategy. Med Chem Res 23: 207-223.

Maroun J (1988) Clinical response to trimetrexate as sole therapy for non small cell lung cancer. Semin Oncol 15: 17−21.

Marques MPM, Amorim da Costa AM, and Ribeiro-Claro Paulo JA (2001) Evidence of C-HâââO Hydrogen Bonds in Liquid 4-Ethoxybenzaldehyde by NMR and Vibrational Spectroscopies. J Phys Chem A 105: 5292-5297

Marr EB, Bogert MT (1935) Researches on Quinazolines. XXXIX. The Synthesis of quinazoline Derivatives Structurally Analogous to the Angostura Alkaloids Galiopine and Galipine. J Am Chem Soc 57: 729-732.

Martin RB (1996) Comparisons of Indefinite self association models. Chem Rev 96 (8): 3043-3064

Martin GJ, Moss J, Avakian S (1947) Folic acid activity of N-(4-(4-quinazoline)- benzoyl)glutamic acid. J Biol Chem 167: 737-743.

Martin SR (1980) Absorption and circular dichroic spectral studies on the selfassociation of daunorubicin. Biopolymers 19: 713-721.

Marvania B, Lee PC, Chaniyara R, Dong H, Suman S, Kakadiya R, Chou TC, Lee TC, Shah A, Su TL (2011) Design, synthesis and antitumor evaluation of phenyl N-mustardquinazoline conjugates. Bioorg Med Chem, 19(6): 1987-1998.

Marzaro G, Guiotto A, Chilin A (2012) Quinazoline derivatives as potential anticancer agents: a patent review (2007-2010). Expert Opin Ther Pat 22: 223-252.

Masur H (1990) Problems in the management of opportunistic infections in patients infected with human immunodeficiency virus. J Infect Dis 161: 858−864.

Matsumoto A, Maeda K, Arai T (2003) Dimerization of Hydrogen Bonding and Photochemical properties of Dipyridone. J Phys Chem A 107: 10039-10045

McCrone W C (1957) Fusion Methods in Chemical Microscopy, Interscience, New York.

Mhaske SB, and Argade NP (2006) The chemistry of recently isolated naturally occurring quinazolinone alkaloids. Tetrahedron 62(42): 9787–9826.

Mohing W, Suckert R, Lataste X (1981) Comparative study of fluproquazone in the management of post-operative pain. Arzneimittelforschung 31: 918-920.

Mohri S (2001) Research and development of synthetic processes for pharmaceuticals: pursuit of rapid, inexpensive, and good processes. Journal of Synthetic Organic Chemistry 59: 514-515.

Morita S, Fujii A, Mikami N, Tsuzuki S (2006) Origin of the Attraction in Aliphatic C−H/π Interactions: Infrared Spectroscopic and Theoretical Characterization of Gas-Phase Clusters of Aromatics with Methane. J Phys Chem A 110: 10583-10590.

Morris GM, Goodsell DS, Halliday RS, Huey R, Hart WE, Belew RK, Olson A (1998) J Automated Docking Using a Lamarckian Genetic Algorithm and and Empirical Binding Free Energy Function. J Comp Chem 19(14): 1639-1662.

Mosmann T (1983) Rapid colorimetric assay for cellular growth and survival: application to proliferation and cytotoxicity assays. J Immunol Methods 65(1-2): 55–63.

Mullarkey MF, Blumenstein BA, Andrade WP, Bailey GA, Olason I, Wetzel CE,(1988) Methotrexate in the treatment of corticosteroid-dependent asthma. A double-blind crossover study. N Engl J Med 318: 603−607.

Muller RH, Jacobs C, Kayer O (2000) Nanosuspensions for the formulation of poorly soluble drugs in Pharmaceutical Emulsion and Suspension, F. Nielloud and G Marti Mestres, Eds, 383 Marcel Dekker, New York, NY, USA, 383-407.

Munshi P, Venugopala KN, Jayashree BS, Row TNG (2004) Concomitant polymorphism in 3-acetylcoumarin: Role of weak CH...O and C-H...pi Interactions. Crys Growth Des 4: 1105-1107.

Murugan V, Padmavaty NP, Ramasarma GVS, Sunil V, Sharma SB (2003) The synthesis of some Quinazoline derivatives as possible anticancer agents. Int J Hetero Chem 13(2): 143-146.

Naama JH, Al-Temimi AA, Al-Amiery AAH (2010) Study the anticancer activities of ethanolic curcumin extract. Afr J Pure Appl Chem 4: 68–73.

Nagarajan M, Morrell A, Fort BC, Meckley MR, Antony S, Kohlhagen G, Pommier Y, Cushman M (2004) Synthesis and anticancer activity of simplified indenoisoquinoline Topoisomerase I inhibitors lacking substituents on the aromatic rings. J Med Chem 47: 5651–5661.

Nanda AK, Ganguli S, Chakraborty R (2007) Antibacterial activity of some 3-(Arylideneamino)-2-phenylquinazoline-4(3H)-ones: synthesis and preliminary QSAR studies. Molecules 12: 2413-2426.

Nandi S, Bagchi MC (2010) 3D-QSAR and molecular docking studies of 4-anilinoquinazoline derivatives: a rational approach to anticancer drug design. Mol Divers 14(1): 27-38.

Nanjwade BK, Derkar GK, Bechra HM, Nanjwade VK, Manvi FV (2011) Design and Characterization of Nanocrystals of Lovastatin for Solubility and Dissolution Enhancement. J Nanomedic Nanotechnol 2: 107.

Nasongkla N, Wiedmann AF, Bruening A, Beman M, Ray D, Bornmann WG, Boothman DA, Gao J (2003) Enhancement of solubility and bioavailability of b-lapachone using cyclodextrin inclusion complexes. Pharm Res 20: 1626–1633.

Navarrete-López A M, Garza J, Vargas R (2007) Relationship between the Critical Points Found by the Electron Localization Function and Atoms in Molecules Approaches in Adducts with Hydrogen Bonds. J Phys Chem A 111: 11147-11152.

Niementowski V. (1895) Niementowski Quinazoline Synthesis. Journal für Praktische Chemie 51: 564.

Nerkar AG, Saxena AK, Ghone SA, Thaker AK (2009) In Silico Screening, synthesis and in vitro evaluation of some quinazolinone and pyridine derivatives as dihydrofolate reductase inhibitors for anti-cancer activity. J. Chem 6: 97–102.

Nzila A (2006) The past, present and future of antifolates in the treatment of Plasmodium falciparum infection. J Antimicrob Chemother 57: 1043–1054.

Oatis JE Jr, Hynes JB (1977) Synthesis of quinazoline analogues of folic acid modified at position 10. J Med Chem 20: 1393-1396.

Ochiai T, Ishida R (1982) Pharmacological studies on 6-amino-2-fluoromethyl- 3-(O-tolyl)-4(3*H*)-quinazolinone (afloqualone), a new centrally acting muscle relaxant. (II) Effects on the spinal reflex potential and the rigidity. Jpn J Pharmacol 32: 427-38.

Ogoshi T, Chujo Y (2003) Synthesis of Organic−Inorganic Polymer Hybrids by Means of Host−Guest Interaction Utilizing Cyclodextrin. Macromolecules 636: 654-660.

Oprea T (2000) Property distribution of drug-related chemical databases, J Comput Aided Mol Des, 14: 251–264.

Osborn MJ, Freeman M, Huennekens FM (1958) Inhibition of dihydrofolic reductase by aminopterinand amethopterin. Proc Soc Exp Biol Med 97: 429–431.

Osborn MJ, Huennekens FM (1958) Enzymatic reduction of dihydrofolic acid. J Biol Chem 233: 969–974.

Ovádeková R, Jantová S, Theiszová M, Labuda J (2005) Cytotoxicity and detection of damage to DNA by 3-(5-nitro- 2-thienyl)-9-chloro-5-morpholin-4-yl[1,2,4]triazolo[4,3-c] quinazoline on human cancer cell line HeLa, Biomed Pap Med Fac Univ Palacky Olomouc Czech Repub 149(2): 455-459.

Palm K, Stenberg P, Luthman K, Artursson P (1997) Polar molecular surface properties predict the intestinal absorption of drugs in humans. Pharma Res 14: 568–571.

Pandey VK, Lohani HC (1979) The anti-tremour activity of 2- aryl/alkyl-3(2-amino ethyl-1, 3, 4-thiadiazol-5-yl)quinazolin-4(3H) ones. J Ind Chem Soc 56: 415-419.

Pandey VK, Misra D, Shukla A (1994) Synthesis and antiviral activity if 2-aryl-5-[3′-2′-methyl-6:8 substituted-quinazolyl)-phenyl], pyrazoles. Indian Drugs 31 (11): 532–536.

Patil DR, Dalal DS (2011) One-Pot, Solvent free synthesis of Hantzsch 1, 4-Dihydropyridines using β-cyclodextrin as a Supramolecular Catalyst. Lett Org Chem 8(7): 477- 486.

Pauling L (1960) The Nature of the Chemical Bond, Cornell University Press, Ithaca, NY. The first edition was published in 1939.

Pecul M, Leszczynski J, Sadlej J (2000) Comprehensive *ab initio* studies of nuclear magnetic resonance shielding and coupling constants in XH···O hydrogen-bonded complexes of simple organic molecules. J Chem Phys. 112: 7930-7938.

Perrenot B , Widman G (1994) Polymorphism by differential scanning calorimetry. Thermochim Acta 234: 31-39.

Pierce CA, Haar E, Binch HM, Kay DP, Patel SR, Li P (2005) CH...O and CH...N hydrogen bonds in ligand design: a novel quinazolin-4-ylthiazol-2-ylamine protein kinase inhibitor. J Med Chem 48: 1278-1281.

Pimente GCL and McClellan AL (1960) The Hydrogen Bond. WH Freeman and Co. San Francisco.

Prins LJ, Reinhoudt D A, Timmerman P (2001) Noncovalent Synthesis Using Hydrogen Bonding. Ange Chem Int Ed Engl 40 (13): 2382-2426.

Rajamohan R, Nayaki SK, Swaminathan M (2012) Host–guest complexation between 5-aminoisoquinoline and b-cyclodextrin and its effect on spectral and prototropic characteristics. J Incl Phenom Macrocycl Chem 73: 99–108.

Ramachandran GN, Ramakrishnan C, and Sasisekharan V (1963) Stereochemistry of polypeptide chain configurations. J Mol Biol 7: 95-99.

Ramírez J-Z, Vargas R, Garza J (2008) The Role of the Linearity on the Hydrogen Bond in the Formamide Dimer: a BLYP, B3LYP, and MP2 Study. J Mex Chem Soc 52(1): 31-35.

Rangel-Yagui CD, Pessoa A, Tavares LC (2005) Micellar solubilisation of drugs. Pharm Pharm Sci 8(2): 147–163.

Ravez S, Castillo-Aguilera O, Depreux P, Goossens L (2015) Quinazoline derivatives as anticancer drugs: a patent review (2011-present). Expert Opin Ther Pat 25: 789–804.

Ribeiro-Claro PJA, Batista de Carvalho LAE, Amado AM (1997) Evidence of dimerization through C—H···O interactions in liquid 4-methoxybenzaldehyde from Raman spectra and *ab initio* calculations. J Raman Spectrosc 2: 867-872.

Rodrı´guez-Spong B, Price CP, Jayasankar A, Matzger AJ, Rodrı´guez HN (2004) General principles of pharmaceutical solid polymorphism: a supramolecular perspective. Adv Drug Del Rev 56: 241–274.

Rodriguez-Spong B, Price CP. A. Jayasankar, A.J. Matzger, N. Rodriguez-Hornedo N (2004) General principles of pharmaceutical solid polymorphism: a supramolecular perspective. Adv Drug Deliv Rev 56: 241-274.

Roskoski Jr R (2014) The ErbB/HER family of protein-tyrosine kinases and cancer. Pharmacol Res 79: 34–74.

Roth B (1986) Design of dihydrofolate reductase inhibitors from X-ray crystal structures. Fed Proc 45: 2665−2772.

Ruiz T P, Fernandez-Gómez M, González JJL, Koziol AE, Roldán JMG (2004) Weak C–H· · ·O and C–H· · ·p hydrogen bonds in crystal 1-indanone. A structural and spectroscopic analysis. J Mol Struct 707: 33-46.

Savjani KT, Gajjar AK, Savjani JK (2012) Drug solubility: importance and enhancement techniques. ISRN Pharm 195727.

Scanlon KJ, Moroson BA, Bertino JR, Hynes JB (1979) Quinazoline analogues of folic acid as inhibitors of thymidylate synthetase from bacterial and mammalian sources. Mol Pharmacol 16: 261-269.

Schneidman-Duhovny D, Dror O, Inbar Y, Nussinov R, Wolfson JH (2008) PharmaGist a webserver for ligand-based pharmacophore detection. Nuc Acids Res 36: W223–W228.

Schnell I, Brown SP, Low HY, Ishida H, Spiess HW (1998) An Investigation of Hydrogen Bonding in Benzoxazine Dimers by Fast Magic-Angle Spinning and Double-Quantum 1H NMR Spectroscopy. J Am Chem Soc 120: 11784-11795.

Sekiguchi K, Obi N (1961) Studies on absorption of eutectic mixtures. I.A. comparison of the behaviour of eutectic mixtures of sulphathiazole and that of ordinary sulphathiazole in man. Chem Pharm Bull 9: 866– 872.

Selvan TP, Kumar PV (2011) Quinazoline Marketed drugs - A Review. Res Pharm 1: 1-21.

Sharma MC, Sharma S (2011) Formulation and Spectroscopic Studies and Dissolution Behavior of Levofloxacin-β Cyclodextrins Inclusion Complex. Int J Pharm Tech Res 3(3): 1883-1888.

Sharma RN, Ravani R (2013) Synthesis and screening of 2-(2-(4-substituted piperazine-1-yl)-5-phenylthiazol-4-yl)-3-aryl quinazolinone derivatives as anticancer agents. Med Chem Res 22: 2788-2794.

Shirodkar PY, Vartak M (2000) Synthesis, biological evaluation and QSAR evaluation of Mannic bases of 6-nitro-quinazolones. Indian J Heterocyclic Chem 9: 239–240.

Shobha RS, Raju B (2015) Review on Quinazoline Deirivatives. Journal of Global Trends in Pharmaceutical Sciences 6: 2510-2527.

Singh M, Sharma R, and Banerjee UC (2002) Biotechnological applications of cyclodextrins. Biotechnol Adv 20: 341-359.

Sinha VR, Anitha R, Ghosh S, Nanda A, Kumria R (2005) Complexation of celecoxib with beta-cyclodextrin: characterization of the interaction in solution and in solid state. J Pharm Sci 94: 676–687.

Sirisoma N, Pervin A, Zhang H, Jiang S, Willardsen JA, Anderson MB, Mather G, Pleiman CM, Kasibhatla S, Tseng B, Drewe J, Cai SX (2009) Discovery of N-(4-methoxyphenyl)-N,2- dimethylquinazolin-4-amine, a potent apoptosis inducer and efficacious anticancer agent with high blood brain barrier penetration. J Med Chem 52(8): 2341-2351.

Smith HO, Blessing JA, and Vaccarello L(2002) Trimetrexate in the treatment of recurrent or advanced leiomyosarcoma of the uterus: a phase II study of the Gynecologic Oncology Group. Gynecol Oncol 84(1): 140-144.

Smyth RD, Lee JK, Polk A, Chemburkar PB, Savacool AM (1973) Bioavailability of methaqualone. J Clin Pharmacol 13: 391-400.

Sneader W (2000) The discovery of aspirin: a reappraisal. Br Med J 321: 1591 -1594.

Sorbera LA, Bartroli J, Castaner J (2003) Albaconazole antifungal. Drugs Fut 28: 529-537.

Stoddart JF (2009) Thither supramolecular chemistry? Nature Chemistry 1: 14-15.

Strober W (1992) Trypan blue exclusion test of cell viability. In: Coligan JE, Kruisbeek AM, Margulis DH, Shevach EM, Strober W, editors. Current Protocols in Immunology. New York: John Wiley & Sons. A.3.3–4.

Sundrud MS, Koralov SB, Feuerer M, Calado DP, Kozhaya AE, Rhule-Smith A, Lefebvre RE, Unutmaz D, Mazitschek R, Waldner H, Whitman M, Keller T, Rao A (2009) Halofuginone inhibits TH17 cell differentiation by activating the amino acid starvation response. Science 324: 1334-1338.

Susich G (1950) Identification of Organic Dyestuffs by X-Ray Powder Diffraction. Anal. Chem 22: 425-430.

Sutor DJ (1963) Evidence for the Existence of C-H-0 Hydrogen Bonds in Crystals. J Chem Soc: 1105-1110.

Tachibana T, Nakamura A (1965) A methode for preparing an aqueous colloidal dispersion of organic materials by using water-soluble polymers: dispersion of β-carotene by polyvinylpyrrolidone. Colloid Polym Sci 203(2): 130–133.

Tambunan USF, Bramantya N, Parikesit AA (2011) In silico modification of suberoylanilide hydroxamic acid (SAHA) as potential inhibitor for class II histone deacetylase (HDAC). BMC Bioinformatics 12(Suppl 13): S23.

Tambunan USF, Bramantya N, Parikesit AA (2011) In silico modification of suberoylanilide hydroxamic acid (SAHA) as potential inhibitor for class II histone deacetylase (HDAC). BMC Bioinformatics 12(Suppl 13): S23.

Tan JH, Ou TM, Hou JQ, Lu YJ, Huang SL, Luo H-B, Wu J-Y, Huang Z-S, Wong K-Y, Gu L-Q (2009) Isaindigotone derivatives: a new class of highly selective ligands for telomeric G-quadruplex DNA. J Med Chem 52(9): 2825-2835.

Taylor R, Kennard O (1982) Crystallographic Evidence for the Existence of C-H-0, C-H-N, and C-H-Cl Hydrogen Bonds. J Am Chem Soc 104: 5063-5070.

Teetsov AS, McCrone WC (1967) The Microscopical Study of Polymorph Stability Diagrams. Microsc Cryst Front 15: 13-29.

Thilagavathy R, Kavitha HP, Arulmozhi R, Vennila JP, Manivannan V (2009) 2- Phenyl-4H-3,1-benzoxazin-4-one. Acta Crystallogr Sect E- Struct Rep 65:127.

Tiwary BK, Pathak RK, Pradhan K, Nanda AK, Bothra AK, Chakraborty R(2014) Evaluation of drug candidature of some quinazoline-4–3H-ones as inhibitor of human dihydrofolate reductase enzyme: Molecular docking and In silico studies. Int J Pharm Pharm Sci. 6 Suppl: 2393–2400.

UH Sk, Prakasha Gowda AS, Crampsie MA, Yun JK, Spratt TE, Amin S, Sharma AK (2011) Development of novel naphthalimide derivatives and their evaluation as potential melanoma therapeutics Eur J Med Chem 46: 3331–3338.

Urakawa K, Mihara M, Suzuki T, Kawamura A, Akamatsu K, Tokeda Y, Kamatani N (2000) Polyglutamation of antifolates is not required for induction of extracellular release of adenosine or expression of their anti-inflammatory effects. Immunopharmacology 48: 137−144.

Uzqueda M, Martin C, Zornoza A, Sanchez M, Martínez-Ohárriz MC, Velaz I (2006). Characterization of complexes between naftifine and cyclodextrins in solution and in the solid state. Pharm Res 23: 980–988.

Vargas R, Garza J, Dixon DA, Hay BPJ (2000) How Strong Is the C^{α}-H..O=C Hydrogen Bond? J Am Chem Soc 122: 4750-4755.

Vishweshwar P, McMahon JA, Oliveira M, Peterson ML, Michael JZ (2005) The Predictably Elusive Form II of Aspirin J. Am. Chem. Soc. 127(48): 16802-16803.

Vogt M, Kunath K, Dressman JB (2008) Dissolution enhancement of fenofibrate by micronization, cogrinding and spray-drying: comparison with commercial preparations. Eur J Pharm Biopharm 68(2): 283–288.

Voress L (1994) DTA heats up material analysis. Anal Chem 66: 1035A-1038A.

Wahl MC, Sundaralingam M (1997) C-H···O hydrogen bonding in biology. Trends Biochem Sci 22: 97-102.

Waisser K, Petrlikova E, Perina M, Klimesova V, Kunes J, Palat K, Kaustova J, Dahse H, Mollmann U (2010) A note to the biological activity of benzoxazine derivatives containing the thioxo group. Eur J Med Chem 45: 2719-2725.

Waisser K, Petrlíková E, Peřina M, Klimešová V, Kuneš J, Palát K, Kaustová J, Dahse HM, Möllmann U (2010) A note to the biological activity of benzoxazine derivatives containing the thioxo group. Eur J Med Chem 45(7): 2719-2725.

Warwicker JO (1960) Comparative studies of fibroins. II. The crystal structures of various fibroins. J Mol Biol 2: 350-362.

Weber C, Demeter A, Szendrie G, Freiner I (2003) Solid-phase synthesis of 2,6-and 2,7-diamino-4(3H)-quinazolinones via palladium-catalyzed amination. Tetrahedron let 44: 7533-7536.

Weinblatt ME, Coblyn JS, Fox DA, Fraser PA, Holdsworth DE, Glass DN, Trentham DE (1985) Efficacy of low-dose methotrexate in rheumatoid arthritis. N Engl J Med 312(13): 818-822.

Weinstein G D, Frost P (1971) Methotrexate for psoriasis. A new therapeutic schedule. Arch Dermatol 103: 33−38.

Welton AF, Dunton AW, McGhee B (1986) The pharmacological profile and initial clinical evaluation of tiacrilast (Ro 22-3747): a new antiallergic agent. Agents Actions 18: 313-317.

Wheatley D (1982) Analgesic properties of fluproquazone. Rheumatol Rehabil 21: 98-100.

Wheatley PJ (1964) The crystal and molecular structure of aspirin. J Chem Soc 6036-6048.

Widemann BC, Balis FM, Godwin KS, McCully C, Adamson PC (1999) The plasma pharmacokinetics and cerebrospinal fluid penetration of the thymidylate synthase inhibitor raltitrexed (Tomudex) in a nonhuman primate model. Cancer Chemother Pharmacol 44: 439–443.

Wu X, Li M, Tang W, Zheng Y, Lian J, Xu L, Ji M (2011) Design, synthesis and in vitro antitumor activity evaluation of novel 4-pyrrylamino quinazoline derivatives. Chem Biol Drug Des 3: 112-118.

Wulff M, Alden M, Tegenfeldt J (2002) Solid-State NMR Investigation of Indomethacin−Cyclodextrin Complexes in PEG 6000 Carrier. Bioconjugate Chem 13: 240-248.

Xia Y, Yang ZY, Hour MJ, Kuo SC, Xia P, et al. (2001) Antitumor agents. Part 204: synthesis and biological evaluation of substituted 2-aryl quinazolinones. Bioorg Med Chem Lett 11: 1193-1196.

Xingwen G, Xuejian C, Kai Y, Baoan S, Lili G, Zhuo C (2007) Synthesis and Antiviral Bioactivities of 2-Aryl- or 2-Methyl-3-(substituted- Benzalamino)-4(3*H*)-quinazolinone Derivatives. Molecules 12: 2621-2642.

Yamini L, Meena KK, Vijjulatha M (2011) Molecular Docking, 3D QSAR and Designing of New Quinazolinone Analogues as DHFR Inhibitors Bull Korean Chem Soc 32 : 2433-2442

Yukhnevich G V, Tarakanova E G (1998) Hydrogen bond CH…O in liquid methanol. J Mol Structure 447 (3): 257-261.

Zayed MF, Hassan MH (2014) Synthesis and biological evaluation studies of novel quinazolinone derivatives as antibacterial and anti-inflammatory agents. Saudi Pharm J 22: 157-162.

Zhang Zhang, S (2009) Structure/Ligand-based Drug Design and Structure Bioinformatics: Basics, Concepts, Methods, and Applications. VDM Verlag.

Zheng Y, Bian M, Deng XQ, Wang SB, Quan ZS (2013) Synthesis and anticonvulsant activity evaluation of 5-phenyl-[1,2,4]triazolo[4,3-c]quinazolin-3-amines. Arch Pharm (Weinheim) 346: 119-126.

INDEX

N

P

S

T

V

PUBLICATIONS

PUBLICATIONS

Thesis related publications:

1. **Bipransh Kumar Tiwary**, Kiran Pradhan, Ashis Kumar Nanda, Ranadhir Chakraborty. (2015). Implication of Quinazoline-4-(3H)-ones in medicinal chemistry: A Brief review. *Journal of Chemical Biology and Therapeutics,* 1:1

2. **Bipransh Kumar Tiwary**, Ravindra Kailasrao Zirmire, Kiran pradhan, Ashis Kumar Nanda, Ranadhir Chakraborty (2014) Preparation and Spectroscopic Characterization of Inclusion Complex of 2-phenyl-4h-benzo[d][1,3]oxazin-4-one and β-Cyclodextrin. *International Journal of Pharmacy and Pharmaceutical Sciences,* Vol 6, Issue 3, 176-179.

3. **Bipransh Kumar Tiwary**, Ravi Kant Pathak, Kiran Pradhan, Ashis Kumar Nanda, Asim Kumar Bothra, Ranadhir Chakraborty (2014). Evaluation of Drug Candidature of some Quinazoline- 4-(3h)-ones as Inhibitor of Human Dihydrofolate Reductase enzyme: Molecular Docking and *In Silico* Studies. *International Journal of Pharmacy and Pharmaceutical Sciences,*Vol 6 suppl 2, , 393-400.

4. **Bipransh Kumar Tiwary,** Kiran Pradhan, Ranadhir Chakraborty, Ashis Kumar Nanda. Investigation of polymorphism in 2-substituted-benzo[d][1,3]oxazine-4-ones by thermo-analytical, spectroscopic evidence and PXRD studies. *Journal of Molecular structure.* (Communicated)

5. **Bipransh Kumar Tiwary,** Kiran Pradhan, Ranadhir Chakraborty, Ashis Kumar Nanda. A New Potential Motif for supramolecular assembly framed with aryl C-H---O=C H-bond and the effect of self association on antibacterial property. (Manuscript under preparation)

6. **Bipransh Kumar Tiwary,** Kiran Pradhan, Ranadhir Chakraborty, Ashis Kumar Nanda. Preparation and characterization of Inclusion complex of 3-aryldeneamino-2-phenyl-quinazoline-4(3H)-one and β-cyclodextrin. (Manuscript under preparation)

Other publications:

1. **Bipransh Kumar Tiway,** Arvind Kumar, Ravikant Pathak, Nishtha Pandey, Krishnakant Yadav, Ranadhir Chakraborty (2016) The Locus *PgaABCD* of *Acinetobacter junii* Putatively Responsible for Poly-*β*-(1, 6)-*N*-Acetylglucosamine Biosynthesis Might Be Related to Biofilm Formation: A Computational Analysis, Advances in Microbiology (In Press).

2. Kiran Pradhan, **Bipransh Kumar Tiwary,** Mossaraf Hossain, Ranadhir Chakraborty and Ashis Kumar Nanda (2016). A mechanistic study of carbonyl activation under solvent-free conditions: evidence drawn from the synthesis of imidazoles, *RSC Advance,* 6, 10743-10749.

3. K.B. Benzon, Hema T. Varghese, C.Y. Panicker, Kiran Pradhan, **Bipransh Kumar Tiwary,** Ashis Kumar Nanda, C. Van Alsenoy (2015) Spectroscopic and theoretical characterization of 2-(4-methoxyphenyl)- 4,5-dimethyl-1H-imidazole 3-oxide, *Spectrochimica Acta Part A: Molecular and Biomolecular Spectroscopy*, 151, 965–979.

4. K.B. Benzon, Hema T. Varghese, C.Y. Panicker, Kiran Pradhan, **Bipransh Kumar Tiwary,** Ashis Kumar Nanda, C. Van Alsenoy (2015) Spectroscopic investigation (FT-IR and FT-Raman), vibrational assignments, HOMOLUMO, NBO, MEP analysis and molecular docking study of 2-(4-hydroxyphenyl)-4,5-dimethyl-1H-imidazole 3- oxide, *Spectrochimica Acta Part A: Molecular and Biomolecular Spectroscopy*, 146; 307–322.

5. **Bipransh Kumar Tiwary,** Sony Bihani, Anoop Kumar, Ranadhir Chakraborty, Runu Ghosh (2015) The in vitro cytotoxic activity of ethno-pharmacological important plants of Darjeeling district of West Bengal against different human cancer cell lines. *BMC Complementary and Alternative Medicine*, 15:22.

6. Arvind Kumar, **Bipransh Kumar Tiwary,** Sangita Kachhap, Ashis Kumar Nanda, Ranadhir Chakraborty (2015) An Escherichia coli strain, PGB01, isolated from feral Pigeon faeces, thermally fit to survive in pigeon, shows high level resistance to trimethoprim. *PLoS ONE* 10(3): e0119329. doi:10.1371/journal.pone.0119329. [Arvind Kumar **and B K Tiwary were contributed equally]**

7. Runu Ghosh, **Bipransh Kumar Tiwary,** Anoop Kumar, Ranadhir Chakraborty (2014). Guava Leaf Extract Inhibits Quorum-Sensing and Chromobacterium violaceum Induced Lysis of Human Hepatoma Cells: Whole Transcriptome Analysis Reveals Differential Gene Expression, *PLoS ONE* 9(9): e107703. doi:10.1371/journal.pone.0107703.

8. **Bipransh Kumar Tiwary,** Anil Kumar, Ashis Kumar Nanda, Ranadhir Chakraborty (2014). A Study on Optimization of Marigold Petal Yield, Pure Lutein, and Formulation of Free-Flowing Lutein Esters, *Journal of Crop Science and Biotechnology* 17 (3) : 175 ~ 181

9. Ranadhir Chakraborty, Arvind Kumar, Suparna Saha Bhowal, Amit Kumar Mandal, **Bipransh Kumar Tiwary,** Shriparna Mukherjee (2013). Diverse Gene Cassettes in Class 1 Integrons of Facultative Oligotrophic Bacteria of River Mahananda, West Bengal, India, *PLoS ONE* 8(8): e71753. doi:10.1371/journal.pone.0071753.

❖ **BOOK CHAPTERS:**

1. **Bipransh Kumar Tiwary**, Kiran Pradhan, Ashis Kumar Nanda, Asim Kumar Bothra, Ranadhir Chakraborty. "**Basics of Computer-aided Drug-design** "Biotechnology for people" ISBN- 978-93-80663-86-9, page no-151-167, Published by- P.D. Women's College and Levant Books

2. Ranadhir Chakraborty, Arvind Kumar, Shriparna Mukherjee, Suparna Saha Bhowal, Amit K Mandal, **Bipransh Kumar Tiwary. Oligotrophic Bacteria of River Mahananda: Spanking Reservoir ofIntegron-Borne Gene Cassettes Coding for Diverse Proteins Including Antibiotic-Resistance.** "Biotechnology for people" ISBN- 978-93-80663-86-9, page no-50-59, Published by- P.D. Women's College and Levant Books.

Abstract and Conference Proceedings

1. A new potential motif for supramolecular assembly: 2-substitueted benzo[d] [1,3] oxazine-4-ones and study of their effect on antibacterial activity. **Bipransh Kumar Tiwary,** Kiran Pradhan, Mossaraf Hossain, Ranadhir Chakraborty, Ashis Kumar Nanda. The 5th Asian Conference on Colloid and Interface Scince, held on November 20-23, 2013 at North Bengal University. (Oral Presentation)

2. Inhibition of recombinant human DHFR activity in presence of 3-{[4-Dimethylaminophenyl) methylene]amino}-2-phenylquinazolin-4(3H)-one and characterization of dimerization property of the inhibitor. **Bipransh Kumar Tiwary,** Kiran Pradhan, Ashis Kumar Nanda and Ranadhir Chakraborty. *World Congress on Biotechnology:Organized by OMICS group USA.* held at HICC, Hyderabad, March 21-23, 2011. (Poster Presentation)

3. Optimizing Petal yield and Process Standardization of Extraction, Purification, and precise Estimation of Marigold Lutein and Lutein Esters. **Bipransh Kumar Tiwary,** Ashis Kumar Nanda and Ranadhir Chakraborty. *International Symposium on System Intensification Towards food and Environmental Security):* held at Bidhan Chandra Krishi Vishwavidyalya, Kalyani, February 24-27, 2011. (Oral Presentation)

4. Discovery of 2-Substituted benzo[d] [1, 3] oxazin-4-ones – as potential new motif for supramolecular assembly and study of the impact of self-assembled dimer on antibacterial activity. **Bipransh Kumar Tiwary,** Kiran Pradhan, Subarna Ganguly, Ranadhir Chakraborty, Swapan Kumar Saha and Ashis Kumar Nanda. *International Symposium on facets of weak interactions in chemistry*: held at University of Calcutta, Kolkata, January 13-15, 2011. (Poster Presentation)

5. Screening of certain medicinal plants from the hill and plain area of Darjeeling district for their anti-quorum sensing activity using *Chromobacterium violaceum.* Dipanwita Deb, **Bipransh Kumar Tiwary,** Saurav Moktan, Dibakar Choudhury, Abhay Prasad Das, Ranadhir Chakraborty and Runu Ghosh. *National Seminar on Micro and Macro resources in Biomolecular Technology,* held at University of North Bengal, Darjeeling, February 25-26, 2013. (Poster Presentation)

6. Molecule to Drug: A basic theoretical approach. **Bipransh Kumar Tiwary,** Ashis Kumar Nanda, Asim Kumar Bothra and Ranadhir Chakraborty *National seminar on Biotechnology for people: Application and Awareness;* held at PD Womens

College, Jalpaiguri on 4th &5th December, 2011. (Oral Presentation)

7. Molecular docking of of Synthesized 3-(Arylideneamino)-2- phenylquinazoline-4(3H)-ones as putative human dihydrofolate reductase inhibitor. **Bipransh Kumar Tiwary,** Kiran Pradhan, Ashis Kumar Nanda, Asim Kumar Bothra and Ranadhir Chakraborty *National Conference on Biology and Bioinformatics of Economically Important Plants and Microbes*: held at University of North Bengal, Darjeeling, on February 17-19, 2012. (Oral Presentation)

8. In Quest of causes for virtual catalytic effects (carbonyl activation) in solventfree multi-component reaction Ashis Kumar Nanda, Kiran Pradhan, **Bipransh Kumar Tiwary,** Ranadhir Chakraborty and Sajal Das. *National Seminar on Frontiers in Chemistry 2011 & Celebration of the International Year of Chemistry 2011:* held at University of North Bengal, Darjeeling, March 14- 16, 2011. (Oral Presentation)

Workshops and Industrial Traininng

1. Participated in Science Academies Lecture workshop on " Spectroscopy of Emerging Materials" held on 26-27 November, 2014, in Department of Chemistry, University of North Bengal.

2. Completed 4 days training on " National Workshop on Drug Design and Discovery" conducted by Institute of Life Sciences, Bhubaneshwar, held on 18-21 February 2013.

3. Completed training on "Basics off Molecular Modelling and computer-aided drug Designing" conducted by BIF, C.V.Sc, Assam Agricultural University from 8th to 10th January 2013.

4. Science Academies Lecture Workshop on "Modern Trends in Chemistry Education" held on November 22-23 Nov, 2012 at Department of Chemistry, University of North Bengal.

5. Science Academies Lecture Workshop on "Recent Trends in Chemistry" held on November 11-12, 2011 at Department of Chemistry, University of North Bengal.

6. UGC sponsored "Research Scholars Training Programme" held on Academic staff college, University of north Bengal on 30th June and 01st July, 2011.
7. 3 days "Training programme on Application of open Software" offered from 28^{th} to 30^{th} March 2011, conducted by University science Instrumentation Centre, North Bengal University.

8. 3 days Seminar cum workshop on Bioinformatics held from 12th to 14th February 2009 at Bioinformatics Facility, University of north Bengal.

Academic Sciences International Journal of Pharmacy and Pharmaceutical Sciences

ISSN- 0975-1491 Vol 6 suppl 2, 2014

Research Article

EVALUATION OF DRUG CANDIDATURE OF SOME QUINAZOLINE- 4-(3H)-ONES AS INHIBITOR OF HUMAN DIHYDROFOLATE REDUCTASE ENZYME: MOLECULAR DOCKING AND IN SILICO STUDIES

BIPRANSH KUMAR TIWARY[1#], RAVI KANT PATHAK[2#], KIRAN PRADHAN[3], ASHIS KUMAR NANDA[3], ASIM KUMAR BOTHRA[4] , RANADHIR CHAKRABORTY[1*]

[1]Omics laboratory, Department of Biotechnology, University of North Bengal, Siliguri, West Bengal 734013, [2]Genetics and Molecular Biology Domain, Department of Biotechnology, Lovely Professional University, Phagwara, Punjab, 144402, [3]Department of Chemistry, University of North Bengal, Siliguri, West Bengal 734013, [4]Cheminformatics Bioinformatics Laboratory, Department of Chemistry, Raiganj College (University College), Raiganj-733134, Uttar Dinajpur, West Bengal , India. Email: rcnbu2003@yahoo.com, asimbothra@gmail.com

Received: 26 Nov 2013, Revised and Accepted: 02 Feb 2014

ABSTRACT

Objectives: Human dihydrofolate reductase (hDHFR) is one of the best targets for the anticancer drug because it plays an important role in the synthesis of purines and pyrimidines. It also maintains intracellular biochemically active reduced folate pools. Quinazoline-containing compounds are more noticed because of their some resemblance with folic acid and also have provided attractive scaffolds for designing anticancer drugs. In this study, molecular docking and *In silico* studies were carried out in an attempt to evaluate the drug candidature of some quinazoline-4-(3H) -ones as inhibitors of human dihydrofolate reductase enzyme.

Methods: The study comprised of 27 compounds belonging to quinazoline-4-(3H)-one along with one standard drug methotrexate. Automated molecular docking of some quinazoline-4(3H)-ones with human DHFR was performed by the AutoDock 4.0 suite. Molecular descriptor properties were predicted by Molinspiration and OSIRIS Property explorer. Ligand based pharmacophore has been generated by PharmaGist tools.

Results: All the derivatives have qualified the Lipinski's Rule of Five and occupied the same cavity (as evidenced by the molecular docking results) in the protein molecule as is occupied by the natural ligand folic acid and the standard drug methotrexate. The binding energies of all the docked complex of compounds have significant negative values as compared to methotrexate.

Conclusion: The molecular docking study signified that the compounds can act as a putative inhibitor of hDHFR. The generated pharmacophore could further be used to design and develop new drugs. This study significantly supports a theoretical perception regarding the candidature of these compounds as inhibitors of human DHFR.

Keywords: Dihydrofolate reductase, Molecular docking, Drug likeliness, Drug score, Anticancer drug.

INTRODUCTION

In cancer chemotherapy, the folate metabolism has long been considered as an attractive target because of its obligatory role in the biosynthesis of nucleic acid precursor [1]. In folate metabolism, dihydrofolate reductase (5, 6, 7, 8 tetrahydrofolate: $NADP^+$ oxidoreductase, EC 1.5.1.3, DHFR) catalyzes the reduction of folate or 7, 8-dihydrofolate to tetrahydrofolate and intimately couples with thymidylate synthase. DHFR plays a fundamental role in the maintenance of intracellular biochemically active reduced folate pools [2]. It is also an important target for the treatment of a wide range of diseases. The abilities of quinazolines to inhibit DHFR activities were reported earlier [3-6].

Quinazoline-containing compounds have provided attractive scaffolds for designing anticancer drugs [7]. They are more noticed because of their diverse biological activity notably as kinase inhibitors [8] and some resemblance with folic acid. [9,10] The 4-anilinoquinazoline derivatives have led to the development and marketing of a new series of antitumor agents, such as gefitinib, erlotinib and lapatinib [11-13]. The quinazoline ring provides a satisfactory backbone for inhibition of mammalian DHFR, establishing contact with the key amino acid residues in the enzyme pocket. The 3-amino-2-aryl-4(3H)-quinazolinone was found to be highly potential against the multiple-antibiotic-resistant bacteria [14] and later antifungal and anti viral properties were also reported [15]. But literatures revealing anticancer property of these compounds are inadequate.

A suitable screening of the compounds, using theoretical and computational approaches prior to real-time experiments, to generate pharmacophore is considered to be the most appropriate strategy in the context of drug discovery research. The physico-chemical properties closely related to drug absorption are used in predicting bioavailability and also to interpret *in vitro* and *in vivo* findings. However, it is also found that the intrinsic biological and physiochemical parameters of the molecules depend on many of these properties. But, the complex structure of the whole drug molecule seems difficult to correlate with these parameters [16].

Additionally, modern drug design process helps to identify and develop new ligands with high binding affinity towards a target protein receptor. The molecular docking approaches help to reveal drug–receptor interaction to a greater detail. The study of receptor-ligand interaction is considered as one of the fundamental approaches for rational drug design and so the prediction of such interactions by molecular docking has been gaining importance [17].

In the present study, the molecular docking study was done for some quinazoline-4-3H-one against human DHFR. This was followed by ADMET prediction and drug likeliness as well as drug score analysis of the docked compounds to evaluate the status of some quinazoline-4-(3H) -one as inhibitors of human DHFR.

MATERIALS AND METHODS

The study comprised of 27 compounds belonging to quinazoline-4-(3H)-one (Fig.1) along with one standard drug methotrexate. The selected compounds have different substituents as shown in Table 1. Molinspiration (http://www.molinspiration.com) and OSIRIS Property explorer (http://www.organic-chemistry.org/prog/peo/) were used to calculate logP, solubility, drug likeliness, polar surface area, molecular weight, number of atoms, number of rotatable bonds, volume, drug score and number of violations to Lipinski's rule. PreADMET (http://preadmet.bmdrc.org/) server was also used to test drug-likeliness and ADMET (Absorption, Distribution, Metabolism, Excretion and Toxicity) profile. The OSIRIS program was used to predict the overall toxicity of the most active derivatives (as it may reveal or indicate the presence of some fragments generally responsible for the irritant, mutagenic, tumorigenic, or reproductive effects of the tested compounds).

The physical properties of the ligands were determined. The similarity coefficient of the ligands was compared with the standard drug methotrexate and a cluster tree representing the similarity of the molecules was generated by ChemMine tools (http://chemmine.ucr.edu). Automated molecular docking was performed using the AutoDock 4.0 suite [18].

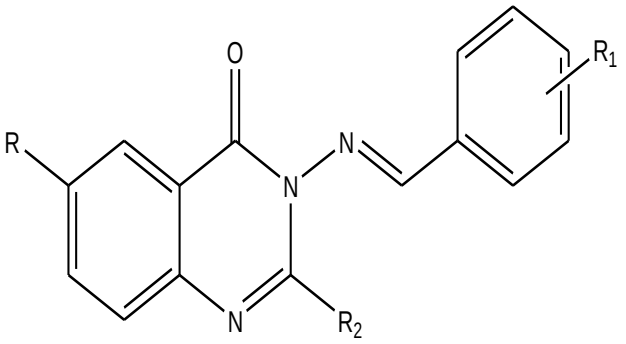

Fig. 1: Structure of 3-amino-2-aryl-4(3H)-quinazolinone

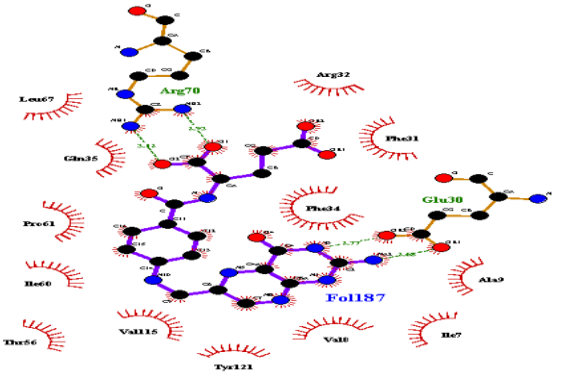

Fig. 2: LigPlot generated snapshot of the residues in the active site of 1DHF interacting with the natural ligand Folate.

Table 1: The substituents of the 3-amino-2-aryl-4(3H)-quinazolinone

Compounds	R	R_1	R_2
4a	H	3,5-Cl	Ph
4b	H	3-NO_2-4-Cl	Ph
4c	H	4-CF_3	Ph
4d	H	3-Cl	Ph
4e	H	2,3-Cl	Ph
4f	H	2,6-Cl	Ph
4g	H	3,4-F	Ph
4h	H	3-CF_3	Ph
4i	6-Br	2-F	Me
4j	6-Br	3-F	Me
4k	6-Br	4-F	Me
4l	6-Br	2-CF_3	Me
4m	6-Br	3-Cl	Me
4n	6-Br	2,4-Cl	Me
4o	6-Br	2,6-Cl	Me
4p	6-Br	3,4-F	Me
4q	6-Br	2-Cl, 5-NO_2	Me
4r	6-Br	4-Cl, 3-NO_2	Me
4s	6-Br	2-F, 3-CF_3	Me
4t	6-Br	3,4-OMe	Me
4u	6-Br	2,3-OMe	Me
4v	6-Br	2,5-OMe	Me
4w	6-Br	3-NO_2	Me
4x	6-Br	2-OH	Me
4y	6-Br	2,4-OMe	Me
4z	6-Br	5-Cl, 3-OH	Me
4	H	2,3-Cl	Me

The three dimensional structure (Fig 2) of the human dihydrofolate reductase was retrieved from the protein data bank (PDB ID: 1DHF) [19]. All water molecules and ligands were removed from the PDB file prior to docking. The receptor molecule was prepared by adding all missing hydrogen and side chain atoms, using the graphic user interface of AutoDock tools (ADT) [20]. The ligand files were also prepared from the 27 compounds used in this study, by adjusting the number of rotatable and non-rotatable bonds in the ligand molecules to assist in flexible docking process. The number of active torsions was set to the maximum number of atoms. As AutoDock requires pre-calculated grid maps, one for each atom type, present in the ligand being docked for storing the interaction potential energy, the grid was prepared in a way that it surrounded the active site based on the amino acid residues, which are involved in folate binding. The grid box size was set at 90, 90, and 90 A° (x, y, and z respectively) using AutoGrid 4.0 Program integrated in AutoDock 4.0. Twenty seven separate molecular docking experiments were set up using Lamarckian Genetic Algorithm (LGA) keeping all other parameters set in default mode. The top ranked model in the lowest energy cluster with maximum cluster size was considered for further interaction studies. Interaction has been compared based on the amino acid residues interacting with the natural ligand folate in the active site of hDHFR [Fig 2]. The docking result was converted from .dlg format to .pdb format by using python script. The compounds were structurally aligned to get a ligand based pharmacophore using PharmaGist tool [21].

RESULTS

Twenty-seven compounds used in this study have successfully qualified Lipinski's Rules, CMC like rule (except 4a and 4f), MDDR like rule and WDI like rule (Table 2). Ligands tested in this study were predicted to have good oral bioavailability (Table 3). Some of the compounds (4e, 4f and 4) have shown excellent permeability, while others have relatively less or poor (in some cases) permeability (Table 4). The physical properties like ionization potential, electronic energy and dipole plays an important role in activity of compounds (data not shown). The drug score and drug likeliness of the ligands were also predicted (Table 5). It revealed that drug score of compounds (4t, 4v, 4k, 4i, 4m, 4o and 4y) in the range of 0.5-0.66 and the rest of the compound in the range of 0.2 0.5.

Table 2: Data representing the qualification of the substituents for drug likeliness using CMC like rule, MDDR like rule and WDI like rule along with Rule of Five as predicted using OSIRIS server

Compound	CMC like rule	MDDR like rule	Rule of five	WDI like rule
4a	Not qualified	Mid structure	Suitable	90%
4b	Qualified	Mid structure	Suitable	90%
4c	Qualified	Mid structure	Suitable	90%
4d	Qualified	Mid structure	Suitable	90%
4e	Qualified	Mid structure	Suitable	90%
4f	Not qualified	Mid structure	Suitable	90%
4g	Qualified	Mid structure	Suitable	90%
4h	Qualified	Mid structure	Suitable	90%
4i	Qualified	Mid structure	Suitable	90%
4j	Qualified	Mid structure	Suitable	90%
4k	Qualified	Mid structure	Suitable	90%
4l	Qualified	Mid structure	Suitable	90%
4m	Qualified	Mid structure	Suitable	90%
4n	Qualified	Mid structure	Suitable	90%
4o	Qualified	Mid structure	Suitable	90%
4p	Qualified	Mid structure	Suitable	90%
4q	Qualified	Mid structure	Suitable	90%
4r	Qualified	Mid structure	Suitable	90%
4s	Qualified	Mid structure	Suitable	90%
4t	Qualified	Mid structure	Suitable	90%
4u	Qualified	Mid structure	Suitable	90%
4v	Qualified	Mid structure	Suitable	90%
4w	Qualified	Mid structure	Suitable	90%
4x	Qualified	Mid structure	Suitable	90%
4y	Qualified	Mid structure	Suitable	90%
4z	Qualified	Mid structure	Suitable	90%
4	Qualified	Mid structure	Suitable	90%

Table 3: Molecular descriptor properties of the ligands

Compound	miLogP	TPSA	nON	nOHNH	Nviolations	nrotb	volume	natoms
4a	5.887	47.261	4	0	1	3	321.379	27.0
4b	5.16	93.08	4	0	0	3	317.532	27.0
4c	4.25	47.261	4	0	0	3	288.64	25.0
4d	5.25	47.26	4	0	1	3	307.843	26.0
4e	5.863	47.261	4	0	1	3	321.379	27.0
4f	5.86	47.26	4	0	1	3	321.37	27.0
4g	4.85	47.26	4	0	0	3	304.17	27.0
4h	5.47	47.26	4	0	1	4	325.60	29.0
4i	3.47	47.26	4	0	0	2	262.27	22.0
4j	3.5	47.26	4	0	0	2	262.27	22.0
4k	3.52	47.26	4	0	0	2	262.27	22.0
4l	4.20	47.26	4	0	0	3	288.64	25.0
4m	4.01	47.26	4	0	0	2	270.88	22.0
4n	4.64	47.26	4	0	0	2	284.41	23.0
4o	4.62	47.26	4	0	0	2	284.41	23.0
4p	3.61	47.261	4	0	0	2	267.20	23.0
4q	3.92	93.08	7	0	0	3	294.21	25.0
4r	3.52	47.261	4	0	0	2	262.27	22.0
4s	4.32	47.261	4	0	0	3	293.57	26.0
4t	3.00	65.729	6	0	0	4	308.43	25.0
4u	3.18	65.729	6	0	0	4	308.43	25.0
4v	3.40	65.729	6	0	0	4	308.43	25.0
4w	3.2	93.08	7	0	0	3	280.67	24.0
4x	3.3	67.489	5	1	0	2	265.36	22.0
4y	3.40	65.729	6	0	0	4	308.43	25.0
4z	3.954	67.489	5	1	0	2	278.898	23.0
4	4.62	47.261	4	0	0	2	284.41	23.0

Table 4: preADME prediction of ligands

Compound name	HIA%	Caco-2 nm/sec	MDCK nm/sec	In vitro plasma%	In vitro blood barrier
4a	98.06	45.898	15.94	96.47	0.84
4b	99.142	17.55	0.044	93.484	0.027
4c	97.68	27.43	0.044	92.11	0.135
4d	97.84	42.28	44.058	93.244	2.07
4e	98.06	45.54	25.09	96.07	1.107
4f	98.06	44.77	34.26	95.998	2.05
4g	97.62	44.77	0.182	93.022	0.269
4h	97.668	27.45	0.044	93.718	0.127
4i	97.589	35.543	0.0958	96.408	2.31
4j	97.589	35.46	0.053	100	1.39
4k	97.589	35.455	0.046	99.18	0.996
4l	97.63	42.27	0.020	100	0.1945
4m	97.809	38.752	0.094	100	1.319
4n	98.003	42.6359	0.0412	100	0.79
4o	98.033	47.7122	0.125	100	1.38
4p	97.592	35.998	0.025	98.44	0.491
4q	99.14	17.55	0.023	100	0.292
4r	99.143	17.34	0.0208	100	0.201
4s	97.64	43.077	0.021	98.35	0.159
4t	97.485	37.517	0.024	95.31	0.241
4u	97.485	37.62	0.026	92.21	1.88
4v	97.485	37.62	0.028	92.71	1.93
4w	99.38	18.775	0.0323	100	0.194
4x	96.169	21.197	0.138	94.513	0.623
4y	97.48	37.06	0.028	89.708	0.358
4z	96.56	22.355	0.037	98.24	0.49
4	97.64	39.17	75.66	91.17	1.67

Table 5: Fragment based drug-likeliness of the ligands

Compound	cLogP	Solubility	MW	Drug likeness	Drug Score
4a	5.26	-6.27	393	1.71	0.23
4b	3.77	-5.44	404	5.07	0.45
4c	4.65	-5.44	393	5.19	0.4
4d	5.26	-5.54	359	5.51	0.31
4e	5.26	-6.27	394	5.59	0.4
4f	4.65	-6.27	394	6.1	0.31
4g	4.16	-5.43	361	2.68	0.42
4h	4.8	-5.58	393	-1.84	0.21
4i	3.42	-4.78	362	1.44	0.59
4j	3.42	-4.78	360	0.12	0.4
4k	3.42	-4.78	360	1.91	0.61
4l	4.12	-5.24	410	-6.99	0.27
4m	3.97	-5.2	376	2.72	0.55
4n	4.59	-5.2	411	3.17	0.44
4o	3.97	-5.94	411	3.76	0.56
4p	3.48	-5.09	378	0.19	0.47
4q	3.71	-5.84	421	1.5	0.45
4r	3.71	-5.84	428	3.16	0.49
4s	4.18	-5.56	402	-4.45	0.25
4t	3.15	-4.5	402	4.56	0.66
4u	3.15	-4.5	402	3.02	0.65
4v	3.15	-4.5	402	3.23	0.66
4w	3.09	-5.1	387	2.57	0.6
4x	3.06	-4.17	358	2.7	0.71
4y	3.15	-4.5	402	1.57	0.61
4z	3.67	-4.9	392	3.41	0.6
4	3.89	-5.1	332	4.94	0.49

The structural similarities of the compounds between each pair of molecules and also with the standard drug methotrexate were calculated. The cluster diagram revealing the relatedness amongst the molecules considering methotrexate as a reference has been shown in Fig. 3. The fate of a promising drug depends on its toxicity. The therapeutic index of a drug would be higher when it shows low toxicity/side effects. Based on this we have performed toxicity predication using Osiris Property Explorer. Results revealed that the compounds have low toxicity. The prediction using Osiris Property Explorer was shown in color codes. Green color represents low toxicity, yellow represents the mediocre toxicity, and red represents high toxicity as shown in table 6.

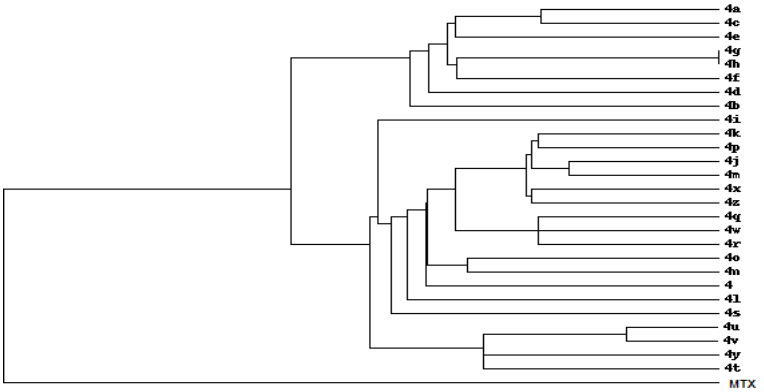

Fig. 3: **The cluster image showing the structural relationship of ligands (4, 4a-4z) with Methotrexate (MTX).The cluster tree drawn by ChemMine tools (http://chemmine.ucr.edu).**

Table 6: Toxicity prediction as per output of Orisis programme

Compound	Mutagenic	Tumorogenic	Irritant	Reproductive effect
4a	Green	Green	Green	Yellow
4b	Green	Green	Green	Yellow
4c	Green	Green	Green	Yellow
4d	Green	Green	Green	Yellow
4e	Green	Green	Green	Yellow
4f	Green	Green	Green	Yellow
4g	Green	Green	Green	Yellow
4h	Green	Green	Green	Yellow
4i	Green	Green	Green	Green
4j	Green	Green	Green	Yellow
4k	Green	Green	Green	Green
4l	Green	Green	Green	Green
4m	Green	Green	Green	Green
4n	Green	Green	Green	Green
4o	Green	Green	Green	Green
4p	Green	Green	Green	Green
4q	Green	Green	Green	Green
4r	Green	Green	Green	Green
4s	Green	Green	Green	Green
4t	Green	Green	Green	Green
4u	Green	Green	Green	Green
4v	Green	Green	Green	Green
4w	Green	Green	Green	Green
4x	Green	Green	Green	Green
4y	Green	Green	Green	Green
4z	Green	Green	Green	Green
4	Green	Green	Green	Green

The molecular docking results revealed that the docked complex of 27 compounds had less binding energy than methotrexate as shown in table 7 .The docking model of the ligand and hDHFR are shown in Fig. 4. The molecular alignment results have shown that all the compounds under study along with the standard drug methotrexate have occupied the same cavity (Fig 5) as is occupied by the natural ligand folate. All the 27 compounds were used to develop a ligand based pharmacophore (Fig. 6) using PharmaGist tool. Pharmacophore with a score of 66.813 showed the following characteristics: five spatial features out of which three are aromatic rings and two are hydrogen bond acceptors. There are no negative or positive centers, hydrophobic groups or hydrogen bond donors.

DISCUSSION

Molecular descriptor properties

The selected compounds used in this study were evaluated as potential hDHFR inhibitors. The oral bioavailability of the compounds projected as potential drugs were evaluated by determining the molecular weight, number of rotatable bonds (nrotb), number of hydrogen bonds (nON and nOHNH), and drug's polar surface (TPSA). Since the individual molecular weights of all the compounds were less than 500, the number of the rotatable bond were <10, the number of hydrogen bond donors and acceptors were < 12, and TPSA values being <140, they qualified to be an ideal oral drug. Ligands tested in this study were also predicted to have good oral bioavailability.

Calculation of the fragment based drug-likeliness of the compounds signifies that the compounds have the same fragments as compared to the existing drug. The drug-likeliness values of all the compounds are reasonably acceptable (except 4h,4i and 4s) as shown in Table 2. The higher drug-likeliness values are found in the case of compounds 4c, 4d, 4e and 4f. Results indicated that these four compounds have the most fragments similar to existing potent drugs to fulfill the potentiality of being drugs.

The drug score values [Table 3] were also calculated which took into account the effect of drug-likeliness, LogP, solubility, molecular weight, and toxicity risk together.

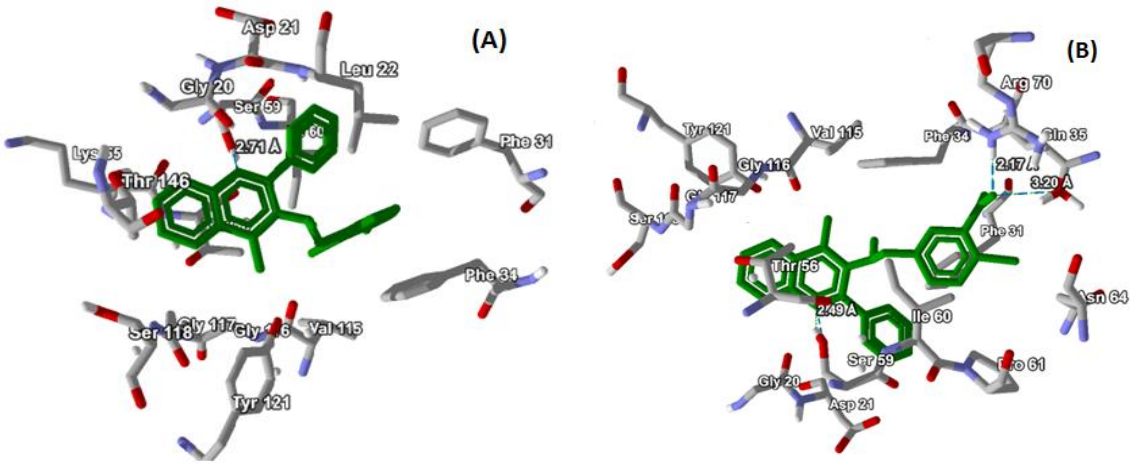

Fig. 4: (A) Ligand 4e docked with hDHFR; (B) ligand 4b docked with hDHFR.

Table 7: Binding energy and Inhibition constant of ligand -human DHFR interaction for each test compound

Compound	Binding energy Kcal/Mol	Inhibition constant (nM)
4a	-11.73	2.5
4b	-12.33	0.91
4c	-11.2	6.61
4d	-11.7	2.35
4e	-12.38	0.846
4f	-11.88	1.96
4g	-11.26	5.55
4h	-11.28	5.43
4i	-10.45	21.82
4j	-10.65	15.49
4k	-10.62	16.23
4l	-10.96	9.26
4m	-11.14	6.79
4n	-11.39	4.44
4o	-10.76	13.0
4p	-10.05	42.94
4q	-11.52	3.59
4r	-11.5	3.72
4s	-10.56	18.06
4t	-10.41	10.09
4u	-10.92	9.91
4v	-10.56	18.18
4w	-12.15	1.23
4x	-10.79	12.35
4y	-10.62	16.35
4z	-10.38	24.81
4	-10.47	21.25
MTX	-8.62.	479.78

Any compound that is considered to be a better drug candidate should exhibit better drug score. Our data showed that compound 4x has the best score (0.71), the compounds 4t,4v,4k,4i,4m,4o and 4y were in the range of 0.5-0.66, and the rest of the compounds were in the range of 0.2-0.5. The hydrophobicity of drugs could be inferred from LogP values [Table 3]. It was found that hydrophobicity and retention time of the drug inside the host are directly related i.e. higher the hydrophobicity, higher is the retention time of the drug in the body [23].

ADME prediction

In the modern drug designing process, computational approaches like preADMET prediction; MDCK and Caco-2 cell permeability, etc. serve as computational screening model for the prediction of intestinal drug absorption. All the compounds under study have qualified HIA%, *in vitro* plasma% (>90% in all the cases) and Caco-2 cell permeability (>25 nm/Sec) to be a good drug candidate. Some of the compounds have shown excellent permeability, while others have relatively less or poor (in some cases) permeability in relation to qualify as CNS drug and MDCK permeability as shown in Table 4. Less permeability is predicted because of the lesser solubility; and solubility, to a certain extent, depends on the arrangement of molecules in the crystal. It is to be noted that the topological aspects cannot be predicted via atom types or substructure fragments.

Molecular Docking and Pharmacophore study

The docked complexes of the receptor (original PDB structure (1DHF:A) and compounds in terms of the occupancy of the active site were compared. The molecular alignment results have shown that all the compounds under study along with the standard drug methotrexate have occupied the same cavity as is occupied by the natural ligand folate. The active site of the human dihydrofolate reductase (hDHFR) is represented by Ile-7, Ala-9, Trp-24, Glu-30, Gln-35, Asn-64, Arg-70, Val-115, Tyr-121 and Thr-136 [24]. It can be inferred that the compounds have an affinity for the active site and can act as competitive inhibitors to the natural ligand.

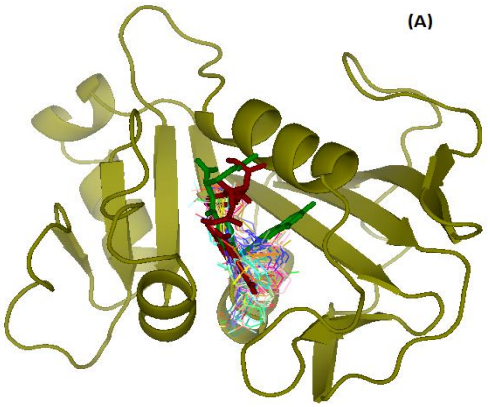

Fig. 5: (A) Docking model of ligands with hDHFR (PDB ID- 1DHF) protein (Folic Acid and methotrexate are represented in green and red sticks respectively, and the other 27 molecules are shown in line representation)

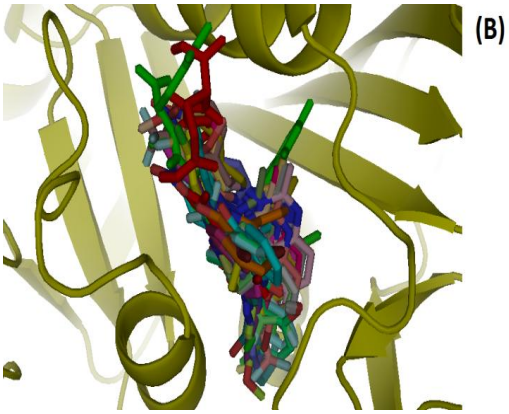

Fig. 5: (B) Zoomed view of the active site showing all the docked molecules (ligands are represented in different color sticks including folic acid and methotrexate represented in green and red sticks respectively)

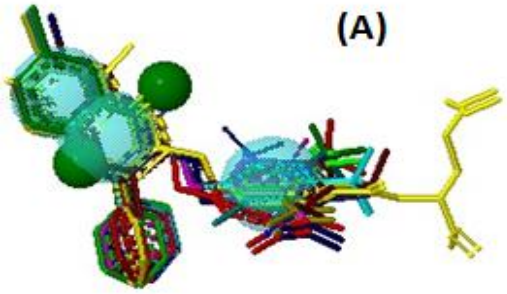

Fig. 6: (A) Structural alignment of 27 molecules along with the reference compound, methotrexate (methotrexate is shown in yellow color)

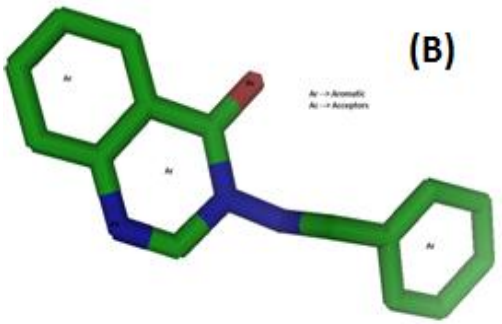

Fig. 6: (B) Structural representation of the derived Pharmacophore

The compounds were evaluated in terms of their binding mode to hDHFR. Based on the binding free energy (ΔG binding) of the protein-ligand interaction and inhibition constant (*Ki*), and one of the 10 models was chosen to be the best one. The docking result showed that all 27 compounds have low binding energy and inhibition constant as compared to the standard drug methotrexate. The minimum binding energy (maximum stability) was found in case of the compound 4e (-12.38 Kcal/Mol). The N1 of 4e forms hydrogen bond with the Ser-59 with a distance of 2.71Å. The amino acids Val-115, Phe-31, Phe-34, Tyr-121, Thr-136 and Asp-21 are found to be involved in making hydrophobic interactions with 4e. Interestingly, all these amino acids are also present in the active site of hDHFR, which infers that 4e binds to the active site region of the enzyme. The ligand 4b has also formed significant stable complex on docking. Similar to 4e, the N1 atom of 4b formed hydrogen bond with the Ser-59. It was reported that the tested quinazoline's recognition with the key amino acid Glu-30 and Ser-59 are essential for binding and biological activity [25]. The maximum binding energy was found in 4p (-10.05 Kcal/mol) which did not form hydrogen bond with the residues of the receptor. It was observed from the calculated binding energies that incorporation of phenyl at 2-C increased the interaction with the enzyme in comparison to compounds substituted with methyl at 2-C. The compounds 4a- 4h have binding energies in the range of -11.28 to -12.38 Kcal/Mol. The inhibition constant is directly proportional to the binding energy as shown in table 7. Many authors have used ligand-based approach for pharmacophore modeling of species-specific DHFR inhibitors. Moreover, a pharmacophore model for hDHFR (human) inhibitors has also been modeled [26]. All the 27 compounds were used to develop a ligand based pharmacophore [Fig. 6 (B)] using PharmaGist tool, which could be used further for the development of new, improved and optimized drug acting as inhibitor to hDHFR.

The pharmacophore has 3 aromatic rings and two hydrogen bond acceptors which enables in making several non covalent interactions like hydrophobic-hydrophobic interactions, hydrogen bonding, pi cloud interactions, etc.

This pharmacophore is qualifying all the four parameters of Lipinski's rule of five and thus could be considered as a lead molecule to generate new conformations for virtual screening library along with more modifications which could enhance its therapeutic index by enhancing the kind of interactions it could possibly make with the target protein.

CONCLUSIONS

Structure based drug design is significantly based on the protein-ligand interaction. The molecular docking study signified that the compounds can act as a putative inhibitor of hDHFR. The binding energy was found to be lesser than that of methotrexate. The compounds have also successfully qualified the rule of five, CMC like rule, WDI like rule and MDDR like rule. Every compound possessed apt pharmacological properties based on the results of Lipinski's Rule, hydrophobicity (based on log P value), and good drug likeliness and drug score. Moreover, the compounds have low toxicity value. The compounds were predicted to be safe (non-mutagenic as well as non-carcinogenic). This study has enabled to broaden the vision for the generation of more specific drugs for hDHFR, and may pave the way for the production and identification of more effective drugs.

Conflicts of Interest: All authors have none to declare.

ACKNOWLEDGEMENTS

Authors are thankful to Tamal Sarkar, Technical officer, USIC, University of North Bengal for assistance in computation. BKT was provided by fellowship funded by DBT Sanction No. BT/BIO-CARe/06/141/2010-2011.

REFERENCES

1. Abali EE, Celikkaya H, Yi-Ching H, Banerjee D, Bertino RJ Novel Therapeutic Approaches to Regulate Human Dihydrofolate Reductase Activity and Expression. *Current enzyme inhibition* 2012;8: 107-117.
2. MacKenzie RE Folates and Pterins. In. (Blakley R L & Benkovic S J eds), Wiley-Interscience, New York. 1984;Vol. 1 pp. 255-306
3. Wyss PC, Gerber P, Hartman PG, Hubschwerlen C, Locher H, Marty H, Stahl M Novel Dihydrofolate Reductase Inhibitors. Structure-Based versus Diversity-Based Library Design and High-Throughput Synthesis and Screening. *J Med Chem* 2003;46: 2304–2312.
4. Rastelli G, Pacchioni S, Sirawaraporn W, Sirawaraporn R, Parenti MD, Ferrari AM Docking and Database Screening Reveal New Classes of *Plasmodium falciparum* Dihydrofolate Reductase Inhibitors. *J Med Chem* 2003;46: 2834–2845.
5. Donkor IO, Li H, Queener SF Synthesis and DHFR inhibitory activity of a homologous series of 6-substituted 2,4-diaminoathieno[2,3-d]pyrimidines'. *Eur J Med Chem* 2003;38: 605–611.
6. Zink M, Lanig H, Troschutz R Structural variations of piritrexim, a lipophilic inhibitor of human dihydrofolate reductase: synthesis, antitumor activity and molecular modeling investigations. *Eur J Med Chem* 2004;39: 1079–1088.
7. Garofalo A**,** Goossens L , Baldeyrou B, Lemoine A , Ravez S , Six P , Cordonnier M, Bonte J, Depreux P , Lansiaux A, Goossens J Design, Synthesis, and DNA-Binding of N-Alkyl(anilino)quinazoline Derivatives. *J Med Chem* 2010;53: 8089–8103.
8. Klutchko SR, Zhou H, Winters RT, Tran TP, Bridges AJ, Althaus IW, Amato DM, Elliott WL, Ellis PA, Meade MA et al Tyrosine Kinase Inhibitors. 19. 6-Alkynamides of 4-Anilinoquinazolines and 4-Anilinopyrido[3,4-*d*]pyrimidines as Irreversible Inhibitors of the erbB Family of Tyrosine Kinase Receptors *J Med Chem* 2006;49: 1475-1485.
9. Hynes JB, Buch JM, Freisheim JH Quinazolines as inhibitors of dihydrofolate reductase. 3. Analogs of pteroic and isopteroic acids. *J Med Chem* 1975;18:1191-1194.
10. Hynes JB. Buch JM Freisheim JH Quinazolines as inhibitors of dihydrofolate reductase. 4. Classical analogs of folic and isofolic acids. *J Med Chem* 1977;20: 588-591.
11. Wakeling AE, Guy SP, Woodburn JR, Ashton SE, Curry BJ, Barker AJ, Gibson KH ZD1839 (Iressa): an orally active inhibitor of epidermal growth factor signaling with potential for cancer therapy. *Cancer Research* 2002;62: 5749–5754.
12. Akita RW, Sliwkowski MX Preclinical studies with Erlotinib (Tarceva). Seminars in Oncology. 2003;30: 15–24.
13. Rusnak DW, Lackey K, Affleck K, Wood ER, Alligood KJ, Rhodes N, Keith BR, Murray DM, Knight WB, Mullin RJ, Gilmer TM The effects of the novel, reversible epidermal growth factor receptor/ErbB-2 tyrosine kinase inhibitor, GW2016, on the growth of human normal and tumor-derived cell lines in vitro and in vivo. *Mol Cancer Ther* 2001;1(2): 85–94.
14. Nanda AK, Ganguli S, Chakraborty R Antibacterial activity of some 3-(Arylideneamino)-2-phenylquinazoline-4(3H)-ones: synthesis and preliminary QSAR studies. *Molecules* 2007;12: 2413-2426.
15. Xingwen G, Xuejian C, Kai Y, Baoan S, Lili G, Zhuo C Synthesis and Antiviral Bioactivities of 2-Aryl- or 2-Methyl-3-(substituted- Benzalamino)-4(3*H*)-quinazolinone Derivatives. *Molecules* 2007;12: 2621-2642.
16. Kadam RU, Roy N Recent trends in Drug-Likeliness Prediction: A comprehensive review of *In Silico* methods. *Indian J Pharm Sci* 2009;14: 609-615.
17. Shoichet BK, McGovern SL, Wei B, Irwin JJ Lead discovery using molecular docking. *Curr Opin Chem Biol* 2002;6: 439-446.
18. Morris GM, Goodsell DS, Halliday RS, Huey R, Hart WE, Belew RK, Olson A J Automated Docking Using a Lamarckian Genetic Algorithm and and Empirical Binding Free Energy Function. *J Comp Chem* 1998;19(14): 1639-1662.
19. Davies JF, Delcamp TJ, Prendergad NJ, Ashford VA , Freisheim JH, Kraut J Crystal structures of recombinant human dihydrofolate reductase complexed with folate and 5-deazafolate. *Biochemistry* 1990;29: 9467-9479.
20. Sanner MF Python: a programming language for software integration and development. *J Mol Graph Model* 1999;17: 57-61.
21. Schneidman-Duhovny D, Dror O, Inbar Y, Nussinov R, Wolfson JH PharmaGist: a webserver for ligand-based pharmacophore detection. *Nucleic Acids Research* 2008;36 : W223–W228
22. Lipinski CA, Lombardo F, Dominy BW, Feeney PJ Experimental and computational approaches to estimate solubility and permeability in drug discovery and development settings. *Adv Drug Deliv Rev* 1997;23: 3-25.
23. Tambunan USF, Bramantya N, Parikesit AA. In silico modification of suberoylanilide hydroxamic acid (SAHA) as potential inhibitor for class II histone deacetylase (HDAC). *BMC Bioinformatics* 2011; 12(Suppl 13): S23.
24. Yamini L, Meena KK, Vijjulatha M Molecular Docking, 3D QSAR and Designing of New Quinazolinone Analogues as DHFR Inhibitors. *Bull Korean Chem Soc* 2011;32 : 2433-2442.
25. Al-Rashood Sarah T, Aboldahab Ihsan A, Nagi Mahmoud N, Laila A. Alaa Abouzeid A, Abdel-Aziz M., Sami G, Abdel-hamide, M. Youssef Khairia, M. Al-Obaid Abdulrahman I. El-Subbagh Hussein Synthesis, dihydrofolate reductase inhibition, antitumor testing, and molecular modeling study of some new 4(3H)-quinazolinone analogs. *Bioorg Med Chem* 2006;14: 8608–8621.
26. Al-Omary FAM, Abou-zeid LA, Nagi MN, Habib EE, Abdel-Aziz AAM., El-Azab AS, Abdel-Hamide SG, Al-Omar MA, Al-Obaid AM, El-Subbagh HI Non-classical antifolates. Part 2: Synthesis, biological evaluation, and molecular modeling study of some new 2,6-substituted-quinazolin-4-ones. *Bioorg Med Chem* 2010;18: 2849-2863.